VOLUME: 18 NO: 5 YEAR: 2021

Indexed in PMC and Web of Science
ULAKBİM / TR Dizin, Scopus

ISSN: 1304-530X

TURKISH JOURNAL OF PHARMACEUTICAL SCIENCES

An Official Journal of the Turkish Pharmacists' Association, Academy of Pharmacy

TURKISH
JOURNAL OF PHARMACEUTICAL SCIENCES

TURKISH
JOURNAL OF PHARMACEUTICAL SCIENCES

TURKISH JOURNAL OF PHARMACEUTICAL SCIENCES

AIMS AND SCOPE

The Turkish Journal of Pharmaceutical Sciences is the only scientific periodical publication of the Turkish Pharmacists' Association and has been published since April 2004.
Turkish Journal of Pharmaceutical Sciences journal is regularly published 6 times in a year (February, April, June, August, October, December). The issuing body of the journal is Galenos Yayinevi/Publishing House level.
The aim of Turkish Journal of Pharmaceutical Sciences is to publish original research papers of the highest scientific and clinical value at an international level. The target audience includes specialists and professionals in all fields of pharmaceutical sciences.
The editorial policies are based on the "Recommendations for the Conduct, Reporting, Editing, and Publication of Scholarly Work in Medical Journals (ICMJE Recommendations)" by the International Committee of Medical Journal Editors (2013, archived at http://www.icmje.org/) rules.

Editorial Independence

Turkish Journal of Pharmaceutical Sciences is an independent journal with independent editors and principles and has no commerical relationship with the commercial product, drug or pharmaceutical company regarding decisions and review processes upon articles.

ABSTRACTED/INDEXED IN

PubMed
PubMed Central
Web of Science-Emerging Sources Citation Index (ESCI)
SCOPUS SJR
TÜBİTAK/ULAKBİM TR Dizin
ProQuest
Chemical Abstracts Service (CAS)
EBSCO
EMBASE
GALE
Index Copernicus
Analytical Abstracts
International Pharmaceutical Abstracts (IPA)
Medicinal & Aromatic Plants Abstracts (MAPA)
British Library
CSIR INDIA
GOALI
Hinari
OARE
ARDI
AGORA
Türkiye Atıf Dizini
Türk Medline
UDL-EDGE
J- Gate
Idealonline
CABI

OPEN ACCESS POLICY

This journal provides immediate open access to its content on the principle that making research freely available to the public supports a greater global exchange of knowledge.
Open Access Policy is based on the rules of the Budapest Open Access Initiative (BOAI) http://www.budapestopenaccessinitiative.org/. By "open access" to peer-reviewed research literature, we mean its free availability on the public internet, permitting any users to read, download, copy, distribute, print, search, or link to the full texts of these articles, crawl them for indexing, pass them as data to software, or use them for any other lawful purpose, without financial, legal, or technical barriers other than those inseparable from gaining access to the internet itself. The only constraint on reproduction and distribution, and the only role for copyright in this domain, should be to give authors control over the integrity of their work and the right to be properly acknowledged and cited.

CORRESPONDENCE ADDRESS

All correspondence should be directed to the Turkish Journal of Pharmaceutical Sciences Editorial Board

Post Address: Turkish Pharmacists' Association, Mustafa Kemal Mah 2147.Sok No:3 06510 Çankaya/Ankara, TURKEY
Phone: +90 (312) 409 81 00
Fax: +90 (312) 409 81 09
Web Page: http://turkjps.org
E-mail: turkjps@gmail.com

PERMISSIONS

Requests for permission to reproduce published material should be sent to the publisher.
Publisher: Erkan Mor
Adress: Molla Gürani Mah. Kaçamak Sok. 21/1 Fındıkzade, Fatih, Istanbul, Turkey
Telephone: +90 212 621 99 25
Fax: +90 212 621 99 27
Web page: http://www.galenos.com.tr/en
E-mail: info@galenos.com.tr

ISSUING BODY CORRESPONDING ADDRESS

Issuing Body : Galenos Yayınevi
Address: Molla Gürani Mah. Kaçamak Sk. No: 21/1, 34093 İstanbul, Turkey
Phone: +90 212 621 99 25 Fax: +90 212 621 99 27
E-mail: info@galenos.com.tr

MATERIAL DISCLAIMER

The author(s) is (are) responsible for the articles published in the JOURNAL.
The editors, editorial board and publisher do not accept any responsibility for the articles.

TURKISH
JOURNAL OF PHARMACEUTICAL SCIENCES

INSTRUCTIONS TO AUTHORS

Turkish Journal of Pharmaceutical Sciences journal is published 6 times (February, April, June, August, October, December) per year and publishes the following articles:

• Research articles

• Reviews (only upon the request or consent of the Editorial Board)

• Preliminary results/Short communications/Technical notes/Letters to the Editor in every field of pharmaceutical sciences.

The publication language of the journal is English.

The Turkish Journal of Pharmaceutical Sciences does not charge any article submission or processing charges.

A manuscript will be considered only with the understanding that it is an original contribution that has not been published elsewhere.

The Journal should be abbreviated as "Turk J Pharm Sci" when referenced.

The scientific and ethical liability of the manuscripts belongs to the authors and the copyright of the manuscripts belongs to the Journal. Authors are responsible for the contents of the manuscript and accuracy of the references. All manuscripts submitted for publication must be accompanied by the Copyright Transfer Form [copyright transfer]. Once this form, signed by all the authors, has been submitted, it is understood that neither the manuscript nor the data it contains have been submitted elsewhere or previously published and authors declare the statement of scientific contributions and responsibilities of all authors.

Experimental, clinical and drug studies requiring approval by an ethics committee must be submitted to the JOURNAL with an ethics committee approval report including approval number confirming that the study was conducted in accordance with international agreements and the Declaration of Helsinki (revised 2013) (http://www.wma.net/en/30publications/10policies/b3/). The approval of the ethics committee and the fact that informed consent was given by the patients should be indicated in the Materials and Methods section. In experimental animal studies, the authors should indicate that the procedures followed were in accordance with animal rights as per the Guide for the Care and Use of Laboratory Animals (http://oacu.od.nih.gov/regs/guide/guide.pdf) and they should obtain animal ethics committee approval.

Authors must provide disclosure/acknowledgment of financial or material support, if any was received, for the current study.

If the article includes any direct or indirect commercial links or if any institution provided material support to the study, authors must state in the cover letter that they have no relationship with the commercial product, drug, pharmaceutical company, etc. concerned; or specify the type of relationship (consultant, other agreements), if any.

Authors must provide a statement on the absence of conflicts of interest among the authors and provide authorship contributions.

All manuscripts submitted to the journal are screened for plagiarism using the 'iThenticate' software. Results indicating plagiarism may result in manuscripts being returned or rejected.

The Review Process

This is an independent international journal based on double-blind peer-review principles. The manuscript is assigned to the Editor-in-Chief, who reviews the manuscript and makes an initial decision based on manuscript quality and editorial priorities. Manuscripts that pass initial evaluation are sent for external peer review, and the Editor-in-Chief assigns an Associate Editor. The Associate Editor sends the manuscript to at least two reviewers (internal and/or external reviewers). The Associate Editor recommends a decision based on the reviewers' recommendations and returns the manuscript to the Editor-in-Chief. The Editor-in-Chief makes a final decision based on editorial priorities, manuscript quality, and reviewer recommendations. If there are any conflicting recommendations from reviewers, the Editor-in-Chief can assign a new reviewer.

The scientific board guiding the selection of the papers to be published in the Journal consists of elected experts of the Journal and if necessary, selected from national and international authorities. The Editor-in-Chief, Associate Editors may make minor corrections to accepted manuscripts that do not change the main text of the paper.

In case of any suspicion or claim regarding scientific shortcomings or ethical infringement, the Journal reserves the right to submit the manuscript to the supporting institutions or other authorities for investigation. The Journal accepts the responsibility of initiating action but does not undertake any responsibility for an actual investigation or any power of decision.

The Editorial Policies and General Guidelines for manuscript preparation specified below are based on "Recommendations for the Conduct, Reporting, Editing, and Publication of Scholarly Work in Medical Journals (ICMJE Recommendations)" by the International Committee of Medical Journal Editors (2013, archived at http://www.icmje.org/).

Preparation of research articles, systematic reviews and meta-analyses must comply with study design guidelines:

CONSORT statement for randomized controlled trials (Moher D, Schultz KF, Altman D, for the CONSORT Group. The CONSORT statement revised recommendations for improving the quality of reports of parallel group randomized trials. JAMA 2001; 285: 1987-91) (http://www.consort-statement.org/);

PRISMA statement of preferred reporting items for systematic reviews and meta-analyses (Moher D, Liberati A, Tetzlaff J, Altman DG, The PRISMA Group. Preferred Reporting Items for Systematic Reviews and Meta-Analyses: The PRISMA Statement. PLoS Med 2009; 6(7): e1000097.) (http://www.prisma-statement.org/);

STARD checklist for the reporting of studies of diagnostic accuracy (Bossuyt PM, Reitsma JB, Bruns DE, Gatsonis CA, Glasziou PP, Irwig LM, et al., for the STARD Group. Towards complete and accurate reporting of studies of diagnostic accuracy: the STARD initiative. Ann Intern Med 2003;138:40-4.) (http://www.stard-statement.org/);

STROBE statement, a checklist of items that should be included in reports of observational studies (http://www.strobe-statement.org/);

MOOSE guidelines for meta-analysis and systemic reviews of observational studies (Stroup DF, Berlin JA, Morton SC, et al. Meta-analysis of observational studies in epidemiology: a proposal for reporting Meta-analysis of observational Studies in Epidemiology (MOOSE) group. JAMA 2000; 283: 2008-12).

GENERAL GUIDELINES

Manuscripts can only be submitted electronically through the Journal Agent website (http://journalagent.com/tjps/) after creating an account. This system allows online submission and review.

TURKISH
JOURNAL OF PHARMACEUTICAL SCIENCES

INSTRUCTIONS TO AUTHORS

Format: Manuscripts should be prepared using Microsoft Word, size A4 with 2.5 cm margins on all sides, 12 pt Arial font and 1.5 line spacing.

Abbreviations: Abbreviations should be defined at first mention and used consistently thereafter. Internationally accepted abbreviations should be used; refer to scientific writing guides as necessary.

Cover letter: The cover letter should include statements about manuscript type, single-Journal submission affirmation, conflict of interest statement, sources of outside funding, equipment (if applicable), for original research articles.

ETHICS COMMITTEE APPROVAL

The editorial board and our reviewers systematically ask for ethics committee approval from every research manuscript submitted to the Turkish Journal of Pharmaceutical Sciences. If a submitted manuscript does not have ethical approval, which is necessary for every human or animal experiment as stated in international ethical guidelines, it must be rejected on the first evaluation.

Research involving animals should be conducted with the same rigor as research in humans; the Turkish Journal of Pharmaceutical Sciences asks original approval document to show implements the 3Rs principles. If a study does not have ethics committee approval or authors claim that their study does not need approval, the study is consulted to and evaluated by the editorial board for approval.

SIMILARITY

The Turkish Journal of Pharmaceutical Sciences is routinely looking for similarity index score from every manuscript submitted before evaluation by the editorial board and reviewers. The journal uses iThenticate plagiarism checker software to verify the originality of written work. There is no acceptable similarity index; but, exceptions are made for similarities less than 15 %.

REFERENCES

Authors are solely responsible for the accuracy of all references.

In-text citations: References should be indicated as a superscript immediately after the period/full stop of the relevant sentence. If the author(s) of a reference is/are indicated at the beginning of the sentence, this reference should be written as a superscript immediately after the author's name. If relevant research has been conducted in Turkey or by Turkish investigators, these studies should be given priority while citing the literature.

Presentations presented in congresses, unpublished manuscripts, theses, Internet addresses, and personal interviews or experiences should not be indicated as references. If such references are used, they should be indicated in parentheses at the end of the relevant sentence in the text, without reference number and written in full, in order to clarify their nature.

References section: References should be numbered consecutively in the order in which they are first mentioned in the text. All authors should be listed regardless of number. The titles of Journals should be abbreviated according to the style used in the Index Medicus.

Reference Format

Journal: Last name(s) of the author(s) and initials, article title, publication title and its original abbreviation, publication date, volume, the inclusive page numbers. Example: Collin JR, Rathbun JE. Involutional entropion: a review with evaluation of a procedure. Arch Ophthalmol. 1978;96:1058-1064.

Book: Last name(s) of the author(s) and initials, book title, edition, place of publication, date of publication and inclusive page numbers of the extract cited.

Example: Herbert L. The Infectious Diseases (1st ed). Philadelphia; Mosby Harcourt; 1999:11;1-8.

Book Chapter: Last name(s) of the author(s) and initials, chapter title, book editors, book title, edition, place of publication, date of publication and inclusive page numbers of the cited piece.

Example: O'Brien TP, Green WR. Periocular Infections. In: Feigin RD, Cherry JD, eds. Textbook of Pediatric Infectious Diseases (4th ed). Philadelphia; W.B. Saunders Company;1998:1273-1278.

Books in which the editor and author are the same person: Last name(s) of the author(s) and initials, chapter title, book editors, book title, edition, place of publication, date of publication and inclusive page numbers of the cited piece. Example: Solcia E, Capella C, Kloppel G. Tumors of the exocrine pancreas. In: Solcia E, Capella C, Kloppel G, eds. Tumors of the Pancreas. 2nd ed. Washington: Armed Forces Institute of Pathology; 1997:145-210.

TABLES, GRAPHICS, FIGURES, AND IMAGES

All visual materials together with their legends should be located on separate pages that follow the main text.

Images: Images (pictures) should be numbered and include a brief title. Permission to reproduce pictures that were published elsewhere must be included. All pictures should be of the highest quality possible, in

JPEG format, and at a minimum resolution of 300 dpi.

Tables, Graphics, Figures: All tables, graphics or figures should be enumerated according to their sequence within the text and a brief descriptive caption should be written. Any abbreviations used should be defined in the accompanying legend. Tables in particular should be explanatory and facilitate readers' understanding of the manuscript, and should not repeat data presented in the main text.

MANUSCRIPT TYPES

Original Articles

Clinical research should comprise clinical observation, new techniques or laboratories studies. Original research articles should include title, structured abstract, key words relevant to the content of the article, introduction, materials and methods, results, discussion, study limitations, conclusion references, tables/figures/images and acknowledgement sections. Title, abstract and key words should be written in both Turkish and English. The manuscript should be formatted in accordance with the above-mentioned guidelines and should not exceed 16 A4 pages.

Title Page: This page should include the title of the manuscript, short title, name(s) of the authors and author information. The following descriptions should be stated in the given order:

TURKISH
JOURNAL OF PHARMACEUTICAL SCIENCES

INSTRUCTIONS TO AUTHORS

1. Title of the manuscript (Turkish and English), as concise and explanatory as possible, including no abbreviations, up to 135 characters

2. Short title (Turkish and English), up to 60 characters

3. Name(s) and surname(s) of the author(s) (without abbreviations and academic titles) and affiliations

4. Name, address, e-mail, phone and fax number of the corresponding author

5. The place and date of scientific meeting in which the manuscript was presented and its abstract published in the abstract book, if applicable

Abstract: A summary of the manuscript should be written in both Turkish and English. References should not be cited in the abstract. Use of abbreviations should be avoided as much as possible; if any abbreviations are used, they must be taken into consideration independently of the abbreviations used in the text. For original articles, the structured abstract should include the following sub-headings:

Objectives: The aim of the study should be clearly stated.

Materials and Methods: The study and standard criteria used should be defined; it should also be indicated whether the study is randomized or not, whether it is retrospective or prospective, and the statistical methods applied should be indicated, if applicable.

Results: The detailed results of the study should be given and the statistical significance level should be indicated.

Conclusion: Should summarize the results of the study, the clinical applicability of the results should be defined, and the favorable and unfavorable aspects should be declared.

Keywords: A list of minimum 3, but no more than 5 key words must follow the abstract. Key words in English should be consistent with "Medical Subject Headings (MESH)" (www.nlm.nih.gov/mesh/MBrowser.html). Turkish key words should be direct translations of the terms in MESH.

Original research articles should have the following sections:

Introduction: Should consist of a brief explanation of the topic and indicate the objective of the study, supported by information from the literature.

Materials and Methods: The study plan should be clearly described, indicating whether the study is randomized or not, whether it is retrospective or prospective, the number of trials, the characteristics, and the statistical methods used.

Results: The results of the study should be stated, with tables/figures given in numerical order; the results should be evaluated according to the statistical analysis methods applied. See General Guidelines for details about the preparation of visual material.

Discussion: The study results should be discussed in terms of their favorable and unfavorable aspects and they should be compared with the literature. The conclusion of the study should be highlighted.

Study Limitations: Limitations of the study should be discussed. In addition, an evaluation of the implications of the obtained findings/results for future research should be outlined.

Conclusion: The conclusion of the study should be highlighted.

Acknowledgements: Any technical or financial support or editorial contributions (statistical analysis, English/Turkish evaluation) towards the study should appear at the end of the article.

References: Authors are responsible for the accuracy of the references. See General Guidelines for details about the usage and formatting required.

Review Articles

Review articles can address any aspect of clinical or laboratory pharmaceuticals. Review articles must provide critical analyses of contemporary evidence and provide directions of or future research. Most review articles are commissioned, but other review submissions are also welcome. Before sending a review, discussion with the editor is recommended.

Reviews articles analyze topics in depth, independently and objectively. The first chapter should include the title in Turkish and English, an unstructured summary and key words. Source of all citations should be indicated. The entire text should not exceed 25 pages (A4, formatted as specified above).

TURKISH
JOURNAL OF PHARMACEUTICAL SCIENCES

CONTENTS

TURKISH
JOURNAL OF PHARMACEUTICAL SCIENCES

CONTENTS

Turk J Pharm Sci 2021;18(5):527-529
DOI: 10.4274/tjps.galenos.2021.52323

LETTER TO EDITOR

May Biodegradable and Biocompatible Polymeric Microneedles be Considered as a Vaccine and Drug Delivery System in the COVID-19 Pandemic?

Biyoparçalanır ve Biyouyumlu Polimerik Mikroiğneler COVID-19 Pandemisinde Aşı ve İlaç Taşıyıcı Sistem Olarak Değerlendirilebilir mi?

Sedat ÜNAL, Osman DOĞAN, Yeşim AKTAŞ

Erciyes University Faculty of Pharmacy, Department of Pharmaceutical Technology, Kayseri, Turkey

Key words: COVID-19, new drug delivery systems, microneedles
Anahtar kelimeler: COVID-19, yeni ilaç taşıyıcı sistemler, mikroiğneler

Dear Editor,

Coronavirus disease-2019 (COVID-19) was first reported in Wuhan, China at the end of December 2019 and declared as a pandemic. COVID-19 is a disease characterized by acute respiratory failure. COVID-19, which is caused by severe acute respiratory syndrome coronavirus 2 (a member of the Coronaviridae family), has spread to the whole world in a short time due to its rapid transmission from person to person.[1] New serious mutations giving rise to increasing virus variants and fast spread of the virus have raised questions regarding the efficiacy of vaccines and current treatment methods. Furthermore, supply, stability, and necessity of administering drugs and vaccines developed/being developed for a large number of individuals in a short time brings up a series of problems on a global scale.

Microneedles (MNs) are drug delivery systems that are designed in micron size (usually 10-2000 μm in length and 10-50 μm in diameter) and developed mainly for use in transdermal treatments. MNs do not cause pain and discomfort and these can be applied without stimulating the nerve endings by crossing the stratum corneum. Also, MNs can be used without the need for any healthcare personnel and are designed as controlled/extended systems. Moreover, MNs do not require cold chain for transport. MNs cross the stratum corneum and carry drug molecules to the dermis layer where vascular and lymphatic vessels are concentrated.[2] Then, drug molecules penetrate lymph or blood capillaries according to their physicochemical properties and enter systemic circulation. MNs, which were first developed in 1976 to overcome obstacles faced with transdermal drug delivery systems, have been designed and scientifically investigated by various research groups as drug delivery systems for various drugs, vaccines, genes, and hormones. On the other hand, parallel to the developments in microfabrication technologies, studies have been performed to increase the applicability of MNs in the pharmaceutical field by obtaining MN types with different designs and characteristics (solid MN, hollow MN, coated MN, and dissolving MN). Intensive scientific studies are being performed by researchers to develop innovative MN systems within the framework of the

*Correspondence: sedatunal@erciyes.edu.tr, Phone: +90 352 207 66 66 – 28381, ORCID-ID: orcid.org/0000-0002-1518-010X
Received: 16.02.2021, Accepted: 04.03.2021

target disease and target molecule to increase potential advantages of MN.[3] Oral drug administration for children is limited mainly due to the difficulty in swallowing. On the other hand, the parenteral route of drug administration presents difficulties for both children and parents. For injecting drugs, healthcare professionals need to adopt a pedagogical approach. However, this is not enough to eliminate pain and emotional trauma that may occur during drug administration. Therefore, MN designs for children are considered a promising array. Nowadays, MNs are being investigated as an alternative route for efficient and painless insulin delivery for the treatment of type-1 diabetes, which occurs more frequently in childhood.[4] In another study, promising results were obtained by using ferric pyrophosphate-loaded MNs for treating iron deficiency anemia in children.[5] In this context, clinical trials are being conducted on MNs developed for children.[6]

In recent years, dissolving MNs have attracted more attention of research groups due to high patient compliance and no residual biological material after application. MN drug delivery systems developed using biocompatible and biodegradable polymers as a basic principle may be used to treat a wide range of diseases. After insertion into the skin, the polymeric matrix forms MN and carrying the drug dissolves and releases the drug molecules. Dissolving MNs also allow modification in release rate and duration according to the type, structure, and molecular weight of the polymers used.[7] There is no physical wound, incision, or non-biocompatible residual on the skin after the application of dissolving MNs. Promising results have been reported with MN arrays prepared using various biodegradable and biocompatible polymers (such as polylactic acid, hyaluronic acid, poly lactic-co-glycolic acid, polyvinyl alcohol PVA, and polyvinylpyrrolidone).[8] MN systems are also flexible systems that can be modified using advanced studies and multidisciplinary approaches to achieve desired design and drug release rate.[3]

Increasing studies on MN systems in recent years are considered as a harbinger and it is possible that MN systems will be more widely used as drug/vaccine carriers in the near future. It is known that MN vaccination, which was developed especially for influenza immunization and evaluated clinically, is a milestone in this field and has been studied intensively over the last decade.[9] During the COVID-19 pandemic, the necessity of fast, efficient, stable, easily applicable, and result-oriented systems that do not require compelling storage conditions has again come to the fore. It should not be overlooked that one of the possible global solutions with important advantages in this sense is MN systems.

The COVID-19 pandemic has brought about a large global production and logistics problem in the healthcare field. The production, stability, efficacy, and safety of many sensitive medical materials, such as medicines and vaccines, as well as their rapid and large-scale applications, pose serious difficulties for both healthcare institutions and governments. Developed vaccine technologies incur more additional costs than drugs. The biggest problem encountered with vaccines today is the lack of healthcare personnels during the use, storage, and transportation of vaccines. Residues such as needles and injectors result in social, environmental, and institutional problems. Therefore, soluble MN systems, which are biodegradable, have the potential to prevent such problems. Being mechanically durable, not requiring any healthcare personnel during application, and being easy to apply without pain are the biggest advantages of MN systems in this field. Studies suggest that MNs can provide controlled/extended release without causing toxicity in the body due to their biocompatible polymeric structure and that it can maintain the immune response for a longer time in vaccine applications.

Biocompatible and biodegradable material-based drug/vaccine carrier MNs are among the most important candidates in the pharmaceutical and vaccine industry in terms of their advantages, such as logistics, storage, stability, and ease of use. For all these reasons, MN technologies should be further studied and exploited for their use in the treatment of COVID-19. Developments and studies in the field of MNs should be followed closely. Vaccines are important in the prevention of epidemic diseases. Considering the fact that we are facing a pandemic, quick and reliable distribution is of great importance to enable widespread use of vaccines. Based on ongoing studies and acquired knowledge in this field, MN-based soluble COVID-19 vaccines are suggested to be promising.

Conflict of interest: No conflict of interest was declared by the authors. The authors are solely responsible for the content and writing of this paper.

REFERENCES

1. Yuki K, Fujiogi M, Koutsogiannaki S. COVID-19 pathophysiology: a review. Clin Immunol. 2020;215:108427.
2. Shaikh S, Bhan N, Rodrigues FC, Dathathri E, De S, Thakur G. Microneedle platform for biomedical applications. In: Shaikh S, Bhan N, Rodrigues FC, Dathathri E, De S, Thakur G, eds. Bioelectronics and Medical Devices. London: Elsevier; 2019:421-441.
3. Vora LK, Moffatt K, Tekko IA, Paredes AJ, Volpe-Zanutto F, Mishra D, Peng K, Raj Singh Thakur R, Donnelly RF. Microneedle array systems for long-acting drug delivery. Eur J Pharm Biopharm. 2021;159:44-76.
4. Norman JJ, Brown MR, Raviele NA, Prausnitz MR, Felner EI. Faster pharmacokinetics and increased patient acceptance of intradermal insulin delivery using a single hollow microneedle in children and adolescents with type 1 diabetes. Pediatr Diabetes. 2013;14:459-465.
5. Maurya A, Nanjappa SH, Honnavar S, Salwa M, Murthy SN. Rapidly dissolving microneedle patches for transdermal iron replenishment therapy. J Pharm Sci. 2018;107:1642-1647.
6. Duarah S, Sharma M, Wen J. Recent advances in microneedle-based drug delivery: special emphasis on its use in paediatric population. Eur J Pharm Biopharm. 2019;136:48-69.

7. van der Maaden K, Jiskoot W, Bouwstra J. Microneedle technologies for (trans)dermal drug and vaccine delivery. J Control Release. 2012;161:645-655.

8. Koyani RD. Synthetic polymers for microneedle synthesis: from then to now. J Drug Deliv Sci Technol. 2020:102071. doi: 10.1016/j.jddst.2020.102071.

9. Frew PM, Paine MB, Rouphael N, Schamel J, Chung Y, Mulligan MJ, Prausnitz MR. Acceptability of an inactivated influenza vaccine delivered by microneedle patch: Results from a phase I clinical trial of safety, reactogenicity, and immunogenicity. Vaccine. 2020;38:7175-7181.

Turk J Pharm Sci 2021;18(5):530-540
DOI: 10.4274/tjps.galenos.2020.01212

ORIGINAL ARTICLE

An Examination of the Factors Affecting Community Pharmacists' Knowledge, Attitudes, and Impressions About the COVID-19 Pandemic

Serbest Eczacıların COVID-19 Pandemisi Hakkında Bilgi, Tutum ve İzlenimleri ve Etkileyen Değişkenlerin İncelenmesi

Zekiye Kübra YILMAZ[1]*, Nazlı ŞENCAN[2]

[1]Acıbadem Mehmet Ali Aydınlar University Faculty of Pharmacy, Department of Clinical Pharmacy, İstanbul, Turkey
[2]Acıbadem Mehmet Ali Aydınlar University Faculty of Pharmacy, Department of Pharmacy Management, İstanbul, Turkey

ABSTRACT

Objectives: Coronavirus disease-2019 (COVID-19)-related cases and deaths are ongoing throughout the world, but there is still no effective drug in its treatment, and the vaccine supply is not adequate for the global population. It is important that pharmacists have sufficient knowledge and awareness to prevent and control the disease. COVID-19 has been widely covered in the media, which has been a source widely used by healthcare professionals. This study aimed to assess the knowledge, attitudes, and impressions of community pharmacists about COVID-19 and the factors affecting them.

Materials and Methods: The questions in this survey were formed using the guideline created by the World Health Organization, a guide composed by the Turkish COVID-19 Scholarly Commission, and data disclosed to the public on the website of the Ministry of Health. The questionnaire was designed with Google forms and then applied to community pharmacists all over Turkey by sharing the survey link.

Results: Analyses of 393 questionnaires showed that Ministry of Health/government statements, the internet (scientific sources), and the media were the preferred sources of information (96.7%, 89.6%, and 84%, respectively). "Ways to avoid COVID-19" was the most searched title (96.9%). It was determined that the names of the two drugs most frequently mentioned by the participants to be used in the treatment of COVID-19 in Turkey were hydroxychloroquine and azithromycin (57.5%; 50.1%, respectively). Participants who received information from the media gave less education to patients/customers on personal protection measures against COVID-19 (83.3%) and symptoms of COVID-19 (78.8%); however, their behavior regarding the training of pharmacy personnel was found to be the opposite. It has been determined that about half of the participants (46.6%) mostly trust the Ministry of Health regarding the COVID-19 pandemic.

Conclusion: Media and other sources influence the knowledge, behavior and impressions of pharmacists'. Having a high level of knowledge positively affects people's behavior. It is important for pharmacists to have accurate information about COVID-19 and to transfer their knowledge to the community to provide patient education and to prevent/control the spread of COVID-19.

Key words: COVID-19, pandemic, community pharmacists, knowledge, attitude

ÖZ

Amaç: Koronavirüs hastalığı-2019 (COVID-19) kaynaklı olgular ve ölümler dünya çapında devam etmekte ancak hala etkili bir aşı ve ilaç bulunmamaktadır. Salgın sürecinde önemli rol oynayan eczacıların, yeterli bilgi ve farkındalığa sahip olmaları hastalığın önlenmesi ve kontrolü için önemlidir. COVID-19 medyada geniş yer bulmakla birlikte medya, sağlık uzmanları tarafından yaygın olarak kullanılan bir kaynak olmuştur. Bu çalışma, serbest eczacıların COVID-19 hakkındaki bilgi, tutum ve izlenimlerini ve bunu etkileyen faktörleri değerlendirmeyi amaçlamaktadır.

Gereç ve Yöntemler: Bu anketteki sorular, Dünya Sağlık Örgütü tarafından oluşturulan kılavuz, Türkiye COVID-19 Bilim Kurulu'nun oluşturduğu COVID-19 kılavuzu ve Sağlık Bakanlığı internet sitesinde açıklanan veriler kullanılarak oluşturulmuştur. Anket Google form üzerinde oluşturuldu ve ardından anketin linki paylaşılarak Türkiye'nin dört bir yanındaki serbest eczacılara uygulandı.

*Correspondence: zekiye.yilmaz@acibadem.edu.tr, Phone: +90 530 391 27 51, ORCID-ID: orcid.org/0000-0002-0041-6140
Received: 31.10.2020, Accepted: 07.12.2020

Bulgular: Üç yüz doksan üç anketin analizi Sağlık Bakanlığı/hükümet açıklamaları, internet (bilimsel kaynaklar) ve medyanın bilgi almak için en çok tercih edilen kaynak (sırasıyla; %96,7; %89,6 ve %84) olduğunu göstermiştir. Katılımcılar tarafından en çok aranan başlığın "COVID-19'a karşı korunma yolları" olduğu bulunmuştur (%96,9). Türkiye'de COVID-19 tedavisinde kullanım için katılımcılar tarafından en çok yazılan iki ilacın adının hidroksiklorokin ve azitromisin (sırasıyla; %57,5; %50,1) olduğu tespit edilmiştir. Medyadan bilgi alan katılımcıların hastalara/müşterilere COVID-19'a karşı kişisel korunma önlemleri (%83,3) ve COVID-19 semptomları (%78,8) konusunda daha az eğitim verdiği; ancak eczane personelinin yetiştirilmesi konusundaki davranışlarının bunun tam tersi olduğu görülmüştür. COVID-19 salgın süreci ile ilgili olarak katılımcıların yaklaşık yarısının (%46,6) en çok T.C. Sağlık Bakanlığı'na güvendiği tespit edilmiştir.

Sonuç: Medya ve diğer kaynaklar eczacıların bilgi, davranış ve izlenimlerini etkilemektedir. Yüksek düzeyde bilgi sahibi olmak, insanların davranışlarını olumlu yönde etkilemektedir. Eczacıların COVID-19 hakkında doğru bilgiye sahip olmaları ve edindikleri bilgileri topluma aktarmaları ve COVID-19'un yayılmasını önlemek ve kontrol altına almak için hasta eğitimi vermeleri önemlidir.

Anahtar kelimeler: COVID-19, pandemi, serbest eczacılar, bilgi, tutum

INTRODUCTION

In December 2019, the pathogen named as the novel coronavirus caused an outbreak of Coronavirus disease-2019 (COVID-19) in Wuhan, Hubei Province, China.[1] The virus was highly infectious, spreading rapidly via human-to-human transmission.[2] Consequently, COVID-19 spread rapidly from the first epicenter, the city of Wuhan, into neighboring countries and was declared a global pandemic by the World Health Organization (WHO). The pathogen was then renamed novel severe acute respiratory syndrome-coronavirus 2 (SARS-CoV-2).[2,3]

Common signs of SARS-CoV-2 infection include respiratory symptoms, fever, cough, shortness of breath, and breathing difficulties. In more severe cases, infection can cause pneumonia, SARS, organ failure, and even death.[1] As of October 20th 2020, SARS-CoV-2 had caused 40,693,256 infections and 1,123,596 deaths worldwide, and there were still no effective vaccine products or drugs to prevent and treat COVID-19 infection.[4] (https://www.worldometers.info/coronavirus/?utm_campaign = homeAdvegas1?#countries).

Pharmacists have always been the initial point of contact for healthcare delivery and have played important roles during pandemics and viral epidemics. These comprise vaccination, drug delivery, health training, and supplying direct patient care in the case of extraordinary circumstances, such as throughout the H1N1 pandemic.[5,6] In addition, it was determined that cases with suspected COVID-19 applied to nearby health centers, such as pharmacies, for medical assistance.[7] For this reason, to prevent and control the disease, it is vital that sufficient knowledge and awareness be created among pharmacists about the pandemic and that the factors directing their perceptions and behaviors be identified.[8]

Since the first day of the outbreak, COVID-19 has been widely covered in the news media, press, and social media.[8] It has been observed that the media assists both healthcare professionals and the general public in acquiring information to improve their knowledge, awareness, and implementation.[9] The media also plays an important part in communication among investigators, scientists, general health experts, and funding organizations for an efficient and swift global response.[9,10] This research aimed to assess the knowledge and attitudes of community pharmacists about COVID-19 and the role of the media and other factors in shaping pharmacists' knowledge, perception, and attitudes during the COVID-19 pandemic.

MATERIALS AND METHODS

This is a cross-sectional study based on a self-report questionnaire. The study was conducted between May 2020 and July 2020 during the quarantine period. As it was not feasible to conduct a population-based survey at that time, a questionnaire was designed on Google forms, and a link was shared using social media applications to invite community pharmacists from all over Turkey to participate in the study. Prior to their participation, pharmacists were given information about the aim and description of the study and informed that their attendance would be anonymous and voluntary, and that their data will be treated as confidential. The mean completion duration of the questionnaire was 13 minutes. Ethical approval to conduct the study was obtained from Acıbadem Mehmet Ali Aydınlar University and Acıbadem Healthcare Institutions Medical Research Ethics Committee (reference number: 2020-15/18). All procedures performed in the study involving human participants followed the ethical standards of the institutional research committee and the 1964 Helsinki Declaration.

The questions in this survey were formed using the guideline [Survey tool and guidance: Behavioral insights on COVID-19 (2020)] created by the WHO, a guide (COVID-19 Guide) composed by the Turkish COVID-19 Scholarly Commission, and the COVID-19 data made public on the Ministry of Health internet site.[11] (https://hsgm.saglik.gov.tr/tr/bulasici-hastaliklar/2019-n-cov.html). The participants' names and surnames were not included in the survey, and the data were collected anonymously. Age, gender, education level, years of experience in the profession, and location and city of their pharmacy were collected as demographic data. The names of the medications that are being used in Turkey for the treatment of COVID-19 were requested to gain an understanding of participants' interest in the treatment of COVID-19 (open-ended, no-option questions). Twenty-nine other multiple-choice questions were about information resources, knowledge, opinions, impressions, and behaviors regarding COVID-19. Participants were instructed to choose a single reply for 9 questions on the questionnaire and multiple replies for the other 14 questions. The questionnaire

also included six true/false questions. For each question, the option "other" was presented as an option, and if this option was selected, an explanation was expected. A total of 26,759 community pharmacists are available in Turkey. (https://dergi.tebeczane.net/public_html/kitaplar/bilgilendirmekitapcigi/html5/index.html?&locale=TRK&pn = 21). The sample size was calculated as 379 participants with a 95% confidence level and 5% margin of error.

Statistical analysis

Analysis was performed using SPSS version 22.0 (Armonk, NY; IBM Corp.). All data were considered statistically significant at $p<0.05$ and with a 95% confidence interval. Percentage, mean with standard deviation, median, and minimum-maximum were used for descriptive data. Chi-square tests were used in the analysis of categorical data.

RESULTS

A total of 393 pharmacists participated in this research. The majority of the participants were female (n=262, 66.7%), and their ages varied from 30 to 39 (n=139, 35.3%). In all, 68.7% (n=270) of the pharmacies were outside of Istanbul. Demographic characteristics of the participants are presented in Table 1.

In all, 58.5% (n=230) of participants declared that the origin of the infection is not known definitively, and 66.9% (n=263) of participants stated that the incubation period of COVID-19 is 14 days (Table 2). In all, 62.8% (n=247) of participants expressed that COVID-19 is a vaccine-preventable disease (Table 3), and 38.7% (n=152) of participants specified that a vaccine will be found within 6-12 months and that it will accelerate the end of the pandemic (Table 4).

Nearly all the participants obtained their information from Ministry of Health/government statements (n=380, 96.7%). The internet (scientific sources) was the second most popular source (n=352, 89.6%), and the media was the third most popular source (n=330, 84%) (Table 5). "Ways to be protected against COVID-19" was the most searched title (n=381, 96.9%). In all, 89.3% (n=351) of participants declared that they had made arrangement(s) in their pharmacies to maintain a physical distance of at least 1-2 m between patients. In all, 77.9% (n=306) of participants had given training to pharmacy staff, and 68.4% (n=269) of the participants had given training to patients/customers about COVID-19 (Table 5).

Participants' knowledge and behaviors toward COVID-19 infection were evaluated in accordance with the first three most preferred sources from which they obtained information

Table 1. Demographic characteristics of the participants

Parameters		n (%)
Gender	Female	262 (66.7)
	Male	131 (33.3)
Age	20-29 years	82 (20.9)
	30-39 years	139 (35.3)
	40-49 years	90 (22.9)
	50-59 years	71 (18.1)
	≥60 years	11 (2.8)
Education level	License	291 (74)
	Master's degree	86 (21.9)
	PhD	16 (4.1)
Professional experience duration	<5 years	98 (25)
	5-10 years	41 (10.4)
	11-20 years	120 (30.5)
	>20 years	134 (34.1)
Location of the pharmacy	District pharmacy	141 (35.9)
	Opposite the health center	157 (39.9)
	Opposite the hospital	78 (19.8)
	Bazaar pharmacy	17 (4.4)
City where the pharmacy is located	İstanbul	123 (31.3)
	Out of İstanbul	270 (68.7)

about COVID-19 infection and statistically significant results were obtained only for the issues specified below.

When the behaviors of the pharmacists "who received information from Ministry of Health/government declarations" and "those who did not" were compared, statistically significant differences were determined in the following:

- Their faith in the protection from COVID-19 offered by the use of a surgical mask (88.4% and 69.2%, respectively p=0.038);
- Their knowledge about airborne transmission of the infection (84.5% and 61.5%, respectively; p=0.028); their knowledge about transmission of the infection through surface contact (95.8% and 76.9%, respectively; p=0.002);
- Their perception that the health of people over 60 years will be the most adversely affected if they are infected with COVID-19 (93.4% and 76.9%, respectively; p=0.023);
- Their belief that covering the mouth and nose with a disposable tissue would protect against the infection (27.6% and 61.5%, respectively; p=0.008);

Table 2. Knowledge questions about COVID-19 disease

Questions	Answers*	n (%)
What is the original source of the infection?	It is not known clearly	230 (58.5)
	Bats	86 (21.9)
	Humans	34 (8.7)
	Other (artificial-produced in the laboratory)	43 (10.9)
How long is the incubation period of COVID-19?	2-4 days	104 (26.5)
	14 days	263 (66.9)
	15-28 days	26 (6.6)
What is the mortality rate from COVID-19?	0-1%	25 (6.4)
	1.1-5%	278 (70.7)
	5.1-10%	78 (19.8)
	10.1-25%	5 (1.3)
	>25%	7 (1.8)
In your opinion, which of the following is the most correct approach about using masks?	Only those who are sick should wear a mask	17 (4.3)
	Everyone in society should wear a mask	372 (94.7)
	Only healthcare professionals should wear a mask	1 (0.3)
	Only people in the risk group (over 60 years, pregnant, etc.) should wear a mask	3 (0.8)
At least how many seconds should hands be washed with soap and water?	20 seconds	244 (62.1)
	30 seconds	90 (22.9)
	45 seconds	30 (7.6)
	1 minute	29 (7.4)

*Only one option was chosen. COVID-19: Coronavirus disease-2019

Table 3. The approach of the participants to true-false knowledge questions about the COVID-19

Proposal	True, n (%)	False, n (%)
Alcohol-based hand sanitizer compensates for washing hands with soap and water	154 (39.2)	239 (60.8)
Soap used to protect against COVID-19 must contain antiseptic	35 (8.9)	358 (91.1)
There is a possibility of transmission of SARS-CoV-2 infection from products from China	204 (51.9)	189 (48.1)
COVID-19 is a vaccine-preventable disease	247 (62.8)	146 (37.2)
Once the person with the COVID-19 infection recovers, they are immune and will not be able to become infected with COVID-19 again	82 (20.9)	311 (79.1)
Even if COVID-19 is treated successfully, it leaves sequelae in patients	270 (68.7)	123 (31.3)

COVID-19: Coronavirus disease-2019, SARS-CoV-2: Severe acute respiratory syndrome-coronavirus 2

Table 4. The participants' impressions on the COVID-19 pandemic process

Questions	Answers*	n (%)
When do you think the pandemic will end?	When the air temperature rises	4 (1.0)
	Within 1-2 months	4 (1.0)
	Within 6-12 months	90 (22.9)
	Within 1-2 years	178 (45.3)
	Within 2-5 years	82 (20.9)
	Within 5-10 years	4 (1.0)
	After 10 years	1 (0.3)
	It will not end	30 (7.6)
Which of the following best describes your thoughts about the COVID-19 vaccine?	I think the vaccine will be found within 6 months, and it will accelerate the end of the pandemic	38 (9.7)
	I think the vaccine will be found within 6 months, but it will not affect the course of the pandemic	18 (4.6)
	I think the vaccine will be found within 6-12 months and it will accelerate the end of the pandemic	152 (38.7)
	I think the vaccine will be found within 6-12 months, but it will not affect the course of the pandemic	40 (10.2)
	I think the vaccine will not be found within 12 months	140 (35.6)
	Vaccine found but not given	5 (1.3)
Which of the following institutions do you trust the most regarding the COVID-19 pandemic process?	T.C. Ministry of Health	183 (46.6)
	World Health Organization	112 (28.5)
	U.S. Food & Drug Administration	27 (6.9)
	Turkish Pharmacists' Association	8 (2)
	International Pharmaceutical Federation	63 (16)
How much do you trust to the source(s) from which you learn about COVID-19?	<10%	27 (6.9)
	10-50%	92 (23.4)
	50%	106 (27)
	50-75%	115 (29.3)
	75-99%	53 (13.5)

*Only one option was chosen. COVID-19: Coronavirus disease-2019

- Their use of behavioral practices to protect themselves against COVID-19 by pouring disinfectant and/or cologne on their hands frequently (94.2% and 76.9%, respectively; p=0.012); washing/wiping everything bought from the outside before bringing it into the home (68.2% and 38.5%, respectively; p=0.025); and not going places such as the market unless absolutely necessary (95% and 76.9%, respectively; p=0.005);
- Their use of behavioral practices to protect against the infection and prevent its spread by putting a plastic shield in front of the existing distribution area in the pharmacy (65.8% and 38.5%, respectively; p=0.042).

When the behaviors of the pharmacists "who used the internet (scientific sources) as an information resource" and "those who did not" were compared, statistically significant differences were determined in the following:

- Their behavioral practice of researching information regarding patient education concerning COVID-19 (79% and 53.7%, respectively p=0.000);
- Their behavioral practice of using a mask while traveling (87.5% and 73.2%, respectively; p=0.012); in crowded environments (100% and 85.4%, respectively p=0.000); while working (95.5% and 68.3%, respectively p=0.000); while wandering the street (90.6% and 56.1%, respectively p=0.000); on public transport (99.1% and 85.4%, respectively p=0.000); whenever leaving home (75% and 41.5%, respectively p=0.000); and all the time (49.7% and 41.5%, respectively p=0.000);
- Their knowledge about transmission of the infection through shaking hands (94.6% and 85.4%, respectively; p=0.002); through sexual intercourse (52% and 34.1%, respectively; p=0.031); and from mother to baby during childbirth (58.2% and 36.6%, respectively; p=0.008);

Table 5. Knowledge and attitude questions about COVID-19 disease

Questions	Answers*	n (%)
From which sources do you get information about COVID-19?	Media (TV, newspaper, magazine)	330 (84)
	Internet (non-scientific sources)	165 (42)
	Internet (scientific sources)	352 (89.6)
	Social media	283 (72)
	Training sessions/scientific meetings	255 (64.9)
	Friends/family	230 (58.5)
	Ministry of Health/government statements	380 (96.7)
Which topics are you researching regarding COVID-19?	Symptoms of COVID-19	368 (93.6)
	Scientific progresses regarding COVID-19 vaccine	266 (67.7)
	Scientific progresses regarding COVID-19 treatment	353 (89.8)
	Patient education	300 (76.3)
	Ways to be protected against COVID-19	381 (96.9)
In which(s) of the following situations do you use a mask for COVID-19?	I use a mask while traveling	338 (86)
	I use a mask when in crowded environments	387 (98.5)
	I use a mask while at work	364 (92.6)
	I use a mask while wandering the street	342 (87)
	I use a mask in public transport	384 (97.7)
	I use a mask every time I leave home	281 (71.5)
	I use a mask all the time	192 (48.9)
Which(s) of the following do you use to protect yourself from COVID-19 during working hours in the pharmacy?	Fabric mask	43 (10.9)
	Surgical mask	345 (87.8)
	N95 mask	125 (31.8)
	Face shield	168 (42.7)
	Glasses	143 (36.4)
	Glove	154 (39.2)
In which way(s) is COVID-19 transmitted?	It is transmitted by airborne	329 (83.7)
	Kissing	393 (100)
	Shaking hands	368 (93.6)
	Surface contact	374 (95.2)
	It is transmitted by blood	195 (49.6)
	During sexual intercourse	197 (50.1)
	From mother to baby during childbirth	220 (56)
What are the symptom(s) of COVID-19?	Fever	393 (100)
	Cough	392 (99.7)
	Dyspnea	390 (99.2)
	Pneumonia	324 (82.4)
	Runny nose	122 (31)
	Kidney failure	68 (17.3)
	Diarrhea	326 (83)
	Bleeding	45 (11.5)
	Sudden loss of consciousness	108 (27.5)
	Asymptomatic	296 (75.3)
	Headache	328 (83.5)

Table 5.continued

Questions	Answers*	n (%)
In case of infection with COVID-19, which person(s)' health will be affected most negatively?	People over 60 years	365 (92.9)
	People with serious chronic diseases such as hypertension, diabetes	380 (96.7)
	Children	67 (17)
	Pregnant women	219 (55.7)
	Young adults	33 (8.4)
	Health workers	198 (50.4)
	Other	4 (1)
Which should be applied to protect from COVID-19?	Washing hands with soap and water	393 (100)
	Avoiding contact with sick people	390 (99.2)
	Using hand sanitizer	375 (95.4)
	Using a N95 mask	96 (24.4)
	Using a surgical mask	380 (96.7)
	Wearing protective clothing	104 (26.5)
	Wearing protective glasses	177 (45)
	Covering the mouth and nose with a disposable tissue	113 (28.8)
	Using medical gloves	114 (29)
What behaviors do you implement to protect against COVID-19?	I wash my hands more often than ever	376 (95.7)
	I frequently pour disinfectant and/or cologne on my hands	368 (93.6)
	I try to touch less frequently surfaces where other people touch	389 (99)
	I take a bath everyday	267 (67.9)
	I wash/wipe everything I bought from the outside before putting it to home	264 (67.2)
	I try to stay away from people who are coughing/sneezing	390 (99.2)
	Except for compulsory situations, I do not go places such as the market	371 (94.4)
	I reduce my use of public transport	378 (96.2)
	I use vitamin supplements	320 (81.4)
Which can prevent COVID-19?	Rinsing the nose with saline	125 (31.8)
	Using vinegar	98 (24.9)
	Consuming ginger	111 (28.2)
	Consuming turmeric	117 (298)
	Consuming echinacea	145 (36.9)
	Consuming vitamin C	345 (87.8)
	Consuming vitamin D	330 (84)
To protect against COVID-19 and prevent its spread, which(s) of the precautions do you apply in your pharmacy?	I change the apron I wear in the pharmacy every day	176 (44.8)
	I placed a plastic shield in front of the existing distribution area in the pharmacy	255 (64.9)
	I made arrangement(s) to keep a distance of at least 1-2 meters between patients	351 (89.3)
	We disinfect the drugs coming from the drug storage before placing them on the shelves	98 (24.9)
	After each patient/customer, we wipe and disinfect the pharmacy counter	223 (56.7)
	After serving each patient/customer, we disinfect our hands with an alcohol-based solution	337 (85.8)

Table 5.continued

Questions	Answers*	n (%)
Have you given training to your pharmacy staff about the COVID-19?	I did not give training	87 (22.1)
	I gave training on personal protection precautions against COVID-19	351 (89.3)
	I gave training on the correct use of masks	320 (81.4)
	I gave training on COVID-19 transmission routes	332 (84.5)
	I gave training about the symptoms of COVID-19 infection	329 (83.7)
Have you given training to your patients/customers about the COVID-19?	I did not give training	124 (31.6)
	I gave training on personal protection precautions against COVID-19	334 (85)
	I gave training on the correct use of masks	326 (83)
	I gave training on COVID-19 transmission routes	315 (80.2)
	I gave training about the symptoms of COVID-19 infection	318 (80.9)

*More than one option was chosen. COVID-19: Coronavirus disease-2019

- Their knowledge about symptoms of the infection is as follows: pneumonia (87.3% and 70%, respectively; p=0.00);
- Their knowledge about people whose health will be most adversely affected if infected with COVID-19 is as follows: Young adults (9.4% and 0%, respectively; p=0.041);
- Their belief in protecting against COVID-19 by using hand sanitizer (96.6% and 85.4%, respectively; p=0.001);
- Their behaviors protecting against COVID-19 by pouring disinfectant and/or cologne on their hands frequently (95.5% and 78%, respectively; p=0.000); trying to touch less often where others touch (99.4% and 95.1%, respectively; p=0.009); having a bath everyday (70.2% and 48.8%, respectively; p=0.005);
- Their knowledge on interception of the infection with using vinegar (22.7% and 43.9%, respectively; p=0.003); consuming ginger (25.9% and 48.8%, respectively; p=0.000); consuming echinacea (33.5% and 65.9%, respectively; p=0.000);
- Their behavioral practices to protect themselves from the infection and prevent its spread by disinfecting their hands with an alcohol-based solution after serving each patient/customer (87.2% and 73.2%, respectively; p=0.015);
- Their behavioral practices in training pharmacy staff regarding personal protection precautions against COVID-19 (91.5% and 70.7%, respectively; p=0.000); regarding correct use of masks (84.1% and 58.5%, respectively; p=0.000); and regarding COVID-19 transmission routes (86.6% and 65.9%, respectively; p=0.001);
- Their behavioral practices in training patients/customers regarding the correct use of masks (84.9% and 65.9%, respectively; p=0.002); regarding symptoms of COVID-19 infection (82.4% and 68.3%, respectively; p=0.030).

When the behaviors of the pharmacists "who received information through the media" and "those who did not" were compared, statistically significant differences were detected in the following:

- Their attitudes in researching information regarding patient education concerning COVID-19 (73% and 93.7%, respectively p=0.000);
- Their behavior in using a mask while working (93.9% and 85.7%, respectively p=0.022);
- Their faith in protection from COVID-19 by fabric mask use (12.7% and 1.6%, respectively p=0.009) and by surgery mask use (89.4% and 79.4%, respectively p=0.026);
- Their knowledge on transmission of the infection via surface contact (96.4% and 88.9%, respectively; p=0.011); through sexual intercourse (46.4% and 69.8%, respectively; p=0.001);
- Their knowledge on the symptoms of COVID-19 is as follows: bleeding (8.8% and 25.4%, respectively; p=0.014); headache (81.5% and 93.7%, respectively; p=0.018);
- Their knowledge about people whose health will be most adversely affected if they are infected with COVID-19 is as follows: People over 60 years (94.2% and 85.7%, respectively; p=0.016); young adults (6.4% and 19%, respectively; p=0.001);
- Their belief in protecting against the infection by using an N95 mask (27% and 11.1%, respectively; p=0.007);
- Their behaviors in protecting against COVID-19 by washing hands more than ever (97% and 88.9%, respectively; p=0.004); by pouring disinfectant and/or cologne on their hands frequently (94.8% and 87.3%, respectively; p=0.025); trying out to touch less often where others touch (99.4% and 95.1%, respectively; p=0.009); washing/wiping everything bought from the outside before bringing it into the home (69.4% and 55.6%, respectively; p=0.032); reducing the use of public transport (97.9% and 87.3%, respectively; p=0.000);

- Their knowledge on interception of the infection by rinsing the nose with saline (35.2% and 14.3%, respectively; p=0.001); using vinegar (28.8% and 4.8%, respectively; p=0.000); and consuming turmeric (31.8% and 19%, respectively; p=0.042);
- Their behavioral practices in protecting themselves from the infection and preventing its spread by changing the apron they wear in the pharmacy every day (48.2% and 27%, respectively; p=0.002);
- Their behavioral practices in training pharmacy staff regarding COVID-19 transmission routes (87% and 71.4%, respectively; p=0.002); regarding symptoms of COVID-19 infection (85.8% and 73%, respectively; p=0.012);
- Their behavioral practices in training patients/customers regarding personal protection precautions against COVID-19 (83.3% and 93.7%, respectively; p=0.036); regarding correct use of masks (80.9% and 93.7%, respectively; p=0.014); regarding symptoms of COVID-19 infection (78.8% and 92.1%, respectively; p=0.014).

Participants were asked to write the names of three drugs that were being used for the treatment of COVID-19 in Turkey. Hydroxychloroquine (n=226, 57.5%) was the most widely mentioned drug. In the second place, azithromycin (n=197, 50.1%) was the most often named drug, followed by oseltamivir (n=166, 42.2%). In all, 9.8% (n=38) of the participants declared that they did not know the name of the drug (Table 6).

Table 6. Participants' responses regarding the names of drugs used in the treatment of COVID-19

Name of the drug	n (%)
I do not know	38 (9.8%)
Hydroxychloroquine	226 (57.5%)
Azithromycin	197 (50.1%)
Oseltamivir	166 (42.2%)
Favipiravir	87 (22.1%)
Enoxaparin	76 (19.3%)
Paracetamol	72 (18.3%)
Clarithromycin	43 (10.9%)
Tocilizumab	42 (10.7%)
Vitamin C	35 (8.9%)
Ritonavir + lopinavir	33 (8.4%)
Ritonavir	21 (5.3%)
Remdesivir	15 (3.8%)
Vitamin D	15 (3.8%)
Doxycycline	12 (3.1%)
Acetylcysteine	9 (2.3%)
Ivermectin	3 (.8%)
Heparin	3 (.8%)
Gemifloxacin	3 (.8%)
Diosmin + hesperidin	2 (.5%)

COVID-19: Coronavirus disease-2019

DISCUSSION

This study aimed to evaluate the knowledge and attitudes of community pharmacists about COVID-19 and the role of the media and other factors in shaping pharmacists' knowledge, perception, and attitudes during the COVID-19 pandemic.

Community pharmacists have always been the most accessible healthcare providers. The fact that they continue to ensure direct patient care despite restrictions implemented by the government because of the pandemic is another indication of this.[12] Community pharmacists have fulfilled a variety of responsibilities in sustaining the health system during COVID-19: Administering medication to patients, training patients, evaluating patients for renewal of chronic medication prescriptions, conducting counseling on minor illnesses, explaining misunderstandings about COVID-19 treatments, creating community cognizance regarding COVID-19, prevention methods, risk elements, signs, and symptoms.[12,13] Although these services vary among pharmacists, there is a relationship between the resources used and the knowledge, attitudes, and perceptions of the pharmacists about COVID-19 disease and treatment.[12]

In this study, it was determined that the participants generally preferred to obtain information from Ministry of Health/government statements, the internet (scientific sources), and the media. It was identified that the resource from which the participants ascertained information about COVID-19 and related topics has a significant impact on their knowledge and behaviors toward COVID-19 disease.

Pharmacists who used the internet (scientific sources) as an information resource had the correct approaches, particularly in terms of behaviors that offered protection from the disease (such as trying to touch less often where others touch, pouring disinfectant, and/or cologne on their hands frequently, using a mask on public transport, using a mask while traveling, working, wandering the street, using a mask in populous places). The pharmacists that obtained information from Ministry of Health/government statements also had the correct approaches to protection from the infection (such as pouring disinfectant and/or cologne on their hands frequently, not going places such as the market except when absolutely necessary, using a surgical mask). The participants that obtained information from media also had the correct approaches to protection from the illness (such as washing hands more than usual, pouring disinfectant and/or cologne on their hands frequently, trying to touch less often where others touch, reducing the use of public transport, using a mask while working, using a surgical mask). However, the participants that obtained information from the household/peers had incorrect approaches, chiefly in prevention of the infection (such as using vinegar, consuming turmeric).

Similar results to our findings were found in a study conducted to assess knowledge and attitudes of hospital pharmacists

about COVID-19. It was determined that the information resource from which the participants learned about COVID-19 and related information has a significant impact on their knowledge and behaviors toward COVID-19 disease. In addition, pharmacists that obtained information from the internet (scientific sources) had the correct approaches, whereas participants that obtained info from the household/peers had incorrect approaches, chiefly regarding interception of the illness.[14]

The participants that obtained their information from the internet (non-scientific sources) had incorrect approaches, particularly with respect to contamination by the infection (such as via blood), interception of the illness (such as consuming turmeric), and protection against the disease (such as eyeglasses and glove use). However, WHO declared that there is no scientific evidence that consuming turmeric prevents COVID-19 (https://www.who.int/southeastasia/outbreaks-and-emergencies/novel-coronavirus-2019/fact-or-fiction). In addition, WHO does not recommend using gloves. The wearing of gloves may increase the risk of infection, since it can lead to self-contamination or transmission to others when touching contaminated surfaces and then the face (https://www.who.int/emergencies/diseases/novel-coronavirus-2019/question-and-answers-hub/q-a-detail/q-a-on-covid-19-and-masks).

Some misleading information, such as washing the nose with saline or consuming it has been recommended by some doctors or certain leading people on television programs in Turkey.[14] Although these explanations were objected to and corrected by other doctors and professionals, the fact that some pharmacists preferred these applications (especially washing the nose with saline) reveals the powerful effect of the press.

In this study it was also found that the participants' attitudes differed according to the sources from which they learned about COVID-19.

It was determined that the participants who received information from social media gave less training to pharmacy staff and patients/customers about personal protection measures against COVID-19, correct use of masks, modes of COVID-19 transmission, and COVID-19 symptoms. It was determined that participants who received information from the media provided less training to patients/customers on personal protection measures against COVID-19, correct use of masks, and COVID-19 symptoms; however, it was observed that their behavior in training pharmacy staff was just the opposite of this. On the other hand, it was determined that participants who used the internet (scientific sources) and obtained information from educational/scientific meetings provided more education both to pharmacy staff and to patients/customers about personal protection measures against COVID-19, correct use of masks, modes of COVID-19 transmission, and COVID-19 symptoms.

Although there is no vaccine application as of yet, many vaccine studies are in progress, and it is hoped that COVID-19 will be prevented by vaccination in the future.[15,16] Even though no vaccine is available at present, more than half of the pharmacists in this study expressed that vaccination can prevent COVID-19, which might be owing to extrapolation of the knowledge of other flu-like viral diseases. Most of the participants also stated that a vaccine will be developed within 6-12 months, and it will accelerate the end of the pandemic. On the other hand, 84.2% of participants stated that a drug being developed for the treatment of COVID-19 will reduce death rates due to COVID-19, whereas 73.5% of participants believed that the drug can be put up for sale without sufficient clinical studies. Many medications are being tested for the treatment of COVID-19, and the effects of these medications have been proven by some observational studies.[15,17] Some of these medications are antiretroviral drugs. In this study, more than half of the pharmacists were aware of this information.

Even though no medication has been discovered for the treatment of COVID-19 as yet, nearly all of the participants stated the names of drugs that are being used in Turkey for the treatment of COVID-19. Thus, it is understood that nearly all the participants are aware of the drugs currently being used for the treatment of COVID-19, whereas it is seen that 9.8% of the participants have no interest in this issue.

In this study it was also determined that approximately half of the participants trust the T.C. Ministry of Health the most regarding the COVID-19 pandemic process, followed by the WHO in second place. Most of the participants stated that their level of trust in the source(s) from which they obtain information about COVID-19 was between 50% and 75%.

Study limitations

This study has several limitations. The study participants were only recruited from Turkey; therefore, this study only reflects the attitudes and behaviors of community pharmacists in Turkey. The participants in this study were only a part of community pharmacists, and for this reason, the generalizability of the study sample may be limited. However, the study participants were from different cities in Turkey, and this constitutes one of the strengths of the study. Although the study results reflect pharmacists' answers from all over Turkey, not only a part of Turkey, to gain a better understanding of community pharmacists' knowledge, attitudes, and impressions about COVID-19, a wider-scale study should be performed.

CONCLUSION

The media and other sources used to obtain information affect pharmacists' knowledge, behavior, and impressions. Having a high level of knowledge positively affects people's behavior. It is also important both for the society and for themselves that pharmacists have accurate information about COVID-19 and increase their own level of knowledge. It should be the responsibility of pharmacists, who are the health profession in the closest contact with the public, to transfer the knowledge they have acquired to society by reflecting it in their behaviors and to provide patient education in order to prevent and control the spread of COVID-19.

Conflict of interest: No conflict of interest was declared by the authors. The authors are solely responsible for the content and writing of this paper.

REFERENCES

1. Han Q, Lin Q, Jin S, You L. Coronavirus 2019-nCoV: A brief perspective from the front line. J Infect. 2020;80:373-377.
2. Liu S, Luo P, Tang M, Hu Q, Polidoro JP, Sun S, Gong Z. Providing pharmacy services during the coronavirus pandemic. Int J Clin Pharm. 2020;42:299-304.
3. Al-Qahtani AA. Severe acute respiratory syndrome coronavirus 2 (SARS-CoV-2): emergence, history, basic and clinical aspects. Saudi J Biol Sci. 2020;27:2531-2538.
4. Balla M, Merugu GP, Patel M, Koduri NM, Gayam V, Adapa S, Naramala S, Konala VM. COVID-19, Modern pandemic: a systematic review from front-line health care providers' perspective. J Clin Med Res. 2020;12:215-229.
5. Miller S, Patel N, Vadala T, Abrons J, Cerulli J. Defining the pharmacist role in the pandemic outbreak of novel H1N1 influenza. J Am Pharm Assoc. 2012;52:763-767.
6. Chin TWF, Chant C, Tanzini R, Wells J. Severe acute respiratory syndrome (SARS): the pharmacist's role. Pharmacotherapy. 2004;24:705-712.
7. World Health Organisation (WHO). Infection prevention and control during health care when novel coronavirus (nCoV) infection is suspected. 2020. Available from. file:///Users/batti/Downloads/WHO-2019-nCoV-IPC-2020.3-eng.pdf.
8. Karasneh R, Al-Azzam S, Muflih S, Soudah O, Hawamdeh S, Khader Y. Media's effect on shaping knowledge, awareness risk perceptions and communication practices of pandemic COVID-19 among pharmacists. Res Social Adm Pharm. 2021;17:1897-1902.
9. Gralinski LE, Menachery VD. Return of the coronavirus: 2019-nCoV. Viruses. 2020;12:135.
10. Ippolito G, Hui DS, Ntoumi F, Maeurer M, Zumla A. Toning down the 2019-nCoV media hype - and restoring hope. Lancet Respir Med. 2020;8:230-231.
11. World Health Organisation (WHO). Survey tool and guidance: behavioural insights on COVID-19. Washington DC: World Health Organisation; 2020.
12. Elbeddini A, Prabaharan T, Almasalkhi S, Tran C. Pharmacists and COVID-19. J Pharm Policy Pract. 2020;13:36.
13. Mukattash TL, Jarab AS, Mukattash I, Nusair MB, Farha RA, Bisharat M, Basheti IA. Pharmacists' perception of their role during COVID-19: a qualitative content analysis of posts on Facebook pharmacy groups in Jordan. Pharm Pract (Granada). 2020;18:1900.
14. Kara E, Demirkan K, Unal S. Knowledge and attitudes of hospital pharmacist about COVID-19. Turk J Pharm Sci. 2020;17:242-248.
15. Li H, Zhou Y, Zhang M, Wang H, Zhao Q, Liu J. Updated Approaches against SARS-CoV-2. Antimicrob Agents Chemother. 2020;64:e00483.
16. Ahmed SF, Quadeer AA, McKay MR. Preliminary Identification of Potential Vaccine Targets for the COVID-19 Coronavirus (SARS-CoV-2) Based on SARS-CoV Immunological Studies. Viruses. 2020;12:254.
17. Sarma P, Prajapat M, Avti P, Kaur H, Kumar S, Medhi B. Therapeutic options for the treatment of 2019-novel coronavirus: an evidence-based approach. Indian J Pharmacol. 2020;52:1-5.

Turk J Pharm Sci 2021;18(5):541-549
DOI: 10.4274/tjps.galenos.2020.65047

ORIGINAL ARTICLE

Exploring the Solvent-Anti-solvent Method of Nanosuspension for Enhanced Oral Bioavailability of Lovastatin

Lovastatinin Gelişmiş Oral Biyoyararlanımı İçin Solvent-Anti-solvent Yöntemi ile Hazırlanan Nanosüspansiyon Formülasyonunun Araştırılması

Archana S. PATIL*, Riya HEGDE, Anand P. GADAD, Panchaxari M. DANDAGI, Rajashree MASAREDDY, Uday BOLMAL

Department of Pharmaceutics, KLE College of Pharmacy Belagavi, KLE Academy of Higher Education and Research Belagavi, Karnataka, India

ABSTRACT

Objectives: Lovastatin is an antilipidemic drug that belongs to the class of statins that has poor oral bioavailability due to its low solubility and variable dissolution rate. The main aim of this study was to enhance the solubility and dissolution rate of the drug and understand its oral bioavailability.

Materials and Methods: Lovastatin nanosuspension was formulated using a solventanti-solvent method using a probe sonication technique. A nanosuspension was prepared, using hydroxypropyl methylcellulose (HPMC) K15M and pluronic F68 as stabilizers. The formulated nanosuspensions were characterized for particle size, polydispersity index (PDI) zeta potential, surface morphology, and *in vitro* release rate. Further, an *in vivo* bioavailability study and stability studies were also performed.

Results: Optimized formulation showed a particle size of 127±0.01 nm, a PDI of 0.492±0.001, and a zeta potential of -37.9 mV, which indicates good stability. Morphological study showed that the particles were in the nano range. The drug content was found to be in the range of 73-87%. *In vitro* release revealed much faster release of the drug in one hour compared to the pure drug and its marketed formulation. *In vivo* bioavailability study was carried out in Wistar rats, which showed improvement in bioavailability by approximately 2.5 folds compared with the marketed formulation. Stability studies indicated that the optimized formulation F2 was more stable at 4˚C±2˚C.

Conclusion: The prepared lovastatin nanosuspension showed improvement in solubility, dissolution rate, and oral bioavailability compared to the pure drug and its marketed formulation. Hence, lovastatin nanosuspension may be a potentially valuable tool for improving the oral bioavailability of lovastatin.

Key words: Lovastatin, oral bioavailability, solubility, nanosuspension

ÖZ

Amaç: Lovastatin, düşük çözünürlüğü ve değişken çözünme hızı nedeniyle oral biyoyararlanımı zayıf olan statinler sınıfına ait antilipidemik bir ilaçtır. Bu çalışmanın temel amacı, ilacın çözünürlüğünü ve çözünme hızını artırmak ve oral biyoyararlanımını belirlemektir.

Gereçler ve Yöntemler: Lovastatin içeren nanosüspansiyon, bir prob sonikasyon tekniği kullanılarak solvent-anti-solvent yöntemi kullanılarak formüle edildi. Stabilizatör olarak hidroksipropil metilselüloz (HPMC) K15M ve pluronic F68 kullanılarak bir nanosüspansiyon hazırlandı. Formüle edilen nanosüspansiyonlar, partikül boyutu, polidispersite indeksi (PDI), zeta potansiyeli, yüzey morfolojisi ve *in vitro* salım profilleri belirlenerek karakterize edildi. Ayrıca, *in vivo* biyoyararlanım çalışması ve stabilite çalışmaları da gerçekleştirilmiştir.

Bulgular: Optimize edilmiş formülasyonun, partikül boyutu 127±0,01 nm, PDI değeri 0,492±0,001 ve zeta potansiyeli -37,9 mV olarak belirlendi, bu da formülasyonun iyi bir stabiliteye sahip olduğunu gösterdi. Morfolojik çalışma, partiküllerin nano aralıkta olduğunu gösterdi. İlaç içeriği %73-87 aralığında bulundu. *İn vitro* salım, saf ilaca ve ticari formülasyona kıyasla ilacın bir saat içinde çok daha hızlı salım profili gösterdiğini ortaya çıkardı. *İn vivo* biyoyararlanım çalışması Wistar sıçanlarında gerçekleştirildi ve nanosüspansiyon formülasyonunda ticari formülasyona kıyasla biyoyararlanımda yaklaşık 2,5 kat iyileşme olduğunu gösterdi. Stabilite çalışmaları, optimize edilmiş F2 formülasyonunun 4˚C±2˚C'de daha stabil olduğunu gösterdi.

***Correspondence:** archupharma@gmail.com, **Phone:** +91 9916883344, **ORCID-ID:** orcid.org/0000-0002-7458-8842

Received: 20.10.2020, **Accepted:** 14.12.2020

Sonuç: Hazırlanan lovastatin nanosüspansiyonu, saf ilaca ve ticari formülasyonuna kıyasla çözünürlük, çözünme hızı ve oral biyoyararlanım açısından gelişme göstermiştir. Bu nedenle, lovastatin nanosüspansiyonunun, lovastatinin oral biyoyararlanımını geliştirmek için potansiyele sahip olduğu sonucuna ulaşıldı.

Anahtar kelimeler: Lovastatin, oral biyoyararlanım, çözünürlük, nanosüspansiyon

INTRODUCTION

Oral route is the highly preferred route for administration of drugs as it provides high patient compliance.[1] A large number of drugs that are available in the market exhibit low oral bioavailability because of their low aqueous solubility and intrinsic dissolution rate. According to the Biopharmaceutical Classification System, drugs with poor aqueous solubility are classified either as class II or class IV drugs.[2] Poor aqueous solubility of the drugs results in low oral bioavailability, varying absorption rate, and inter/intrasubject proportionality.[3] Oral bioavailability of various drugs is also affected by another factor (i.e., poor gastrointestinal permeability). According to the literature, various techniques like solubilization, salt formation, micronization, change in physical form, use of prodrug and drug derivatives, addition of surfactants, and pH alteration have been utilized for improving the dissolution and bioavailability of the drugs having poor aqueous solubility.[4]

Nanotechnology has reshaped the field of drug delivery and research. Pharmaceutical nanoparticles are solid submicron sized (<100 nm in diameter) drug carriers that may or may not be biodegradable.[5] Types of nanoparticles that are applied in drug delivery include nanosuspensions, polymeric nanoparticles, and lipid nanoparticles. Nanosuspension is the colloidal dispersion of solid drug particles in a liquid phase having a particle size of <1 μm with an average particle size of 200-600 nm.[6] It consists of pure drug and stabilizers (surfactants or polymers). Their small particle size facilitates effective transportation of drug molecules to cells with an optimum therapeutic effect and reduced adverse effects.[7] The potential benefits of nanosuspension technology for poorly soluble drug delivery are increased drug dissolution rate, increased rate, and extent of absorption, and hence the bioavailability of drugs. The selection of a suitable stabilizer or surfactant as well as the manufacturing method may offer nanosuspension with highest stability for long-term storage. Nanosuspension may be formulated by a bottom-up or top-down approach.

Cardiovascular disease remains the leading cause of morbidity and mortality worldwide, and hyperlipidemia is a major factor contributing to its development.[8] Lovastatin is a cholesterol-lowering agent that has been isolated from a strain of *Aspergillus ferreus*. It is very effective and well tolerated by patients with moderate hypercholesterolemia. Lovastatin also manifests pharmacological activities of bone formation and chemoprevention. Due to its rapid metabolism in the gut and liver, lovastatin exhibits poor oral bioavailability of <5% and a shorter half-life of 2-5 h.[9] According to the literature, various attempts have been made to improve the aqueous solubility and bioavailability of lovastatin by preparing self-emulsifying drug delivery systems, nanostructured lipid carriers (NLC), and extended-release formulation by one-step melt granulation method. For instance, Sunil et al.[10], Jun and Daxin[11] and Gande et al.[12] prepared stabilized self-emulsifying drug delivery systems in the form of hydrogel, NLC, and solid lipid nanoparticles (SLN) of lovastatin, respectively, with an objective to enhance the solubility and bioavailability of lovastatin, but there are no comparative data of their formulation with the already existing marketed product to justify the enhancement in bioavailability of the drug.

Hence, attempts were made to improve solubility and oral bioavailability of lovastatin by formulating lovastatin nanosuspension via the solvent-anti-solvent method using probe sonication technique in this study. Further, nanosuspensions were evaluated for particle size, polydispersity index (PDI), zeta potential, drug content, an *in vitro* release study, *in vivo* bioavailability study, and stability study.

MATERIALS AND METHODS

Materials

Lovastatin was procured as a gift sample from Lupin Pharmaceuticals, Goa. Hydroxypropyl methylcellulose (HPMC) K15M was purchased from Yarrow Chem Products, Mumbai. Pluronic F68 was purchased from Ozone Pharmaceuticals, Mumbai. Acetone, Chloroform, Methanol, and Ethanol were purchased from Molychem, Mumbai. Dialysis membrane having a cutoff molecular weight between 12,000 and 14,000 Dalton was purchased from Hi Media.

Methods

Optimization of process parameters

Selection of a suitable solvent-anti-solvent ratio

Before proceeding toward formulation of the lovastatin nanosuspension, a solvent and anti-solvent were selected based on the solubility studies of drugs in different solvents. In the solvent-anti-solvent method, the selected solvent should be a water-miscible solvent and capable enough to dissolve the drug to a greater extent so that a clear solution is obtained. Conversely, the solvent in which the drug was least soluble or was completely insoluble was selected as an anti-solvent. As the drug exhibits maximum solubility in methanol, it was selected as a solvent, and water was selected as an anti-solvent since the drug was least soluble in water. Different ratios like 1:1, 1:2, 1:3, 1:4, and 1:5 were tried for formulating a nanosuspension. The ratio of solvent:anti-solvent that resulted in a production of nanosuspension with the best reproducible particle size, and PDI was selected as an optimized ratio.

Optimization of sonication time

Optimization of sonication time was done by sonicating the formulation for 2, 5, 10, 15, and 20 mins. Based on the best and reproducible results of particle size and PDI, an optimized sonication time was selected.

Selection of polymer and surfactant

A suitable polymer was selected by screening various polymers like HPMC K15M, HPMC K100M, and PVPK30. Based on the best and reproducible results of particle size, PDI, and the ability to inhibit crystal growth, a suitable polymer was selected. Various surfactants like pluronic F68, pluronic F127, and polyethylene glycol 6000 were tested to determine the surfactant effective in reducing the particle size of the drug.

Effect of flow rate

Particle size of the obtained nanosuspension was measured at varied flow rates of drug solution into polymer solution at 2-8 mL/min to select the optimum flow rate during the formulation of nanosuspension. All the process optimization parameters are depicted in Table 1.

Formulation of nanosuspension by solvent-anti solvent technique

Six formulations of (F1-F6) lovastatin nanosuspensions were prepared by the solvent-anti-solvent method using a probe sonication technique. Briefly, a specified amount of drug was completely dissolved in the water-miscible solvent (methanol). In another beaker, polymer/surfactant was added to the water (anti-solvent) and further sonicated till a clear polymeric solution was formed. The prepared drug solution was then added to the polymeric solution at a rate of 2 mL/min and maintained in an ice bath to prevent particle collision till precipitation occurred.[13-16] The quantities of ingredients used in the formulation are mentioned in Table 2, and the solvent-anti-solvent technique is depicted in Figure 1.

Evaluation of lovastatin-loaded nanosuspensions

Particle size analysis

The particle size of the prepared nanosuspension was determined using a dynamic light scattering (DLS) particle size analyzer. For analysis, the nanosuspension was diluted with Millipore water at a ratio of 1:5 and further sonicated for 2 min. Samples were analyzed in triplicate.[17]

Polydispersity index

PDI is also measured using a DLS particle size analyzer. The obtained PDI values give an idea about the particle size distribution of nanoparticles. Their values range from 0.000 to 1.000, which demonstrate that the lower the value, the narrower the size distribution of nanoparticles and vice versa.[18]

Table 1. Optimization of process parameters and their evaluation

Optimization of the solvent:anti-solvent ratio and sonication time				
Solvent (methanol):anti-solvent (water) ratio	1:1	1:2	1:3	1:4
Sonication time (min)	05	10	15	20
Particle size (nm)	1595	623	407	379
PDI	1.6	1.5	0.04	0.4
Effect of polymer on particle size and PDI				
Polymer	**Particle size (nm)**	**PDI**		
HPMC K15M	483	0.5		
HPMC K100M	1054	0.5		
PVP K30	1064	0.5		
Effect of a surfactant on particle size and PDI				
Surfactant	**Particle size (nm)**	**PDI**		
PEG 6000	1205	1.9		
Pluronic F127	926	0.4		
Pluronic F68	442	0.6		
Effect of flow rate on particle size and PDI				
Flow rate	**Particle size (nm)**	**PDI**		
2 mL/min	487	0.4		
4 mL/min	604	0.5		
6 mL/min	798	0.5		
8 mL/min	1023	0.6		

PDI: Polydispersity index, HPMC: Hydroxypropyl methylcellulose, PVP: Polyvinylpyrrolidone, PEG: Polyethylene glycol

Table 2. Formulation design of lovastatin nanosuspension using the solvent-anti-solvent method

Formulation number	Lovastatin (mg)	HPMC K15M (mg/mL)	Pluronic F68 (mg/mL)	Methanol (mL)	Water (mL)
F1	10	1.0	-	10	50
F2	10	1.5	-	10	50
F3	10	-	1.0	10	50
F4	10	-	1.5	10	50
F5	10	1.0	1.5	10	50
F6	10	1.5	1.0	10	50

HPMC: Hydroxypropyl methylcellulose

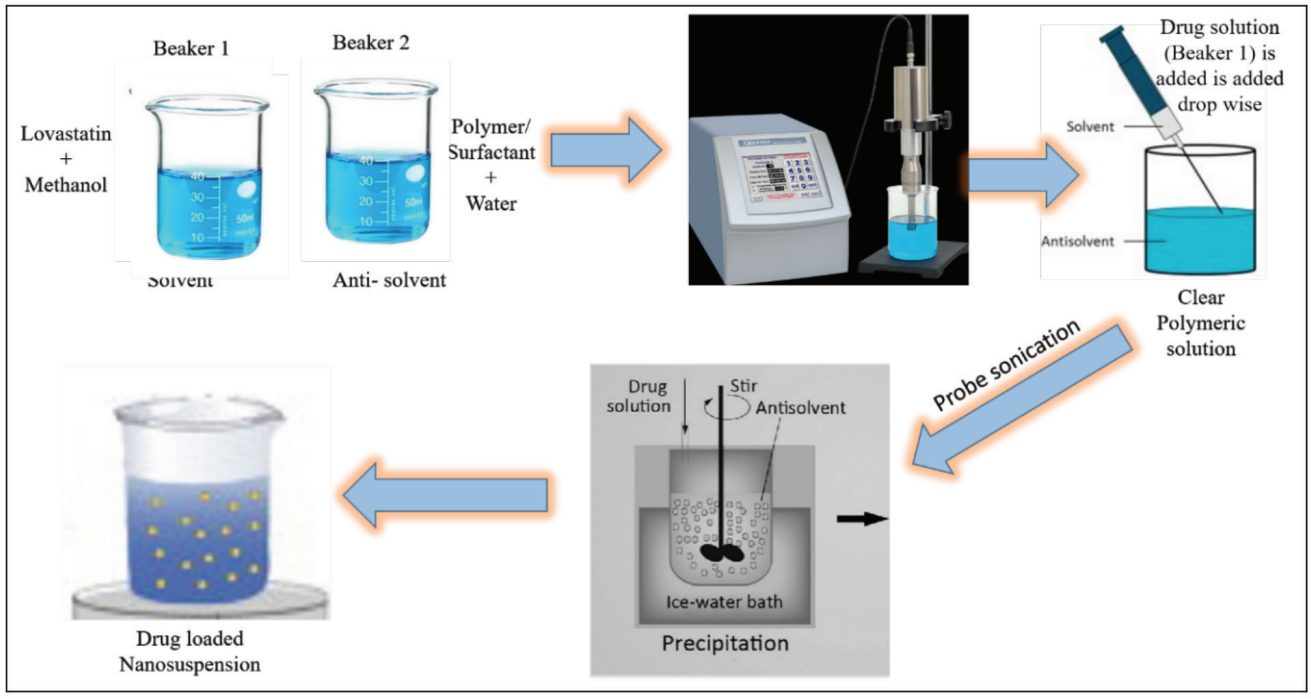

Figure 1. Formulation of nanosuspension by the solvent-anti-solvent technique

Drug content

Lovastatin nanosuspension was equivalent to 1 mg and was added to 10 mL of methanol; it was further diluted with a phosphate buffer up to 100 mL and stirred continuously for 2 h. It was subjected to ultracentrifugation at 15,000 rpm for 20 min. The supernatant was collected, suitably diluted, and analyzed spectrophotometrically at 238 nm.[19]

Zeta potential

A physical property exhibited by particles in suspension is zeta potential. It is used for the optimization of emulsions and suspensions as its knowledge reduces the number of trial formulations. It is also an important parameter to predict long-term stability.[20]

Transmission electron microscopy (TEM)

The external morphology of lovastatin nanosuspension was studied using TEM, and it was performed at SAIF, Cochin. Samples for TEM were prepared by initially diluting with Millipore water. Then, a drop of nanosuspension was kept on a copper grid (carbon coated) and stained with phosphotungstic acid. The grid was air dried and observed at different magnifications under TEM.[21]

In vitro drug release study

The *in vitro* drug release of lovastatin was performed using the dialysis bag diffusion technique. An accurately weighed quantity of nanosuspension (equivalent to 10 mg of the drug) was placed in a dialysis bag, and the bag was sealed. Then, the bag was suspended initially for 1 h in a basket containing 900 mL of pH 6.8 phosphate buffer. Aliquots of 5 mL of the sample were withdrawn at pre-determined intervals from the compartment, and the same amount was replaced by the fresh buffer. The sample was analyzed spectrophotometrically after suitable dilution by determining the absorbance at 238 nm.[22]

In vivo bioavailability study

Healthy Wistar rats weighing 180-200 g were housed in polypropylene cages and maintained at room temperature for 12 h dark/light cycles. They were fed with standard pelleted diet and water. The animals were acclimatized for one week under laboratory conditions before experiments were done on the animals. Ethical clearance was obtained from the Institutional Animal Ethics Committee (resolution no: KLECOP/CPCSEA/ Re.no.221/ PO/RE/S/2000/CPCSEA Res.27-24/12/2018) prior to the beginning of the research. The *in vivo* study was aimed to mainly estimate the amount of drug in the blood withdrawn from rats at various time intervals.[23]

Twelve healthy male Wistar rats weighing 180-200 gms were selected and divided into two groups, each containing six rats. Group 1 received the marketed product of lovastatin, and group 2 received lovastatin nanosuspension equivalent to 0.108 mg in normal saline through the oral route. After 0.5, 2, 4, 6, 8, 10, and 24 h, 0.5-1 mL blood was collected from the tail vein into an Eppendorf tube containing 10-µL EDTA and centrifuged at 5000 rpm for 20 min. Supernatant plasma was collected, filtered through a 0.45 µm membrane into clean vials and analyzed spectrophotometrically to determine the concentration.

Short term stability studies

The optimized formulation was subjected to stability studies as per International Council on Harmonisation (ICH) guidelines. The formulation was exposed to varying conditions of temperature and relative humidity, i.e., 25°C/65% RH and 4°C/65% RH, for a period of three months in a humidity control oven. The samples were collected and evaluated for particle size and percent cumulative drug release at intervals of 0, 1, 2, and 3 months, respectively.

RESULTS AND DISCUSSION

Optimization of process parameters

For the drug lovastatin, maximum solubility was observed in methanol, and least solubility was observed in water. Hence, methanol was selected as a solvent and water as an anti-solvent. Based on the effect of the solvent: anti-solvent volume ratio on particle size, a 1:4 ratio was considered optimum as the particle size was obtained in the nano range. Based on the best and reproducible results, the optimized sonication time was found to be 20 mins, which produced particles in the nano range.

Polymer screening was performed using various polymers like HPMC K15M, HPMC K100M, and PVPK30. Particle size was measured immediately after precipitation. HPMC K15M was found to be more effective in inhibiting crystal growth as compared to particles prepared without the use of a polymer. Hence, HPMC K15M was selected as the stabilizer for the experiment. Pluronic F68 surfactant was found to have more potential as the obtained particle size of nanosuspension was observed in the nano range.

It was observed that an increase in flow rate (2-8 mL/min) increased the particle size from 487 nm to 1023 nm because of large crystal formations. Hence, a flow rate of 2 mL/min was found to be optimum to get the particle size in the nano range. The process optimization parameters and their evaluation results are depicted in Table 1.

Formulation of nanosuspension by the solvent-anti-solvent technique

Lovastatin nanosuspension was successfully prepared by the solvent-anti-solvent method using a probe sonication technique. A total of six formulations were prepared using HPMC K15M and pluronic F68 as stabilizers. In the technique, the addition of the drug solution to the anti-solvent leads to higher supersaturation. This produces many nuclei because of a high nucleation rate, which in turn reduces the mass of the solute for subsequent growth. Submicron particles are thus produced, provided that the nucleating crystals' growth is arrested by the stabilizer via stearic or electrostatic mechanism. Because lovastatin is a hydrophobic drug, the most generally used anti-solvent is water. With respect to the solvent, it has more potential if it solubilizes a higher amount of drug and possesses a greater diffusion rate to the anti-solvent, whereas the stabilizer should possess good affinity toward the drug particles and result in a fast diffusion rate as well as sufficient adsorption onto the surface of the drug particles in the solvent-water mixture. Hence, a pair of solvent-stabilizer is crucial to achieve the submicron particles.[24]

Evaluation of lovastatin-loaded nanosuspension

Particle size analysis

Particle size of the prepared formulation was determined to confirm the production of the particles in the nano range. All formulations were found to be in the range of 127-401 nm (Table 3). It was observed that the particle size was decreased from 284 nm to 127 nm, as the HPMC concentration increased from 1.0 mg/mL to 1.5 mg/mL. This is attributed to the good affinity of the hydrophobic portion of HPMC for drug particles, which leads to an effective stearic barrier against growth. Similarly, when the concentration of pluronic F68 increased from 1.0 mg/mL to 1.5 mg/mL, the particle size decreased from 401 nm to 239 nm. This result may be due to the high affinity of lovastatin particles toward this stabilizer, which provided an effective stearic barrier against crystal growth. Additionally, particle size of the formulations containing the combination of both HPMC K15M and pluronic F68 (F5 and F6) were in the nano range.

Polydispersity index

PDI determines particle size distribution, which ranges from 0 to 1. The sample is said to be monodisperse when the PDI value is close to zero. When the PDI value is <0.2, it is regarded as a narrow size distribution. PDI of all the formulations are shown in Table 3. However, when the PDI value is >0.2, it is considered as polydisperse distribution. Among the prepared nanosuspension formulation, F1 and F3 showed monodisperse size distribution with PDI values of 0.28 and 0.048, respectively. F2, F4, F5, and F6 exhibited polydisperse-sizes distributions with PDI values of 0.492, 0.81, 0.61, and 0.30, respectively.

Zeta potential

The zeta potential was analyzed to determine the stability of the optimized formulation. The zeta potential of the optimized formulation was found to be -37.9 mV, which indicates good stability.

Transmission electron spectroscopy

TEM images of the optimized formulation F2 revealed that the particles were spherical in shape, evenly distributed, and were in the range of 64.62-157.82 nm, which is close to the value obtained from the particle size analyzer (Nanotrac). TEM images are shown in Figure 2.

Drug content

Drug content was calculated for the formulations F1-F6, and it was found to be in the range of 73-86.29%. Drug content was found to be maximum for the formulation F2 and least for the formulation F3.

In vitro drug release study

An *in vitro* drug release study performed in phosphate buffer (pH 6.8) for 1 h to check the release of drug is depicted in Figure 3. The results indicated that the formulation F2 with the least particle size showed a maximum release rate. Based on the drug content, particle size, and drug release profile, the formulation F2 was selected as an optimized formulation. The release profile of the optimized formulation was then compared to the release profile of the pure drug and its marketed formulation, as shown in Figure 4. The percent cumulative drug release obtained at the end of 1 h for optimized, marketed, and pure drug formulations were 92.83%, 60.47%, and 39.73%, respectively. This is because smaller the particle size, larger the surface area. Hence, the drug that is at or near the surface is easily released.

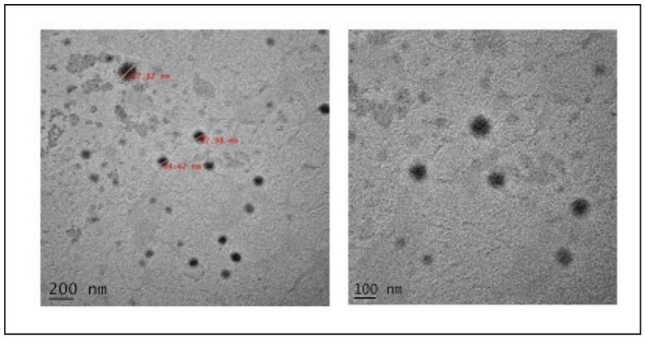

Figure 2. Transmission electron microscopy images of the optimized formulation F2

In vivo bioavailability study

The study was performed in Wistar rats to compare the plasma concentration of the optimized formulation F2 with that of the marketed product given orally in a normal saline. The average concentration was obtained at regular intervals for both the formulations. A comparative graph of plasma concentration vs. time of the optimized formulation F2 and the marketed product is shown in Figure 5. This graph revealed that the formulation F2 showed a greater bioavailability than that of the marketed product. Area under the concentration (AUC) of 29.34 µg h/mL, C_{max} of 4.9 µg/mL, and T_{max} of 4 h was observed for the marketed product when given orally. However, the optimized formulation showed AUC of 63.05 µg h/mL, C_{max} of 6.5 µg/mL, and T_{max} of 1 h, which was calculated by the trapezoidal method (Table 4). Thus, the lovastatin nanosuspension was able to improve the bioavailability by approximately 2.5 folds when compared to the marketed product.

Few more studies have been conducted with respect to the bioavailability enhancement of lovastatin. For instance, Roshan

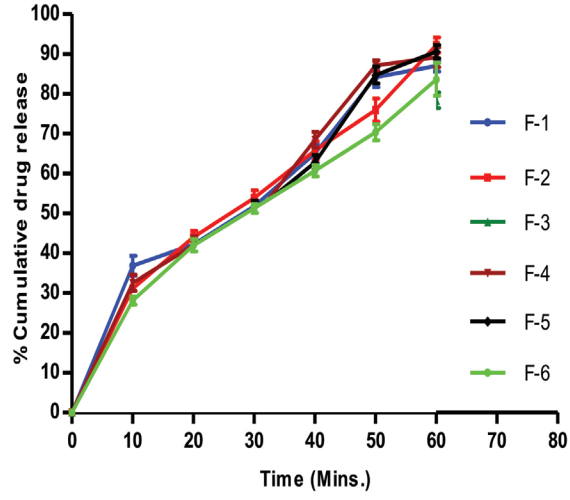

Figure 3. *In vitro* drug release profile for all the formulations

Table 3. Particle size, polydispersity index, percent drug content, and percent CDR of the nanosuspension formulations F1-F6

Formulation code	Particle size (nm)	PDI (Mv)	Drug content %	CDR %
F1	284±0.04	0.28±0.022	76.90±08	87.44±06
F2	127±0.01	0.492±0.001	86.33±07	92.83±08
F3	401±0.06	0.048±0.004	73.25±06	78.19±07
F4	239±0.002	0.81±0.003	78.02±06	89.53±05
F5	224±0.02	0.61±0.005	82.51±08	90.33±06
F6	319±0.03	0.30±0.02	74.00±05	80.25±05

Data are expressed as the mean ± SD (n=3). CDR: Constant default rate, PDI: Polydispersity index, SD: Standard deviation

Table 4. Pharmacokinetic parameters of marketed formulation and optimized formulation F2

Formulation	C_{max} (µg/mL)	T_{max} (h)	AUC_{0-t} (µg/mL/h)
F2	6.5	01	63.05
Marketed product	4.9	04	29.34

C_{max}: Maximum plasma concentration, T_{max}: Time of maximum plasma concentration, AUC_{0-t}: Area under the concentration-time curve from dosing (time 0) to time t

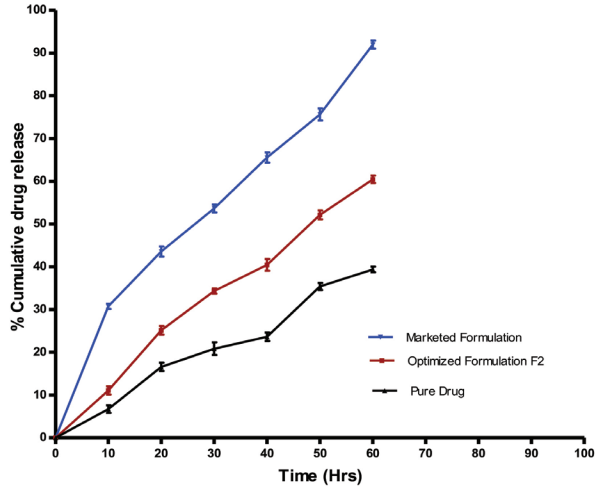

Figure 4. Comparison of *in vitro* drug release profile of the optimized formulation (F2) with that of a pure drug and marketed formulation

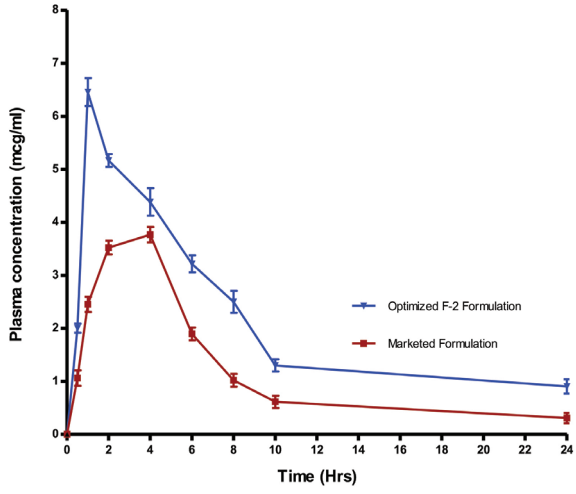

Figure 5. *In vivo* plasma drug concentration time curve of the optimized formulation (F2) and marketed formulation

et al.[25] performed comparative *in vivo* pharmacokinetic studies among solid lipid nanoparticle SLN carrier and NLC and concluded that the lovastatin-encapsulated NLC presented increased bioavailability (10.56%) compared to SLN (7.5%). Keerthi and Bhikshapath[26] developed a self-nanoemulsifying drug delivery system (SNEDDS) of lovastatin to increase its solubility and bioavailability. This study concluded that the optimized formulation of SNEDDS significantly improved the oral bioavailability of lovastatin as compared with the pure drug (no comparison with the marketed product).[26] Recently, Gaber[27] prepared and optimized nanoparticles by an ultrasonication-assisted precipitation method. *In vivo* studies confirmed that there was a 1.45-fold enhancement in C_{max} of lovastatin nanoparticles as compared to a marketed tablet.[27] These studies have also led to enhanced bioavailability of the drug, but not to the extent of a 2.5-fold increment compared with the marketed product. Thus, a developed nanosuspension by the solvent-anti-solvent method may be a potential technique to produce submicron particles of poorly water-soluble drugs, thereby enhancing oral bioavailability.

Short-term stability studies

Stability studies were conducted for the optimized formulation F2 as per ICH guidelines for a period of 3 months. Physical appearance of F2 changed slightly when samples were stored at room temperature 25˚C±2˚C/RH 65%±5% for 3 months. A sediment of thin layer was observed. However, it disappeared immediately with slight shaking. No change in the physical appearance was observed when nanoparticles were stored in the refrigerator at 4˚C±2˚C/RH 65%±5% for 3 months. On comparing the stability study data with the initial data, it was observed that there was not much change in the particle size and the *in vitro drug* release for the formulation stored at 4˚C±2˚C/RH 65%±5% to that stored at room temperature. Thus, the formulation stored at 4˚C±2˚C/RH 65%±5% showed better stability as compared to the formulation stored at 25˚C±2˚C/RH 65%±5%.

CONCLUSION

In the present study, the solvent-anti-solvent method was employed to formulate nanosuspension of lovastatin for enhancing the solubility, dissolution rate, and thereby its oral bioavailability. Lovastatin nanosuspension was formulated using methanol as a solvent, water as an anti-solvent, and HPMC K15M and Pluronic F68 as stabilizers. Fourier transform infrared spectroscopy and differential scanning calorimetry studies showed no interaction between the drug and the excipients that were used in the formulation (results not shown). On the basis of drug content, particle size, and drug release profile, formulation F2 was selected as an optimized formulation. TEM images suggest that the particle size of all the formulations were in the nano range. Zeta potential of optimized formulation F2 was found to be -37.9 mV, which showed a good stability. The dissolution rate depends upon the particle size. The smaller the particle size, the faster will be the dissolution. Formulation F2 showed a maximum dissolution rate of 92.83% in 1 h when compared with the pure drug and the marketed formulation, which showed 39.73% and 60.47% dissolution in the same time. A pharmacokinetic analysis of *in vivo* bioavailability data

indicated a 2.5-fold increase in comparison with the marketed formulation. Stability studies were conducted according to ICH guidelines for optimized formulation F2, and it was more stable at 4˚C±2˚C. Thus, it may be concluded that the solvent-anti-solvent method is a simple and potential technique to produce submicron particles of poorly water-soluble drugs, thereby enhancing oral bioavailability for commercial production.

ACKNOWLEDGMENTS

The authors would sincerely like to thank Lupin Pharmaceuticals, Goa for providing a gift sample of lovastatin. The authors are also thankful to the principal of KLE College of Pharmacy, Belagavi and Dr. Prabhakar Kore Basic Science Research Centre, Belagavi for providing laboratory facilities. The authors are thankful to Kesar Control System, AICTE-MODROB 2017-2018 for providing the stability chamber to carry out the stability studies for this research. The authors are also thankful to AICTE-MODROBE for providing the Ultrasonic probe sonicator VC750.

Conflict of interest: No conflict of interest was declared by the authors. The authors are solely responsible for the content and writing of this paper.

REFERENCES

1. Heran Z, Jin H, Yihua Y, Erxi C. Development of novel mesoporous nanomatrix-supported lipid bilayers for oral sustained delivery of the water-insoluble drug, lovastatin. Colloids Surf B. 2015;128:77-85.
2. Preshita PD, Abhijit AD, Vandana BP. Overcoming poor oral bioavailability using Nanoparticle formulations opportunities and limitations. Drug Discov Today Technol. 2012;09:87-95.
3. Sandip C, Garima J, Kailash P, Krutika S. Enhanced bioavailability and hypolipidemic activity of Simvastatin formulations by particle size engineering: Physicochemical aspects and *in vivo* Investigations. Biochem Eng J. 2013;79:221-229.
4. Konwar R, Ahmed AB. Nanoparticle: an overview of preparation, characterization and application. Int Res J Pharm. 2013;4:47-57.
5. Ying X, Wei W, Zongning Y, Ruyue L. Enhanced dissolution and oral bioavailability of Aripiprazole Nanosuspensions prepared by nanoprecipitation/homogenization based on acid-base neutralization. Int J Pharm. 2012;438:287-295.
6. Alptug K, Zeynep ST, Hakan E, Nevin C. Evaluation of improved oral bioavailability of Ritonavir Nanosuspension. Eur J Pharm Sci. 2019;131:153-158.
7. Chia HC, Jyh CY, Yow SU, Chun JL. Improved dissolution rate and oral bioavailability of Lovastatin in red yeast rice products. Int J Pharm. 2013;444:18-24.
8. Roth GA, Mensah GA, Johnson CO, Addolorato G, Ammirati E, Baddour LM, Barengo NC, Beaton AZ, Benjamin EJ, Benziger CP, Bonny A, Brauer M, Brodmann M, Cahill TJ, Carapetis J, Catapano AL, Chugh SS, Cooper LT, Coresh J, Criqui M, DeCleene N, Eagle KA, Emmons-Bell S, Feigin VL, Fernández-Solà J, Fowkes G, Gakidou E, Grundy SM, He FJ, Howard G, Hu F, Inker L, Karthikeyan G, Kassebaum N, Koroshetz W, Lavie C, Lloyd-Jones D, Lu HS, Mirijello A, Temesgen AM, Mokdad A, Moran AE, Muntner P, Narula J, Neal B, Ntsekhe M, Moraes de Oliveira G, Otto C, Owolabi M, Pratt M, Rajagopalan S, Reitsma M, Ribeiro ALP, Rigotti N, Rodgers A, Sable C, Shakil S, Sliwa-Hahnle K, Stark B, Sundström J, Timpel P, Tleyjeh IM, Valgimigli M, Vos T, Whelton PK, Yacoub M, Zuhlke L, Murray C, Fuster V; GBD-NHLBI-JACC Global Burden of Cardiovascular Diseases Writing Group. Global Burden of Cardiovascular Diseases and Risk Factors, 1990-2019: Update From the GBD 2019 Study. J Am Coll Cardiol. 2020;76:2982-3021.
9. Chih CC, Tung HT, Zih RH, Jia YF. Effects of lipophilic emulsifiers on the oral administration of lovastatin from nanostructured lipid carriers: Physicochemical Characterization and Pharmacokinetics. Eur J Pharm Biopharm. 2010;74:474-482.
10. Sunil KY, Jitendra BN, Jayesh SP, Vinod JM, Ruby S. Enhanced solubility and bioavailability of Lovastatin using stabilized form of self-emulsifying drug delivery system. Colloids Surf A. 2015;481:63-71.
11. Jun Z, Daxin Z. Improvement of oral bioavailability of Lovastatin by using nanostructured lipid carriers. Drug Des Devel Ther. 2015;9:5269-5275.
12. Gande S, Kopparam M, Vemula S. Preparation, Characterization and *in vitro* and *in vivo* evaluation of Lovastatin solid lipid nanoparticles. AAPS PharmSciTech. 2007;8:E1-E9.
13. Mohammad HS, Sharmin S, Jahan I, Reza HM, Kazi M. The impact of process parameters on carrier free paracetamol nanosuspension prepared using different stabilizers by antisolvent precipitation method. J Drug Deliv Sci Technol. 2018;43:123-128.
14. Hamid RP. Preparation and characterization of azithromycin nanodrug using solvent/antisolvent method. Int Nano Lett. 2014;4:2-9.
15. Mansour M, Hamid RP, Vida V. Preparation and characterization of ibuprofen nanoparticles by using solvent/antisolvent precipitation. Open Conf Proc J. 2011;2:88-94.
16. Enubi C, Wonkyung C, Junsung P, Min SK. Enhanced dissolution of megestrol acetate microcrystals prepared by antisolvent precipitation process using hydrophilic additives. Int J Pharm. 2010;396:91-98.
17. Mohammad HS, S. Sharmin, I.Jahan, H.M.Reza, Kazi M. The impact of process parameters on carrier free Paracetamol Nanosuspension prepared using different stabilizers by antisolvent precipitation method. J Drug Deliv Sci Technol. 2018;43:123-128.
18. Bhupesh KA, Sunil KJ, Sharan KP, Surbhi B, Sarasija S. Formulation, optimization and *in vitro-in vivo* evaluation of febuxostat nanosuspension. Int J Pharm. 2015;478:540-552.
19. Rupall LS, Shashikant ND, Nilesh K, Santosh LS. Formulation and evaluation of nanosuspension delivery system for simvastatin. Int J Pharm Sci Nanotechnol. 2014;7:2459-2476.
20. Zhang T, Chen J, Zhang Y, Shen Q, Pan W. Characterization and evaluation of nanostructured lipid carrier as a vehicle for oral delivery of etoposide. Eur J Pharm Sci. 2011;43:174-179.
21. Patricia CD, Alejandro CO, Maria R. Rapid determination of paracetamol in blood serum samples by first-derivative UV absorption spectroscopy. Anal Lett. 1995;28:2219-2226.
22. Arpana PG, Varsha P. Montelukast-Loaded nanostructured lipid carriers: Part I Oral bioavaiability improvement. Eur J Pharm Biopharm. 2014;88:160-168.
23. Prabhat RM, Rainer HM. Production and characterization of hesperetin nanosuspensions for dermal delivery. Int J Pharm. 2009;371:182-189.
24. Wai KN, Sanggu K, Reginald BHT. Preparation and characterization of spironolactone nanoparticles by antisolvent precipitation. Int J Pharm. 2009;375:84-88.

25. Roshan KP, Kalaiselvan S, Balamurugan K. *In vivo* pharmacokinetic studies to investigate the enhancement of bioavailability of lovastatin. J Pharm Int Bio Sci. 2018;3:19-25.

26. Keerthi P, Bhikshapath DVRN. Development and *in vivo* evaluation lovastatin by self-nanoemulsifying drug delivery System. Int J Pharm Sci Drug Res. 2018;10:165-172.

27. Gaber DA. Nanoparticles of lovastatin: design, optimization and *in vivo* evaluation. Int J Nanomedicine. 2020;15:4225-4236.

Turk J Pharm Sci 2021;18(5):550-556
DOI: 10.4274/tjps.galenos.2020.76753

ORIGINAL ARTICLE

Stability-indicating LC Method for Quantification of Azelnidipine: Synthesis and Characterization of Oxidative Degradation Product

Azelnidipin Miktar Tayini İçin Stabilite Göstergeli LC Yöntemi: Oksidatif Bozunma Ürününün Sentezi ve Karakterizasyonu

Sandeep S. SONAWANE*, Pooja C. BANKAR, Sanjay J. KSHIRSAGAR

MET's Institute of Pharmacy, MET League of Colleges, Bhujbal Knowledge City, Nashik, India

ABSTRACT

Objectives: In the work presented here, the degradation behavior of azelnidipine under diverse forced degradation conditions was studied. A stability-indicating liquid chromatographic method was established which could separate and resolve azelnidipine from its degradation products. Further, chemical kinetics under acidic and alkaline conditions were studied, and validation studies were performed.

Materials and Methods: Using reversed-phase chromatography, azelnidipine and its formed degradants were resolved using phosphate buffer (pH 3.0) and methanol in a mixture of 10:90% v/v as a mobile phase at a flow rate of 1.0 mL/min. All eluents were detected at a wavelength of 256 nm.

Results: Azelnidipine was degraded under acid, alkali, wet heat, and oxidized environment. The pH-dependent rate of hydrolysis of azelnidipine was studied under acidic and alkaline conditions and chemical kinetics were determined. Further, the oxidative degradation product of azelnidipine was synthesized and characterized as 3-(1-benzhydrylazetidin-3-yl) 5-isopropyl 2-amino-6-methyl-4-(3-nitrophenyl) pyridine-3,5-dicarboxylate (dehydro-AZD).

Conclusion: The susceptibility of azelnidipine to hydrolysis was attributed to the presence of ester at 3 and 5 positions of 1,4 dihydropyridine. Further, under oxidative conditions, the aromatization of 1,4 dihydropyrinine resulted in dehydro-AZD. Azelnidipine followed the first-order reaction under acid and alkali hydrolysis, and was more susceptible to degradation under acidic conditions. The synthesized and confirmed dehydro-AZD was found as one of the metabolites and impurities of azelnidipine. The evaluated validation parameters ascertained the practicality of the method for the quantification of azelnidipine tablets.

Key words: Azelnidipine, chemical kinetics, degradation product, HPLC, method validation, stability-indicating

ÖZ

Amaç: Bu çalışmada, azelnidipinin çeşitli zorlu bozunma koşulları altında bozunma davranışı incelenmiştir. Azelnidipinin stabilitesini gösteren, azelnidipini bozunma ürünlerinden ayırabilen ve çözebilen sıvı kromatografik yöntem geliştirilmiştir. Ayrıca asidik ve alkali koşullar altında kimyasal kinetikler incelendi ve doğrulama çalışmaları yapıldı.

Gereç ve Yöntemler: Azelnidipin ve oluşan bozunma ürünleri, mobil faz olarak kullanılan fosfat tamponu (pH 3,0) ve metanol (%10:90 h/h) ile, 1,0 mL/dk akış hızında ters faz kromatografisi kullanılarak ayrıştırıldı. Tüm eluentler 256 nm dalga boyunda tespit edildi.

Bulgular: Azelnidipin asit, alkali, ıslak ısı ve oksitlenmiş ortam koşullarında degrade edildi. Azelnidipinin pH'ye bağlı hidroliz hızı asidik ve alkali koşullar altında çalışılmış ve kimyasal kinetik belirlenmiştir. Ayrıca, azelnidipinin oksidatif bozunma ürünü olan 3-(1-benzhidrilazetidin-3-il) 5-izopropil 2-amino-6-metil-4-(3-nitrofenil) piridin-3,5-dikarboksilat (dehidro-AZD) sentezlendi ve karakterize edildi.

Sonuç: Azelnidipinin hidrolize duyarlılığı, 1,4 dihidropiridinin 3 ve 5 pozisyonlarındaki esterin varlığı ile ilişkilendirildi. Ayrıca, oksidatif koşullar altında 1,4 dihidropirinin aromatizasyonu dehidro-AZD eldesi ile sonuçlandı. Azelnidipin için, asit ve alkali hidroliz altında bozunmasının birinci derece kinetiğe uyduğu belirlendi ve asidik koşullar altında bozunmaya daha duyarlıydı. Sentezlenen ve doğrulanan dehidro-AZD, azelnidipinin

*Correspondence: sandeeps.iop@gmail.com, Phone: +912532555947, ORCID-ID: orcid.org/0000-0002-4858-7651

Received: 15.09.2020, Accepted: 21.12.2020

metabolitlerinden ve safsızlıklarından biri olarak bulundu. Değerlendirilen doğrulama parametreleri, azelnidipin tabletlerinin miktar tayini için yöntemin pratikliğini belirlemiştir.

Anahtar kelimeler: Azelnidipin, kimyasal kinetik, bozunma ürünü, HPLC, metot validasyonu, stabilite göstergesi

INTRODUCTION

Stability experiments aim to recognize the likely alterations with drug substances and products with regards to time under various storage conditions. It is anticipated that all the analytical methods used during the study should be stability-indicating. Although any method evaluating changes in the physico-chemical properties of a drug substance or product should indicate stability, chromatographic methods are the most common stability-indicating methods (SIM).[1] A major challenge in SIM development is the generation of stability test samples which are the real-time samples and contain all degradation products which may form under normal storage conditions. For stability evaluation, forced degradation experiments are conducted where the drug substances and products are heated to elevated temperatures under different pH conditions at different intervals, oxidation, dry heat, and photolytic conditions.

Chemically, AZD (Figure 1) is (±) 3-(1-benzhydrylazetidin-3-yl) 5-isopropyl 2-amino-6-methyl-4-(3-nitrophenyl) -1,4-dihydropyridine (DPH)-3,5-dicarboxylate.[2] AZD is official in Indian Pharmacopoeia 2014[3] and Japanese Pharmacopoeia 2016.[4]

AZD is a third-generation calcium channel antagonist and an effective antihypertensive agent used in patients suffering from hypertension.[5] It specifically suppresses the L-type calcium channels of smooth muscle cells, and prevents the influx of transmembrane calcium.[6]

A literature review found numerous analytical methods stated for the estimation of AZD, including AZD estimation in pharmaceutical formulations by high performance liquid chromatography (HPLC),[7-10] ultraviolet (UV) spectroscopy[11] in biological fluids by hyphenated LC-mass spectrometry (MS) techniques,[12,13] enantiomeric separation and estimation of AZD by HPLC[14] and LC-tandem MS.[15] Along with these, an extensive literature exists on SIM for the estimation of AZD, including HPLC[16,17] and HPTLC.[18] Two SIM have been reported for the simultaneous estimation of AZD and olmesartan.[19,20] Further, the degradation of AZD under radical initiator-based oxidative conditions was studied.[21]

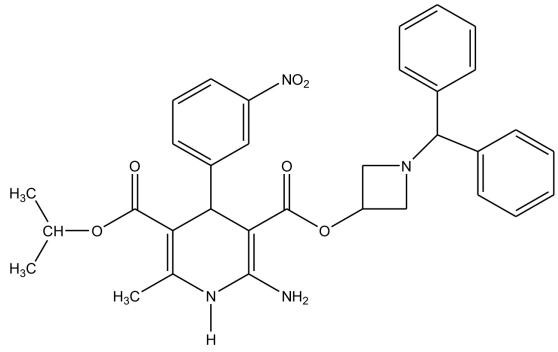

Figure 1. Chemical Structure of AZD

Moreover, limited shreds of evidence have been reported regarding the degradation behavior of AZD under different degradation conditions as well as no chemical kinetic study has been performed to date.

To address these unaccounted phenomena, the objectives of the current investigation was to ascertain an LC approach for AZD quantification in bulk and tablets which could separate and resolve the AZD from its degradants, to validate the method to prove the accuracy, precision, robustness, and stability-indicating power of the method. The study was set out to explore the degradation behavior of AZD under different forced degradation conditions and to study the kinetics under acidic and alkaline conditions.

Further, from the literature, it was revealed that 3-(1-benzhydrylazetidin-3-yl) 5-isopropyl 2-amino-6-methyl-4-(3-nitrophenyl) pyridine-3,5-dicarboxylate (dehydro-AZD) is the oxidative degradation product of AZD [21] as well as one of the major AZD metabolites.[22] According to the literature 1,4-DHP derivates oxidize in the liver by cytochrome P-450 into pyridine derivatives (aromatization of 1,4-DHP).[23] This was of high interest and therefore, the study was continued to synthesize and interpret the oxidative degradation product of AZD.

MATERIALS AND METHODS

Chemicals and reagents

A pharmaceutical grade AZD (certified to contain 99.91% w/w on dried basis) was obtained from Precise Pharmaceuticals Ltd, Nashik, India as a gift sample. In the investigation, methanol was of HPLC grade and other chemicals were of Analytial Reagent grade. All chemicals were bought from SDFLC - SD Fine Chem Ltd, Mumbai, India. The varying strengths of hydrochloric acid, sodium hydroxide, and hydrogen peroxide were prepared freshly by diluting appropriately with double distilled water, and were further used after filtering through membrane filter papers (Millipore India Pvt. Ltd., Bengaluru, India). The tablets containing AZD 16 mg were bought from the residential market.

Instrumentation and chromatographic conditions

HPLC system used in the analyses consisted of binary pumps (PU 2080 plus), Jasco Corporation, Tokyo, Japan with 20 μL sample injector and multi-channel UV-visible detector, UV-2077, Jasco Corporation, Tokyo, Japan. All signals were recorded using Borwin software (version 1.50).

All chromatographic analyses were conducted on the C18 column with dimensions of 250×4.6 mm, 5 μm using a blend of

25 mM phosphate buffer (pH 3.0), and methanol (10:90% v/v) at a constant flow of 1.0 mL/min. The detector wavelength was set out at 256 nm, which was the absorbance maxima of the AZD.

Forced degradation studies

Forced degradation trials were carried out on AZD bulk drug sample and on AZD tablets as per ICH Q2A (R1).[24] Preliminary experiments were conducted to decide the strength of the stressor used, temperature of exposure, and time of heating. Under acidic and alkaline degradation, AZD was exposed to 0.1 N HCl and 0.1 N NaOH at 70°C for 35 min, respectively. Wet heat degradation was achieved by refluxing the drug into double distilled water for 8 h at 70°C. Further, AZD was exposed to 3% v/v hydrogen peroxide under dark for 24 h. The oxidized sample was heated on water bath to eliminate the leftover hydrogen peroxide. Degradation under dry heat condition occured by heating the AZD for 6 h in a hot air oven at 70°C and photolytic degradation by exposing the AZD under 7-day cycles to direct sunlight.

After exposure, degradation samples were collected and diluted suitably with the mobile phase. The obtained 10 μg/mL of samples were injected in the LC system. The decrease in the area under curve (AUC) of AZD compared to the standard AZD sample and with the appearance of secondary peaks in the chromatograms were noted as degradation. Appropriate counter blank samples were used to impede errors.

Chemical kinetic studies

To study the chemical kinetics of AZD under acidic and alkaline conditions, 10 mg of AZD was transferred to two separate round bottom flasks, and in each flask, 10 mL of 0.1 N HCl and 0.1 N NaOH were added, respectively. The resulting solutions were heated in a thermostatic water bath at 50°C for 35 min. After 5 min intervals, the appropriate quantity was quenched, diluted with the mobile phase to obtain 10 μg/mL, and injected in the LC system.

Synthesis and characterization of dehydro-AZD

An accurately weighed 1 g quantity of AZD was transferred to a conical flask, to which 20 mL of acetonitrile was added and the solution was stirred for 10 min. To it, 1 g of 2,3-dichloro-5,6-dicyano-1,4-benzoquinon was added. The resulting mixture was again stirred for 20 min and was kept in dark at room temperature for 7 h. The obtained reaction mixture was washed with double distilled water. The resulting product was characterized using MS.

Preparation of standard stock solution, calibration curve standards, and estimation of AZD in tablets

The standard stock solution of 1 mg/mL of AZD was prepared in methanol. The prepared standard stock solution was diluted appropriately with the mobile phase to obtain 10, 20, 30, 40, 50, and 60 μg/mL of calibration curve standards and injected in triplicate. To obtain the calibration curve equation, the recorded AUC at each calibration standard was plotted against respective concentrations, and the regression coefficient (r^2), y-axis intercept, and the slope of the line were determined.

To estimate the AZD in tablets, twenty tablets were weighed and ground to a fine powder. The amount equal to the total weight of one tablet was weighed and moved to a 100 mL volumetric flask. The mixture was sonicated for 10 min after the addition of 70 mL methanol and diluted further to 100 mL with methanol. The obtained solution was filtered, subsequently diluted to obtain 10 μg/mL, and injected in triplicate. The corresponding concentrations and the % label claim were calculated using the calibration curve equation.

Method validation

The developed method was validated as per the ICH Q2 R1 guidelines[25] to evaluate the accuracy, precision, detection limit (DL), quantitation limit (QL), robustness, and specificity.

Accuracy and precision were executed by spiking the standard sample of AZD in the tablet solution at 80%, 100%, and 120% levels across the calibration range in triplicate for three successive days. The acceptable accuracy was established by the closeness of the % amount recovered with the % amount added and the precision with low relative standard deviation % (RSD). Further, the obtained data of accuracy and precision were subjected to One-Way ANOVA to ascertain the intermediate precision of the method. DL and QL were determined as DL: (3.3 σ/S) and QL: (10 σ/S), where σ: SD of AUC and S is the slope of the calibration curve, respectively. Robustness of the method was verified by executing minor changes in the flow rate (±0.2 mL), % methanol (±10%) and the detection wavelength (±5 nm) and the effects on the system of the AZD peak were observed. To prove the specificity of the method, absolute separation of AZD from its degradation products and the absence of the interfering peaks at the retention times of AZD were evaluated.

Statistical analysis

In the results and discussion section, the statistical analysis was discussed in chemical kinetics and method validation.

RESULTS AND DISCUSSION

Optimization of the chromatographic conditions

To obtain the adequate retention time of AZD with acceptable system suitability, different mobile phases were tried. Initially, water was tried as an aqueous phase along with acetonitrile and methanol. However, the splitting of the AZD peak suggests a buffer in the mobile phase. Good peak shape and acceptable system suitability parameters (theoretical plates: 8991, asymmetry: 1.10) were obtained when phosphate buffer at pH 3.0 was tried with methanol using Phenomenex Hyperclone ODS (C18) column (250×4.6 mm, 5 μm). The adequate retention time of AZD at 4.703±0.12 min was obtained when 25 mM phosphate buffer was used with methanol in the ratio of 10:90% v/v, respectively. All eluents were detected at 256 nm in an isocratic mode at the flow rate of 1 mL/min.

Forced degradation studies

Under acidic conditions, two degradation products were obtained, whereas, under alkaline conditions, wet heat, and oxidative conditions, one degradation product was obtained.

Inconsiderable decrease in the peak area of AZD or appearance of secondary degradation products were detected in dry heat and photolytic conditions.

The degradation behavior of AZD under different forced degradation conditions is presented in Table 1 and the respective chromatograms are presented in Figure 2.

From the degradation behavior of AZD under different conditions, it was observed that AZD is more susceptible to degrade under acidic and alkaline conditions followed by oxidation and wet heat conditions.

Chemical kinetics

A gradual decrease in the peak area (Figure 3) confirmed that AZD follows the first-order reaction under acidic and alkaline conditions. The rate constant (K), half-life ($t_{1/2}$), and shelf-life (t_{90}) were determined using the following equations, respectively.

$$K = \frac{2.303}{t}\log\frac{C_0}{C} \quad \text{equation (1)}$$

$$t_{1/2} = \frac{0.693}{K} \quad \text{equation (2)}$$

$$t_{90} = \frac{0.104}{K} \quad \text{equation (3)}$$

From Table 2, the K value was found to be higher under acidic condition than alkaline condition which concludes that the rate of hydrolysis of AZD is higher in acid as compared to that in alkali. Also, the $t_{1/2}$ and t_{90} values were the lowest for acid and highest for alkali. AZD contains two ester groups and a lactone ring; both groups are susceptible to hydrolysis. However, the rate of hydrolysis depends upon pH, temperature, and substituents.

Table 1. Forced degradation behavior of AZD

Degradation condition	Degradation %	RT of a drug (min)	RT of degradation products (min)
Acid	21.27	4.82	2.76, 3.18
Alkali	17.88	4.57	2.85
Wet heat	8.59	4.82	3.45
Hydrogen peroxide induced oxidation	10.07	4.82	2.21 (peroxide blank), 3.27

RT: Room temperature

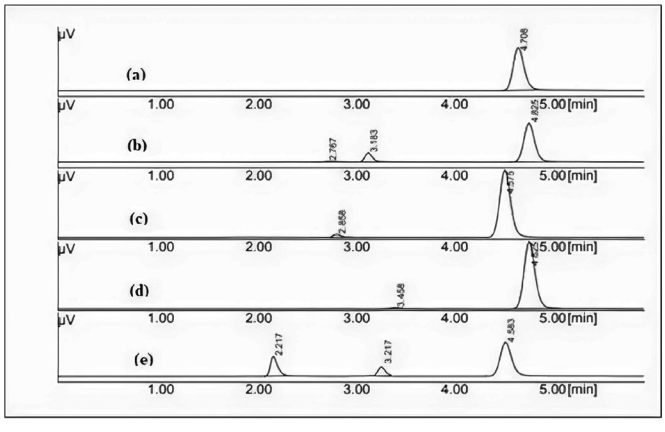

Figure 2. Representative chromatograms of AZD under (a) standard AZD (10 mg/mL), (b) acidic condition, (c) alkaline condition, (d) wet heat degradation (e) hydrogen peroxide induced oxidation

Characterization of synthesized dehydro-AZD

The MS of the synthesized compound is depicted in Figure 4, where the major fragments identified had an m/z ratio of 581.45 (molecular ion), 342.18, 238.14, and 167.11, respectively. The mass fragmentation pattern is depicted in Figure 5, and it confirmed the synthesis of dehydro-AZD.

Table 2. Summary of AZD acid and alkali hydrolysis kinetics

Degradation condition	K (1/min)	$t_{½}$ (min)	t_{90} (min)
Acid degradation	1.10×10^{-2}	63	9.45
Alkali degradation	5.99×10^{-3}	115.69	17.36

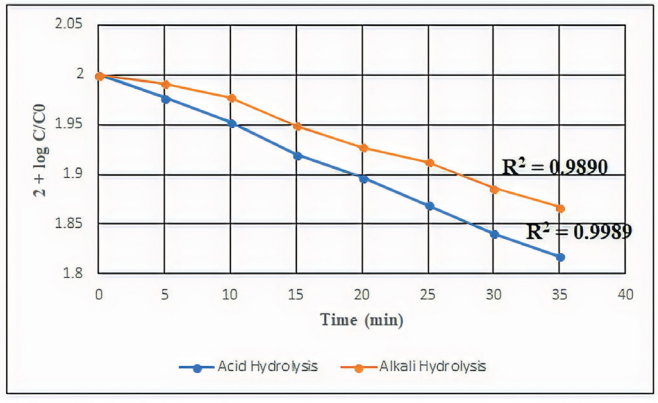

Figure 3. First-order plots of AZD under acidic and alkaline conditions

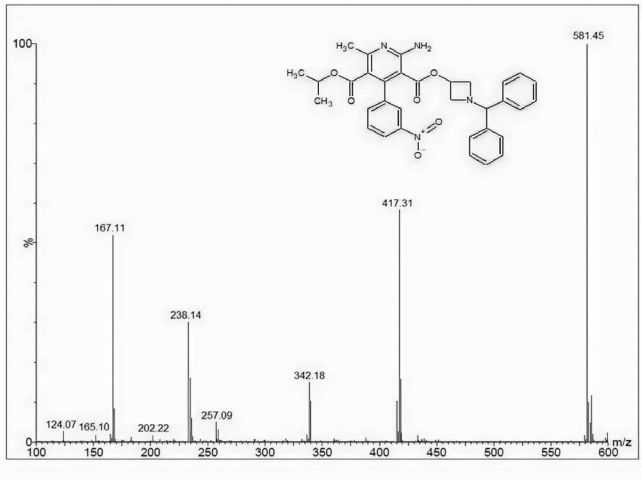

Figure 4. Mass spectrum of dehydro-AZD

Calibration curve and estimation of AZD in tablets

AZD was found to be linear in the range of 10-60 µg/mL with r^2: 0.9989 with the calibration curve equation, *y*: 53455*x*+121119.

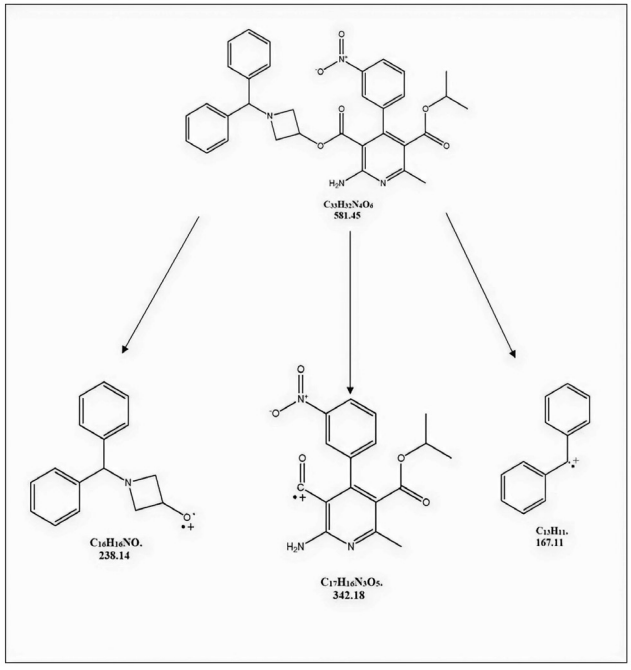

Figure 5. Fragmentation pattern of dehydro-AZD

The calibration curve is depicted in Figure 6. The analysis of the tablet showed 100.54±0.30 of AZD.

Method validation

The results of accuracy and precision studies are presented in Table 3; mean concentration values were close to the spiked concentration of AZD, indicating good recovery. The precision was indicated by the low values of RSD %. When the obtained data of accuracy and precision studies were subjected to ANOVA, the F (observed) at each QC level was lower than the F (theoretical) at 95% confidence interval, indicating insignificant

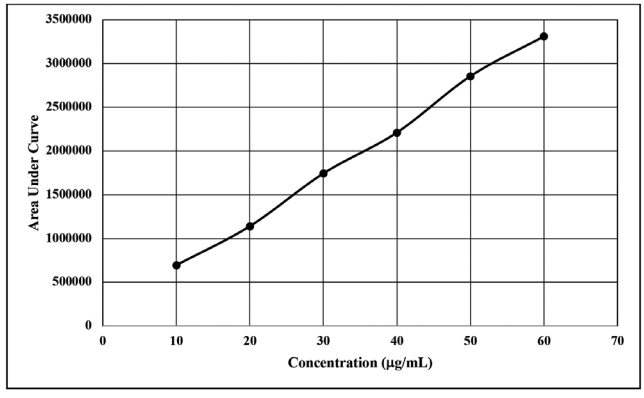

Figure 6. Calibration curve of AZD

Table 3. Summary of accuracy and precision of AZD

Amount added (µg/mL)	Amount found(µg/mL)			Within mean square	Between mean square	F value
	Day 1	Day 2	Day 3			
25+20=45 (80%)	44.78	44.52	44.51	0.0606	0.1541	2.5438
	44.92	44.73	44.85			
	44.92	44.02	44.49			
Mean	**44.87**	**44.42**	**44.62**			
± SD	**0.08**	**0.36**	**0.20**			
RSD %	**0.18**	**0.82**	**0.45**			
25+25=50 (100%)	49.33	49.12	49.15	0.0495	0.0825	1.6673
	49.06	49.36	49.46			
	49.14	49.15	49.82			
Mean	**49.18**	**49.21**	**49.48**			
± SD	**0.14**	**0.13**	**0.33**			
RSD %	**0.28**	**0.26**	**0.67**			
25+30=55 (120%)	54.77	54.18	54.83	0.2100	0.0546	0.2598
	54.69	55.37	54.80			
	55.05	54.22	54.19			
Mean	**54.83**	**54.59**	**54.61**			
± SD	**0.18**	**0.67**	**0.36**			
RSD %	**0.34**	**1.24**	**0.66**			

SD: Standard deviation, RSD: Relative standard deviation

difference of the data of intra- and inter-day precision and proved the intermediate precision. The DL and QL were 0.43 μg/mL and 1.32 μg/mL, respectively. In the robustness experiment, no significant changes were observed in the system suitability parameters for AZD when minor changes were executed in the established chromatographic condition, demonstrating the robustness of the method. AZD was well separated and resolved from its degradation products; the absence of interfering peaks at the retention time of the AZD designated specificity.

CONCLUSION

The main conclusions of this work are drawn together and presented in this section:

- In the present work, LC method was stated for the estimation of AZD in bulk and tablets. The method proved to be simple and economic as the separation was achieved on a C18 column with the mixture of 25 mM phosphate buffer (pH 3.0) and methanol as a mobile phase in the proportion of 10: 90% v/v in an isocratic mode, and all the formed degradation products along with AZD were separated out within less than 10 min of the run time.
- The method proved to be accurate with satisfactory precision. No significant alterations in the system suitability ascertained the robustness of the method. The acceptable specificity proved the stability-indicating nature of the method. The method was linear in the range of 10-60 μg/mL and the assay of the tablet was found to be 100.54%±0.30% of the stated label of AZD.
- The forced degradation trials resulted in the degradation of AZD under acidic, alkaline, wet heat conditions, and peroxide-mediated oxidation.
- Hydrolysis is the major degradation pathway for drug substances with an ester functional group in their structure. The AZD has two ester groups present at 3 and 5 positions of the 1,4-DHP moiety, and hence, AZD may be susceptible to acid, alkali, and wet heat hydrolysis. Further, the pH-dependent rate of hydrolysis of AZD under acid and alkali conditions was determined by the chemical kinetic study, which proved the first-order reaction of AZD under acidic and alkaline conditions, respectively. The $t_{1/2}$ and t_{90} values proved that AZD was more susceptible to degrade under an acidic enviornment than under an alkaline environment.
- Considering the atomization of 1,4-DHP to pyridine derivative under oxidative conditions, the oxidative degradation product of AZD was synthesized and confirmed using MS, which was found as one of the impurities and metabolites of AZD.

Conflict of interest: No conflict of interest was declared by the authors. The authors are solely responsible for the content and writing of this paper.

REFERENCES

1. Aubry AF, Tattersall P, Ruan Joan. Development of Stability Indicating Methods. In: Huynh-Ba K, ed. Handbook of Stability Testing in Pharmaceutical Development. New York: Springer Science and Business Media; 2009:139-161.
2. O'Neil MJ, ed. The Merck Index An Encyclopedia of Chemicals, Drugs, and Biological. 14th ed. New Jersy USA,: Merck research laboratories Division of Merck and Co. Inc.; 2006:153.
3. Indian Pharmacopoeia. Ghaziabad: Indian Pharmacopoeia. 7th ed New Delhi: Indian Pharmacopeia Commission; 2014:1115.
4. The Japanese Pharmacopeia (English Version) [Internet]. The Ministry of Health, Labour and Welfare. 2016. Last Accessed Date: 03.11.2019. Available from: http://www.mhlw.go.jp/file/06-Seisakujouhou-11120000-Iyakushokuhinkyoku/JP17_REV_1.pdf
5. Chen BL, Zhang YZ, Luo JQ, Zhang W. Clinical use of azelnidipine in the treatment of hypertension in Chinese patients. Ther Clin Risk Manag. 2015;24:309-318.
6. Catterall WA, Perez-Reyes E, Snutch TP, Striessnig J. International Union of Pharmacology. XLVIII. Nomenclature and structure-function relationships of voltage-gated calcium channels. Pharmacol Rev. 2005;57:411-425.
7. Hua-min A, Ju-cai W. Determination of content and related substances of azelnidipine by HPLC. West J Pharm Sci. 2006;21:581.
8. Pan YF, Zang JB, Ding J, Wang TM. Determination of azelnidipine tablets by HPLC. Qilu Pharm Aff. 2008:398-399.
9. Prabhakar D, Sreekanth J, Jayaveera KN. Method development and validatoin of azelnidipine by RP-HPLC. Int J ChemTech Res. 2018;11:7-12.
10. Gore MG, Dabhade PS. RP-HPLC method development and validation of azelnidipine. Int J Pharm Sci Res. 2016;7:5111.
11. Raskapur KD, Patel MM, Captain AD. UV-spectrophotometric method development and validation for determination of azelnidipine in pharmaceutical Dosage form. Int J Pharm Pharm Sci. 2012;4:238-240.
12. Gao Y, Li B, Zhu B, Liu D, Zhao H, Fang Z, Wang H, Lou H. A liquid chromatography-tandem mass spectrometric assay for the antihypertensive agent azelnidipine in human plasma with application to clinical pharmacokinetics studies; biomedical chromatography. Biomed Chromatogr. 2015;29:970-974.
13. Jian-Jun Z, Hong-Jian J, Xiao-Hua, Z, Yu-Bin Z, Hong-Wei F, Da-Wei X, Qin Hu. Determination of azelnidipine by LC-ESI-MS and its application to a pharmacokinetic study in healthy Chinese volunteers. Pharmazie. 2008;63:568-570.
14. Zhang K, Xue N, Li L, Li F, Du Y. Enantiomeric separation of azelnidipine by high performance liquid chromatography with chiral stationary phase. Chinese J Chromatogr. 2010;28:215-217.
15. Kawabata K, Samata N, Urasaki Y, Fukazawa I, Uchida N, Uchida E, Yasuhara H. Enantioselective determination of azelnidipine in human plasma using liquid chromatography-tandem mass spectrometry. J Chromatogr B Anal Technol Biomed Life Sci. 2007;852:389-397.
16. Modi J, Patel SK, Parikh N, Shah SR, Pradhan PK, Upadhyay UM. Stability indicating analytical method development and validation for estimation of azelnidipine. World J Pharm Res. 2016;5:831-847.

17. Rele RV, Sawant SA. Development and validation of stability indicating reverse phase liquid chromatographic method for the assay of azelnidipine in bulk and pharmaceutical formulations. Int J Pharma Biosci. 2016;7:376-380.

18. Rane AS, Mahajan SK. Validation and forced stability-indicating HPTLC method for determination of azelnidipine. World J Pharm Res. 2016;5:1053-1062.

19. Ganduri R, Peddapapireddigari J, Vurimindi H, Ramprakash. Stability indicating liquid chromatographic method for the simultaneous determination of olmesartan medoxomil and azelnidipine in combined tablet dosage form. Int J Pharma Sci Res. 2014;5:275-282.

20. Patel JK, Patel NK. Validated stability-indicating RP-HPLC method for the simultaneous determination of azelnidipine and olmesartan in their combined dosage form. Sci Pharm. 2014;82:541-554.

21. Ueyama E, Takahashi F, Ohashi J, Konse T, Kishi N, Kano K. Mechanistic study on degradation of azelnidipine solution under radical initiator-based oxidative conditions. J Pharm Biomed Anal. 2012;61:277-283.

22. Kawabata K, Urasaki Y. Simultaneous determination of azelnidipine and two metabolites in human plasma using liquid chromatography-tandem mass spectrometry. J Chromatogr B Anal Technol Biomed Life Sci. 2006;844:45-452.

23. Guengerich FP, Sari MA, Brian WR, Iwasaki M, Bäärnhielm C, Berntsson P. Oxidation of Dihydropyridine Calcium Channel Blockers and Analogues by Human Liver Cytochrome P-450 IIIA4. J Med Chem. 1991;34:1838-1844.

24. ICH Guideline, Q1A (R2): Stability Testing of New Drug Substances and Products. Last Accessed Date: 17.12.2019. Available from: https://database.ich.org/sites/default/files/Q1A%28R2%29%20Guideline.pdf

25. ICH Guideline, Q2(R1): Validation of Analytical Procedures: Text and Methodology. Last Accessed Date: 12.01.2020. Available from: https://database.ich.org/sites/default/files/Q2%28R1%29%20Guideline.pdf

Turk J Pharm Sci 2021;18(5):557-564
DOI: 10.4274/tjps.galenos.2021.71235

ORIGINAL ARTICLE

Metabolomics-driven Approaches on Interactions Between *Enterococcus faecalis* and *Candida albicans* Biofilms

Enterococcus faecalis ve *Candida albicans* Biyofilmleri Arasındaki Etkileşimler Üzerine Metabolomik Odaklı Yaklaşımlar

Didem KART[1]*, Samiye YABANOĞLU ÇİFTÇİ[2], Emirhan NEMUTLU[3]

[1]Hacettepe University Faculty of Pharmacy, Department of Pharmaceutical Microbiology, Ankara, Turkey
[2]Hacettepe University Faculty of Pharmacy, Department of Biochemistry, Ankara, Turkey
[3]Hacettepe University Faculty of Pharmacy, Department of Analytical Chemistry, Ankara, Turkey

ABSTRACT

Objectives: This study aimed to determine the effect of *Enterococcus faecalis* on the cell growth and hyphal formation of *Candida albicans* and to understand the exact mechanism of candidal inhibition by the existence of *E. faecalis* by metabolomic analysis.

Materials and Methods: Single- and dual-species biofilms of *E. faecalis* and *C. albicans* were formed in a microtiter plate, and the metabolomic profiles of both biofilms was determined by gas chromatography-mass spectrometry. The hyphal cell growth of *C. albicans* after treatment with both the supernatant and biofilm cells of *E. faecalis* was examined microscopically. The expression levels of Efg1 and the images of *C. albicans* cell wall in single- and dual-species biofilms were determined by real-time quantitative polymerase chain reaction and transmission electron microscopy, respectively. The violacein levels produced by *Chromobacterium violaceum* were measured to determine the quorum sensing (QS) inhibitory activity of single- and dual-species biofilms.

Results: The biofilm cell growth, Efg1 expression, and hyphal development of *C. albicans* were inhibited by *E. faecalis*. Compared to single-species biofilms, alterations in carbohydrate, amino acid, and polyamine metabolites were observed in the dual-species biofilm for both microorganisms. Putrescine and pipecolic acid were detected at high levels in dual-species biofilm. A thicker β-glucan chitin and a denser and narrower fibrillar mannan layer of *C. albicans* cell wall were observed in dual-species biofilm. QS inhibitory activity was higher in dual-species biofilm suspensions of *E. faecalis* and *C. albicans* than in their single-species biofilms.

Conclusion: *E. faecalis* inhibited the hyphal development and biofilm formation of *C. albicans*. Biofilm suspensions of *C. albicans* and *E. faecalis* showed an anti-QS activity, which increased even further in the environment where the two species coexisted. Investigation of putrescine and pipecolic acid can be an important step to understand the inhibition of *C. albicans* by bacteria.

Key words: Dual-biofilm, *Candida albicans*, *Enterococcus faecalis*, fungal inhibition, metabolomic

ÖZ

Amaç: *Enterococcus faecalis*'in *Candida albicans*'ın hücre büyümesi ve hifal gelişimi üzerine etkisini değerlendirmeyi ve *E. faecalis* varlığında candidal inhibisyonunun ana mekanizmasını metabolomik analizler ile belirlemeyi amaçladık.

Gereç ve Yöntemler: *E. faecalis* ve *C. albicans*'ın tek ve ikili biyofilmleri mikroplak içinde geliştirildi ve her iki biyofilmin metabolit profili gaz kromatografisi-kütle spektrometresi ile belirlendi. *C. albicans*'ın hifal hücre büyümesi, *E. faecalis*'in hem süpernatant hem de biyofilm hücreleri ile muamelesi sonrasında mikroskobik olarak incelendi. Efg1 ekspresyon seviyeleri ve tek ve ikili biyofilmlerdeki *C. albicans*'ın hücre duvarı görüntüleri sırasıyla RT-qPCR ve transmisyon elektron mikroskobu ile belirlendi. *Chromobacterium violaceum* tarafından üretilen violacein seviyeleri, tek ve ikili biyofilmlerin quorum sensing (QS) inhibitör aktivitelerini belirlemek amacıyla ölçüldü.

*Correspondence: dturk@hacettepe.edu.tr, Phone: +90 533 690 76 37, ORCID-ID: orcid.org/0000-0001-7119-5763

Received: 05.08.2020, Accepted: 11.01.2021

Bulgular: *C. albicans*'ın biyofilm hücre büyümesi, Efg1 ekspresyonu ve hifal gelişimi *E. faecalis* tarafından inhibe edilmiştir. Tekli biyofilmler ile karşılaştırıldığında, her iki mikroorganizma için ikili biyofilmde karbonhidrat, amino asit ve poliamin metabolitlerinde değişiklikler gözlenmiştir. İkili biyofilmde putresin ve pipekolik asit yüksek düzeyde tespit edilmiştir. *C. albicans* hücre duvarının daha kalın β-glukan kitin ve daha yoğun ve daha dar fibrillar mannan tabakası ikili biyofilmde gözlenmiştir. *E. faecalis* ve *C. albicans*'ın ikili tür biyofilm süspansiyonlarında ölçülen QS inhibitör aktivitesinin tekli biyofilmlerine kıyasla daha yüksek olduğu bulunmuştur.

Sonuç: *E. faecalis, C. albicans*'ın hifal gelişimini ve biyofilm oluşumunu inhibe etmiştir. *C. albicans* ve *E. faecalis*'in biyofilm süspansiyonları, iki türün bir arada bulunduğu ortamda daha da artan bir anti-QS aktivitesi göstermiştir. Putresin ve pipekolik asitin araştırılması, *C. albicans*'ın bakteriler tarafından inhibisyonunu anlamak için önemli bir adım olabilir.

Anahtar kelimeler: İkili-biyofilm, *Candida albicans*, *Enterococcus faecalis*, fungal inhibisyon, metabolomik

INTRODUCTION

Biofilms formed in non-sterile mucosal sites are polymicrobial, and interspecies interactions in biofilms vary. They can interact either in a synergistic or antagonistic manner.[1-4] *Candida albicans* and *Enterococcus faecalis* are frequently found together in biofilm-related infections.[5-7] They have common features such as strong biofilm-forming capability that complicates the treatment of chronic infections, especially infections associated with foreign bodies.[8,9]

Microbial metabolomics has attracted great attention in microbiology in recent years.[10,11] To better understand the biofilm structure of microorganisms, metabolic differences between planktonic and biofilm forms of the same microorganism have been investigated, but the results of the polymicrobial biofilm environment containing multiple species have not been reported in the literature yet.[6]

Studies concerning the details of the relationship between *C. albicans* and *E. faecalis* are limited.[4] Thus, this study aimed to investigate the interactions at the metabolic level in the dual-species biofilm model formed by *E. faecalis* and *C. albicans*. The metabolic profile that both cells exhibit alone and in a common biofilm environment were compared by gas chromatography-mass spectrometry (GC-MS)-based metabolic analysis. Besides metabolomics analysis, the effects of each other were also investigated by several analyses including microscopy, quorum sensing (QS), and mRNA expression.

MATERIALS AND METHODS

Microbial strains

E. faecalis ATCC 47077/OG1RF and *C. albicans* ATCC MYA-2876 were cultured in brain heart infusion broth (BHI) (Oxoid, Basingstoke, UK) overnight at 37°C. *Chromobacterium violaceum* ATCC 12472 was grown in Luria Bertani broth (Merck, Darmstadt, Germany).

Effect of E. facealis on C. albicans hyphal morphogenesis

C. albicans were cultured in Yeast extract-peptone-dextrose broth (Merck, Darmstadt, Germany) at 30°C for 24 h. The inoculum suspension of the cell pellet was prepared in Roswell Park Memorial Institute Medium (RPMI) as 10^5 cfu/mL. After the addition of 1 mL of the inoculum to the wells of cell culture slides, which were coated with 20% fetal bovine serum (FBS), they were incubated for 90 min at 30°C. After the incubation period, the wells were rinsed with phosphate-buffered saline (PBS); then, RPMI containing 20% FBS and *E. faecalis* supernatant at a ratio of 1:1 (v/v) were transferred into wells.

To evaluate the direct effect of *E. faecalis* cells on hyphal cells, 50 µL of *E. faecalis* suspension was transferred to *C. albicans*, which had previously adhered to slides via incubation for 90 min. Finally, 950 µL of Spider medium containing 20% FBS was transferred onto slides and incubated at 37°C for 24 h.[4] To assess the effect of *E. faecalis* supernatant on the development of *C. albicans* hyphal cells, the supernatant of *E. faecalis* was used instead of its cell suspension in the same method above. Slides containing biofilms were rinsed with PBS, and microscopic images were acquired using an inverted microscope (Thermo Scientific, MA, USA).

Development of single- and dual-species biofilm models

Inoculum suspensions with final concentrations of ~10^6 cfu/mL for *E. faecalis* and 10^5 cfu/mL for *C. albicans* were made in BHI. Mature biofilms were formed as described previously.[12] Our experimental conditions include the biofilm formation of *E. facealis* and *C. albicans* alone and culturing both microorganisms together.

For the quantification of biofilm cells, plates containing biofilms were sonicated after 5 min of vortexing, thereby allowing biofilm cells to break out of the wells.[12] Tryptic soy agar [(TSA); Merck, Darmstadt, Germany] and sabouraud dextrose agar [(SDA); Merck] were used for the enumeration of single-species *E. faecalis* and *C. albicans* biofilm cells, respectively. For the enumeration of *E. faecalis* and *C. albicans* cells in dual-species biofilms, TSA media with amphotericin B (0.025 mg/mL) and SDA media with vancomycin (0.100 mg/mL) were used.

Quantitative real-time polymerase chain reaction (PCR)

C. albicans biofilms (single and dual) were harvested as described above. The mRNA expression changes of Efg1 in *C. albicans* biofilms were evaluated using qPCR method adopted from a study.[12] The sequence of each primer was compared in *C. albicans* database using Basic Local Alignment Search Tool to assess its specifity.[13,14]

Quantification of violacein in single- and dual-species biofilms

The production of purple-colored violacein, which is regulated by the QS system in *C. violaceum*, is an easily observable and

measurable marker and is widely used in QS research.[15] In the present study, after obtaining *E. faecalis* and *C. albicans* cells and supernatants in single- and dual-species biofilms as described above, QS activities were evaluated by slightly modified violacein measurement analysis according to methods by Sankar Ganesh and Ravishankar Rai[15] The amounts of violacein produced by *C. violaceum* after separate treatment with both cell and supernatant solutions of single- and dual-species biofilms were compared with each other.

Metabolomic analysis

As mentioned above, the biofilms (single and dual) were formed in 96-well micro plates with minor revisions. Shortly, *C. albicans* (10^6 cfu/mL) was attached for 4 h individually. After transferring *E. faecalis* (10^6 cfu/mL) to the culture medium after 4 h, the coculture was incubated at 37°C for 24 h.[16]

The preparation of samples and GC-MS-dependent conditions was conducted following methods reported by previous a study.[16]

Freeze-substitution transmission electron microscopy (TEM) analysis

TEM analysis was applied as described previously.[17] Briefly, *C. albicans* biofilm cells were harvested by sonication and centrifugation as described above. Briefly, the cell pellets were mixed in 1% agarose and moved to the sample carriers. After freeze-substitution of the cells in liquid nitrogen, the samples were embedded in epoxy resin. Ultra-thin sections were obtained (100 nm thickness). Samples were visualized with a Hitachi HT7800 TEM.

Statistical analysis

SPSS version 23 (SPSS, Chicago, IL, USA) was used for the statistical analyses. Groups were compared by Student's t-test. P values <0.05 were significant, and each test was performed at least three times.

Ethics committee approval

The authors declared that an ethics committee approval was not needed for this study.

RESULTS

Effects of E. faecalis supernatant and biofilm cells on C. albicans hyphal morphogenesis and biofilm development

When grown in the common medium, *E. faecalis* biofilm cells prevented the growth of *C. albicans* cells. However, no significant change was seen in the growth of *E. faecalis* (Figure 1). Although it was not statistically significant, *C. albicans* biofilm cell counts treated with biofilm culture supernatant of *E. faecalis* decreased (Figure 1).

To analyze the influence of both *E. faecalis* cells and factors released by *E. faecalis* on *C. albicans* hyphal cell formation, *C. albicans* biofilms were formed on the slides. At 48 h of mature *C. albicans* single-species biofilm formation, a significant number of hyphal cells were observed (Figure 1b). However, the hyphal formation of *C. albicans* cells was inhibited by both *E. faecalis* biofilm cells and its supernatant when they were incubated together (Figure 1c, d).

EFG1 gene expression profile in C. albicans

To research the inhibitory activity of biofilm cells and supernatant of *E. faecalis* on *C. albicans* hyphae formation, Efg1 expression in *C. albicans* was determined by RT-qPCR. The expression of *Efg1* gene in *C. albicans* was significantly downregulated for both treatment ($p<0.05$) (Figure 2).

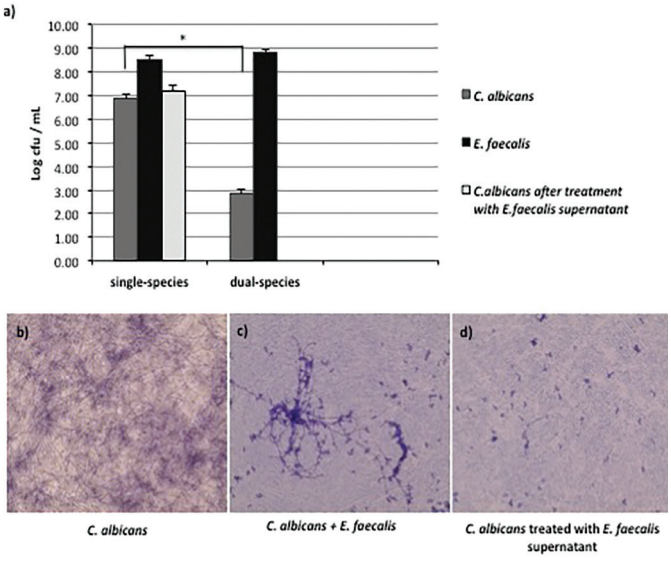

Figure 1. *Enterococcus faecalis* biofilm cells prevent the proliferation and hyphal development of *Candida albicans*. a) Proliferation of cells in single- and dual-species biofilms (cfu/mL). Compared with *C. albicans* in single-species biofilm, *E. faecalis* prevented the proliferation of *C. albicans* cells in dual-species biofilm (*p<0.05). Optical microscope images of b) *C. albicans* biofilm cells formed in six-well cell culture plate. c) *C. albicans* biofilms with *E. faecalis* cells and d) *C. albicans* biofilms exposed to the supernatant of biofilm culture of *E. faecalis*

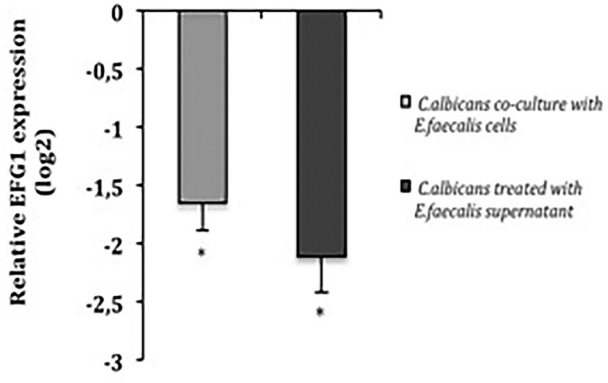

Figure 2. Expression of *Efg1* gene in *Candida albicans*. It was significantly downregulated both in the presence of *Enterococcus faecalis* cells and in treatment with biofilm culture supernatant of *E. faecalis*. Statistical significance (*p<0.05) was relative to untreated *C. albicans* single-species biofilm

Changed metabolite levels in the single- and dual-species biofilms

In this study, GC-MS-based metabolomic analyses were performed to understand how the presence of one microbial species in the dual-species biofilm environment developed by *E. faecalis* and *C. albicans* affects the other at the metabolic level. A total of 172 different metabolites were determined, and 112 of them were identified by the index library. Partial least squares discriminant analysis methods were used for both multivariate statistical analysis of GC-MS metabolomic results and the determination of the differences in metabolomic profiles between single- and dual-species biofilms (Figure 3). First, statistical analysis of the models was performed using R2 and Q2 values. All biofilms with values >0.7 show that the method was valid and the models were stable.

The changed metabolite levels determined in the biofilms (single and dual) are shown separately in Table 1. No significant difference was found in the amounts of the remaining tricarboxylic acid (TCA) cycle intermediates, except for succinate and citric acid in both biofilms of *E. faecalis* (Table 1). This result is not surprising considering that *E. faecalis* lacks the TCA cycle. *C. albicans* has lower concentrations of TCA intermediates in the dual-species biofilm than in the single-species biofilm (Table 1). Levels of maltose, glucose, and leucrose were high in *C. albicans* biofilm alone. The existence of *E. faecalis* in the same environment caused a significant decline in the amounts of these metabolites.

When comparing both biofilms (single and dual), the concentrations of valine, leucine, glycine, methionine, threonine, and phenylalanine were significantly reduced, specifically for *E. faecalis*, and a decrease in the level of tyrosine was also notable for *C. albicans*. Putrescine and pipecolic acid concentrations in the dual-species biofilm remained significant, which are the most promising results of this study.

Changes in Candida cell wall architecture in single- and dual-species biofilms

The cell wall biomass was significantly different in dual-species biofilm including the thicker β-glucan-chitin layer and the more dense and narrower fibrillar layer of mannan, when compared with the cells in biofilm alone (Figure 4).

Measurement of violacein in single- and dual-species biofilms

The amount of violacein produced by *C. violaceum* was determined in single- and dual-species biofilms formed by *E. faecalis* and/or *C. albicans* (Figure 5). Compared with untreated media containing only *C. violaceum* (control), *C. violaceum* produced less violacein after separate treatment of *E. faecalis* and *C. albicans* single- and dual-species biofilms with both supernatant and cell culture suspensions. When single- and dual-species biofilms of both microorganisms were compared, *C. violaceum*, which was treated with both cell and supernatant suspensions of the dual-species biofilms, produced less violacein for all test conditions, except for the supernatant of *E. faecalis*.

DISCUSSION

Infections are often considered and treated as a condition caused by a single microorganism; however, in several microorganisms, coexistence of many human microbiome members is observed. These microorganisms live together harmoniously under physiological conditions. Many environmental factors may disrupt this balance; consequently, single or several species become dominant in the environment.[18]

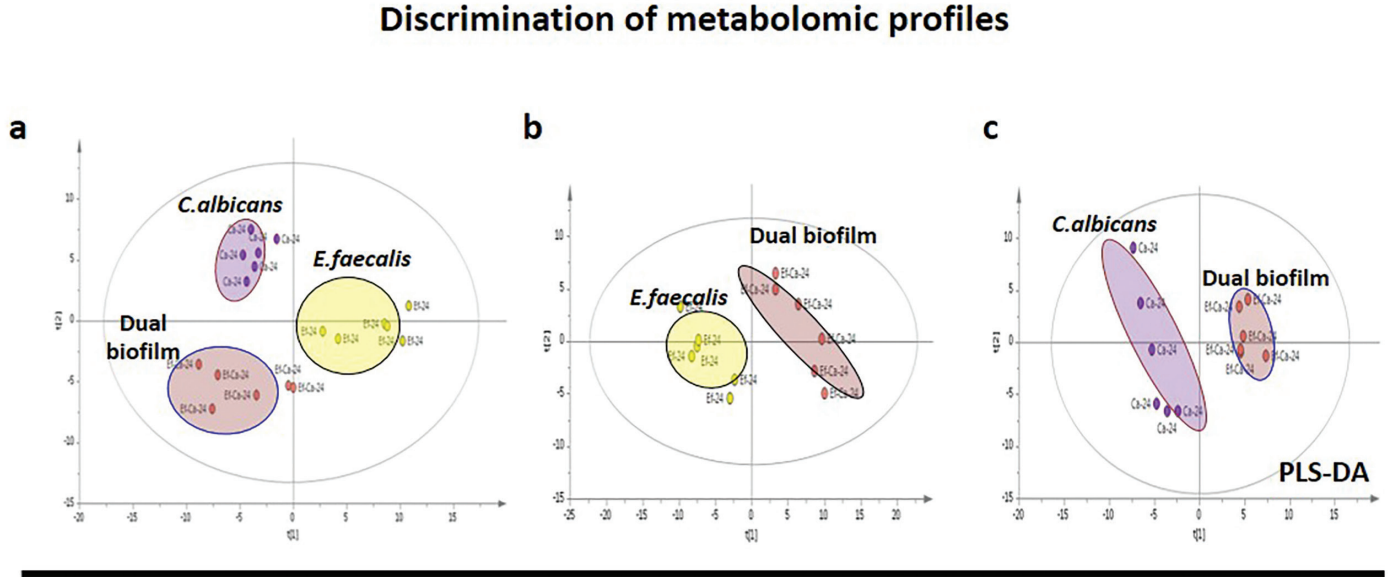

Figure 3. a) PLS-DA score graphs of single- and dual-species biofilm of *Candida albicans* for metabolomic profile comparison. b) PLS-DA score plots show clear separation between *Enterococcus faecalis* and its dual-species biofilm. c) PLS-DA score plots demonstrate apparent distinction with *C. albicans* and its dual-species biofilm. Each circle represents the sharp metabolomic distinction in the biofilms

PLS-DA: Partial least squares discriminant analysis

Table 1. Relative metabolite amounts in the biofilms of *Enterococcus faecalis* or *Candida albicans*

Metabolites	Ef-Ca/Ca		Ef-Ca/Ef		Pathways
Tricarboxylic acid cycle					
Citric acid	0.09***	↓	3.95**	↑	Carbohydrate metabolism
Fumaric acid	0.49*	↓	1.58**	↑	
Lactic acid	0.38**	↓	-		
Malic acid	2.1**	↑	-		
Ketoglutaric acid	5.42**	↑	-		
Oxalic acid	0.4**	↓	-		
Pyruvic acid	-		-		
Succinate	0.45*	↓	0.3**	↓	
Maltose	0.49*	↓	5.11**	↑	
Glucose	0.29**	↓	-		
Leucrose	0.49*	↓	5.43**	↑	
Amino acid metabolism					
Cysteine	0.21**	↓	0.44*	↓	Amino acid metabolism
Serine	0.15***	↓	0.4**	↓	
Threonine	-		0.33**	↓	
Aspartate	2.05**	↑	-		
Glutamic acid	2.37**	↑	1.63**	↑	
Proline	0.40**	↓	0.41**	↓	
Tyrosine	0.06***	↓	-		
Valine	-		0.36**	↓	
Leucine	-		0.33**	↓	
Alanine	0.44**	↓	0.45*	↓	
Glysine	-		0.40**	↓	
Methionine	-		0.37**	↓	
Lysine	-		-		
Tryptophan	-		-		
Phenylalanine	-		0.43**	↓	
Metabolism of nitrogen-containing compounds					
Urea	-		0.45*	↓	Nitrogen metabolism
Ornithine	8.74***	↑	-		
Ornithine-arginine	7.33***	↑	-		
Creatine	-		0.43**	↓	
Other metabolisms					
Putrescine	9.99***	↑	3.38***	↑	Polyamine metabolism
Pipecolic acid	24.2***	↑	14.10***	↑	
Ethanolamine	-		3.09**	↑	Lipid metabolism
Glycerol-1-phosphate	-		9.37***	↑	
Glycerol	-		2.53**	↑	

*Compared with dual-species biofilm, the metabolite level was significantly changed in single-species biofilm, *p<0.5, **p<0.05, ***p<0.001

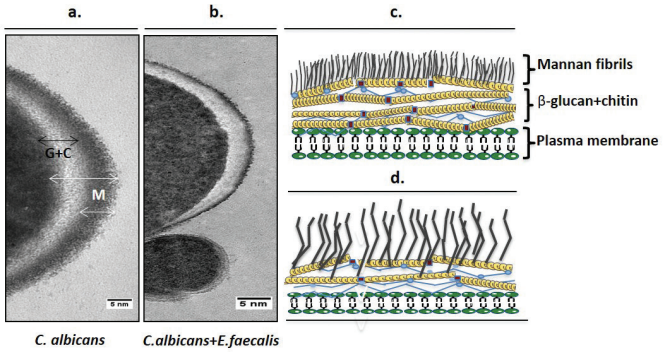

Figure 4. Visualizaton of *Candida albicans* cell walls grown in single-species (a) and dual-species biofilms (b). (Figures consisted of ≈100 cell images); bar, 5 nm. G + C, β-glucan and chitin; M, mannan. Drawings representing the possible structural changes are shown in c (for the cell wall of *C. albicans* in dual-species biofilm) and d (for the cell wall of *C. albicans* in single-species biofilm)

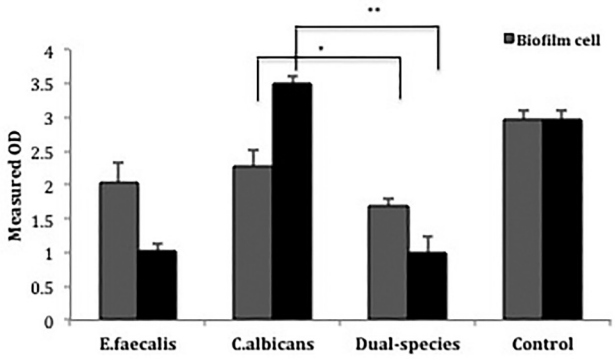

Figure 5. Quantitative measurement of violacein in both single- and dual-species biofilms. Asterisks indicate significance ($p<0.05$). A significant decrease was shown for all test conditions compared with the control

In this study, the effect of the interaction between *E. faecalis* and *C. albicans* on biofilm formation was investigated based on microscopy and metabolomics. The results revealed that in dual-species biofilms, the proliferation of *E. faecalis* is not affected by the presence of *C. albicans*; however, the existence of these species in the same environment has an antagonistic effect on the growth of *C. albicans* (Figure 1). Compared with controls, the reduction of the production of violacein, which provides QS signal communication in *C. violaceum* treated by single-biofilm cells of *C. albicans*, also indicates the presence of a molecule that provides *C. albicans*-induced anti-QS activity in the environment.

In this study, compared with the untreated *C. albicans* cells, the number of *C. albicans* hyphal cells decreased when treated with cell suspension or supernatant of *E. faecalis* biofilm (Figure 2). Therefore, both *E. faecalis* cells and factors released into the medium have been found to inhibit the hyphal development of *Candida*. Similar to this finding, in recent studies, bacterial-fungal cooccurrence has been reported to have an antagonizing effect on *Candida* cell growth. A study that investigated the interference between *C. albicans* and *Lactobacillus* species showed that *C. albicans* did not grow on the surface of the vaginal mucosa because of the lactic acid produced by the *Lactobacillus* species.[19] The coexistence of *Staphylococcus aureus* and *C. albicans* in the biofilm environment leads to a substantial increase in the attachment and colonization abilitity of *S. aureus*. Thus, *S. aureus* can use *C. albicans* hyphal cells as a scaffold to the development of a biofilm.[20]

In this study, the coexistence of *E. faecalis* and *C. albicans* in the biofilm model developed may have supported the formation of an anaerobic environment because of increased oxygen consumption. Under this condition, *Candida* relies on the glycolytic pathway to produce energy. No significant difference was found in the single- and dual-species biofilms of *E. faecalis* in glucose consumption. The elevated levels of maltose and leucrose in the dual-species biofilm are thought to be caused by the existence of *C. albicans*. The bacteria within the biofilm are exposed to various environmental conditions, causing the population to be highly heterogeneous in terms of oxygen content.[21] Fox et al.[22] showed that the hypoxic nature of *C. albicans* biofilms supports the growth of anaerobic bacteria that share the same environment.

Compared with *C. albicans* alone, reduced amounts of citric acid, fumaric acid, and oxalic acid in the dual-species biofilm indicate that *C. albicans* need more energy in the presence of *E. faecalis*. A study reported that α-ketoglutarate dehydrogenase, a TCA cycle enzyme, is suppressed by Efg1, which is a crucial factor for the hyphal development of *C. albicans*.[23] The downregulation of Efg1 in *C. albicans* obtained in our study may have led to the suppression of a-ketoglutarate dehydrogenase, which may lead to the transition of *C. albicans* into the glyoxylate cycle. Thus, it can be a reason for the accumulation of large amounts of ketoglutaric acid and malic acid in the dual-species biofilm.

Glycerol metabolism is an important pathway for the synthesis of lipids and (lipo) teichoic acids in *E. faecalis*. Lipids, one of the main membrane components, are needed for energy accumulation.[24] *E. faecalis* has increased lipid-related metabolite synthesis when grown with *C. albicans*. This increase indicates the greater need for lipid-related cell membrane products such as phospholipids and/or lipoteichoic acids in *E. feacalis*.

Putrescine, an important polyamine in cellular survival, does not support cell proliferation in low amounts; by contrast, the overabundant quantity of internal cells led to the inhibition of cell proliferation.[25,26] In this study, one of the most important differences was the concentration of putrescine. Compared with *C. albicans* biofilm alone, it enhanced approximately by 10- and 3.4-fold in dual-species biofilm and *E. faecalis*, respectively. In our previous study, the high level of putrescine detected in the dual-species biofilms formed by *C. albicans* and *Proteus mirabilis* supports our current data.[16]

Another interesting result of our study was that the pipecolic acid level increased by 24- and 14-fold for *C. albicans* and *E. faecalis* in dual-species biofilm environment when compared with both *C. albicans* and *E. faecalis* single biofilms, respectively. The naturally occurring alkyl derivatives of pipecolic acid

(piperidine-2-carboxylic acid) are structural components of many biologically active compounds.[27] Detailed studies have also shown that the organic compound pipecolic acid is an osmoprotectant and plays a role in protecting macromolecules from denaturation. In the osmoregulation stages, which are generally the same in all living organisms, the first stage is the accumulation of potassium and glutamate, followed by the accumulation of small organic compounds by intracellular synthesis or uptake by external media.[28] In our study, higher levels of sugars such as maltose and leucrose in the dual-species biofilm than *E. faecalis* biofilm alone may have been a threat for *E. faecalis* because of increased osmolarity. *E. faecalis* may have synthesized pipecolic acid known to be an osmoprotectant to deal with this threat. The synthesis of bacterial pipecolic acid is a byproduct during the catalysis of the proline amino acid, which may explain the low level of proline in the dual-species biofilm obtained from our study.

The alterations in the yeast cell wall as an adaptation to osmotic stress have been highlighted in the literature.[29] We detected the more dense and shorter mannan layer and thicker β-glucan-chitin layer in *Candida* cell wall grown in dual-species biofilm than in the single-species biofilm. In both cases, alterations in the cell wall of *C. albicans* are similar to those in cells with and without salt-induced osmotic stress in the study of Ene et al.[29] This strengthens the possibility of increased osmotic stress in the dual-species biofilm environment.

Compared with the single-species biofilm of both microorganisms, significant decrease was observed in many amino acid levels in the dual-species biofilm. This reduction in amino acid levels in the dual-species biofilm shows that anabolic reactions are dominant for both species to grow, develop, and multiply. Clearly, amino acid synthesis is required for *C. albicans* biofilm development

CONCLUSION

The metabolite diversity of both microorganisms, which was affected by each other by increasing the cellular stress due to high carbohydrate consumption, more energy needs, etc., was demonstrated in our results. The high levels of putrescine and pipecolic acid synthesized as osmoprotectant by both species may have suppressed the growth of *Candida*. This study provided preliminary data for a detailed investigation of the possible role of putrescine and pipecolic acid in the prevention of *C. albicans* via bacterial species.

Conflict of interest: No conflict of interest was declared by the authors. The authors are solely responsible for the content and writing of this paper.

Funding sources: This work was supported by funding from TUBITAK (grant no. 115S550).

REFERENCES

1. Burmolle M, Ren DW, Bjarnsholt T, Sorensen SJ. Interactions in multispecies biofilms: do they actually matter? Trends Microbiol. 2014;22:84-91.
2. Morales DK, Grahl N, Okegbe C, Dietrich LEP, Jacobs NJ, Hogan DA. Control of *Candida albicans* metabolism and biofilm formation by *Pseudomonas aeruginosa* phenazines. mBio. 2013;4:e00526-12.
3. Tampakakis E, Peleg AY, Mylonakis E. Interaction of *Candida albicans* with an intestinal pathogen, *Salmonella enterica* Serovar Typhimurium. Eukaryot Cell. 2009;8:732-737.
4. Cruz MR, Graham CE, Gagliano BC, Lorenz MC, Garsin DA. *Enterococcus faecalis* inhibits hyphal morphogenesis and virulence of *Candida albicans*. Infect Immun. 2013;81:189-200.
5. Ten Oever J, Netea MG. The bacteriome-mycobiome interaction and antifungal host defense. Eur J Immunol. 2014;44:3182-3191.
6. Pfaller MA, Diekema DJ. Epidemiology of invasive mycoses in North America. Crit Rev Microbiol. 2010;36:1-53.
7. Wenner JJ, Rettger LF. A systematic study of the Proteus group of bacteria. J Bacteriol. 1919;4:331-353.
8. Nobile CJ, Johnson AD. *Candida albicans* biofilms and human disease. Annu Rev Microbiol. 2015;69:71-92.
9. Mayer FL, Wilson D, Hube B. *Candida albicans* pathogenicity mechanisms. Virulence. 2013;4:119-128.
10. Reaves ML, Rabinowitz JD. Metabolomics in systems microbiology. Curr Opin Biotechnol. 2011;22:17-25.
11. Xu YJ, Wang CS, Ho WE, Ong CN. Recent developments and applications of metabolomics in microbiological investigations. Trac-Trend Anal Chem. 2014;56:37-48.
12. Kart D, Tavernier S, Van Acker H, Nelis HJ, Coenye T. Activity of disinfectants against multispecies biofilms formed by *Staphylococcus aureus*, *Candida albicans* and *Pseudomonas aeruginosa*. Biofouling. 2014;30:377-383.
13. Bandara HM, Cheung BP, Watt RM, Jin LJ, Samaranayake LP. Secretory products of *Escherichia coli* biofilm modulate *Candida* biofilm formation and hyphal development. J Investig Clin Dent. 2013;4:186-199.
14. Altschul SF, Madden TL, Schaffer AA, Zhang J, Miller W, Lipman DJ. Gapped BLAST and PSI-BLAST: a new generation of protein database search programs. Nucleic Acids Res. 1997;25:3389-3402.
15. Sankar Ganesh P, Ravishankar Rai V. Attenuation of quorum-sensing-dependent virulence factors and biofilm formation by medicinal plants against antibiotic resistant *Pseudomonas aeruginosa*. J Tradit Complement Med. 2018;8:170-177.
16. Kart D, Yabanoglu Ciftci S, Nemutlu E. Altered metabolomic profile of dual-species biofilm: interactions between *Proteus mirabilis* and *Candida albicans*. Microbiol Res. 2020;230:126346.
17. Netea MG, Gow NA, Munro CA, Bates S, Collins C, Ferwerda G, Hobson RP, Bertram G, Hughes HB, Jansen T, Jacobs L, Buurman ET, Gijzen K, Williams DL, Torensma R, McKinnon A, MacCallum DM, Odds FC, Van der Meer JW, Brown AJ, Kullberg BJ. Immune sensing of *Candida albicans* requires cooperative recognition of mannans and glucans by lectin and Toll-like receptors. J Clin Invest. 2006;116:1642-1650.
18. Gulati M, Nobile CJ. Candida albicans biofilms: development, regulation, and molecular mechanisms. Microbes Infect. 2016;18:310-321.
19. Strus M, Kucharska A, Kukla G, Brzychczy-Wloch M, Maresz K, Heczko PB. The in vitro activity of vaginal *Lactobacillus* with probiotic properties against *Candida*. Infect Dis Obstet Gynecol. 2005;13:69-75.
20. Kean R, Rajendran R, Haggarty J, Townsend EM, Short B, Burgess KE, Lang S, Millington O, Mackay WG, Williams C, Ramage G. *Candida albicans*

mycofilms support *Staphylococcus aureus* colonization and enhances miconazole resistance in dual-species interactions. Front Microbiol. 2017;8:258.

21. Blank LM, Sauer U. TCA cycle activity in Saccharomyces cerevisiae is a function of the environmentally determined specific growth and glucose uptake rates. Microbiology (Reading). 2004;150:1085-1093.
22. Fox EP, Cowley ES, Nobile CJ, Hartooni N, Newman DK, Johnson AD. Anaerobic bacteria grow within *Candida albicans* biofilms and induce biofilm formation in suspension cultures. Curr Biol. 2014;24:2411-2416.
23. Pan J, Hu C, Yu JH. Lipid biosynthesis as an antifungal target. J Fungi (Basel). 2018;4:50.
24. Doedt T, Krishnamurthy S, Bockmühl DP, Tebarth B, Stempel C, Russell CL, Brown AJ, Ernst JF. APSES proteins regulate morphogenesis and metabolism in Candida albicans. Mol Biol Cell. 2004;15:3167-3180.
25. Porat Z, Wender N, Erez O, Kahana C. Mechanism of polyamine tolerance in yeast: novel regulators and insights. Cell Mol Life Sci. 2005;62:3106-3116.
26. Valdes-Santiago L, Ruiz-Herrera J. Stress and polyamine metabolism in fungi. Front Chem. 2014;1:42.
27. Hibi M, Mori R, Miyake R, Kawabata H, Kozono S, Takahashi S, Ogawa J. Novel enzyme family found in filamentous fungi catalyzing trans-4-hydroxylation of l-pipecolic acid. Appl Environ Microbiol. 2016;82:2070-2077.
28. Gouesbet G, Jebbar M, Talibart R, Bernard T, Blanco C. Pipecolic acid is an osmoprotectant for *Escherichia coli* taken up by the general osmoporters ProU and ProP. Microbiology (Reading). 1994;140:2415-2422.
29. Ene IV, Walker LA, Schiavone M, Lee KK, Martin-Yken H, Dague E, Gow NA, Munro CA, Brown AJ. Cell wall remodeling enzymes modulate fungal cell wall elasticity and osmotic stress resistance. mBio. 2015;6:e00986.

Turk J Pharm Sci 2021;18(5):565-573
DOI: 10.4274/tjps.galenos.2021.91145

ORIGINAL ARTICLE

Development and Validation of a Discriminative Dissolution Medium for a Poorly Soluble Nutraceutical Tetrahydrocurcumin

Zayıf Çözünür Bir Nutrasötik Olan Tetrahidrokurkumin İçin Ayırt Edici Bir Dissolüsyon Ortamının Geliştirilmesi ve Yöntemin Doğrulanması

Habibur Rahman SHIEK ABDUL KADHAR MOHAMED EBRAHIM[1]*, Telny Thomas CHUNGATH[2], Karthik SRIDHAR[1], Karthik SIRAM[1], Manogaran ELUMALAI[3], Hariprasad RANGANATHAN[1], Sivaselvakumar MUTHUSAMY[4]

[1]PSG College of Pharmacy, Department of Pharmaceutics, Coimbatore, India
[2]Chemists College of Pharmaceutical Sciences and Research, Department of Pharmaceutical Analysis, Ernakulum, India
[3]UCSI University Faculty of Pharmaceutical Sciences, Department of Pharmacology, Kuala Lumpur, Malaysia
[4]PSG Institute of Medical Sciences & Research Centre for Molecular Medicine and Therapeutics, Department of Pharmaceutical Analysis, Coimbatore, India

ABSTRACT

Objectives: The present study aimed to develop and validate a discriminative dissolution method for tetrahydrocurcumin (THC), a Biopharmaceutical Classification System class II drug, by a simple ultraviolet (UV) spectrophotometric analysis. The final dissolution medium composition was selected based on the solubility and stability criteria of the drug.

Materials and Methods: As a prerequisite for this, the solubility of the drug was assessed in media of different pH (1.2-7.4), and surfactant concentrations of 0.5-1.5% (w/v) sodium lauryl sulfate (SLS) in water, and pH 7.4 phosphate buffer. The dissolved drug concentration in each medium was quantified by UV analysis at 280 nm wavelength.

Results: The drug solubility was found to be high at a pH of 1.2 and 7.4. The media with surfactant enhanced solubility of the drug by approximately 17-fold and exhibited better sink conditions. The discriminative power of the developed dissolution medium (i.e., 1% w/v SLS in pH 7.4) was determined by performing *in vitro* dissolution studies of the prepared THC tablets and comparing their release profiles using fit factors (f1 and f2). The results of the fit factor comparisons made between the dissolution profiles of THC tablets proved the discriminative ability of the medium. The validation of the developed dissolution method was performed by international guidelines and the method showed specificity, linearity, accuracy, and precision within the acceptable range.

Conclusion: The proposed dissolution method was found to be adequate for the routine quality control analysis of THC, as there is no specified dissolution method for the drug in the pharmacopoeia.

Key words: Tetrahydrocurcumin, sodium lauryl sulfate, solubility, dissolution medium, dissolution comparison, fit factors

ÖZ

Amaç: Bu çalışma, bir Biyofarmasötik Sınıflandırma Sistemi sınıf II ilacı olan tetrahidrokurkumin (THC) için basit bir ultraviyole (UV) spektrofotometrik analiz ile tayinini sağlayacak bir dissolüsyon yöntemi geliştirmeyi ve doğrulamayı amaçlamıştır. Nihai dissolüsyon ortamı bileşimi, ilacın çözünürlük ve stabilite kriterlerine göre seçildi.

Gereç ve Yöntemler: Bunun için bir ön koşul olarak, ilacın çözünürlüğü suda ve pH 7,4 fosfat tamponunda farklı pH (1,2-7,4) değerlerinde ve %0,5-1,5 (a/h) sodyum lauril sülfat (SLS) yüzey aktif madde konsantrasyonlarında değerlendirildi. Her bir ortamdaki çözünmüş ilaç konsantrasyonu, 280 nm dalga boyunda UV analizi ile ölçülmüştür.

Bulgular: İlaç çözünürlüğünün pH 1,2 ve 7,4'te yüksek olduğu bulundu. Yüzey aktif madde içeren ortam, ilacın çözünürlüğünü yaklaşık 17 kat artırdı ve daha iyi sink koşulları sergiledi. Geliştirilen çözünme ortamının ayırt edici gücü (pH 7,4'te %1 w/v SLS), hazırlanan THC tabletlerinin *in vitro* çözünme çalışmaları yapılarak ve uygunluk faktörleri (f1 ve f2) kullanılarak salım profillerinin karşılaştırılması yoluyla belirlendi. THC tabletlerin

*Correspondence: hablet1@gmail.com, Phone: 09894229078, ORCID-ID: orcid.org/0000-0003-2609-4677
Received: 29.07.2020, Accepted: 19.01.2021

çözünme profilleri arasında yapılan uyum faktörü karşılaştırmalarının sonuçları, ortamın ayırt etme kabiliyetini kanıtlamıştır. Geliştirilen çözünme yönteminin validasyonu uluslararası kılavuzlar kullanılarak gerçekleştirildi ve yöntem kabul edilebilir aralık içinde özgüllük, doğrusallık, doğruluk ve kesinlik gösterdi.

Sonuç: Farmakopede ilaç için belirlenmiş bir dissolüsyon yöntemi olmadığından önerilen dissolüsyon yöntemi THC'nin rutin kalite kontrol analizi için yeterli bulunmuştur.

Anahtar kelimeler: Tetrahidrokurkumin, sodyum lauril sülfat, çözünürlük, çözünme ortamı, çözünme karşılaştırması, uyum faktörleri

INTRODUCTION

In recent years, significant attention has been paid to nutraceuticals, as they are advantageous over synthetic drugs having many pharmacological actions with little or no toxic effects. However, the bioavailability of nutraceuticals is often compromised due to their poor aqueous solubility. Many formulation methods have been proposed to enhance the solubility and bioavailability of these hydrophobic entities.[1] Dissolution testing is an important quality control tool to identify the effects of manufacturing variability on product performance and to ensure batch to batch equivalence.[2] In this context, there is an utmost need for a suitable and validated dissolution method for analyzing the nutraceutical formulations which endorses the development.

The choice of a medium for the dissolution studies of class II drugs of the Biopharmaceutical Classification System (BCS) is critical, and developing a suitable dissolution media has always been a challenge because of the hydrophobicity exhibited by the drugs of this class. More importance should be given to the solubility factor of a drug while designing a dissolution method. The medium used should be able to homogenously solubilize the drug for an accurate quantification of the released amount from the total drug dose of the dosage form at each time interval. On the other hand, the solubility of a drug is directly or indirectly dependent on many variables like the pH of the medium, temperature, log P, pK_a, and ionic behavior of the drug.[3] Maintaining large aqueous sink conditions, alteration of pH, and addition of co-solvents or surfactants are a few approaches that have been adopted in the development of a dissolution medium for poorly soluble drugs.[4] Addition of surfactants is preferred widely as they enhance the solubility of hydrophobic drugs by reducing the surface tension of the medium, increasing the wetting of the drug, and by micellar solubilization [above critical micelle concentration (CMC)] in the media. Although bile salts in the gastro-intestinal (GI) system acts as surfactants that help in solubilization of the drug *in vivo*, use of these bile salts externally for routine *in vitro* analysis is not possible as they are expensive. Hence, the use of surfactants in the dissolution medium may serve well as a reliable alternative to mimic GI conditions.[5] Among the different surfactants, anionic surfactants, like sodium lauryl sulfate (SLS),[6-8] and non-ionic surfactants, like polysorbate-80, were commonly used by the researchers.[9,10]

Moreover, the medium chosen to perform the *in vitro* dissolution studies of drug formulations should be discriminative enough to differentiate drug release patterns and help in identifying the formulation and process variables that affect the release of the drug from the dosage form during the initial stages of product development.[11] For this purpose, the *in vitro* dissolution profiles of different batches of the formulation are often compared to understand the similarities or differences in the release pattern. Various statistical methods like analysis and calculated by a least square regression method and analysis of variance (ANOVA), model-dependent, and model independent approaches are being adopted to compare the dissolution profiles.[12,13] Determination of fit factors, which include difference factor (f1) and similarity factor (f2), are one of the effective and feasible model independent methods of dissolution comparison. The Food and Drug Administration (FDA) also recommends the use of these fit factors for dissolution comparison in the guides for industry.[14-16]

The natural herb curcumin [(1E,6E)-1,7-Bis(4-hydroxy-3-methoxyphenyl)-1,6-heptadiene-3,5-dione] falls under the category of nutraceuticals, and tetrahydrocurcumin [(THC), 1,7-Bis(4-Hydroxy-3-Methoxyphenyl)Heptane-3,5-Dione] is one of the active metabolites of curcumin that exhibits similar pharmacological actions.[17] THC showed potent anti-inflammatory and antioxidant effects while compared to other curcuminoids.[18] It inhibits the amyloid precursor protein based on QSAR studies and has the potential to be utilized to treat Alzheimer's disease.[19] The bioavailability of THC is limited due to its poor solubility and absorption. The aqueous solubility of these drugs is low, and hence, it is classified into class II of BCS.[20] The role of pH and surfactants in the dissolution of curcumin was previously studied by Rahman et al.[21] In the present study, an attempt was made to develop a suitable dissolution medium for *in vitro* analysis of THC by employing a surfactant to enhance its solubility and to maintain the sink conditions. To the best of our knowledge, no previous study on the dissolution medium development for THC has been done. The solubility of THC in different pH media and in the presence of anionic surfactant SLS was studied, and the effect of different media on the solubility of the drug was assessed. The discriminative power of the developed dissolution medium was determined by comparing the dissolution profiles of the prepared THC tablets using fit factors (f1 and f2).

MATERIALS AND METHODS

Materials

THC was a gift sample from Sami labs (Bangalore, India). SLS, disodium hydrogen phosphate, sodium dihydrogen phosphate, sodium acetate trihydrate, hydrochloric acid, and

glacial acetic acid were purchased from Himedia (Mumbai, India). Microcrystalline cellulose [(MCC), Avicel PH 102, FMC biopolymer, USA] and polyvinyl pyrrolidone (Povidone K 30, BASF, Ludwigshafen, Germany) were purchased from Signet chemical corporation Pvt. Ltd. (Mumbai, India). Sodium starch glycolate (SSG), magnesium stearate, and talc were purchased from Amishi drugs and chemicals Pvt. Ltd. (Ahmedabad, India).

Media preparation for dissolution studies

The buffer solution of pH 1.2 [0.1 N Hydrochloric acid (HCl)] was prepared by dissolving 8.5 mL of concentrated HCl in 1000 mL of purified water. The acetate buffer of pH 4.0 was prepared by transferring 362 mL of 0.2 M glacial acetic acid + 148 mL of 0.2 M sodium acetate solution into a volumetric flask, and the volume was made up to 1000 mL with purified water. For the preparation of phosphate buffers, 0.2-M sodium dihydrogen phosphate (NaH_2PO_4) and 0.2-M disodium hydrogen phosphate (Na_2HPO_4) solutions were prepared initially. Then 255 mL of 0.2-M NaH_2PO_4 + 245 mL of 0.2-M Na_2HPO_4 and 100 mL of 0.2-M NaH_2PO_4 + 400 mL of 0.2-M Na_2HPO_4 were mixed to obtain buffer solutions of pH 6.8 and 7.4, respectively. The pH of the solutions was adjusted with NaOH or acetic acid, and final, they volume was made up to 1000 mL with a purified water.

Formulation of THC tablets by direct compression method

THC tablets were prepared in our lab since no commercial THC tablets are available in the market yet. The tablets were prepared using MCC, Avicel PH 102 as filler, polyvinyl pyrrolidone (Povidone K-30) as a binder, and SSG as a disintegrating agent. Magnesium stearate and talc were used as an antiadhesive agent and glidant. Three different tablet batches: TF1, TF2, and TF3 with three different concentrations of binder (5%, 7.5%, and 10% w/w) were formulated to determine the effect of binding strength on drug release and to evaluate the discriminative ability of the dissolution medium in identifying formulation changes among the three tablet batches. The amount of drug was equivalent to 100 mg in every tablet, and the total tablet weight was 200 mg (Table 1).

Before preparing the tableting mixtures, all the materials were sieved manually through a sieve with a mesh size of 0.595 mm. The weighed quantities of the drug, filler, disintegrant, and binder were mixed in a polybag for 10 min. Finally, magnesium stearate and talc were added to the initial mixture and blended for 3 min. A total of 100 tablets from each batch with a 8.7-mm diameter and 4.6-mm thickness were produced by the direct compression method using Rimek minipress II (Karnavati engineering Ltd., Ahmedabad, India). All tablets were compressed with a constant compression pressure of 12 kN.

Determination of mechanical strength of the tablet

The mechanical strength or crushing strength of the prepared tablets was determined by using the tablet testing apparatus (Model DHT-250, THERMONIK, Campbell electronics, Mumbai, India).

Determination of critical micellar concentration

The micelle formation is an intrinsic property of a surfactant which plays a major role in the solubilization of the drug. The two generally accepted models explaining the aggregation of surfactant monomers into micelles are the "mass-action model" and the "phase-separation model", and the concentration of surfactant at which the micelles are formed (CMC) is dependent on many factors.[22,23] The CMC of SLS in water and pH 7.4 phosphate buffers (PB) were determined by dye solubilization and drop number methods prior to the solubility studies of the drug in these media. In the former method, eosin Y was added to various concentrations of SLS (0.25-2% w/v) prepared in water and pH 7.4 PBs, and shaken for 24 hr at 37°C. The residue was filtered, and the absorbance of the resultant solutions was measured at 542 nm (λ_{max} of eosin Y) using a ultraviolet (UV)-visible spectrophotometer (Shimadzu1650PC, Tokyo, Japan). The obtained absorbance values were plotted against the concentrations of a surfactant expressed in millimoles (0.009-0.069 mM/mL: 0.25-2% w/v).[24] The surface tension of the surfactant solutions prepared in water and pH 7.4 PBs were also determined by the drop number method using the following equation:

$$\frac{\gamma_l}{\gamma_w} = \frac{n_w}{n_l} \times \frac{d_l}{d_w},$$

where $\gamma_l\ \gamma_l$ and $\gamma_W\ \gamma_W$ are surface tensions of the liquid in test and water (71.97 dynes/cm), $n_W\ n_W$ and $n_l\ n_l$are number of drop counts for water and liquid, and $d_l\ d_l$ and $d_W\ d_W$ are the densities of liquid and water.

Table 1. Composition of prepared tetrahydrocurcumin tablets showing weight in mg of excipients per tablet for a total average tablet weight of 200 mg

	TF1		TF2		TF3	
Ingredients	**Weight per tablet (mg)**	**w/w %**	**Weight per tablet (mg)**	**w/w %**	**Weight per tablet (mg)**	**w/w %**
THC	100	50%	100	50%	100	50%
Avicel PH 102	80	40%	75	37.5%	70	35%
Sodium starch glycolate	6	3%	6	3%	6	3%
Povidone K-30	10	5%	15	7.5%	20	10%
Magnesium stearate	2	1%	2	1%	2	1%
Talc	2	1%	2	1%	2	1%

THC: Tetrahydrocurcumin

A plot of surface tension vs. log concentrations of surfactant in millimoles (-2.665 to -1.158 mM/mL equivalent to 0.25-2% w/v) was made to determine the point of micelle formation in both the media.[25]

Solubility study of pure THC

To assess the role of pH and surfactant in the solubility of THC, the equilibrium solubility of the drug was determined in dissolution media of different pH (1.2-7.4) and 0.5-1.5% (w/v) SLS in water (pH 5.5) and PB (pH 7.4). Excess of drug (approximately 50 mg) was poured into 20 mL of each of the media and were kept over the shaker at 37˚C and shaken for 2 hr. Then, 2 mL of samples were withdrawn at the end of 1 h and 2 h, filtered (0.45 µ pore size cellulose esters membrane filter, Millipore Corp., Billerica, MA, USA) and diluted in methanol. The concentration of the dissolved drug in each medium was determined by measuring the absorbance and correlating it with the standard concentration curve of THC built using a UV-visible spectrophotometer (Shimadzu 1650PC, Tokyo, Japan) at a corresponding wavelength of 280 nm (λ_{max} of THC). The solubility parameter was kept as one of the main criteria for selecting the composition of the dissolution medium.

Dissolution method validation for the analysis of THC tablets

The developed dissolution method was validated by evaluating specificity, accuracy, precision, linearity, filter suitability, and stability.

Specificity

Specificity testing was done to demonstrate the absence of interference of excipients or dissolution medium with the drug response at 280 nm. For this purpose, the solutions of placebo (excipients without drug), placebo with drug, and reference standard was prepared and analyzed in a UV spectrophotometer (Shimadzu 1650PC, Tokyo, Japan).

Accuracy and precision

The accuracy of the method was determined by the recovery test of a known amount of THC added to the placebo. An initial stock solution was prepared in methanol, and the final concentrations of 4.8, 6, and 7.2 µg mL^{-1} in dissolution medium were obtained corresponding to 80%, 100%, and 120% of the nominal assay concentration. The samples were analyzed in triplicate on different days. The same solutions were used to evaluate the precision of the method. Repeatability and inter-day precision were evaluated based on the relative standard deviation (RSD) of the results.

Linearity

Aliquot of a stock solution containing 100 µg/mL of THC was prepared in methanol. It was then transferred into 25 mL volumetric flask and diluted with dissolution medium to obtain final concentrations of 2, 4, 6, 8, and 10 µg mL^{-1} and analyzed in a UV spectrophotometer (Shimadzu 1650PC, Tokyo, Japan). The solutions were analyzed in triplicate, and the linearity was evaluated by linear regression ANOVA.

Filter suitability

Generally, the filters used in the dissolution sample preparation must be evaluated to verify that it does not adsorb the drug and is adequate enough to filter the excipients which would otherwise interfere with drug analysis. The standard and sample drug solutions with a final concentration of 6 µg mL^{-1} prepared in the dissolution medium were used to carry out the test. The sample solutions were prepared using the placebo. Both the reference and sample solutions were subjected to filtration through a 0.45-µ pore size cellulose esters membrane filter (Millipore Corp., Billerica, MA, USA), and recovery of the drug after passing through the filters was assessed. For a filter to be acceptable, the recovery must be within 98-102%.[26,27]

Standard and sample solution stability

The stability of THC in the dissolution medium was evaluated to demonstrate that the drug solution created during the dissolution test is stable over the period of dissolution and analysis of the samples. For this purpose, both the standard and sample were subjected to dissolution in the developed dissolution medium at 37±0.5˚C for 2 h to obtain a final concentration of 10 µg mL^{-1} solution. The samples were assayed at 0 h at room temperature (25±2˚C), and after 24 and 48 hr at both room and refrigerator temperature (8±2˚C). The assay was performed in triplicate and observed for any change in the absorbance values as indicates the degradation of the drug. The acceptable assay range to confirm the sample and standard stability is 98-102%.[28]

In vitro dissolution study of pure THC and tablet formulations

The dissolution of pure THC and *in vitro* release studies of the prepared THC tablets in the developed dissolution medium were performed using USP II rotating paddle apparatus (Electrolab TDT-08L, Mumbai, India). The dissolution study of the pure drug was carried out by filling 100 mg of pure THC into the hard gelatin capsules (capsule size two) and allowing it to sink in each of the dissolution media with the help of sinkers. The dissolution flask was filled with 900 mL of each dissolution medium, and the temperature was maintained at 37˚C. The speed of paddles was set at 50 rpm, and the distance between the paddle and bottom of the flask was 25 mm. The same conditions were maintained to study the dissolution of prepared THC tablets in the developed dissolution medium. Six tablets of uniform weight were chosen from each batch (TF1, TF2, and TF3), and the study was carried out for 2 h. The samples were collected at 5, 10, 15, 30, 45, 60, 90, and 120 min. A total of 5 mL sample was withdrawn at each time interval and replaced with a fresh dissolution medium to maintain the sink condition. The collected samples were filtered (0.45-µ pore size cellulose esters membrane filter, Millipore Corp., Billerica, MA, USA) and the amount of drug released, and the cumulative percentage of the drug released was determined by UV spectrophotometric analysis at 280 nm. The method was repeated thrice (n=3).

Discriminating test on a developed dissolution medium

The discriminative power of the developed dissolution medium was determined by comparing the dissolution profiles of the prepared THC tablets. Model independent approach of

dissolution comparison was used to differentiate the *in vitro* release profiles of the tablets. The difference factor (f1) and similarity factor (f2) were determined using the following equations:[29]

$$\text{Difference factor (f1)} = \frac{\sum_{t=1}^{n}(R_t - T_t)}{\sum R_t} \times 100$$

$$\text{Similarity factor (f2)} = 50 \log\{[1 + \frac{1}{n}\sum_{t=1}^{n}(R_t - T_t)^2]^{-0.5} \times 100\},$$

where n is the number of time points, R_t and T_t are the dissolution values of the reference, and test formulations at time *t*.

No statistical method was used in this study.

RESULTS

Determination of mechanical strength of the tablet

The hardness of the tablets increased with the increase in binder concentration due to increased interparticular bonding. The tablets with lowest binder concentration (5% w/w) exhibited an average crushing strength of 31.30 N, whereas those of intermediate (7.5% w/w) and highest (10% w/w) concentrations exhibited 46.06 N and 61.74 N, respectively.

Determination of critical micellar concentration

From the dye solubilization study, it was observed that the solubility of the dye gradually increased below CMC, and a sharp increase was observed at 0.017 mM (0.5% w/v) of SLS in water media, whereas the maximum solubility of the dye was at 0.035 mM (1% w/v) of SLS in pH 7.4 buffer (Figure 1a). The concentration of the surfactant showing maximum solubility of the dye indicated CMC. Surfactants tend to reduce the surface tension of the solutions. The surface tensions of the aqueous and buffer solutions gradually decreased with increasing concentration of SLS below CMC. A sudden drop in surface tension was seen at -1.76 mM (0.5% w/v) in aqueous solution. On the other hand, this drop in surface tension was observed at -1.46 mM (1% w/v) of SLS in PB of pH 7.4, indicating the CMC (Figure 1b).

Solubility study of pure THC

The solubility of the drug was high at an acidic pH of 1.2 (113.4±3.41 µg/mL) and a basic pH of 7.4 (88.54±4.5 µg/mL), and the drug exhibited less solubility at an intermediate pH of 6.8 which was only 66.7±5.05 µg/mL after 2 h of study (Figure 2a). A previous stability study on curcumin and its metabolites in various pH conditions indicated that THC was more stable in basic pH conditions than acidic.[30-32] On the basis of the available stability information, further evaluation of drug dissolution in the presence of surfactants was carried out in a PB of pH 7.4, though the solubility of drugs seems to be slightly higher in an acidic pH of 1.2 than a pH 7.4. A substantial increase in the solubility of the drug was observed when tested in media with a surfactant. The dissolution of the drug increased with an increase in surfactant concentrations in both media (e.g., from 617.67±6.55-808.33±5.31 µg mL^{-1}, 933.0±4.08-998.33±6.94 µg mL^{-1}, and 1746.33±5.31-1944.70±4.92 µg mL^{-1} in water; and from 589.33±4.50-714.00±5.35 µg mL^{-1}, 1228.33±4.92-1271.67±5.73 µg mL^{-1}, and 1421.00±5.35-1572.33±5.79 µg mL^{-1} in pH 7.4 PB saline (PBS) (Figure 2b). The high initial solubility of THC at 0.5% w/v SLS in an aqueous surfactant medium relative to pH 7.4 PB was due to micelle formation and attainment of CMC at low levels of surfactant in water. However, CMC of SLS in pH 7.4 PB was attained only at 1% w/v, which led to a high solubilization of the drug at this surfactant concentration in a PB than in water. The increase in solubility of the drug above CMC in both media is due to the increase in the micelle aggregation with an increase in the amounts of a surfactant.[20] From the experimentally determined CMC and solubility data, it was observed that the CMC of SLS reached below 1.5%. Thus, 1% SLS in pH 7.4 PB was chosen as a suitable dissolution medium. The results are subjected to statistical analysis of ANOVA, and the standard error is incorporated in the solubility graph (Figure 2).

Dissolution method validation

Specificity

The specificity test demonstrated that there was no interference of the excipients and the dissolution medium in the quantitative determination of THC at 280 nm. There was no change in the UV spectrum of the drug in the presence of excipients used for tablet preparation. This indicates that the developed UV

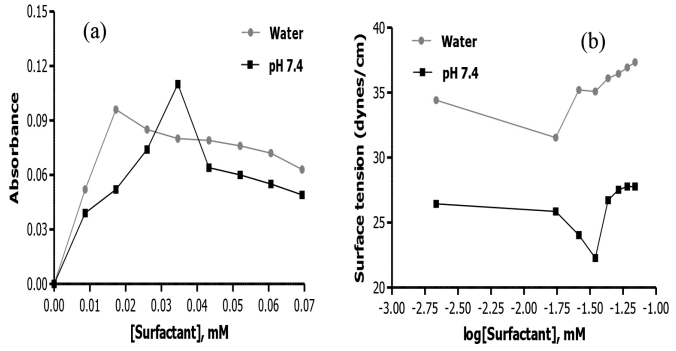

Figure 1. Experimental CMC values of SLS in water and pH 7.4 phosphate buffer determined by (a) dye solubilization method and (b) surface tension method.

CMC: Critical micelle concentration, SLS: Sodium lauryl sulfate

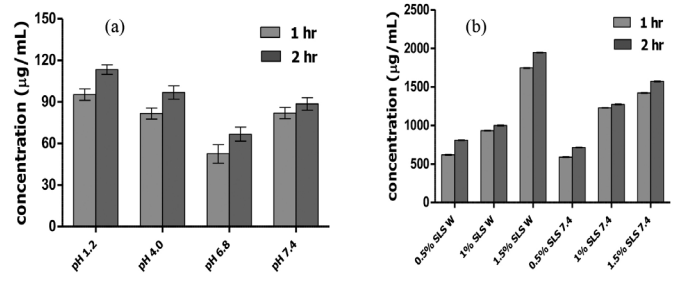

Figure 2. (a) Solubility profiles of pure tetrahydrocurcumin (THC) at 1 h and 2 h in different pH solutions of 1.2-7.4. (B) Solubility profiles of pure THC at 1 h and 2 h in water and pH 7.4 containing 0.5-1.5% w/v sodium lauryl sulfate

(p value less than 0.05)

spectrophotometric method may be used for an assay of THC in dissolution studies.

Accuracy and precision

The accuracy of the method is evaluated by the recovery of the known amount of drug added to the placebo. The recommended recoveries in the dissolution tests should be in the range of 95-105%. The mean recoveries of the drug for three different concentrations on different days were in the range 99.50-99.78%, which demonstrated the accuracy of the method. The recovery results are presented in Table 2. The inter-day and intra-day precisions were also evaluated for three different concentrations (4.8, 6.0, 7.2 µg mL^{-1}) in two days. For a method to be precise, the RSD should be low (i.e., ≤2%. From the results, the RSD was found to be <2%, which demonstrated good precision of the method (Table 3).

Linearity

The linearity of the THC calibration curve for the concentration range of 2-10 µg mL^{-1} was evaluated by a least square regression method and analyzed by ANOVA. The results showed good linearity, and the regression equation obtained was y=0.031x+0.028. The correlation coefficient was found to be 0.9996. Analysis by ANOVA showed significant linear regression ($p<0.05$), and no significant deviation from the linearity.

Filter suitability

The average percentage recoveries of the standard and sample solutions after filtration were found to be within the range of 98-102%. This showed the absence of any interference of the filter used in the analysis of the drug and that the filter used is suitable for the routine sample preparation in the dissolution test.

Standard and sample solution stability

The stability test of both standard and sample solutions showed that the drug is stable in the dissolution medium for a period of 48 h at both 25±2°C (room temperature) and 8±2°C (refrigerated conditions).This indicates that the drug did not form any degradation products in the dissolution medium (1% SLS in pH 7.4 PBS). The results of the stability test are shown in Table 2.

In vitro release study of pure THC and tablet formulations

The dissolution of pure THC in different dissolution media was found to be solubility dependent. The cumulative percentage of the drug that released in pH 1.2, 4.0, 6.8, and 7.4 was 40±1.8, 30±4.7, 23.8±2.67, and 35.3±2.6, respectively, at the end of 120 min (Figure 3a). The percentage of drug dissolved was found to be linearly dependent on the surfactant concentration, and a maximum drug release of 93±3.2% and 92±2.8% was seen in 1.5% w/v of SLS in water and pH 7.4 PBS, respectively, at the end of 120 min (Figure 3b).

The release study of three tablet formulations TF1, TF2, and TF3 in 1% w/v SLS in pH 7.4 PB showed varying drug release profiles. The prepared THC tablets differed in the amount of binder, the effect of which was reflected on their drug release pattern. Formulations TF1, TF2, and TF3 showed an initial drug release of 87.3±2.14%, 73.16±2.49%, and 64.6±2.04%, respectively in the first 5 min of the study (Figure 3c). The overall release of a drug from tablet formulations was found to be retarded with an increase in the binder concentrations. As is evident from the hardness test, the crushing strength of the tablets increased as the amount of the binder increased. This caused a delay in the disintegration of the tablets, and hence, the formulations with higher binder concentrations showed a slow-release rate of the drug.

Discriminating test on a developed dissolution medium

The release profiles of formulations TF1, TF2, and TF3 were compared choosing four time points (5, 15, 60, and 120 min) of the drug release curve, and the fit factors (f1 and f2) were determined. Two release profiles were said to be similar when the value of difference factor (f1) is between 0 and 15, and that of similarity factor (f2) is between 50 and 100.[14,33] From the fit values, the release profile of formulation TF3 was found to be different from TF1 and TF2, and a slight similarity was observed between TF1 and TF2 (Table 3). Though similarity was observed between formulations TF1 and TF2 in terms of f2, which was at a border value of 51.61, a noticeable difference existed in the cumulative percentages of the drug released at initial time points of the study. This showed that the medium was able to differentiate the release rates of the prepared THC tablets.

Table 2. Stability data of tetrahydrocurcumin showing assay concentration of the drug in percentage at different storage temperatures and time periods

	At 0 h Initial: 10 µg mL^{-1}		At 24 h		At 48 h	
	Standard	Sample	Standard	Sample	Standard	Sample
Room temperature (25±2°C)	100.0%	100.0%	100.0%	99.76%	99.75%	99.65%
Refrigerator (8±2°C)	100.0%	100.0%	100.21%	100.0%	100.14%	99.75%

Table 3. Fit factor values obtained from the drug release comparison of tetrahydrocurcumin tablets

Fit factors	TF1/TF2	TF2/TF3	TF1/TF3
f1	12.50	15.18	26.74
f2	51.61	41.29	33.52

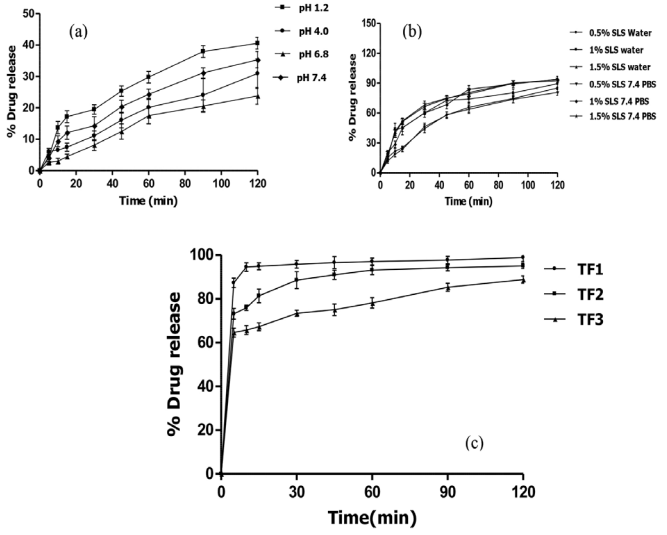

Figure 3. (a) Dissolution profiles of tetrahydrocurcumin (THC)-filled capsules in solutions of pH 1.2-7.4 (n=3). (b) Dissolution profiles of THC filled capsules in water and pH 7.4 containing 0.5-1.5% w/v sodium lauryl sulfate (n=3). (c) Cumulative percent drug release profiles of the prepared THC tablets in 900 mL of 1% w/v SLS in pH 7.4 PBS at 50 rpm (n=3)

PBS: Phosphate buffer saline

DISCUSSION

In the past decade, dissolution testing has undergone much transition in its application and value. Based on FDA guidance, dissolution test is applied as a surrogate marker for bioequivalence test along with quality control.[34] On the other hand, there is very little published on the application of a dissolution in the development and testing of natural and nutraceutical products. Recently, there is lot of attention given for the nutraceutical product development because of its proven pharmacological actions.[35-37] The present investigation was focused on the development of a discriminative dissolution medium, and its validation may serve as a reliable medium for quality assessment of THC formulations.

The initial CMC determination aimed to assess the contribution of surfactant in the solubility of the THC. The results of CMC determination by the drop number method was in agreement with those of the dye solubilization method. The critical concentration for micelle formation of the surfactant was low in aqueous solutions whereas it had increased in pH 7.4. This is due to the presence of ions, which would have reduced the aggregation and formation of micelles at lower concentrations of SLS in pH 7.4 buffers.[38]

The increase in solubility of the drug in media with SLS was apparently due to the micellar solubilization of the drug by the surfactant. Surfactants are generally employed in developing the dissolution media of low soluble class II drugs to maintain sink conditions, and the required surfactant concentration depends on its CMC to solubilize 85% of the drug. The usual concentrations of SLS being used in the dissolution media are between 0.1 and 3%.[39,40] Apart from solubility of the drug, the suitability of a dissolution medium depends on the stability of the drug in the medium. Considering the stability of the drug, and on the basis of solubility data, 1% SLS in a pH of 7.4 PBS was chosen as a suitable dissolution medium for THC.

Further *in vitro* release test of the prepared THC tablets was performed in 900 ml of 1% w/v SLS in pH 7.4 PB with a paddle speed of 50 rpm, and the release profiles were compared. Generally, a paddle speed of 50/75 rpm was used to carry out the *in vitro* release studies of tablets by USP II paddle method. However, the dissolution medium may become indiscriminative when paddles are rotated at a higher agitation rate.[41,42] Hence release studies were carried out at low agitation speed of 50 rpm to produce the steepest drug release profiles. The rate of release of the drug from each tablet formulation differed owing to the effect of the binder on a mechanical strength and disintegration of the tablets.

To elucidate the discriminative power of the medium, the dissolution curves of THC tablets were compared using the fit factors (f1 and f2). The release curves of THC tablets were compared at three different release time points before and one point after 85% of drug dissolution from all the tablets as per FDA guidelines.[43] The difference or similarity observed between the release profiles of THC tablets was due to changes made in the formulation composition, and the developed dissolution medium was able to discriminate this. Further plasma absorption studies of THC formulations are required to establish reliable *in vitro-in vivo* correlation, and confirm the bio relevance of the medium.

CONCLUSION

Dissolution is crucial for low water-soluble compounds, because the absorption of these molecules is limited by their dissolution rate. In the case of THC, dissolution is an important rate-limiting step for absorption, so developing a suitable dissolution medium is necessary to predict differences in the bioavailability of the THC formulations.[43] In the present study, the dissolution method for THC by UV spectroscopy was developed and validated. The results suggest that the pH of the medium and micellar aggregation of a surfactant in aqueous and ionic solutions influence the solubility of the drug. The final conditions for the dissolution test are 900 ml of 1% SLS in pH 7.4 PBS at 37±0.5˚C as a dissolution medium using USP apparatus II with a paddle speed of 50 rpm. The validation showed that the developed dissolution method is appropriate for quantification of THC. The release profiles comparison of prepared THC tablets by a model independent approach and the determination of fit factors showed that 1% SLS in pH 7.4 is a discriminative dissolution medium. Considering this, it may be concluded that the developed dissolution method is simple, cost effective, and adequate for the routine quality control analysis of THC, since there is no official monograph and validated method available.

ACKNOWLEDGMENTS

The authors would like to thank Sami labs (Bangalore, India) for providing the gift sample of the drug.

Conflict of interest: No conflict of interest was declared by the authors. The authors are solely responsible for the content and writing of this paper.

REFERENCES

1. Kaya-Celiker H, Mallikarjunan K. Better nutrients and therapeutics delivery in food through nanotechnology. Food Eng Rev. 2012;4:114-123.
2. Dressman JB, Amidon GL, Reppas C, Shah VP. Dissolution testing as a prognostic tool for oral drug absorption: immediate release dosage forms. Pharm Res. 1998;15:11-22.
3. Hörter D, Dressman JB. Influence of physicochemical properties on dissolution of drugs in the gastrointestinal tract. Adv Drug Deliv Rev. 2001;46:75-87.
4. Jinno J, Oh DM, Crison JR, Amidon GL. Dissolution of ionizable water-insoluble drugs: The combined effect of pH and surfactant. J Pharm Sci. 2000;89:268-274.
5. Amidon GL, Lennernäs H, Shah VP, Crison JR. A theoretical basis for a biopharmaceutic drug classification: the correlation of *in vitro* drug product dissolution and *in vivo* bioavailability. Pharm Res. 1995;12:413-420.
6. Bajerski L, Rossi RC, Dias CL, Bergold AM, Fröehlich PE. Development and validation of a discriminating *in vitro* dissolution method for a poorly soluble drug, olmesartan medoxomil: comparison between commercial tablets. AAPS PharmSciTech. 2010;11:637-644.
7. Jamzad S, Fassihi R. Role of surfactant and pH on dissolution properties of fenofibrate and glipizide—a technical note. AAPS PharmSciTech. 2006;7:E17-E22.
8. Lee H, Park SA, Sah H. Surfactant effects upon dissolution patterns of carbamazepine immediate release tablet. Arch Pharm Res. 2005;28:120-126.
9. da Fonseca LB, Labastie M, de Sousa VP, Volpato NM. Development and validation of a discriminative dissolution test for nimesulide suspensions. AAPS PharmSciTech. 2009;10:1145-1152.
10. El-Massik MA, Darwish IA, Hassan EE, El-Khordagui LK. Development of a dissolution medium for glibenclamide. Int J Pharm. 1996;140:69-76.
11. Anand OM, Lawrence XY, Conner DP, Davit BM. Dissolution testing for generic drugs: an FDA perspective. AAPS J. 2011;13:328-335.
12. Yuksel N, Kanık AE, Baykara T. Comparison of *in vitro* dissolution profiles by ANOVA-based, model-dependent and-independent methods. Int J Pharm. 2000;209:57-67.
13. Costa P, Lobo JM. Modeling and comparison of dissolution profiles. Eur J Pharm Sci. 2001;13:123-133.
14. Guidance FD. Guidance for industry, immediate release solid oral dosage forms scale-up and postapproval changes: chemistry, manufacturing, and controls. Vitro dissolution testing, and *in vivo* bioequivalence documentation (SUPAC-IR). US Department of Health and Human Services, Food and Drug Administration, Center for Drug Evaluation and Research (CDER). 1995.
15. Guidance FDA. Guidance for industry: Dissolution testing of immediate release solid oral dosage forms. US Department of Health and Human Services. Food and Drug Administration, Center for Drug Evaluation and Research (CDER). 1997.
16. SUPAC-MR FD. Modified release solid oral dosage forms: scale-up and post-approval changes: chemistry, Manufacturing, and Controls. Vitro dissolution testing and *in vivo* bioequivalenee documentation [S/OL]. (1997-09)[2009-08-18]. Available from: http://www. fda. gov/downloads/Dmgs/GuidanceComplianceRegalatorvlnformation/Guidances/UCM070640, pdf. 1997.
17. Wu JC, Tsai ML, Lai CS, Wang YJ, Ho CT, Pan MH. Chemopreventative effects of tetrahydrocurcumin on human diseases. Food Funct. 2013;5:12-17.
18. Xiang L, Nakamura Y, Lim YM, Yamasaki Y, Kurokawa-Nose Y, Maruyama W, Osawa T, Matsuura A, Motoyama N, Tsuda L. Tetrahydrocurcumin extends life span and inhibits the oxidative stress response by regulating the FOXO forkhead transcription factor. Aging (Albany NY). 2011;3:1098-1099.
19. Kumar B, Garg V, Singh A, Pandey NK, Singh S, Panchal S, Melkani I Raji R, Axel M, Mohanta S, Jyoti J, Som S, Gulati M, Bhatia A, Prakash T, Singh SK. Investigation and optimization of formulation parameters for self nanoemulsifying delivery system of two lipophilic and gastrointestinal labile drugs using box-behnken design. Asian J Pharm Clin Res. 2018;11:12-18.
20. Setthacheewakul S, Kedjinda W, Maneenuan D, Wiwattanapatapee R. Controlled release of oral tetrahydrocurcumin from a novel self-emulsifying floating drug delivery system (SEFDDS). AAPS PharmSciTech. 2011;12:152-164.
21. Rahman SM, Telny TC, Ravi TK, Kuppusamy S. Role of surfactant and pH in dissolution of curcumin. Indian J PharmSci. 2009;71:139-142.
22. Katritzky AR, Pacureanu LM, Slavov SH, Dobchev DA, Shah DO, Karelson M. QSPR study of the first and second critical micelle concentrations of cationic surfactants. Comput Chem Eng. 2009;33:321-332.
23. Drew M. Physical properties of surfactants used in cosmetics. In: Martin, M.R.; Linda, D.R. (eds.) Surfactants in cosmetics, New York: Marcel Dekker, INC; 1997:29-81.
24. Patist A, Bhagwat SS, Penfield KW, Aikens P, Shah DO. On the measurement of critical micelle concentrations of pure and technical-grade nonionic surfactants. J Surfactants Deterg. 2000;3:53-58.
25. Mata J, Varade D, Bahadur P. Aggregation behavior of quaternary salt based cationic surfactants. Thermochim Acta. 2005;428:147-155.
26. Pharmacopoeial forum. Pharmacopoeial previews, 2004;30:351-363. Available from: https://www.uspnf.com/pharmacopeial-forum
27. Marques MR, Brown W. Desenvolvimento e validação de métodos de dissolução para formas farmacêuticas sólidas orais. Rev Analytica. 2002;1:48-51.
28. United States Pharmacopeial Convention. The United States Pharmacopeia 2011: USP 34; The national formulary: NF 29. Rockville, MD: United States Pharmacopeial Convention; 2010.
29. Shah VP, Tsong Y, Sathe P, Williams RL. Dissolution profile comparison using similarity factor, f2. Dissolution Technol. 1999;6:15.
30. Pan MH, Huang TM, Lin JK. Biotransformation of curcumin through reduction and glucuronidation in mice. Drug Metab Dispos. 1999;27:486-494.
31. Hegde K, Shabaraya AR, Rao MN. Scavenging potential of reactive oxygen species by tetra-hydrocurcumin. J Appl Pharm Sci. 2011;1:114-118.

32. Wang YJ, Pan MH, Cheng AL, Lin LI, Ho YS, Hsieh CY, Lin JK. Stability of curcumin in buffer solutions and characterization of its degradation products. J Pharm Biomed Anal. 1997;15:1867-1876.

33. Chow SC, Shao J. On the assessment of similarity for dissolution profiles of two drug products. J Biopharm Stat. 2002;12:311-321.

34. Dosage IS. Guidance for Industry Guidance for Industry Waiver of In Vivo Bioavailability and. Drugs, vol. FDA Guidan, no. August. 2000;16. Available from: https://www.fda.gov/files/drugs/published/Guidance-for-Industry-Bioavailability-and-Bioequivalence-Studies-for-Orally-Administered-Drug-Products---General-Considerations.PDF

35. Dillard CJ, German JB. Phytochemicals: nutraceuticals and human health. J Sci Food Agric. 2000;80:1744-1756.

36. Lee J, Koo N, Min DB. Reactive oxygen species, aging, and antioxidative nutraceuticals. Compr Rev Food Sci Food Saf. 2004;3:21-33.

37. Mecocci P, Tinarelli C, Schulz RJ, Polidori MC. Nutraceuticals in cognitive impairment and Alzheimer's disease. Front Pharm. 2014;5:147.

38. Goddard ED, Harva O, Jones TG. The effect of univalent cations on the critical micelle concentration of sodium dodecyl sulphate. Transactions of the Faraday Society. 1953;49:980-984.

39. Noory C, Tran N, Ouderkirk L, Shah V. Steps for development of a dissolution test for sparingly water-soluble drug products. Am Pharm Rev. 2002;5:16-21.

40. Zhao F, Malayev V, Rao V, Hussain M. Effect of sodium lauryl sulfate in dissolution media on dissolution of hard gelatin capsule shells. Pharm Res. 2004;21:144-148.

41. Soni T, Nagda C, Gandhi T, Chotai NP. Development of discriminating method for dissolution of aceclofenac marketed formulations. Dissolution Technol. 2008;15:31.

42. Lagace M, Gravelle L, Di Maso M, McClintock S. Developing a discriminating dissolution procedure for a dual active pharmaceutical product with unique solubility characteristics. Dissolution Technol. 2004;11:13-18.

43. Guidance FD. Guidance for Industry: Dissolution Testing of Immediate Release Solid Oral Dosage Forms. US Department of Health and Human Services. Food and Drug Administration, Center for Drug Evaluation and Research (CDER). Rockville: U.S. Department of Health and Human Services Food and Drug Administration Center for Drug Evaluation and Research; 1997.

Turk J Pharm Sci 2021;18(5):574-580
DOI: 10.4274/tjps.galenos.2021.24571

ORIGINAL ARTICLE

Antioxidant, Anti-inflammatory, and Analgesic Activities of Alcoholic Extracts of *Ephedra nebrodensis* From Eastern Algeria

Doğu Cezayir'den *Ephedra nebrodensis* Bitkisinin Alkol ile Hazırlanan Ekstrelerinin Antioksidan, Anti-inflamatuvar ve Analjezik Aktiviteleri

Meriem HAMOUDI[1]*, Djouher AMROUN[1], Abderrahmane BAGHIANI[2], Seddik KHENNOUF[1], Saliha DAHAMNA[1]

[1]Ferhat Abbas Setif 1 University Faculty of Natural and Life Sciences, Laboratory of Phytotherapy Applied to Chronic Diseases, Setif, Algeria
[2]Ferhat Abbas Setif 1 University Faculty of Natural and Life Sciences, Laboratory of Applied Biochemistry, Setif, Algeria

ABSTRACT

Objectives: *Ephedra nebrodensis* (Ephedraceae) presents a wide range of biological activities. It is used to treat respiratory problems and hepatic pathologies in traditional medicine. The aim of this study is to evaluate the antioxidant, *in vitro* and *in vivo* anti-inflammatory and analgesic properties of two hydro-alcoholic extracts of *E. nebrodensis* in mice.

Materials and Methods: The antioxidant capacity of hydro-methanolic (HM) and hydro-ethanolic (HE) extracts of *E. nebrodensis* was evaluated *via* assays of their superoxide radical scavenging capacity and ferrous ion chelating activity. The *in vitro* anti-inflammatory activity of the extracts (5, 10, and 20 mg/kg) was also determined using the bovine serum albumin denaturation test. Croton oil-induced ear edema was then employed to evaluate the *in vivo* anti-inflammatory effect of the extracts (200 and 400 mg/kg). Finally, the analgesic activity of the extracts (200 and 400 mg/kg) was determined by the acetic acid-induced torsion test.

Results: The hydro-alcoholic extracts of *E. nebrodensis* present significant antioxidant activity. The HE and HM could inhibit protein denaturation by 82.99%±20.21% and 56.25%±2.12%, respectively. The extracts (HM and HE) also show strong anti-inflammatory effects *in vivo* and could reduce ear edema by 70.37%±2.00% and 72.22%±1.94%, respectively. The HM extract (72.51%±2.43%) demonstrates greater pain inhibitory effects than HE (70.76%±2.58%).

Conclusion: The hydro-alcoholic extracts of *E. nebrodensis* produce antioxidant, anti-inflammatory, and analgesic effects. These results confirm the traditional use of the herb in the treatment of various diseases.

Key words *Ephedra nebrodensis,* anti-inflammatory activity, analgesic test, antioxidant capacity, hydro-alcoholic extracts

ÖZ

Amaç: *Ephedra nebrodensis* (Ephedraceae) bitkisinin çok çeşitli biyolojik aktivitesi bulunmaktadır. Geleneksel tıpta solunum problemlerini ve karaciğer patolojilerini tedavi etmek için kullanılır. Bu çalışmanın amacı, *in vitro* ve *in vivo* (farelerde) koşullarda *E. nebrodensis*'in iki hidro-alkollü ekstresinin antioksidan, anti-inflamatuvar ve analjezik özelliklerini değerlendirmektir.

Gereç ve Yöntemler: *E. nebrodensis*'in hidro-metanolik (HM) ve hidro-etanolik (HE) ekstrelerinin antioksidan kapasitesi, süperoksit radikal süpürme kapasiteleri ve demirli iyon şelatlama aktivitelerinin belirlenmesi ile değerlendirildi. Ekstrelerin (5, 10 ve 20 mg/kg) *in vitro* anti-inflamatuvar aktivitesi de sığır serum albümin denatürasyon testi kullanılarak belirlendi. Daha sonra ekstrelerin (200 ve 400 mg/kg) *in vivo* anti-inflamatuvar etkisini değerlendirmek için kroton yağı ile indüklenen kulak ödemi modeli kullanıldı. Son olarak ekstrelerin analjezik aktivitesi (200 ve 400 mg/kg), asetik asit ile indüklenen kıvranma testi ile belirlendi.

Bulgular: *E. nebrodensis*'in hidro-alkolik ekstreleri, önemli antioksidan aktiviteye sahiptir. HE ve HM, protein denatürasyonunu sırasıyla %82,99±%20, 21 ve %56,25±%2,12 oranında inhibe edebilir. Ekstreler (HM ve HE) ayrıca *in vivo* olarak güçlü anti-inflamatuvar etkiler gösterir ve kulak ödemini

*Correspondence: meryoumamm2009@hotmail.fr, Phone: +213777150029, ORCID-ID: orcid.org/0000-0001-6659-3943
Received: 10.11.2020, Accepted: 03.02.2021

sırasıyla %70,37±%2,00 ve %72,22±%1,94 oranında azaltabilir. HM ekstresi (%72,51±%2,43) HE'den (%70,76±%2,58) daha yüksek analjezik aktiviteye sahiptir.

Sonuç: *E. nebrodensis*'in hidro-alkolik ekstreleri, antioksidan, anti-inflamatuvar ve analjezik etkiler üretir. Bu sonuçlar, bitkinin çeşitli hastalıkların tedavisinde geleneksel kullanımını doğrulamaktadır.

Anahtar kelimeler: *Ephedra nebrodensis*, anti-inflamatuvar aktivite, analjezik test, antioksidan kapasite, hidro-alkolik ekstreler

INTRODUCTION

Inflammation is a reaction of the immune system in response to external pathogens or injury to cells and tissues. The local coronary system, the immune system, inflammatory cells, mediators, and cytokines are implicated in this process. Macrophages play an important role in the production of numerous cytokines, reactive oxygen and nitrogen molecules, and growth factors and chemicals, such as lipopolysaccharides (LPS), which are organic mediators of inflammatory stimuli.[1] Pain is a sign of tissue lesions due to mechanical, chemical, or physical stimulation. Pain perception is controlled by the neurosensory system and afferent nerve lanes in response to potential damage.[2] Pain stimulates the production of substances called pain mediators, such as histamine, bradykinin, leukotriene, and prostaglandin;[2] these substances activate pain receptors that channel the stimulus through to the brain via nerve points with numerous synapses through the spinal cord, bone marrow, and midbrain. Pain relief is achieved by a class of drugs known as analgesics. Despite their many benefits, however, analgesics also present a number of adverse side effects, including gastric ulcer.[3]

Over the last few years, the use of medicinal plants as potential therapeutic agents for the treatment of pain and inflammation has generated great interest. *Ephedra* (Ephedraceae), a genus of non-flowering grained plants,[4] includes approximately 67 species and is principally found in desert zones across Asia, Europe, North Africa, and North America.[5] Over 145 organic molecules have been isolated from *Ephedra*, included alkaloids, polysaccharides, flavonoids, and tannins.[6] *Ephedra* is known to show anti-asthmatic,[7] anti-inflammatory,[8] antiproliferative,[9] hypoglycemic,[10] antioxidant,[11] and weight-reduction[12] properties.

Research on *Ephedra nebrodensis* is scarce. Sureka et al.[13] for example, showed that the aerial part of *E. nebrodensis* has cardio-protective effects. Short-term low-dose consumption of the hydro-ethanolic (HE) extract of *Ephedra major* has shown protective effects in cirrhotic patients.[14]

The ethanol:acetone extract of *E. nebrodensis* Tineo exhibits antihistaminic, adaptogenic, and antinociceptive activities.[15] The data reported by Shah et al.[16] suggest that the ethanol:acetone extract of *E. nebrodensis* has preventive effects against the cardio-toxicity induced by doxorubicin.

To date, however, no study describing the anti-inflammatory and antinociceptive effects of *E. nebrodensis* has yet been published. In this research, we studied the *in vitro* antioxidant and anti-inflammatory properties, the *in vivo* anti-inflammatory effect, and the analgesic activity of hydro-methanolic (HM) and HE extracts of the aerial parts of *E. nebrodensis.*

MATERIALS AND METHODS

Plant materials

The aerial parts of *E. nebrodensis* were collected in May 2017 from the mountains of Nafla, Commune de Hidoussa, Batna, Algeria. Species identification was conducted by Prof. Laouer Hocine (Laboratory of Natural Resources Valorization, Department of Biology and Vegetal Ecology, University of Setif 1, El Bez, 19000, Algeria). A plant specimen was deposited in the herbarium of the Laboratory of Botany of the Faculty of Natural and Life Sciences, University of Setif 1 (no: SNV004/20). The collected samples were dried in the shade in open air for 7 d.

Test animals

Two-month-old mice weighing 22-29 g were purchased from Institut Pasteur d'Algérie, Algiers. The animals were acclimatized in the pet shop at a temperature of 25-27 °C, relative humidity of 50–62%, and light/dark cycle of 12 h prior to the start of the experiments. All animal experimental protocols performed in this study were approved by the Ethics Committee of the Algerian Association of Sciences in Animal Experimentation (http://aasea.asso.dz/articles/) under Law No. 88-08/1988, which describes guidelines for veterinary medical activities and animal health protection (N° JORA: 004/1988).

Preparation of extracts

Approximately 100 g of the aerial part of *E. nebrodensis* in powder form was extracted with methanol (85%) and ethanol (70%). The samples were macerated for 72 h at room temperature prior to extraction. The sample/solvent mixtures were filtered, and the filtrates obtained were evaporated in an evaporator to eliminate the solvent. The residues were then dried in the oven to obtain crude HM and HE.[17]

Determination of antioxidant capacity by alkaline dimethyl sulfoxide (DMSO) assay

Scanning capacity was established by the superoxide anion (produced in a non-enzymatic solution) assay with alkaline DMSO assay.[18] Test mixtures consisting of 0.03 mL of NBT (1 mg/mL), 0.130 mL of alkaline DMSO (0.02 g of NaOH/100 mL of DMSO), and 0.04 mL of the crude extracts or standard were prepared and incubated for 5 min. The absorption of the solutions was then determined at 560 nm. The scavenging capacity of the samples was evaluated according to the following formula:

$$[\% \text{ inhibition}] = [(A_{Ct} - A_{TS}) / A_{Ct}] \times 100$$

where A_{TS} is the absorbance of the sample and A_{Ct} is the absorbance of the control.

Determination of iron-chelating activity

The ability of the extracts to chelate iron and inhibit the formation of the Fe^{2+}-ferrozine complex was tested.[19] Briefly, 40

µL of ethylenediamine tetraacetic acid (EDTA) or the samples was added to 40 µL of $FeCl_2$ (0.2 mM) and 0.04 mL of methanol. Five minutes later, the complexation reaction was initiated *via* the addition of 0.08 mL of ferrozine (0.5 mM) and allowed to proceed for 10 min at ambient temperature. The absorption of the Fe^{2+}-ferrozine complex produced was measured at 562 nm, and chelating ability was calculated in terms of inhibition percentage according to the following equation:

Fe^{2+} chelating effect (%) = $[(A_C - A_{TS}) / A_C] \times 100$

where A_{TS} is the absorbance of the test sample and A_C is the absorbance of the control sample.

Determination of in vitro anti-inflammatory activity

In vitro anti-inflammatory capacity was evaluated according to the method of Karthik et al.[20] with slight modifications. Briefly, 100 µL of different doses of the extracts or diclofenac was treated with 1 mL of 0.2% bovine serum albumin (BSA) solution prepared in Tris-HCl (pH: 6.6) and then kept in the oven for 15 min at 37°C. Thereafter, the solutions were placed in a water bath for 5 min at 72°C. The chilling turbidity of the solutions was determined at 660 nm by spectrophotometry. Blanks containing 1 mL of extract and 1 mL of Tris-HCl were prepared for each extract concentration.

Determination of in vivo anti-inflammatory activity by the croton oil-induced ear edema method

The anti-inflammatory properties of HM and HE from *E. nebrodensis* were tested *via* the croton oil-induced ear edema method according to Manga et al.[21]

The internal surface of the right ear of five groups of mice with a mean weight of 24.815±1.66 g was treated with 15 µL of acetone: water solution (1:1) containing 80 µg of croton oil as an irritant to induce skin inflammation. The same volume of solution without croton oil was applied to the left ear. The experimental mice were orally administered different concentrations of the extracts 1 h after croton oil application, the positive control group received 50 mg/kg indomethacin, and the negative control group received distilled water. Ear thickness was evaluated with a digital caliper 6 h after edema induction.[22]

The mice were randomized into six groups, each of which included six mice.

Negative control group: Received distilled water.

Positive control group: Received indomethacin (50 mg/kg).

Groups A1 and A2: Received 200 and 400 mg/kg HE, respectively.

Groups B1 and B2: Received 200 and 400 mg/kg HM, respectively.

The percentage of edema inhibition was defined in relation to the control group, which received the croton oil solution, according to the following formula:

Inhibition % = $(D_{Control} - D_{Treated} / D_{Control}) \times 100$

where $D_{Control}$ is the difference in edema thickness in the control group and $D_{Treatment}$ is the difference in edema thickness for the treated groups.

Determination of in vivo analgesic activity by the acetic acid-induced writhing test

Analgesic activity against acetic acid-induced pain was evaluated according to the method described by Koster et al.[23] The negative control group was given distilled water orally, the treatment groups were given a single dose of 200 or 400 mg/kg HM or HE orally, and the positive control group was given 100 mg/kg aspirin. The mice were then injected with acetic acid (0.6%, 10 mL/kg) intra-peritoneally. The number of twitches exhibited by each mouse was counted at 5 min intervals for 30 min. The percentage of pain inhibition was determined using the following equation:

Inhibition % = $100 \times (C_{nc} - C_{tr}) / C_{nc}$

where C_{nc} is the average number of twitches in the negative control group and C_{tr} is the average number of twitches in groups given various doses of HM or HE extracts or aspirin.

Statistical analysis

The results of the *in vitro* test were expressed as mean ± standard deviation, while the results of the *in vivo* experiments were expressed as mean ± standard error of the mean. Results were evaluated by One-Way analysis of variance and Dunnett's test by using GraphPad Prism (version 5.01). $P<0.05$ was regarded as statistically significant.

RESULTS

Antioxidant capacity

The capacity of the extracts to capture superoxide anion radicals was examined in our study. According to the results shown in Table 1, the scavenging ability (IC_{50}) of HE (1.84±0.46 µg/mL) was significantly greater ($p<0.001$) than those of ascorbic acid (7.59±1.16 µg/mL) and α-tocopherol (31.52±2.22 µg/mL). HM showed effects (7.81±0.28 µg/mL) comparable with those of ascorbic acid.

All samples showed moderate chelation ability for Fe^{2+} (Table 1). Compared with other samples, HE appeared to be a more active chelator, and the IC_{50} of HE (168.12±1.13 µg/mL) was greater than that of HM (174.60±4.28 µg/mL). Neither extract appeared to be a more powerful Fe^{2+} chelator than the EDTA positive standard (8.80±0.47 µg/ mL) in the present test system.

In vitro anti-inflammatory activity

The *in vitro* anti-inflammatory effect of the *E. nebrodensis* extracts was evaluated *via* the BSA denaturation method, and the results are presented in Figure 1. HE could inhibit BSA denaturation in a dose-dependent manner and demonstrated a maximum inhibition rate of 82.99% at a dose of 20 mg/mL. HM inhibited protein denaturation by 56.25%. Diclofenac at a dose of 5 mg/mL inhibited inflammation by 99.82%.

Anti-inflammatory effects against croton oil-induced ear edema

The anti-inflammatory effects of HE and HM on ear edema induced by croton oil are presented in Figure 2. Edema was inhibited by the extracts in a dose-dependent manner, and the highest dose of the extracts demonstrated the most significant activity. HM and HE reduced ear edema with maximum

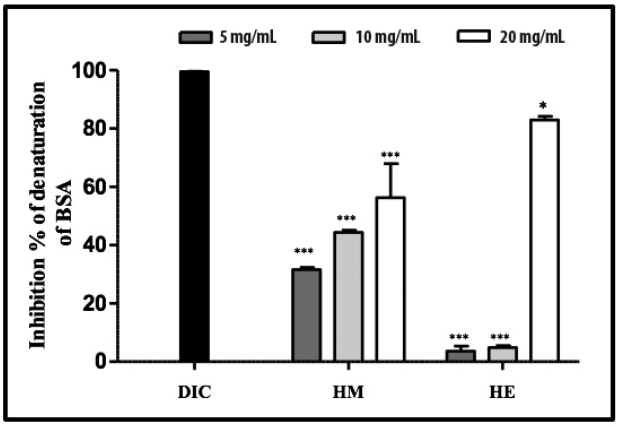

Figure 1. *In vitro* anti-inflammatory effect of hydro-alcoholic extracts of *Ephedra nebrodensis*. Data are presented as mean ± SD (n=3). *P<0.05 compared with the diclofenac group, ***P<0.001 compared with the diclofenac group.

HE: Hydro-ethanolic extract (70%), HM: Hydro-methanolic extract (85%), DIC: Diclofenac group 5 g/kg, SD: Standard deviation, BSA: Bovine serum albumin

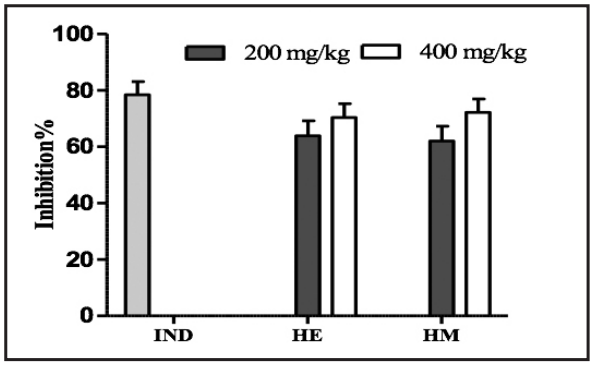

Figure 2. Effects of *Ephedra nebrodensis* on inflammation in Swiss albino mice (n=6; W: 24.815±1.66 g). Inflammation was induced by applying 15 µL of acetone:water solution (1:1, v:v) containing 80 µg of croton oil to the internal surface of the right ear. The same volume of solution without croton oil was applied to the left ear. After 1 h, the mice were orally administered the extracts. Ear thickness was measured after 6 h. The results are expressed as mean ± SEM. P>0.05 compared with 50 mg/kg indomethacin

HE: Hydro-ethanolic extract (70%), HM: Hydro-methanolic extract (85%), IND: Indomethacin (50 mg/kg), SEM: Standard error of the mean

inhibition percentages of 72.22% and 70.37%, respectively, at a dose of 400 mg/kg. This effect is statistically similar to that of indomethacin (78.49%).

Antinociceptive effects against acetic acid-induced pain

The results presented in Figure 3 show that administration of 200 and 400 mg/kg *E. nebrodensis* extracts exerts a protective effect against pain caused by acetic acid. HM and HE demonstrated good analgesic activity with inhibition rates of 63.74% and 59.06%, respectively, when administered at a dose of 200 mg/kg. Higher doses of HM and HE (400 mg/kg) resulted in higher pain inhibition rates of 72.51% and 70.76%, respectively. These effects are similar to that of aspirin at 100 mg/kg (79.14%). No significant difference between the effects of the extracts at different concentrations and the standard (aspirin) was observed.

DISCUSSION

Herbal medicines are widely acknowledged to represent a beneficial approach for the treatment of many types of human diseases. Numerous sources have documented the ethno-pharmacological use of herbs by many populations since ancient times.[24] Phytochemicals are ubiquitous compounds found in herbs that provide a wide range of benefits, such as anticancer, antibacterial, anti-inflammatory, antidiabetic, and antioxidant activities.[25] In this study, we report the antioxidant, anti-inflammatory (*in vitro* and *in vivo*), and analgesic effects of *E. nebrodensis* extracts on a mouse model.

HE demonstrated stronger *in vitro* antioxidant activity compared with HM. Hamoudi et al.[11] used 2,2-diphenyl-1-picrylhydrazyl and 2,2'-Azino-bis(3-ethylbenzothiazoline-6-sulfonic acid) assays to show that an ethyl acetate fraction of *E. nebrodensis* exhibits potent antioxidant properties.

The superoxide radical scavenging activity of our extracts may be related to their contents of flavonoids and polyphenols, which are major contributors to the antioxidant potential of the aerial parts of *E. nebrodensis*. Good correlations between the antioxidant effect and polyphenol and flavonoid contents of various plant extracts have been well established in the literature.[11,26,27]

The results obtained in this work indicate that HE and HM are strongly able to chelate Fe^{2+}. Previous research found no

Table 1. Superoxide radical scavenging and metal-chelating activities of *Ephedra nebrodensis*

Extracts/standard	O^{-2} DMSO alkaline		Fe^{2+} ion chelating ability	
	Inhibition % at 200 µg/mL	IC_{50} (µg/mL)[a]	Inhibition % at 200 µg/mL	IC_{50} (µg/mL)[a]
HM	94.86±0.10[c]	7.81±0.28[c]	54.55±0.84[c]	174.60±4.28[c]
HE	94.17±0.01[c]	1.84±0.46[c]	55.73±0.63[c]	168.12±1.13[c]
EDTA[b]	-	-	95.87±0.06	8.80±0.47
Ascorbic acid[b]	94.28±1.12	7.59±1.16	-	-
α-tocopherol[b]	96.54±0.10	31.52±2.22	-	-

[a]IC_{50} values correspond to the mean ± standard deviation of three simultaneous measures, [b]Standard compounds, [c]p≤0.001. HE: Hydro-ethanolic extract, HM: Hydro-methanolic extract, DMSO: Dimethyl sulfoxide, EDTA: Ethylenediamine tetraacetic acid

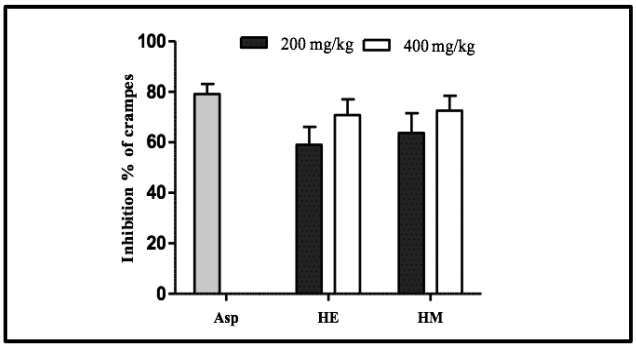

Figure 3. Effects of hydro-alcoholic extracts of *Ephedra nebrodensis* on peripheral nociception in Swiss albino mice (n=6; W: 27±5 g). Peripheral antinociceptive activity was determined by the acetic acid-induced writhing test. The results are expressed as mean ± SEM. P>0.05 compared with 100 mg/kg aspirin

HE: Hydro-ethanolic extract (70%), HM: Hydro-methanolic extract (85%), Asp: Aspirin 100 mg/kg, SEM: Standard error of the mean

relationship between phenolic level and Fe^{2+}-chelating activity.[28] This result suggests that the iron-chelating effect of the extracts may be attributed to the existence of other antioxidants that able to chelate metal ions, such as phosphoric acid, carnosine, acid citric, amino acids, protein, and ascorbic acid.[29]

Protein denaturation refers to changes in the structure of proteins as a result of altered hydrogen, hydrophobic, electrostatic, and disulfide bonds. The majority of proteins loses their biological activities following denaturation and generates auto-antigens, leading to a series of autoimmune dysfunctions, such as inflammatory and rheumatoid disorders. Thus, drugs that could inhibit the denaturation of proteins are regarded as essential anti-inflammatory agents.[30] The *in vitro* anti-inflammatory effect of the hydro-alcoholic extracts observed in this work indicates that the extracts could preserve the three-dimensional profile of proteins that control the production of auto-antigens. This finding may be explained by the presence of phytochemicals, such as flavonoids and phenols, in *Ephedra*.

Croton oil is often used as an inflammatory agent.[31] The oil activates phospholipase A2, which induces the secretion of arachidonic acid from the cell membrane. This compound is then metabolized to prostaglandins and leukotrienes.[32] Dermal exposure to croton oil can cause reactive oxygen species production and an inflammatory skin response resembling that occurring during contact dermatitis.[33,34]

Analogues of ephedrine, which consist mainly of ephedrine, ephedrroxane, and pseudoephedrine, have potent *in vivo* anti-inflammatory capacity, which has been attributed to the blockage of prostaglandin E2 biosynthesis.[35] Kim et al.[36] found that ephedranin A and ephedranin B in *Ephedra* root extracts have anti-inflammatory effects. These substances can impede the transcription of IL-1β and TNF-α and block the inflammation induced by LPS. These substances could also inhibit the translocation of NF-κB and phosphorylation of p38 kinase in mitogen-activated protein.

Acute inflammation reactions are manifested by the formation of swelling and infiltration of leukocytes into the inflamed tissue. The chemicals released by resident cells promote the alteration of vascular permeability and, in turn, the formation of edema. Sequential processes and activities between the endothelium and inflammatory tissue cells (principally neutrophils) then lead to the development of inflammatory cells at the tissue.[37,38]

We noted that the *E. nebrodensis* extracts and indomethacin, which was used as a positive control, similarly inhibited the formation of atrial edema. Anti-inflammatory effects may be achieved through various mechanisms of action, including inhibition of histamine release, 5-lipooxygenase, complement and elastase functions.[39,40] Many studies have attributed the anti-inflammatory properties of phenolic compounds to their antioxidant activity.[41,42]

In acetic acid assay, it is apparent that abdominal muscle pain is not a specific pattern and involuntary abdominal muscle pain may be due to its similarities to some of the known visceral pain patterns.[43] Activation of prostaglandins, histamines, serotonin, lipooxygenases, cyclooxygenases, and endogenous cytokines (e.g., IL-8 and IL-1β) in peripheral tissues is activated by acetic acid injection into the abdominal cavity of mice.[44] These substances penetrate the dorsal horn of the central nervous system and stimulate primary nociceptors, resulting in enzyme pain and torsion disorder.[45] In our experiment, the hydro-alcoholic extracts significantly ($p<0.001$) and dose-dependently reduced the number of acetic acid-facilitated abdominal contractions or torsions manifested by the mice. This finding clearly indicates that the anti-nociceptive effect produced by the extracts prevents the endogenous synthesis of inflammatory substances or directly inhibits their receptors.[46]

The peripheral analgesic capacity of the different extracts studied in this work may be due to the phenolic compounds and alkaloids produced by the plant. These compounds are known to be responsible for the analgesic properties of other medicinal plants, such as *Jasminum amplexicaule* and *Elephantopus tomentosus*.[47,48]

CONCLUSION

This study reports for the first time the antioxidant and anti-inflammatory activities of hydro-alcoholic extracts (i.e., HE and HM) of *E. nebrodensis.* The extracts exhibited excellent *in vitro* antioxidant activity, as determined by superoxide radical scavenging and metal chelation assays. The extracts also demonstrated significant *in vitro* anti-inflammatory effects, with inhibition rates of 56-82%.

The plant extracts studied in this work demonstrated important *in vivo* anti-inflammatory effects, as well as moderate analgesic activity, in mice. Further phytochemical characterization of the active compounds responsible for these biological activities is necessary to improve the understanding on the mechanism through which *E. nebrodensis* reduces inflammation and pain.

ACKNOWLEDGMENTS

This work was supported by the Algerian Ministry of Higher Education and Scientific Research (MESRS, DGRSDT). We

would like to thank Pr. Laouer Hocine (Laboratory of Natural Resources Valorization, Department of Biology and Vegetal Ecology, University of Ferhat Abbas Setif 1, El Bez, 19000, Algeria) for identifying the plant materials used in this study.

Conflict of interest: No conflict of interest was declared by the authors. The authors are solely responsible for the content and writing of this paper.

REFERENCES

1. Somsil P, Ruangrungsi N, Limpanasitikul W, Itthipanichpong C. *In vivo* and *in vitro* anti-infammatory activity of Harrisonia perforata root extract. Pharmacogn J. 2012;4:38-44.
2. Ghosh, AK, Banerjee M, Mandal TK, Mishra A, Bhowmik M.K. A study on analgesic efficacy and adverse effects of aloe vera in Wistar rats. Pharmacologyonline. 2011;1:1098-1108.
3. Nalamachu S. An overview of pain management: the clinical efficacy and value of treatment. Am J Manag Care. 2013;19(Suppl 14):s261-s266.
4. D'Auria M, Emanuele L, Racioppi R. FT-ICR-MS analysis of lignin. Nat Prod Res. 2012;26:1368-1374.
5. Xie M, Yang Y, Wang B, Wang C. Interdisciplinary investigation on ancient *Ephedra* twigs from Gumugou Cemetery (3800 B.P.) in Xinjiang region, northwest China. Microsc Res Tech. 2013;76:663-672.
6. Zhang BM, Wang ZB, Xin P, Wang QH, Bu H, Kuang HX. Phytochemistry and pharmacology of genus *Ephedra*. Chin J Nat Med. 2018;16:811-828.
7. ILiu YG, Luo JB. [Effects of among compositions of Herba Ephedrae decoction on genic xpression of 5-lipoxygenase activating protein, IL-4 and leukotriene C4 in asthmatic mice]. Zhongguo Zhong Yao Za Zhi. 2007;32:246-249.
8. Aoki K, Yamakuni T, Yoshida M, Ohizumi Y. Ephedorae herba decreases lipopolysaccharide-induced cyclooxgenase-2 protein expression and NF-kappaB-dependent transcription in C6 rat glioma cells. J Pharmacol Sci. 2005;98:327-330.
9. Danciu C, Muntean D, Alexa E, Farcas C, Oprean C, Zupko I, Bor A, Minda D, Proks M, Buda V, Hancianu M, Cioanca O, Soica C, Popescu S, Dehelean CA. Phytochemical characterization and evaluation of the antimicrobial, antiproliferative and pro-apoptotic potential of ephedra alata decne. Hydroalcoholic extract against the MCF-7 breast cancer cell line. Molecules. 2018;24:13.
10. Ben Lamine J, Boujbiha MA, Dahane S, Cherifa AB, Khlifi A, Chahdoura H, Yakoubi MT, Ferchichi S, El Ayeb N, Achour L. α-Amylase and α-glucosidase inhibitor effects and pancreatic response to diabetes mellitus on Wistar rats of *Ephedra* alata areal part decoction with immunohistochemical analyses. Environ Sci Pollut Res Int. 2019;26:9739-9754.
11. Hamoudi M, Amroun D, Khennouf S, Dahamna S. Antioxidant evaluation and polyphenol contents of hydro ethanolic extract's fractions from *Ephedra nebrodensis*. Journal of Drug Delivery and Therapeutics. 2020;10:314-319.
12. Lim J, Lee H, Ahn J, Kim J, Jang J, Park Y, Jeong B, Yang H, Shin SS, Yoon M. The polyherbal drug GGEx18 from Laminaria japonica, Rheum palmatum, and *Ephedra sinica* inhibits hepatic steatosis and fibroinflammtion in high-fat diet-induced obese mice. J Ethnopharmacol. 2018;225:31-41.
13. Sureka M, Sumathi R, Kanagavalli U. A Comprehensive Review on Cardiotoxic Drugs and Cardioprotective Medicinal Plants. IJPRR. 2016;5:21-34.
14. Hassanzadeh M, Dianat M, Torabizadeh P, Badavi M. Protective effect of hydroalcoholic extract of *ephedra* major on an experimental model of bile duct ligation in rats. Int. J. LifeSc. Bt & Pharm Res. 2014;3:44-50.
15. Ballero M, Foddis C, Sanna C, Scartezzini P, Poli F, Petitto V, Serafini M, Stanzione A, Bianco A, Serilli AM, Spina L, Longoni R, Kasture S. Pharmacological activities on *Ephedra nebrodensis* Tineo. Nat Prod Res. 2010;24:1115-1124.
16. Shah S, Mohan MM, Kasture S, Sanna C, Maxia A. Protective Effect of *Ephedra nebrodensis* on Doxorubicin-Induced Cardiotoxicity in Rats. Iranian Journal of Pharmacology & Therapeutics. 2009;8:61-66.
17. Annapandian VM, Rajagopal SS. Phytochemical evaluation and *in vitro* antioxidant activity of various solvent extracts of *Leucas aspera* (willd.) link leaves. Free Radic Antioxid. 2017;7:166-171.
18. Kunchandy E, Rao MNA. Oxygen radical scavenging activity of curcumin. Int J Pharm. 1990;58:237-240.
19. Decker EA, Welch B. Role of ferritin as a lipid oxidation catalyst in muscle food. J Agric Food Chem. 1990;38:674-677.
20. Karthik K, Bharath R, Kumar P, Priya VR, Kumar SK, Rathore RSB. Evaluation of anti-inflammatory activity of *canthium parviflorum* by *in-vitro* method. IJRPB. 2013;1:729-731.
21. Manga HM, Brkic D, Marie DE, Quetin-Leclercq J. *In vivo* anti-inflammatory activity of *Alchornea cordifolia* (Schumach. & Thonn.) Müll. Arg. (Euphorbiaceae). J Ethnopharmacol. 2004;92:209-214.
22. Delaporte RH, Sarragiotto MH, Takemura OS, Sánchez GM, Filho BP, Nakamura CV. Evaluation of the antioedematogenic, free radical scavenging and antimicrobial activities of aerial parts of Tillandsiastreptocarpa Baker-Bromeliaceae. J Ethnopharmacol. 2004;95:229-233.
23. Koster R, Anderson M, De Beer EJ. Acetic acid for analgesic screening. Federal Proceeding. 1959;8:412-416.
24. Zengin G, Mahomoodally F, Picot-Allain C, Diuzheva A, Jekő J, Cziáky Z, Cvetanović, A Aktumsek, A, Zeković Z, Rengasamy KRR. Metabolomic profile of *Salvia viridis* L. root extracts using HPLC-MS/MS technique and their pharmacological properties: a comparative study. Ind Crops Prod. 2019;131:266-280.
25. Guldiken B, Ozkan G, Catalkaya G, Ceylan FD, Ekin Yalcinkaya I, Capanoglu E. Phytochemicals of herbs and spices: Health versus toxicological effects. Food Chem Toxicol. 2018;119:37-49.
26. Bouaziz A, Djidel S, Bentaher A, Khennouf S. Polyphenolic content, antioxidant and anti-inflammatory activities of melon (cucumis melo L. var. inodorus) seeds. J Drug Deliv Ther. 2020;10:22-26.
27. Mamache W, Amira S, Ben Souici C, Laouer H, Benchikh F. *In vitro* antioxidant, anticholinesterases, anti-α-amylase, and anti-α-glucosidase effects of Algerian *Salvia aegyptiaca* and *Salvia verbenaca*. J Food Biochem. 2020;00:e13472.
28. Belkhiri F, Baghiani A, Zerroug MM, Arrar L. Investigation of antihemolytic, xanthine oxidase inhibition, antioxidant and antimicrobial properties of *Salvia verbenaca* L. aerial part extracts. Afr J Tradit Complement Altern Med. 2017;14:273-281.
29. Lee J, Renita M, Fioritto RJ, St Martin SK, Schwartz SJ, Vodovotz Y. Isoflavone characterization and antioxidant activity of ohio soybeans. J Agric Food Chem. 2004;52:2647-2651.

30. Mouffouk C, Hambaba L, Haba H, Mouffouk S, Bensouici C, Hachemi M, Khadraoui H. Acute toxicity and *in vivo* anti-inflammatory effects and *in vitro* antioxidant and anti-arthritic potential of *Scabiosa Stellata*. Orient Pharm Exp Med. 2018;18:335-348.

31. Lan M, Wan P, Wang ZY, Huang XL. [GC-MS analysis of chemical components in seeds oil from Croton tiglium]. Zhong Yao Cai. 2012;35:1105-1108.

32. Shah B, Seth A, dan Maheshwari K. A review on medicinal plants as a resource of antiinflammatory agents. Res J Med Plant. 2011;5:101-115.

33. Pinto NDCC, Machado DC, da Silva JM, Conegundes JLM, Gualberto ACM, Gameiro J, Chedier LM, Castañon MCMN, Scio E. Pereskia aculeata Miller leaves present *in vivo* topical anti-inflammatory activity in models of acute and chronic dermatitis. Journal of Ethnopharmacology. 2015;173:330-337.

34. Siddiqui F, Naqvi S, Abidi L, Faizi S, Lubna, Avesi L, Mirza T, Farooq AD. Opuntia dillenii cladode: opuntiol and opuntioside attenuated cytokines and eicosanoids mediated inflammation. J Ethnopharmacol. 2016;182:221-234.

35. Kasahara Y, Hikino H, Tsurufuji S, Watanabe M, Ohuchi K. Antiinflammatory actions of ephedrines in acute inflammations. Planta Med. 1985;325-331.

36. Kim IS, Park YJ, Yoon SJ, Lee HB. Ephedrannin A and B from roots of *Ephedra sinica* inhibit lipopolysaccharide-induced inflammatory mediators by suppressing nuclear factor-κB activation in RAW 264.7 macrophages. Int Immunopharmacol. 2010;10:1616-1625.

37. Tamura EK, Jimenez RS, Waismam K, Gobbo-Neto L, Lopes NP, Malpezzi-Marinho EA, Marinho EA, Farsky SH. Inhibitory effects of Solidago chilensis Meyen hydroalcoholic extract on acute inflammation. J Ethnopharmacol. 2009;122:478-485.

38. Vestweber D. How leukocytes cross the vascular endothelium. Nat Rev Immunol. 2015;15:692-704.

39. Díaz AM, Abad MJ, Fernández L, Recuero C, Villaescusa L, Silván AM, Bermejo P. *In vitro* anti-inflammatory activity of iridoids and triterpenoid compounds isolated from *Phillyrea latifolia* L. Biol Pharm Bull. 2000;23:1307-1313.

40. Ryu SY, Oak MH, Yoon SK, Cho DI, Yoo GS, Kim TS, Kim KM. Anti-allergic and anti-inflammatory triterpenes from the herb of *Prunella vulgaris*. Planta Med. 2000;66:358-360.

41. Middleton E Jr, Kandaswami C. Effects of flavonoids on immune and inflammatory cell functions. Biochem Pharmacol. 1992;43:1167-1179.

42. Kassim M, Achoui M, Mansor M, Yusoff KM. The inhibitory effects of Gelam honey and its extracts on nitric oxide and prostaglandin E(2) in inflammatory tissues. Fitoterapia. 2010;81:1196-1201.

43. Hajhashemi V, Sajjadi SE, Heshmati M. Anti-inflammatory and analgesic properties of Heracleum persicum essential oil and hydroalcoholic extract in animal models. J Ethnopharmacol. 2009;124:475-480.

44. Lu TC, Ko YZ, Huang HW, Hung YC, Lin YC, Peng WH. Analgesic and anti-inflammatory activities of aqueous extract from Glycine tomentella root in mice. J Ethnopharmacol. 2007;113:142-148.

45. Le Bars D, Gozariu M, Cadden SW. Animal models of nociception. Pharmacol Rev. 2001;53:597-652.

46. Franzotti EM, Santos CV, Rodrigues HM, Mourão RH, Andrade MR, Antoniolli AR. Anti-inflammatory, analgesic activity and acute toxicity of *Sida cordifolia* L. (Malva-branca). J Ethnopharmacol. 2000;72:273-277.

47. Jia Q, Su W, Peng W, Li P, Wang Y. Anti-diarrhoea and analgesic activities of the methanol extract and its fractions of *Jasminum amplexicaule* Buch.-Ham. (Oleaceae). J Ethnopharmacol. 2008;119:299-304.

48. Yam MF, Ang LF, Ameer OZ, Salman IM, Aziz HA, Asmawi MZ. Anti-inflammatory and analgesic effects of Elephantopus tomentosus ethanolic extract. J Acupunct Meridian Stud. 2009;2:280-287.

Turk J Pharm Sci 2021;18(5):581-588
DOI: 10.4274/tjps.galenos.2021.45389

ORIGINAL ARTICLE

Trend Analysis of Lead Content in Roadside Plant and Soil Samples in Turkey

Türkiye'de Yol Kenarında Bulunan Bitki ve Toprak Örneklerinde Kurşun İçeriğinin Eğilim Analizi

Gamze ÖĞÜTÜCÜ, Gülce ÖZDEMİR, Zeynep ACARARICIN, Ahmet AYDIN*

Yeditepe University Faculty of Pharmacy, Department of Pharmaceutical Toxicology, İstanbul, Turkey

ABSTRACT

Objectives: Lead (Pb) is one of the most common heavy metals which contaminate the environment. People may be exposed to Pb by inhaling the contaminated air droplets and dust particles through drinking water or eating contaminated foods such as vegetables grown in lead-contaminated soils. This study aimed to examine the changes in Pb levels measured in roadside plant and soil samples that have been exposed to heavy traffic for years.

Materials and Methods: Sixty-three articles were searched using keywords from different databases. Twenty-five of the scanned articles were found to be relevant for the determined criteria. The Pb levels were evaluated according to the previously measured Pb levels in plant and soil samples collected from the roadside by years.

Results: In the data collected from databases over the years, it was observed that there was a decrease in Pb accumulation in both soil and plant samples. Pb levels were higher in industrial cities and metropolitan areas than in rural areas.

Conclusion: In ealier studies, Pb levels have often been found to exceed safety limits. This may be due to the Pb added to gasoline in the past, as well as the low sensitivity of analytical methods used for measurement. The decrease over the years has been interpreted as the use of unleaded gasoline after 2004, taking essential measures to improve air quality and at the same time increasing the sensitivity of analytical methods.

Key words: Heavy metal, herbal, plant, highway, roadside, lead

ÖZ

Amaç: Kurşun (Pb), çevreyi kirleten yaygın elementlerden birisidir. İnsanlar, kontamine olmuş hava damlacıklarını ve toz parçacıklarını soluma yoluyla, içme suyuyla veya Pb ile kirlenmiş topraklarda yetişen sebzeleri yiyerek Pb'ye maruz kalabilir. Trafik hareketliliğinin yoğun olduğu yol kenarlarında yetişen bitki ve topraklarda ölçülen Pb düzeylerinin yıllara göre değişiminin incelenmesi amaçlanmıştır.

Gereç ve Yöntemler: Farklı veri tabanlarından anahtar kelimeler kullanılarak 63 makale taranmıştır. Taranan makalelerin 25'i belirlenen kriterlere uygun bulunmuştur. Yol kenarında yaşayan bitki ve toprak örneklerinde ölçülen Pb düzeyleri yıllara göre değerlendirilmiştir.

Bulgular: Yıllar içinde toplanan verilerde hem toprak hem de bitki örneklerinde Pb birikiminde azalma olduğu görülmüştür. Sanayi şehirlerinden ve metropollerde Pb seviyeleri kırsal bölgelere göre daha yüksek bulunmuştur.

Sonuç: Daha önceki çalışmalarda, Pb seviyelerinin çoğunlukla güvenlik limitlerini aştığı tespit edilmiştir. Bu durum, önceki zamanlarda benzine katılan Pb nedeniyle olabileceği gibi aynı zamanda ölçüm için kullanılan analitik yöntemlerin hassasiyetlerinin düşük olmasıyla da ilişkilendirilebilmektedir. Yıllara göre azalmanın ise 2004 yılından sonra kurşunsuz benzin kullanılması, hava kalitesinin artırılması için önemli tedbirlerin alınması ve aynı zamanda analitik yöntemlerin hassasiyetinin yükselmesi olarak yorumlanmıştır.

Anahtar kelimeler: Ağır metal, bitkisel, bitki, otoyol, yol kenarı, kurşun

***Correspondence:** ahmet.aydin@yeditepe.edu.tr, **Phone:** +90 533 342 25 65, **ORCID-ID:** orcid.org/0000-0003-3499-6435

Received: 30.10.2020, **Accepted:** 12.02.2021

INTRODUCTION

Chemical substances form the core of our world for both the living systems and the environment. When produced, used, and managed appropriately, the chemicals make things easy and benefit our everyday needs. However, chemicals may also be a significant threat to the living systems and the ecosystem in some circumstances. In 2010, the World Health Organization (WHO) published a report on ten chemicals or groups considered major public health concerns. WHO listed them as air pollution, arsenic, asbestos, benzene, cadmium, dioxin, and dioxin-like substances, inadequate or excess fluoride, lead (Pb), mercury, and highly hazardous pesticides. There are several heavy metals on the list, including Pb.[1]

Environmental pollution has been a primary global health concern since the early phases of the industry. This issue is getting more threatening and becoming much more critical day by day. Heavy metals are accepted as one of the primary sources of environmental pollution. Thanks to technological developments, actions are being taken to diminish the hazardous effects of these pollutants using environmentally-friendly solutions, such as abandoning the use of Pb in gasoline.[2] Due to the high usage of heavy metals in technological equipment, their existence in living systems is inevitable. When the amount exceeds the acceptable ranges, heavy metals can be accumulated in organisms.

Heavy metal accumulation has become a predominant problem for the world, especially in developing countries, and it may cause several harmful effects on humans, animals, plant species, and the environment itself.[3] Contaminated soil can be a critical source for heavy metal exposure due to farming, agriculture, horticulture, and animal breeding. Roadside soils should also be a focus because many people, especially in the rural regions, collect, and consume plant substances growing on the roadside. Therefore, it is necessary to estimate harmful substances' qualitative and quantitative content, particularly heavy metals in the soil.[4]

Heavy metal can be considered the naturally occurring metallic elements with densities higher than 5 g/cm^3, equal to more than five times that of water, and relatively high atomic numbers.[2,5] Several definitions had been proposed for heavy metals. The Oxford English Dictionary indicates that the oldest definition in the scientific literature of heavy metal is "those metals with an elemental density above 7 g/cm^3".[6] More specific definitions have been published, but none of these have been widely accepted. Ali and Khan[6] defined heavy metals as naturally occurring metals having an atomic number greater than 20 and an elemental density greater than 5 g/cm^3.

Heavy metal exposure results in toxicities and tissue damages with various symptoms. Toxic effects vary depending on the amount and route of exposure and personal characteristics like age, gender, hereditary characteristics, and eating habits of the exposed individual.[2,5]

Heavy metal contamination is caused by exhaust gases from industrial activities, motor vehicles, chemical and pharmaceutical manufacturings, and fertilizers and pesticides used for agricultural purposes, eventually leaking into the soil. The contamination of heavy metals in the soil is harmful because of their non-biodegradable nature; they may persist and accumulate in the soil for many years. Additionally, as the soil's heavy metal content increases, the amount is taken up by the plant also rises.[2,3] The United States Environmental Protection Agency (US EPA) and the International Agency for Research on Cancer classify arsenic, cadmium, chromium, Pb, and mercury as probable or known human carcinogens.

This study focused on the Pb accumulation levels throughout the years because of their high content in the roadside plants and soils.[5] Pb is naturally occurring in the environment and is one of the most important and commonly contaminated heavy metals. It has an atomic number of 82 and a molecular weight of 207.2 u.[5] According to the US EPA, Pb is a naturally occurring element found in small amounts in the earth's crust. It causes severe toxicities besides some beneficial impacts.[7]

People may be exposed to Pb by inhaling the contaminated air droplets and dust particles, exhaling the household paintings, drinking contaminated water, or ingesting contaminated food such as vegetables grown in Pb-contaminated soils.[5]

Pb shows its toxic effects by particular mechanisms after entering the systemic circulation in the body. It may interfere with the enzymes by binding their amide and sulfhydryl groups and inhibiting their action. It competitively binds to the sites of some essential elements like calcium and alters their activities. Also, it induces oxidative stress generating reactive oxygen species. Oxidative stress is a widely known toxicity mechanism for its role in cellular damage.[5]

The central nervous system is the primary target for Pb toxicity, which results in headaches, memory deficits, attention deficits, or hallucinations. In addition, studies report that Pb poisoning causes neurobehavioural and intelligence-related damages in children. Furthermore, Pb exposure is a significant problem for pregnant women, including possible preterm labor and post-natal complications in the child because it may cross the placental barrier.[5]

In this study, a literature review was conducted by collecting data from 25 studies regarding the Pb accumulation in the roadside plants and soils from several different regions in Turkey between 2001 and 2020. Then, Pb levels' changes throughout the years were examined, and possible reasons beneath them were discussed.

MATERIALS AND METHODS

In this study, 63 articles about heavy metal accumulation in plants and soil were searched. All studies about heavy metal accumulation included Pb but other heavy metals were varied. The study targeted the roadside plants and soil. Heavy metal, herbal, plant, highway, and roadside keywords were used while searching the articles. Initially, articles throughout the world were read, then narrowed down to studies from Turkey. The articles that did not examine Pb, not collected samples at the roadside, and were not studied in Turkey were eliminated. Twenty-five articles were left to be put on the tables. Table 1 shows Pb accumulation in plants (fruit and leaves).

Table 1. Lead content and its safe limit in different plant samples of different regions in Turkey

Year	Sample	Pb level (ppm)	Pb in portion (100 g)	Safe limits (ppm)	Proportion of safe limit	Location	Reference
2001	*Robinia pseudo-acacia* (leaves)	72.69	7.27	2	36.34	Denizli	Celik et al.[13]
2002	Apple	180	18.0	2	90.00	Elazığ	Bakirdere and Yaman[14]
2002	Grape	213	21.3	2	106.50	Elazığ	Bakirdere and Yaman[14]
2002	Apple (leaves)	866	86.6	2	433.00	Elazığ	Bakirdere and Yaman[14]
2002	Grape (leaves)	547	54.7	2	273.50	Elazığ	Bakirdere and Yaman[14]
2002	Tomato	175	17.5	2	87.50	Elazığ	Bakirdere and Yaman[14]
2002	Bell pepper	139	13.9	2	69.50	Elazığ	Bakirdere and Yaman[14]
2002	Parsley	585	58.5	2	11.70	Elazığ	Bakirdere and Yaman[14]
2003	Grass	1.75	0.175	2	0.875	Konya	Onder et al.[15]
2003	Lavender (flowers)	0.5	0.05	2	0.25	Western Anatolia	Divrikli et al.[16]
2003	Laurel (root)	0.1	0.01	2	0.05	Western Anatolia	Divrikli et al.[16]
2003	Chard (leaves)	0.2	0.02	2	0.10	Western Anatolia	Divrikli et al.[16]
2003	Chard (root)	2.8	0.28	2	14.0	Western Anatolia	Divrikli et al.[16]
2003	Lavender (leaves)	0.8	0.08	2	0.40	Western Anatolia	Divrikli et al.[16]
2006	Parsley	9.9	0.99	2	4.95	Kayseri	Demirezen and Aksoy[17]
2006	Tomato	9.7	0.97	2	4.85	Kayseri	Demirezen and Aksoy[17]
2007	Cabbage	0.91	0.091	2	0.455	İstanbul	Osma et al.[18]
2007	Parsley	0.95	0.095	2	0.475	İstanbul	Osma et al.[18]
2007	Chard	0.99	0.099	2	0.495	İstanbul	Osma et al.[18]
2007	*Rosmarinus officinalis*	6.9	0.690	2	3.45	Mersin	Koc and Sari[19]
2008	Apple	2.21	0.221	2	1.10	Konya	Hamurcu et al.[20]
2008	Cornelian	2.65	0.265	2	1.32	Konya	Hamurcu et al.[20]
2008	Plum	2.82	0.282	2	1.41	Konya	Hamurcu et al.[20]
2008	Rose	2.86	0.286	2	1.34	Konya	Hamurcu et al.[20]
2009	*Pinus nigra*	0.35	0.035	2	0.175	Denizli	Keskin and Ili[21]
2010	*Pinus nigra*	0.00	0	2	0	Denizli	Keskin and Ili[21]
2012	Sweet cherry (leaves)	8.74	0.874	2	4.37	Aras valley	Pehluvan et al.[22]
2012	Sweet cherry (fruits)	1.75	0.175	2	0.875	Aras valley	Pehluvan et al.[22]
2012	Black mullberry (leaves)	3.48	0.348	2	1.74	Aras valley	Pehluvan et al.[22]
2012	Black mullberry (fruits)	1.62	0.162	2	0.81	Aras valley	Pehluvan et al.[22]
2012	White mullberry (leaves)	4.15	0.415	2	2.07	Aras valley	Pehluvan et al.[22]
2012	White mullberry (fruits)	2.15	0.215	2	1.07	Aras valley	Pehluvan et al.[22]
2012	Apricot (leaves)	10.23	10.23	2	5.11	Aras valley	Pehluvan et al.[22]
2012	Apricot (fruits)	3.15	0.315	2	1.57	Aras valley	Pehluvan et al.[22]

Table 1. continued

Year	Sample	Pb level (ppm)	Pb in portion (100 g)	Safe limits (ppm)	Proportion of safe limit	Location	Reference
2012	Plum (leaves)	15.47	1547	2	7.73	Aras valley	Pehluvan et al.[22]
2012	Plum (fruits)	3.42	0.342	2	1.71	Aras valley	Pehluvan et al.[22]
2012	Peach (leaves)	7.69	0.769	2	3.84	Aras valley	Pehluvan et al.[22]
2012	Peach (fruits)	3.15	0.315	2	1.57	Aras valley	Pehluvan et al.[22]
2012	Pear (leaves)	10.43	1043	2	0.52	Aras valley	Pehluvan et al.[22]
2012	Pear (fruits)	2.15	0.215	2	1.07	Aras valley	Pehluvan et al.[22]
2012	Hawthorn (leaves	8.67	0.867	2	4.33	Aras valley	Pehluvan et al.[22]
2012	Hawthorn (fruis)	3.1	0.31	2	1.55	Aras valley	Pehluvan et al.[22]
2012	Rosehip (leaves)	10.36	1.36	2	5.18	Aras valley	Pehluvan et al.[22]
2012	Rosehip (fruits)	2.85	0.285	2	1.42	Aras valley	Pehluvan et al.[22]
2012	Sweet cherry (leaves)	47.83806947	4.784	2	23.92	Aras valley	Pehluvan et al.[22]
2012	*Rosmarinus officinalis (leaves)*	1.19	0.119	2	0.595	İzmir	Colak Esetlili et al.[23]
2012	Parsley	1.14	0.114	2	0.57	İzmir	Colak Esetlili et al.[23]
2014	*Passiflora coccinea*	8.94	0.894	2	4.47	Adana-Gaziantep highway	Kirpik et al.[24]
2014	Nerium oleander	4.86	0.486	2	2.43	Adana-Gaziantep highway	Kirpik et al.[24]
2014	*Rosmarinus officinalis*	8.16	0.816	2	4.08	Adana-Gaziantep highway	Kirpik et al.[24]
2014	*Rosmarinus officinalis* (refuge-stem)	9.48	0.948	2	4.74	Hatay	Bozdogan Sert et al.[25]
2014	*Rosmarinus officinalis* (refuge-leaves)	9.70	0.97	2	4.85	Hatay	Bozdogan Sert et al.[25]
2014	*Rosmarinus officinalis* (slope-stem)	11.21	1.121	2	5.60	Hatay	Bozdogan Sert et al.[25]
2014	*Rosmarinus officinalis* (slope-leaves)	10.01	1.00	2	5.00	Hatay	Bozdogan Sert et al.[25]
2016	*Celtis australis* (leaves)	34	3.4	2	17.00	İstanbul	Ozturk et al.[26]
2017	Hollyhock (leaves)	2.59	0.26	2	1.29	Lake Van	Kaya and Gülser[27]
2020	Pomegranate (fruits)	0.375	0.0375	2	0.1875	Pirinçli village-Siirt	Demirhan Aydın and Pakyürek[2]
2020	Pomegranate (fruits)	0.351	0.0351	2	0.1755	Kapılı village-Siirt	Demirhan Aydın and Pakyürek[2]
2020	Pomegranate (leaves)	0.614	0.0614	2	0.307	Pirinçli village-Siirt	Demirhan Aydın and Pakyürek[2]
2020	Pomegranate (leaves)	0.625	0.0625	2	0.3125	Kapılı village-Siirt	Demirhan Aydın and Pakyürek[2]

Pb: Lead

Table 2 shows Pb accumulation in soil. Tables 3 and 4 show Pb accumulation in parsley and rosemary (*Rosmarinus officinalis*). These two plants were used because they have more data available. We have to compare the same plants to make a correct comparison since each plant species has different bioaccumulation factors. Parsley and rosemary data were listed in different tables to achieve a more accurate comparison. Table 5 shows the exposure limits of five different national and international authorities for Pb, including Occupational Safety and Health Administration (OSHA), National Institute for Occupational Safety and Health (NIOSH), WHO, European Chemicals Agency (ECHA), and the Ministry of Family, Labor and Social Services of Turkey. The permissible exposure limit of Pb according to OSHA and NIOSH is 0.00005 ppm.[8] The safety limit of Pb for soil and plants according to WHO are 85 and 2 ppm, respectively.[9] Occupational exposure limits of Pb according to the Ministry of Family, Labour and Social Services of Turkey and ECHA are 0.00015 and 0.00003 ppm, respectively.[10-12]

Statistical analysis was not used in this manuscript due to the meta-analysis of published studies.

RESULTS

Pb accumulation in roadside plants

From the research, 60 results from different plants and places were collected. All plant data are listed in Table1 according to the year. The safe level of Pb in plants is 2 ppm, according to WHO. However, the results vary ranging from 0.00 to 866.0 ppm; 30% of plants were safe according to their Pb level. The Pb levels were higher in studies conducted in the early years than the recent years' results. Before 2003, all data were higher than the safe limit. The highest values were found in a study in 2002 in Elazığ, Turkey, and apple leaves had the most Pb accumulated. The second and third highest values were found in grape leaves and parsley, respectively, in the same study. The lowest values were found in Denizli, Turkey, in 2010. In that study, researchers found no Pb accumulation in *Pinus nigra*.

Table 2. Lead level and its safe limit in various soil samples of different places in Turkey

Year	Sample	Pb level (ppm)	Pb level in portion (100 g)	Safe limit	Proportion of safe limit	Location	Reference
2001	Soil	336.55	33.66	85	3.959	Denizli	Celik et al.[13]
2002	Soil	73	7.3	85	0.8588	Tokat	Tüzen[28]
2002	Soil	26	2.6	85	0.3059	Elazığ	Bakirdere and Yaman[14]
2002	Soil	13.28	1.328	85	0.1562	Elazığ	Bakirdere and Yaman[14]
2003	Soil	2.66	0.266	85	0.0313	Konya	Onder et al.[15]
2006-2007	Soil	1.55	0.16	85	0.0182	Edirne	Aktaş and Kocabaş[29]
2007	Soil	235.1	23.51	85	2.766	Bursa-İzmir highway	Aydinalp[30]
2008	Soil	191	19.1	85	2.247	İstanbul	Guney et al.[31]
2009	Soil	31.50	3.15	85	0.3705	Eskişehir	Malkoc et al.[32]
2009	Soil	1.72	0.172	85	0.0202	Fatsa	Özkutlu et al.[33]
2010	Central soil	401	40.1	85	4.7176	Ankara	Akbulut and Çevik[34]
2010	Highway soil	567	56.7	85	6.6705	Ankara	Akbulut and Çevik[34]
2010	Central soil	442	44.2	85	5.20	Bursa	Akbulut and Çevik[34]
2010	Highway soil	405	40.5	85	4.7647	Bursa	Akbulut and Çevik[34]
2012	Soil	124.36	12.436	85	1.4631	Gümüşhane	Vural[35]
2013	Soil	102.8514	10.285	85	1.21	Sakarya	Çelenk and Kızıloğlu[36]
2014	*Passiflora coccinea (soil)*	33.70	3.37	85	0.3965	Adana-Gaziantep highway	Kirpik et al.[24]
2014	*Nerium oleander (soil)*	25.56	2.556	85	0.3007	Adana-Gaziantep highway	Kirpik et al.[24]
2014	*Rosmarinus officinalis (soil)*	35.76	3.576	85	0.4207	Adana-Gaziantep highway	Kirpik et al.[24]
2016	Soil	27.4-51.55	2.74-5.155	85	0.3224 - 0.6065	İstanbul	Ozturk et al.[26]

Pb: Lead

The lethal dose of Pb is 450 ppm in the lowest published data. Three of the 60 results collected were higher than the lethal dose. The Pb values are mostly higher than 2 ppm but lower than the lethal dose.

Pb accumulation in roadside soil

During the research, 20 results were collected. All soil data are listed in Table 2 according to the year. The safe level of Pb in the soil is 85 ppm, according to WHO. Results were varied in the range of 1.55 to 567.00 ppm, whereas 55% of the samples were within the safe limit. The highest results were obtained in 2010 in Ankara, Turkey, while the lowest was in 2006 in Edirne, Turkey.

Comparison of Pb values in parsley

In Table 3, Pb accumulation in parsley from various locations are listed according to year. Four values were found. The values varied in the range of 0.95 to 585 ppm. Fifty percent of these results are under the safe limit. After 2007, the values are within safe limits even though the results are from metropolises. The highest accumulation, where Pb accumulation was higher than the lethal dose, was seen in 2002 in Elazığ, Turkey.

Comparison of Pb accumulation in R. officinalis

In Table 4, Pb accumulation in *R. officinalis* leaves from different areas are listed according to year. Four values were found, and two of them were from the same study where they investigated differences in Pb accumulation according to place (slope or refuge). Values vary from 1.19 to 10.01 ppm, in which 25% of the collected data were within the safe limit. Additionally, none of the reported values were above lethal dose. The highest value was seen in 2014 in Hatay, Turkey, in slope.

DISCUSSION

Heavy metal accumulation is one of the primary health concerns worldwide, affecting millions of people and ecosystems. Pb is a naturally occurring heavy metal that may accumulate through waste products and exhaust gases in the soils plants.

Initially, articles on heavy metal accumulation in plants and soil were searched. Then, the search was limited to the Pb accumulation of roadside plants and soil. After finding the Pb levels in plants and soil from diverse articles, the safe limit values of Turkish and International authorities were examined. The Pb levels were evaluated base on the WHO data. More data were obtained from plants, thus, making separate tables for

Table 3. Lead level and its safe limit in parsley samples of different places in Turkey

Year	Pb level (ppm)	Pb level in portion (100 g)	Safe limit	Proportion of safe limit	Location	Reference
2002	585	58.5	2	11.70	Elazığ	Bakirdere and Yaman[14]
2006	9.9	0.99	2	4.95	Kayseri	Demirezen and Aksoy[17]
2007	0.95	0.095	2	0.475	İstanbul	Osma et al.[18]
2012	1.14	0.114	2	0.57	İzmir	Colak Esetlili et al.[23]

Pb: Lead

Table 4. Lead level and its safe limit in *Rosmarinus officinalis* samples of various places in Turkey

Year	Pb level (ppm)	Pb level in portion (100 g)	Safe limit	Proportion of safe limit	Location	Reference
2007	6.9	0.690	2	3.45	Mersin	Koc and Sari[19]
2012	1.19	0.119	2	0.595	İzmir	Colak Esetlili et al.[23]
2014	9.70	0.97	2	4.85	Hatay-refugee	Bozdogan et al.[25]
2014	10.01	1.001	2	5.005	Hatay-slope	Bozdogan et al.[25]

Pb: Lead

Table 5. Exposure limits of lead according to different national and international authorities

Exposure limits of lead (ppm)					
OSHA PEL	NIOSH REL	WHO		Ministry of Family, Labour and Social Services	ECHA
		Soil	Plant		
0.0005[a]	0.0005[b]	85[c]	2[d]	0.00015[e]	0.00003[f]

[a]Permisible exposure limit of lead according to OSHA, [b]Recommended exposure limit of lead according to, NIOSH, [c]Safety limit of lead for soil according to WHO, [d]Safety limit of lead for plants according to WHO, [e]Occupational exposure limit of lead according to the Ministry of Family, Labour and Social Services of Turkey, [f]Occupational exposure limit of lead according to ECHA. OSHA: Occupational Safety and Health Administration, NIOSH: National Institute for Occupational Safety and Health, WHO: World Health Organization, ECHA: European Chemicals Agency

a more accurate comparison regarding their bioaccumulation factors.

In Table 1, accumulated Pb values (ppm) for several plant samples from different locations are listed throughout the years with their safe limits and percentages.

All the Pb values from the studies before 2003 exceed the safe limits. This findings gave rise to the thought that this is probably resulted from the low sensitivity of the analytical methods used back then due to the lack of the quality parameters of measurements. Analytical methods used for determining the heavy metal content in the plants were not precise enough to give a correct measurement, which led to inaccurate results.

On the other hand, banning the use of Pb in gasoline in 2004 positively decreased the accumulation rates. The Pb content in the plants generally diminished. This change may have resulted from a more proper and accurate analytical system and the ban of Pb in gasoline. However, the reported values were still high in metropolises and industrial cities.

By examining studies conducted from various cities with different economic backgrounds and means of livings, it can be concluded that, in the industrially-developed cities, Pb levels exceed the safe limits because of exhaust gases, heavy industry factories, waste products, and heavy traffic.

In addition, the differences in plants' bioaccumulation factors affect the results, such as different accumulation rates of perennial and annual plants.

In Table 2, the Pb contents in soil samples from the different regions in Turkey are listed by the year. Once again, the Pb content determined from the studies of earlier years is high, probably also because of the inaccuracy in the analytical methods and measurement systems. Furthermore, most industrialized cities had exceeded the safe limits.

According to a study conducted in 2010, Pb accumulation in the highway soil is higher in Ankara than in Bursa, the central soil's Pb content is more elevated in Bursa than in Ankara.[30] This contrast could be due to the heavier traffic on the highways of Ankara and intense industrial activity in Bursa. As a capital city, Ankara is the center of several routes, and Pb can be quickly accumulated in the plants and soils near the highway. In contrast, Bursa is known for its heavy industrial activity, especially the machinery industry. This industrialization is in the city center, which may release high exhaust gases containing Pb from the factories and cause accumulation in the central soil.

For Istanbul, Pb contents were measured in 2008 and 2016, and a significant decrease was found when comparing the results. Although the population has risen from 2008 to 2016 in İstanbul, which directly affect the traffic's heaviness, the Pb content in the soil reduced from 191 ppm to 27.4-51.55 ppm. This change probably is due to the banning of Pb in gasoline in 2004. Even after the ban, Pb levels in the given data did not decrease immediately but took some time, as shown in the results. The results indicated that it requires time to reduce the accumulation of Pb in the soil.

In Table 3, Pb levels in parsley samples determined from the different regions in Turkey are listed. The earlier years results seem to be much higher; this can be caused by improved measurement technologies and increased environmental awareness in the later years. For instance, the value measured in Elazığ in 2002 is within the lethal range. The cause of this high level may be explained by the technical problem, or low sensitivity of methods or a high metal level.

According to data from 2006 and 2007, although samples were collected within almost the same year in Kayseri and İstanbul, Pb accumulation in Istanbul is nearly one-tenth of Kayseri. Probably resulted from different industrial activities in those cities where Kayseri has many heavy metal industrial applications releasing a high amount of solid waste to the environment.

In Table 4, Hatay has the highest values, although it is long after the ban of Pb in gasoline. Air pollution can be the reason for this high amount. Besides, the slope had a higher accumulation than the refuge in Hatay. Mersin and Hatay are close cities geographically, and the accumulation rate decreased from 2007 to 2014, which may be the result of unleaded gasoline use since 2004.

CONCLUSION

In conclusion, Pb accumulation is a global concern, including in Turkey. Although the soil and plants' Pb contents generally decrease with time, the environmental and health risks are still present. The banning of gasoline is one of the primary causes of reduced concentrations.

The studies conducted by far provide us an insight into the contamination status of Pb in Turkey. The methods used for analyses can be more problematic in the earlier years due to the lack of quality parameters of measurements in published studies; however, more accurate and precise results are given in recent studies. For a better analysis, further studies must be done. The concentration levels of Pb should be followed more closely for different purposes, and research can be widen for different areas.

Conflict of interest: No conflict of interest was declared by the authors. The authors are solely responsible for the content and writing of this paper.

REFERENCES

1. Ten chemicals of major public health concern. Access date: 28 January 2021. Available from: https://www.who.int/ipcs/assessment/public_health/chemicals_phc/en/
2. Demirhan Aydın Ş, Pakyürek M. Heavy metal accumulation potential in pomegranate fruits and leaves grown in roadside orchards. PeerJ. 2020 Apr 14;8:e8990.
3. Tang J, Zhang J, Ren L, Zhou Y, Gao J, Luo L, Yang Y, Peng Q, Huang H, Chen A. Diagnosis of soil contamination using microbiological indices: A review on heavy metal pollution. J Environ Manage. 2019;242:121-130.

4. Fei X, Lou Z, Xiao R, Ren Z, Lv X. Contamination assessment and source apportionment of heavy metals in agricultural soil through the synthesis of PMF and GeogDetector models. Sci Total Environ. 2020;747:141293.
5. Tchounwou PB, Yedjou CG, Patlolla AK, Sutton DJ. Heavy metal toxicity and the environment. Exp Suppl. 2012;101:133-164.
6. Ali H, Khan E. What are heavy metals? Long-standing controversy over the scientific use of the term 'heavy metals' - proposal of a comprehensive definition. Toxicol Environl Chem. 2018;100:6-19.
7. Learn about Lead | US EPA. Access date: 28 January 2021. Available from: https://www.epa.gov/lead/learn-about-lead#lead
8. Marcotte S, Estel L, Minchin S, Leboucher S, Le Meur S. Monitoring of lead, arsenic and mercury in the indoor air and settled dust in the Natural History Museum of Rouen (France). Atmos Pollut Res. 2017;8:483-489.
9. Ogundele DT, Adio AA, Oludele OE. Heavy metal concentrations in plants and soil along heavy traffic roads in North Central Nigeria. J Anal Toxicol. 2015;5:6.
10. Kimyasal maddelerle çalışmalarda sağlık ve güvenlik önlemleri hakkında yönetmelik. Access date: 26 January 2021. Available from: https://www.mevzuat.gov.tr/File/GeneratePdf? mevzuat No=18709&mevzuatTur=KurumVeKurulusYonetmeligi&mevzuatTertip=5
11. ECHA Scientific report. Access date: 26 January 2021. Available from: https://echa.europa.eu/documents/10162/68cf7011-9c04-2634-efa6-b712f1b34a85
12. Guidance on information requirements and chemical safety assessment. Available from: 26 January 2021. Available from: https://echa.europa.eu/documents/10162/23047722/draft_inforeq_csr_e_caracal_clean_en.pdf/3720f759-186c-4280-bd56-2124735bfd91
13. Celik A, Kartal AA, Akdoğan A, Kaska Y. Determining the heavy metal pollution in Denizli (Turkey) by using *Robinio pseudo-acacia* L. Environ Int. 2005;31:105-112.
14. Bakirdere S, Yaman M. Determination of lead, cadmium and copper in roadside soil and plants in Elazig, Turkey. Environ Monit Assess. 2008;136:401-410.
15. Onder S, Dursun S, Gezgin S, Demirbas AH. Determination of heavy metal pollution in grass and soil of city centre green areas (Konya, Turkey). Pol J Environ Stud. 2007;16:145-154.
16. Divrikli U, Horzum N, Soylak M, Elci L. Trace heavy metal contents of some spices and herbal plants from western Anatolia, Turkey. Int J Food Sci Technol. 2006;41:712-716.
17. Demirezen D, Aksoy A. Heavy Metal Levels in Vegetables in Turkey are within safe limits for Cu, Zn, Ni and exceeded for Cd and Pb. J Food Qual. 2006;29:252-265.
18. Osma E, Serin M, Leblebici Z, Aksoy A. Heavy Metals Accumulation in Some Vegetables and Soils in Istanbul. Ekoloji. 2012;21:1-8.
19. Koc H, Sari H. Trace metal contents of some medicinal, aromatic plants and soil samples in the Mediterranean region, Turkey. J Applied Chemical Research. 2009;8:52-57.
20. Hamurcu M, Ozcan MM, Dursun N, Gezgin S. Mineral and heavy metal levels of some fruits grown at the roadsides. Food Chem Toxicol. 2010;48:1767-1770.
21. Keskin N, Ili P. Investigation of particular matters on the leaves of *Pinus nigra* Arn. subsp. pallasiana (Lamb.) Holmboe in Denizli (Turkey). Pak J Bot. 2012;44: 1369-1374.
22. Pehluvan M, Turan M, Kaya T, Şimşek U. Heavy metal and mineral levels of some fruit species grown at the roadside in the east part of Turkey. Fresenius Environ Bull. 2015;24:1302-1309.
23. Colak Esetlili B, Pekcan T, Çobanoğlu Ö, Aydoğdu E, Turan S, Anaç D. Essential plant nutrients and heavy metals concentrations of some medicinal and aromatic plants. Journal of Agricultural Sciences. 2014;20:239-247.
24. Kirpik M, Büyük G, Inan M, Çelik A. The Heavy Metal Content of Some Herbal Plants on the Roadside of Adana-Gaziantep Highway. JAFAG. 2017;34:129-136.
25. Bozdogan Sert E, Turkmen M, Cetin M. Heavy metal accumulation in rosemary leaves and stems exposed to traffic-related pollution near Adana-İskenderun Highway (Hatay, Turkey). Environ Monit Assess. 2019;191:553.
26. Ozturk A, Yarci C, Ozyigit I. Assessment of heavy metal pollution in Istanbul using plant (*Celtis australis* L.) and soil assays. Biotechnology & Biotechnological Equipment. 2017;31:1-7.
27. Kaya I, Gülser F. Determining heavy metal contents of hollyhock (*Alcea rosea* L.) in roadside soils of a Turkish lake basin. Pol J Environ Stud. 2018;27:2081-2087.
28. Tüzen M. Determination of heavy metals in soil, mushroom and plant samples by atomic absorption spectrometry. Microchem J. 2003;74:289-297.
29. Aktaş Y, Kocabaş A. Heavy Metal Content of Roadside Soil in Edirne, Turkey. Anal Lett. 2010;43:1869-1878.
30. Aydinalp C. The Status of Some Selected Heavy Metals in Roadside Soils of Bursa Province, Turkey. Environ Eng Manag J. 2010;9:559-563.
31. Guney M, Onay TT, Copty NK. Impact of overland traffic on heavy metal levels in highway dust and soils of Istanbul, Turkey. Environ Monit Assess. 2010;164:101-110.
32. Malkoc S, Yazıcı B, Savas Koparal A. Assessment of the levels of heavy metal pollution in roadside soils of Eskisehir, Turkey. Environ Toxicol Chem. 2010;29:2720-2725.
33. Özkutlu F, Turan M, Korkmaz K, Huang YM. Assessment of heavy metal accumulation in the soils and hazelnut plant (*Corylus avellena* L.) from Black Sea Coastal Region of Turkey. Asian J Chem. 2009;21:4371-4388.
34. Akbulut S, Çevik U. Accumulation of metals in roadside soil, dust and pine needles in different characteristic traffic areas. Fresenius Environmental Bulletin. 2014;23:516-522.
35. Vural A. Assessment of heavy metal accumulation in the roadside soil and plants of *Robinia pseudoacacia*, in Gumushane, Northeastern Turkey. Ekoloji. 2013;1-10.
36. Çelenk FK, Kızıloğlu FT. Distribution of lead accumulation in roadside soils : a case study from D 100 highway in Sakarya, Turkey. Int J Agric For Life Sci. 2015;2:1-10.

Turk J Pharm Sci 2021;18(5):589-596
DOI: 10.4274/tjps.galenos.2021.95680

ORIGINAL ARTICLE

Development of Oral Tablet Formulation Containing Erlotinib: Randomly Methylated-β-cyclodextrin Inclusion Complex Using Direct Compression Method

Doğrudan Basım Yöntemi Kullanılarak Randomize Metillenmiş-β-siklodekstrin İnklüzyon Kompleksi İçeren Erlotinib Oral Tablet Formülasyonu Geliştirilmesi

Nazlı ERDOĞAR*

Hacettepe University Faculty of Pharmacy, Department of Pharmaceutical Technology, Ankara, Turkey

ABSTRACT

Objectives: Erlotinib (ERL) is a tyrosine kinase inhibitor that has been used in the treatment of metastatic non-small cell lung cancer (NSCLC). However, its low aqueous solubility limits its absorption and oral bioavailability. To overcome these pharmacokinetic drawbacks, complexation of ERL can be applied. The aim of this study was to develop and characterize an oral tablet formulation containing ERL: Randomly methylated-β-cyclodextrin (RAMEB-CD) inclusion complex to enhance solubility and oral bioavailability of ERL.

Materials and Methods: An inclusion complex was prepared with RAMEB-CD using co-lyophilization technique. Structural characterization was performed using X-ray diffractometry and fourier-transform infrared spectroscopy. Tablet formulation of ERL: RAMEB-CD inclusion complex were prepared using direct compression technique. Tablet characteristics like hardness, diameter, thickness, friability, weight variability, disintegration and dissolution were evaluated. Flow properties of the powder were also determined.

Results: Characterization studies suggested that stable complexes between ERL and RAMEB-CD were obtained with co-lyophilization method. Tablet formulation using inclusion complex of ERL and RAMEB-CD with drug dose equivalent to 25 mg was successfully prepared using direct compression technique. Physical properties of the powder mixture were studied - angle of repose (°): 34.27±1.78; flow time: 2.2±0.4; HR: 1.05±0.02; compressibility index: 14.27±1.55. Moisture content (%) was found to be 0.27±0.05. The thickness, diameter and hardness values were 3.92±0.05 mm, 11.3±0.06 mm and 81.38±2.27 N, respectively. In uniformity of weight test, the average weight was 404.57±1.6 mg, with less than 5% deviation in 20 randomly selected tablets. Friability value was 0.27% and the disintegration time was found to be less than 15 min. Importantly, dissolution study showed that solubility of ERL was increased by complexation with RAMEB-CD. After 60 minutes, 99% of drug was released from the tablet formulation.

Conclusion: These results demonstrate that a new tablet formulation of ERL: RAMEB-CD inclusion complex could be an alternative approach to achieve increased dissolution and oral bioavailability of ERL for NSCLC treatment.

Key words: Erlotinib, inclusion complex, direct compression, dissolution

ÖZ

Amaç: Erlotinib (ERL) metastatik küçük hücreli akciğer kanserinde (NSCLC) kullanılan tirozin kinaz inhibitörüdür. Bununla birlikte, düşük suda çözünürlüğü absorpsiyonunu ve oral biyoyararlanımını sınırlamaktadır. Bu sakıncaların üstesinden gelmek için kompleksleşme yöntemi kullanılmaktadır. Çalışmanın amacı ERL'nin çözünürlüğünü ve oral biyoyararlanımını artırmak için ERL: Randomize metillenmiş β-siklodekstrin (RAMEB-CD) inklüzyon kompleksi içeren oral tablet formülasyonu geliştirilmesi ve bu formülasyonun karakterize edilmesidir.

Gereç ve Yöntemler: RAMEB-CD siklodekstrin içeren inklüzyon kompleksi ko-liyofilizasyon yöntemi ile hazırlanmıştır. X-ray difraktometresi ve fourier-transform infrared spektroskopisi kullanılarak fizikokimyasal karakterizasyon yapılmıştır. Direkt basım yöntemi ile ERL: RAMEB-

*Correspondence: nerdogar@hacettepe.edu.tr, Phone: +90 5334879527, ORCID-ID: orcid.org/0000-0003-2527-5484

Received: 07.11.2020, Accepted: 15.02.2021

CD siklodekstrin inklüzyon kompleksi içeren tablet formülasyonu hazırlanmıştır. Sertlik, çap, kalınlık, kırılganlık, ağırlık değişkenliği, dağılma ve dissolüsyon gibi tablet özellikleri belirlenmiştir. Tozun akış özellikleri de tayin edilmiştir.

Bulgular: Karakterizasyon çalışmaları ko-liyofilizasyon tekniği ile ERL ve RAMEB-CD arasında stabil kompleks elde edildiğini göstermiştir. Buna göre, direkt basım yöntemi ile 25 mg ilaç dozuna eşdeğer olacak şekilde ERL ve RAMEB-CD inklüzyon kompleksi kullanılarak tablet formülasyonu hazırlanmıştır. Toz karışımının fiziksel özellikleri belirlenmiştir yığın açısı (˚): 34,27±1,78; akış süresi: 2,2±0,4; Hausner oranı: 1,05±0,02; basılabilirlik indeksi: 14,27±1,55). Nem içeriği %0,27±0,05 bulunmuştur. Kalınlık, çap ve sertlik değerleri sırasıyla 3,92±0,05 mm, 11,3±0,06 mm ve 81,38±2,27 N olarak bulunmuştur. Ağırlık sapması testinde; ortalama tablet ağırlığı 404,57±1,6 mg olup rastgele seçilen 20 tablet için sapma %5'ten küçüktür. Kırılganlık değeri %0,27'dir. Dağılma zamanı 15 dakikadan az bulunmuştur. Dissolüsyon çalışması RAMEB-CD ile kompleksleşme ile ERL'nin suda çözünürlüğünün önemli ölçüde arttığını göstermiştir. Altmış dakika sonunda ilacın %99'u salınmıştır.

Sonuç: Elde edilen veriler ile ERL: RAMEB-CD inklüzyon kompleksi içeren yeni tablet formülasyonunun daha iyi çözünme ve oral biyoyararlanım elde etmek için NSCLC tedavisinde alternatif bir yaklaşım olabileceği sonucuna varılmıştır.

Anahtar kelimeler: Erlotinib, inklüzyon kompleksi, direkt basım, dissolüsyon

INTRODUCTION

Erlotinib (ERL) is a selective tyrosine kinase inhibitor which targets epidermal growth factor receptor (EGFR). ERL shows anticancer activity in EGFR-overexpressing tumors such as non-small cell lung cancer and pancreatic cancer.[1] ERL is commercially manufactured and available as a film-coated tablet (Tarceva®), approved by the European Medicines Agency and Food and Drug Administration (FDA). However, several properties of ERL have created challenges to its clinical use. ERL is a weak base with low aqueous solubility (0.4 mg/mL at pH 2). Its low dissolution rate results in limited absorption and low bioavailability. When administered orally, ERL reaches its peak plasma concentration after approximately 4 h, with bioavailability of 60%. A plasma concentration of 44% is adequate for antitumor activity.[2] Moreover, ERL can cause a wide range of adverse effect including diarrhea, rash, renal failure, thrombocytopenia, and neutropenia.[3,4] Hence, novel formulations of ERL are needed to enhance its efficacy and safety. Different approaches reported to increase ERL solubility include solid dispersion, polymorphism, size reduction, and complexation.[5,6] Also, a self-emulsifying formulation,[7] a reverse micelle-loaded lipid nanocarrier formulation,[8] and a sulfobutyl-ether-β-cyclodextrin (CD) complex formation[9] have been utilized to improve ERL bioavailability.

Recently, CD complexation has been employed to increase the solubility and bioavailability of hydrophobic drugs. CDs are cyclic oligosaccharides comprised of 6 or more glucopyranose units bound via α-(1, 4) bonds. Natural CDs include α-, β- and γ-CDs with have 6, 7, and 8 glucose units, respectively.[10] CDs contain a hydrophilic outer surface that results in their high aqueous solubility and a lipophilic cavity capable of accommodating several molecules to form inclusion complexes. Its structure impacts the physicochemical properties of encapsulated drugs by increasing their solubility, dissolution, and bioavailability.[11-13]

However, utilization of natural CDs as drug carriers has been limited due to their low solubility. Different chemical modifications of CD have resulted in various CD derivatives with enhanced aqueous solubility.[9,14-16] Among the modified CDs, randomly methylated ß-CD (RAMEB-CD) complexation with ERL has not been studied.

The purpose of this work was to develop and characterize a new tablet formulation containing the ERL: RAMEB-CD inclusion complex to increase dissolution and oral bioavailability of ERL. Additionally, flow properties and quality control parameters of the formulation were evaluated.

MATERIALS AND METHODS

Materials

ERL hydrochloride (molecular weight: 429.9 g/mol, Hetero Labs, Telangana, India) was a kind gift from Nobel İlaç. RAMEB-CD was a kind gift from cyclolab (Budapest, Hungary). Acetone was purchased from Sigma-Aldrich (St. Louis, USA). Tween 80 was obtained from Merck-Schuchardt (Hohenbrunn, Germany). All other chemicals were of reagent grade and solvents were of high performance liquid chromatography (HPLC) grade. Lactose monohydrate and Avicel pH 102 was purchased from Sigma-Aldrich. Magnesium stearate was provided by Nitika Pharmaceuticals (Maharashtra, India). Sodium starch glycolate was purchased from Avebe (Foxhol, Netherlands).

Preparation of ERL: RAMEB-CD inclusion complex

ERL: RAMEB-CD inclusion complex was prepared by a lyophilization technique that could be was demonstrated in another study (data not shown). Briefly, ERL (27.8 mg, 21 mM) was dissolved in acetone (3 mL) and then slowly added to RAMEB-CD aqueous solution (82.1 mg in 3 mL or 21 mM) to achieve a molar ratio of 1:1. The suspension was magnetically stirred at room temperature for 24 h. The organic solvent was evaporated using a rotary evaporator (IKA RV 10 basic, Germany). The obtained solution was frozen at -20˚C and was lyophilized at -80˚C under 0.1 mbar for 24 h, resulting in a white fluffy powder (Labconco Freezone 4.5 Plus, USA).

Characterization of ERL: RAMEB-CD inclusion complex

Fourier-transform infrared (FT-IR) spectroscopy

FT-IR spectra of ERL, RAMEB-CD, physical mixture (PM), and ERL: RAMEB-CD inclusion complex were obtained using Perkin Elmer BX Spectrum (USA) at the range of 4000-500 cm^{-1} at ambient temperature.

X-ray diffractometry (XRD)

The XRD patterns of ERL, RAMEB-CD, PM, and ERL: RAMEB-CD inclusion complex were obtained using a Multipurpose X-ray Diffraction Multipurpose Diffractometer (X'Pert Pro MPD, Malvern PANalytical, UK) with Cu Ka radiation powered at

voltage 45 kV and current 40 mA. The diffraction angle (2θ) was between 3˚-40˚ and the scanning rate was 2˚/min.

Preparation of tablet formulation containing ERL: RAMEB-CD inclusion complex

Tablet formulations containing lyophilized ERL: RAMEB-CD inclusion complex (equivalent to 25 mg ERL) was prepared by direct compression method using excipients shown in Table 1. Tablet formulations were manufactured based on the commercial drug Tarceva®.[17] It contains 31% lactose monohydrate and 33% Avicel pH 102 as fillers, 8% sodium starch glycolate as a super disintegrant, and 1% magnesium stearate as a lubricant. Using a roller mixer, ERL: RAMEB-CD inclusion complex was blended with lactose monohydrate and Avicel pH 102 for 5 min. Sodium starch glycolate was added into the mixture in small increments. Finally, the powder mixture was mixed with magnesium stearate. Tablet weight was adjusted to 400 mg and tablets were compressed using Erweka AR 400 (Heusenstamm, Germany) to manufacture oral tablet formulations containing ERL: RAMEB-CD complex.

Powder flow properties

The angle of repose (˚)

The angle of repose was determined using the fixed height funnel standing technique. A standard funnel was physically secured and powder was allowed to flow through the orifice of the funnel cone. The radius (r) of the base and height of powder mass (h) was measured, and was calculated using this formula:

$$\tan(\alpha) = \frac{height}{0.5xbase}$$

The flow time was evaluated with a standard funnel. The results were given as mean ± standard deviation (SD).

Hausner ratio (HR) and compressibility index:

The HR and compressibility index are two parameters that can be calculated to predict the characteristics of powder flow. The two indices are calculated as follows:

$$Hausner\ ratio = \frac{Vo}{Vf}$$

$$Compressibility\ index = 100x\frac{Vo - Vf}{Vo}$$

where V_0: Bulk volume; V_f: Tapped volume of powder.

Table 1. Components of tablet formulation containing ERL: RAMEB-CD inclusion complex

Components	Amount (mg)	Percent (%)
ERL-RAMEB complex	109	27
Lactose monohydrate	123	31
Avicel pH 102	132	33
Sodium starch glycolate	32	8
Magnesium stearate	4	1

ERL: Erlotinib, RAMEB-CD: Randomly methylated-β-cyclodextrin

Bulk/tapped volume and density

The bulk (V_0) and apparent volumes (V_{10},V_{500}, and V_{1250}) of powder mixture (50 g) were measured in a 100 mL cylindrical vessel. Because the difference between V_{500} and V_{1250} was less than 2 mL, V_{1250} was considered as the tapped volume. Bulk and tapped densities were calculated as below:

$$Bulk\ density = \frac{m}{Vo}$$

$$Tapped\ density = \frac{m}{\mathrm{V1250}}$$

m: Sample weight (g), V_0: The bulk volume (mL), V_{1250}: The tapped volume (mL).

Moisture content (%)

3 g of powder were heated at 102˚C (Ohaus MB45 Moisture Analyzer, Parsippany, USA) until the weight remained constant.

Quality control tests for tablets containing ERL: RAMEB-CD inclusion complex

Hardness, thickness and diameter

Hardness (n=10), diameter (n=20), and thickness (n=20) of tablets were measured using a Pharma test PTB 311E (Hainburg, Germany).

Friability

Tablets (n=20) were weighed, then placed in a friabilator (Pharma test PTF 10E, Hainburg, Germany). After rotating at 100 cycles, the final weight of tablets was checked. Percent weight loss was calculated.

Uniformity of weight

Tablets (n=20) were weighed individually. The average mass and SD were calculated.

Disintegration test

The disintegration test of tablets was performed using Pharma test PTZ-S (Hainburg, Germany) in 1 L of purified water at 37˚C. Tablets (n=6) were placed in cylindrical tubes of the system and, then the device started to move in a periodic upward-downward manner automatically. The time for each tablet to disintegrate was recorded.

Dissolution test

The dissolution experiment was undertaken using the FDA dissolution methods database.[18] It was performed using a paddle (USP Apparatus 2) in 0.02% Tween 80 in 0.01 N HCl (1000 mL) at 75 rpm. Tablets containing ERL: RAMEB-CD inclusion complex and ERL tablets (containing 25 mg ERL) were added to 1000 mL medium (Sotax Dissolution Testing Device, Switzerland). At various time points (5, 10 15, 20, 30, 45, 60 min), 2 mL of aliquot was withdrawn and replaced with the same volume of fresh medium. All samples were filtered through a 0.45 µm filter. The filtrate was analyzed by an analytically validated HPLC method (r^2: 0.9992). These methods consist of a Kromasil® reversed-phase C18 (250x4.6 mm) column andammonium acetate buffer (pH 4): Acetonitrile (65:35 v/v) as the mobile phase, with injection volume: 20 µL and flow rate: 1 mL min^{-1}.

RESULTS AND DISCUSSION

Characterization of ERL: RAMEB-CD inclusion complex

ERL: RAMEB-CD inclusion complex was prepared with lyophilization technique and resulted in improved ERL solubility. Complexation between drugs and CD may be mediated by van der Waals and non-bonding forces. The ERL: CD ratio (1:1) used resulted in adequation interactions between the hydrophobic region of the drug and CD and allowed successful complexation. Moreover, a stronger interaction between RAMEB-CD and ERL could be due to the lipophilic methyl groups on the RAMEB-CD ring which confers higher solubility and solubilization properties.[19,20]

Figure 1 shows the FT-IR spectra of ERL, RAMEB-CD, PM and ERL: RAMEB-CD inclusion complex. ERL spectrum displayed strong absorption bands at 3277 cm^{-1} (for CH_3, C-H stretching vibrations), 1634 cm^{-1} (for NH, secondary amine bending vibrations), 3277 cm^{-1} (for ≡C-H stretching vibrations), 1238 cm^{-1}, 1069 cm^{-1} (for phenyl ether group) and 1021 cm^{-1} (for aliphatic ether group), which is in agreement with findings reported by Parthasaradhi et al.[21] The spectrum of RAMEB-CD was characterized by intense bands at 3300-3500 cm^{-1} (O-H stretching vibration) and 2800-3000 cm^{-1} (for -CH and $-CH_2$-groups).[22] FT-IR spectrum of PM showed bands that appear as the superposition of the spectra of both ERL and RAMEB-CD, with no shift of the absorption band at 3277 cm^{-1} and 1634 cm^{-1}. However, significant changes were observed in the peak widths at the center-frequencies (1634 cm^{-1} and 3277 cm^{-1}) of the characteristic absorption peaks of ERL. This peak broadening and disappearance of the ERL characteristic peak indicated ERL-RAMEB-CD interaction and validates the formation of the inclusion complex of ERL: RAMEB-CD (Figure 1).

The XRD patterns of ERL, RAMEB-CD, PM and ERL: RAMEB-CD inclusion complex are shown in Figure 2. The XRD pattern of ERL showed the presence of strong, sharp peaks at 5.66, 9.74, 11.32, 18.95, 22.78, 23.6, 24.24, 30.07 on 2θ, confirming the crystalline nature of ERL. The XRD pattern of RAMEB-CD displayed two broad peaks and multiple undefined, diffuse peaks with low intensities, indicating the amorphous structure of CD.[23] The PM showed very few of the crystalline ERL peaks, but with decreased intensities and no sharp peaks. In contrast,

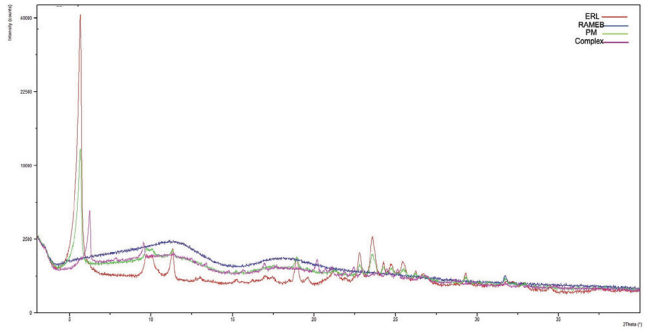

Figure 2. X-ray diffractometry patterns of ERL, RAMEB-CD, PM, and ERL: RAMEB-CD inclusion complex

ERL: Erlotinib, RAMEB-CD: Randomly methylated-β-cyclodextrin, PM: Physical mixture

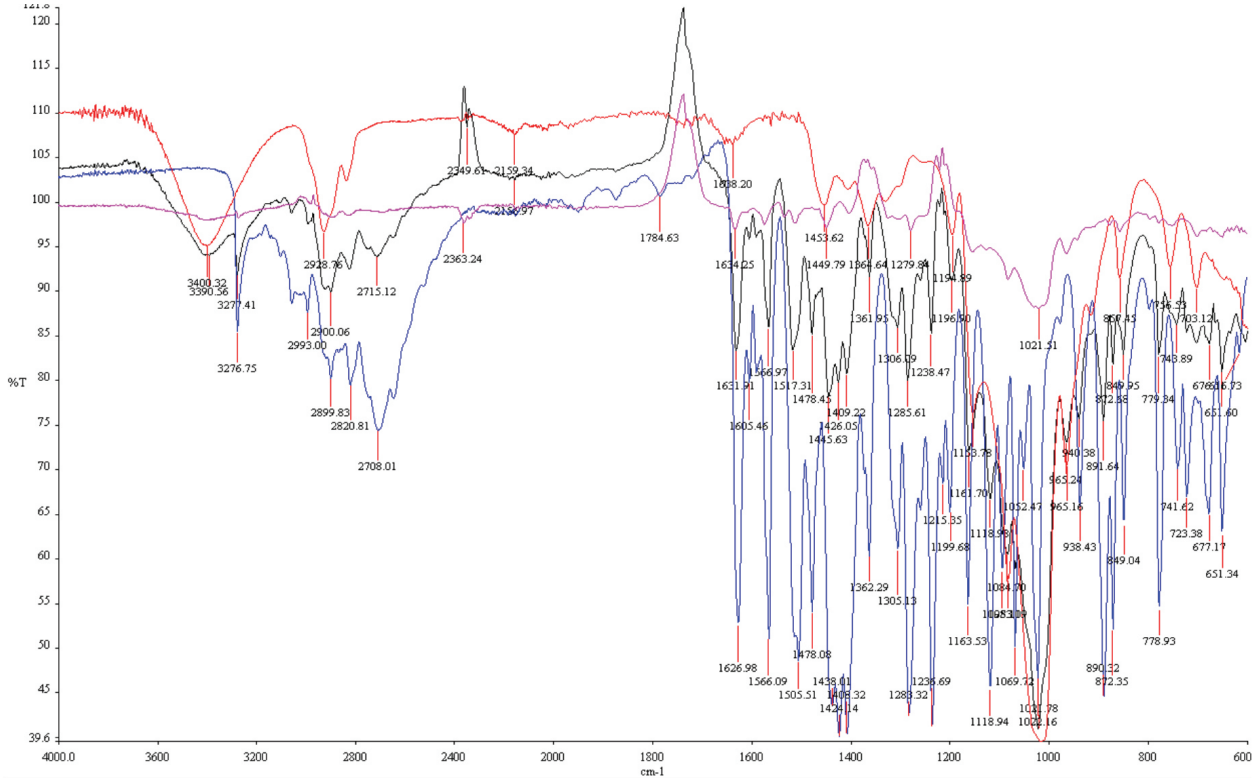

Figure 1. FT-IR spectra of ERL, RAMEB-CD, PM, and ERL: RAMEB-CD inclusion complex

FT-IR: Fourier-transform infrared, ERL: Erlotinib, RAMEB-CD: Randomly methylated-β-cyclodextrin, PM: Physical mixture

compared to the XRD patterns of ERL and RAMEB-CD, the inclusion complex presented an amorphous state, due to both the CD structure and post-lyophilization effects.[9] The inclusion complex diffractometric profile had less intense RAMEB-CD peaks and the absence of the ERL sharp characteristic peaks, thus suggesting that ERL is in an amorphous state. This reduction in ERL crystallinity provides further evidence to the formation of the ERL: RAMEB-CD inclusion complex in solid-state, in agreement with FT-IR results.[24]

The flow properties of powder mixture in tablet formulation

The powder mixture, consisting of drug-CD inclusion complex and excipients, was prepared and its flow properties, such as the angle of repose, compressibility index, HR and moisture content, were measured. The angle of repose is a predictor of flow characteristics of all powder mixtures. In ERL: RAMEB-CD formulation in this study, the angle of repose measured was 34.27±1.78, indicating good flow property according to the United States Pharmacopeia (USP) specifications. HR and compressibility index were 1.05±0.02 and 14.27±1.55, respectively, which further support good flow properties according to USP 30.[25] The moisture content is another important parameter contributing to powder flow. In our study, the moisture content (%) was found 0.27±0.05%, which can enable binding of drugs with excipients during the manufacturing process. These data showed that the prepared powder displayed good flow properties and was favorable for direct compression technique.

Quality-control tests for tablets containing ERL: RAMEB CD inclusion complex

In this study, all of the tablets were manufactured with uniform appearance and appropriate physical characteristics. The thickness and diameter of tablets are between 3.92±0.05 mm and 11.3±0.06 mm, respectively. The very low variabilities in thickness and diameter showed that the operation and weighing of the powder mixture are appropriate during the manufacturing process. The hardness value was 81.38±2.27 N for tablets containing ERL: RAMEB-CD inclusion complex, showing that tablets had suitable crushing strength to resist abrasion.

Friability is a significant parameter that points out the tablet's capability to resist abrasion along with packaging, transport, and handling; compendial specification not more than 1%.[26] Friability value was 0.27% for tablet formulation containing ERL: RAMEB-CD inclusion complex (Table 2). This data correlates the pharmacopeia criteria and shows that tablets probably have adequately high mechanical stress during the process, handling and transportation.[27]

The uniformity of weight (or weight variation) of prepared tablets was evaluated by USP 30. The average weight of prepared tablets was found 404.57±1.6 mg, with less than 5% deviation for 20 tablets, which meets the acceptability criteria of USP.[28] These results suggested that the powder mixture retained homogeneity during the preparation and manufacturing process.

For all tablets, the first important step towards drug dissolution is the breakdown of the tablets into granules or primary powder particles in a process known as disintegration. The disintegration time of the tablet formulation containing ERL: RAMEB-CD inclusion complex was compatible to USP 30 standards which require that uncoated tablets have disintegration time standard values less than 15 minutes (Table 2).

Before performing the dissolution test, the HPLC method was validated. The linearity of the calibration curves was established over the concentration range of 1-200 µg/mL with a correlation coefficient value of 0.9992±0.01, indicating acceptable linearity in this range. The values (mean ± standard error; n=3) of the slope and intercept were 60.103 and 19.837, respectively. The limit of detection was 0.21 µg/mL and the limit of quantitation was 0.71 µg/mL, both with acceptable accuracy and precision. To determine the accuracy of analytical method, six solutions with three different concentrations (0.5, 10 and 50 mg/mL) of the formulation were prepared and HPLC analysis was done. Mean recovery of ERL recovery and coefficient of variation (CV) were calculated as shown in Table 3. The recovery value was determined as 101.82%± 3.7 with CV below 2%. The calculated CV was found suitable according to FDA, International Council for Harmonisation of Technical Requirements for Pharmaceuticals for Human Use, and USP's validation guidelines. To determine the precision of the analytical method, reproducibility and inter-day precision analysis were done. Data are shown in Table 4 and Table 5. CVs was found to be below 2% therefore, indicating that the precision and accuracy of the method were sufficient.

Figure 3 represents dissolution profiles of ERL tablet and ERL: RAMEB-CD tablet. The tablet containing the inclusion complex showed 70.43% dissolved drug at 10 minutes; an approximately 2.5-fold increase in drug dissolution comparison to ERL alone (30.2%). At one hour, the tablet containing the inclusion complex released 98.57% of the drug, while the ERL tablet dissolved 46.51%, indicating an approximately two-fold increase in dissolution. This increase in dissolution may due to the solubilization effect of CD, the particle size reduction at the molecular level, and the formation of hydrogen bonds in the complex.[29]

Table 2. Results from the quality control tests for tablets containing ERL: RAMEB-CD inclusion complex

Parameter	Value (mean ± SD)
Thickness (n=20)	3.92±0.05 mm
Diameter (n=20)	11.3±0.06 mm
Hardness (n=10)	81.38±2.27 N
Friability (n=20)	0.27%
Uniformity of weight (n=20)	404.57±1.6 mg
Disintegration time (n=6)	5 min

ERL: Erlotinib, RAMEB-CD: Randomly methylated-β-cyclodextrin, SD: Standard deviation

Table 3. Coefficient of variation and % recovery of erlotinib

Sample number	10 µg/mL % recovery	50 µg/mL % recovery	150 µg/mL % recovery
1	9.87	50.59	150.07
2	10.19	51.85	154.55
3	9.75	51.95	156.66
4	9.8	50.28	154.92
5	9.82	51.21	155.7
6	9.84	49.54	150.46
X	9.88	50.9	153.73
SD	0.18	0.94	2.78
CV	1.79	1.85	1.81

SD: Standard deviation, CV: Coefficient of variation

Table 4. Repeatability results of erlotinib (n=6)

Sample	Concentration (µg/mL)	X	SD	CV
1	50.28	50.82	0.89	1.76
2	50.43			
3	50.26			
4	50.37			
5	51.04			
6	52.55			

SD: Standard deviation, CV: Coefficient of variation

Table 5. Inter-day precision results of erlotinib (n=6)

Sample	Concentration (µg/mL)	X	SD	CV
1	50.59	51.47	0.76	1.49
2	51.92			
3	51.91			

SD: Standard deviation, CV: Coefficient of variation

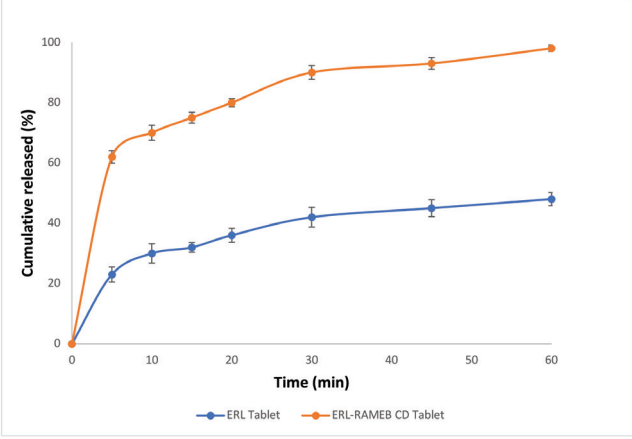

Figure 3. Dissolution profiles of erlotinib tablet and ERL: RAMEB-CD tablet in 0.02% Tween 80 in 0.01 N HCl under sink conditions (n=6, mean ± SD)

ERL: Erlotinib, RAMEB-CD: Randomly methylated-β-cyclodextrin, SD: Standard deviation

The similarity factor (f_2) was used to compare the dissolution profiles. If the f_2 value is 50-100, the curves can be considered as similar.[30] f_2 obtained between the two dissolution curves of ERL and inclusion complex was 11, suggesting that release behaviors for inclusion complex differed from that for ERL. These findings suggest that RAMEB-CD was able to form a water-soluble inclusion complex with ERL and improved its dissolution rate.[31,32] This improvement in the solubility properties of ERL could result in enhanced bioavailability and could possibly minimize the dose-limited side effects. Therefore, complexation with RAMEB-CD possesses great potential in improving the therapeutic and safety profile of ERL.

CONCLUSION

In this study, ERL: RAMEB-CD inclusion complex was successfully developed and evaluated. The inclusion complex was characterized by XRD and FT-IR studies and confirmed the formation of the inclusion complex. A novel tablet formulation

of ERL: RAMEB-CD inclusion complex was prepared by a direct compression method. *In vitro* dissolution studies demonstrated the increase in aqueous solubility and dissolution rate of the complex. In summary, this study applies an effective method of CD complexation to overcome limited drug solubility and allow the preparation of an efficient oral dosage form of ERL to increase its efficacy and reduce its adverse effects.

Conflict of interest: No conflict of interest was declared by the author. The author are solely responsible for the content and writing of this paper.

REFERENCES

1. Soulieres D, Senzer NN, Vokes EE, Hidalgo M, Agarwala SS, Siu LL. Multicenter phase II study of erlotinib, an oral epidermal growth factor receptor tyrosine kinase inhibitor, in patients with recurrent or metastatic squamous cell cancer of the head and neck. J Clin Oncol. 2004;22:77-85.
2. Thomas SM, Grandis JR. Pharmacokinetic and pharmacodynamic properties of EGFR inhibitors under clinical investigation. Cancer Treat Rev. 2004;30:255-268.
3. Fan L, Hu L, Yang B, Fang X, Gao Z, Li W, Sun Y, Shen Y, Wu X, Shu Y, Gu Y, Wu X, Xu Q. Erlotinib promotes endoplasmic reticulum stress-mediated injury in the intestinal epithelium. Toxicol Appl Pharmacol. 2014;278:45-52.
4. Herchenhorn D, Dias FL, Viegas CM, Federico MH, Araujo CM, Small I, Bezerra M, Fontao K, Knust RE, Ferreira CG, Martins RG. Phase I/II study of erlotinib combined with cisplatin and radiotherapy in patients with locally advanced squamous cell carcinoma of the head and neck. Int J Radiat Oncol Biol Phys. 2010;78:696-702.
5. Chaudhari SP, Dugar RP. Application of surfactants in solid dispersion technology for improving the solubility of poorly water-soluble drugs. J Drug Deliv Sci Tech. 2017;41:68-77.
6. Vimalson DC, Parimalakrishnan S, Jeganathan NS, Anbazhagan S. Techniques to enhance solubility of hydrophobic drugs: an overview. Asian J Pharm. 2016;10:S67-S75.
7. Truong DH, Tran TH, Ramasamy T, Choi JY, Lee HH, Moon C, Choi HG, Yong CS, Kim JO. Development of Solid Self-Emulsifying Formulation for Improving the Oral Bioavailability of Erlotinib. AAPS PharmSciTech. 2016;17:466-473.
8. Vrignaud S, Hureaux J, Wack S, Benoit JP, Saulnier P. Design, optimization and *in vitro* evaluation of reverse micelle-loaded lipid nanocarriers containing erlotinib hydrochloride. Int J Pharm. 2012;436:194-200.
9. Devasari N, Dora CP, Singh C, Paidi SR, Kumar V, Sobhia ME, Suresh S. Inclusion complex of erlotinib with sulfobutyl ether-beta-cyclodextrin: Preparation, characterization, in silico, *in vitro* and *in vivo* evaluation. Carbohydr Polym. 2015;134:547-556.
10. Kwon S, Lee W, Shin HJ, Yoon SI, Kim YT, Kim YJ, Lee K, Lee S. Characterization of cyclodextrin complexes of camostat mesylate by ESI mass spectrometry and NMR spectroscopy. J Mol Struct. 2009;938:192-197.
11. Karathanos VT, Mourtzinos I, Yannakopoulou K, Andrikopoulos NK. Study of the solubility, antioxidant activity and structure of inclusion complex of vanillin with beta-cyclodextrin. Food Chem. 2007;101:652-658.
12. Lyra MAM, Soares-Sobrinho JL, Figueiredo RCBQ, Sandes JM, Lima AAN, Tenorio RP, Fontes DAF, Santos FLA, Rolim LA, Rolim-Neto PJ. Study of benznidazole-cyclodextrin inclusion complexes, cytotoxicity and trypanocidal activity. J Incl Phenom Macrocycl Chem. 2012;73:397-404.
13. Wang DW, Ouyang CB, Liu Q, Yuan HL, Liu XH. Inclusion of quinestrol and 2,6-di-O-methyl-beta-cyclodextrin: Preparation, characterization, and inclusion mode. Carbohydr Polym. 2013;93:753-760.
14. Vaidya B, Parvathaneni V, Kulkarni NS, Shukla SK, Damon JK, Sarode A, Kanabar D, Garcia JV, Mitragotri S, Muth A, Gupta V. Cyclodextrin modified erlotinib loaded PLGA nanoparticles for improved therapeutic efficacy against non-small cell lung cancer. Int J Biol Macromol. 2019;122:338-347.
15. Gontijo S, Guimarães P, Viana C, Denadai A, Gomes A, Campos P, Andrade S, Sinisterra R, Cortés M. Erlotinib/hydroxypropyl-β-cyclodextrin inclusion complex: characterization and in vitro and in vivo evaluation. J Incl Phenom Macrocycl Chem. 2015;83:267-279.
16. Polat HK, Bozdag Pehlivan S, Ozkul C, Calamak S, Ozturk N, Aytekin E, Firat A, Ulubayram K, Kocabeyoglu S, Irkec M, Calis S. Development of besifloxacin HCl loaded nanofibrous ocular inserts for the treatment of bacterial keratitis: *In vitro, ex vivo* and *in vivo* evaluation. Int J Pharm. 2020;585:119552.
17. ANNEX I Summary of Product Characteristics. Available from: https://www.ema.europa.eu/en/documents/product-information/tarceva-epar-product-information_en.pdf
18. Dissolution Methods. Available from: https://www.accessdata.fda.gov/scripts/cder/dissolution/dsp_SearchResults.cfm
19. Jansook P, Ogawa N, Loftsson T. Cyclodextrins: Structure, physicochemical properties and pharmaceutical applications. Int J Pharm. 2018;535:272-284.
20. Fenyvesi F, Nguyen TLP, Haimhoffer A, Rusznyak A, Vasvari G, Bacskay I, Vecsernyes M, Ignat SR, Dinescu S, Costache M, Ciceu A, Hermenean A, Varadi J. Cyclodextrin complexation improves the solubility and caco-2 permeability of chrysin. Materials. 2020;13:3618.
21. Parthasaradhi B, Rathnakar K, Raji R, Muralidhara D, Srinivasa T. Erlotinib hydrochloride polymorph Form A substantially free of polymorph Form B. EP2218713A1, 2007. Available from: https://patents.google.com/patent/EP2218713A1/en
22. Nicolescu C, Arama C, Monciu CM. Preparation and characterization of inclusion complexes between repaglinide and β-cyclodextrin, 2-hydroxypropyl-β-cyclodextrin and randomly methylated β-cyclodextrin. Farmacia. 2010;58:78-88.
23. Sbarcea L, Udrescu L, Dragan L, Trandafirescu C, Szabadai Z, Bojita M. Fosinopril-cyclodextrin inclusion complexes: phase solubility and physicochemical analysis. Pharmazie. 2011;66:584-589.
24. Tănase I, Sbârcea L, Ledeţi A, Vlase G, Barvinschi P, Văruţ R, Dragomirescu A, Axente C, Ledeţi I. Physicochemical characterization and molecular modeling study of host-guest systems of aripiprazole and functionalized cyclodextrins. J Therm Anal Calorim. 2020;141:1027-1039.
25. USP 30-NF 25 Powder Flow. 2005:643. Available from: https://www.uspnf.com/?gclid=CjwKCAjw7rWKBhAtEiwAJ3CWLJz0pJM7-h9SjpcrNDZQnGNSDABpbbTXflMyMcjKtACsWz56Guu0AxoCc0YQAvD_BwE
26. Second Interim Revision Announcement: ‹1216› Tablet Friability. 2016:32. Available from: https://www.usp.org/sites/default/files/usp/document/harmonization/gen-chapter/g06_pf_ira_32_2_2006.pdf
27. European Pharmacopoeia. Shutdown of European Pharmacopoeia. (8th ed). Strasbourg: European Pharmacopoeia; 2014.

28. Uniformity of Dosage Units Content Uniformity USP 30-NF 25. 2005;905-910. Available from: https://www.usp.org/sites/default/files/usp/document/harmonization/gen-method/q0304_stage_6_monograph_25_feb_2011.pdf

29. Jadhav P, Petkar B, Pore Y, Kulkarni A, Burade K. Physicochemical and molecular modeling studies of cefixime-L-arginine-cyclodextrin ternary inclusion compounds. Carbohydr Polym. 2013;98:1317-1325.

30. Dissolution Testing of Immediate Release SolidOral Dosage Forms; Guidance for Industry; U.S. Department of Health and Human Services, Food and Drug Administration, Center for Drug Evaluation and Research (CDER), U.S. Government Printing Office: Washington, DC, 1997. Last Accessed Date: 29.09.2008. Available from: http://www.fda.gov/ cder/guidance/1713bp1.pdf

31. Loftsson T, Hreinsdottir D, Masson M. Evaluation of cyclodextrin solubilization of drugs. Int J Pharm. 2005;302:18-28.

32. Loftsson T, Jarho P, Masson M, Järvinen T. Cyclodextrins in drug delivery. Expert Opin Drug Deliv. 2005;2:335-351.

Turk J Pharm Sci 2021;18(5):597-603
DOI: 10.4274/tjps.galenos.2021.30676

ORIGINAL ARTICLE

Flusilazole Induced Cytotoxicity and Inhibition of Neuronal Growth in Differentiated SH-SY5Y Neuroblastoma Cells by All-Trans-Retinoic Acid (Atra)

All-Trans-Retinoik Asit (Atra) ile Farklılaştırılmış SH-SY5Y Nöroblastoma Hücrelerinde Flusilazole Bağlı Sitotoksisite ve Nöronal Büyüme İnhibisyonu

Elif KARACAOĞLU*

Hacettepe University Faculty of Science, Department of Biology, Ankara, Turkey

ABSTRACT

Objectives: Flusilazole (FLUS) is a broad-spectrum organosilicon triazole fungicide used for protecting economically important cereals and orchard fruits. Considering the exposure route of pesticides, pesticide contamination of food is inevitable. Furthermore, excessive exposure to pesticides causes health problems in both target and non-target organisms. It was aimed to evaluate the effects of the triazole fungicide FLUS on cytotoxicity and neurite extension in differentiated SH-SY5Y neuroblastoma cells.

Materials and Methods: The SH-SY5Y cells were differentiated into mature neurons using 10-μM all-trans-retinoic acid (RA) treatment for 7 days. Then the differentiated SH-SY5Y cells were treated with 50, 100 and 200 μM FLUS for 24 h. Afterwards, cell viability assays were performed including crystal violet, neutral red cell viability, and lactate dehydrogenase leakage assays. The morphological examinations were performed and neurite lenghts of the cells were measured in all experimental groups.

Results: FLUS treatment induced cytotoxicity in SH-SY5Y cells differentiated with RA. Significant decreases in cell viability percentages were observed. Furthermore, neurite lengths were negatively affected by the treatment of FLUS at the highest concentration.

Conclusion: FLUS is a fungicide widely used in agriculture to protect crops from fungal diseases. However, the intensive use of these compounds causes a potential risk to human and environmental health. According to the results of the study, it can be concluded that high concentrations of FLUS cause neurotoxicity by causing neural cell death and adverse effects on neurite outgrowth in differentiated SH-SY5Y cells. FLUS exposure can cause neuronal degeneration in mammals.

Key words: Flusilazole, cytotoxicity, SH-SY5Y cell differentiation, neurite growth

ÖZ

Amaç: Flusilazol (FLUS) ekonomik açıdan önemli tahıl ve tahıl ürünlerini ve meyve bahçelerini korumak için kullanılan geniş spektrumlu bir organosilikonlu triazol fungisittir. Pestisitlerin maruziyet yolları dikkate alındığında besin yoluyla pestisit maruziyeti kaçınılmaz olmaktadır. Ayrıca pestisitlere aşırı derecede maruz kalmak hedef ve hedef olmayan organizmalarda sağlık sorunlarına neden olmaktadır. Çalışmanın amacı, bir triazol fungisit olan FLUS'nin farklılaştırılmış SH-SY5Y nöroblastoma hücrelerinde sitotoksisite ve nörit uzaması üzerine etkilerinin değerlendirilmesidir.

Gereç ve Yöntemler: SH-SY5Y hücreleri 10 μM all-trans retinoik asit (RA) ile 7 gün boyunca olgun nöronlara farklılaştırılmıştır. Farklılaştırılmış SH-SY5Y hücreleri 50, 100 ve 200 μM FLUS ile 24 saat boyunca muamele edilmiştir. Kristal viyole, nötral kırmızısı canlılık testleri ile laktat dehidrogenaz salım testlerini kapsayan hücre canlılık testleri yapılmıştır. Ek olarak, morfolojik incelemeler yapılmış ve hücrelerin nörit uzunlukları ölçülmüştür.

Bulgular: FLUS uygulaması RA ile farklılaştırılan SH-SY5Y hücrelerinde sitotoksisiteyi indüklemiştir. Hücre canlılık yüzdelerinde dikkate değer düşüşler gözlenmiştir. Ayrıca en yüksek konsantrasyondaki FLUS uygulaması ile nörit uzunlukları olumsuz yönde etkilenmiştir.

Sonuç: FLUS tarımda ekinleri fungal hastalıklardan koruma amacıyla yaygın olarak kullanılan bir fungisittir. Fakat bu bileşiklerin yoğun kullanımı insan ve çevre sağlığı açısından potansiyel risk oluşturmaktadır. Çalışma sonuçlarına göre, yüksek konsantrasyonlarda FLUS'nin farklılaştırılmış SH-SY5Y hücrelerinde nöral hücre ölümüne ve nörit büyümesinde olumsuz etkilere neden olarak nörotoksisiteye yol açtığı sonucu çıkarılabilir. FLUS maruziyeti memelilerde nöronal dejenerasyona neden olabilir.

Anahtar kelimeler: Flusilazol, sitotoksisite, SH-SY5Y hücre farklılaşması, nörit büyümesi

***Correspondence:** elif.kus@hacettepe.edu.tr, **Phone:** +90 312 297 80 38, **ORCID-ID:** orcid.org/0000-0003-3426-4584

Received: 09.01.2021, **Accepted:** 17.02.2021

INTRODUCTION

The use of pesticides in agriculture enhances the production quality of food and feeds. However, it causes several health problems due to environmental and food contaminations. Among these pesticides, triazole fungicides are commonly used in agriculture for preventing fungal infections in fruits, cereals, and vegetables and have pharmacological uses for human and animal health.[1,2] Consequently, flusilazole (FLUS) is a broad-spectrum organosilicon triazole fungicide that is used for protecting economically important cereals and orchard fruits.[3,4] Its action mechanism can be attributed to the inhibition of the lanosterol 14 alpha-demethylase (CYP51) enzyme that plays a key role in sterol biosynthesis in fungus.[5] The CYP51 inhibition causes a reduction in the synthesis of ergosterol, which is the basic element of the fungal cell wall and prevents fungal cell growth. Consequently, the cell growth inhibition results in fungal cell death. As CYP51 enzyme exists in human, studies have reported that CYP51 inhibition caused by triazole fungicides can adversely affect mammalian cells.[6] Previous *in vitro* and *in vivo* studies asserted that triazole fungicides have adverse effects on mammalian steroidogenesis and may induce developmental toxicity such as craniofacial malformations.[7,8] One study revealed that the estimated acceptable daily intake of FLUS is about 0-0.007 mg/kg bw for humans.[9] However, considering the exposure route of pesticides, pesticide contamination of food is inevitable and excessive exposure to pesticides can cause health problems on both target and non-target organisms. Although previous studies have already focused on cytotoxicity and oxidative stress of FLUS on dopaminergic PC12 cells,[6] it is believed that the present study is the first to reveal the effects of FLUS on neurite growth and to compare cytotoxicity assays on differentiated SH-SY5Y cells.

The human neuroblastoma cell line SH-SY5Y cells are commonly used in neurotoxicity and neurodegenerative disease models.[10] *In vitro* models of SH-SY5Y can be differentiated into mature dopaminergic neuron-like phenotype via the induction of retinoic acid (RA),[11] which is known to regulate the cell cycle.[12] This differentiation of the neuronal cells in experimental studies could provide homogenous neuronal cells.[11] Additionally, studies have shown that RA-induced differentiation can elevate the susceptibility of SH-SY5Y cells against neurotoxins and protective agents.[13] Furthermore, differentiated SH-SY5Y cells are known to serve as a good model for studying experimental Parkinson's disease model.[13] The increased incidence of neurological diseases in recent years has necessitated the increase in experimental studies evaluating the relationship between chemicals and diseases. As exposure to environmental contaminants is inevitable, revealing the potential neurotoxicity effects of commonly used fungicides is important. In the present study, it is aimed to evaluate the effects of FLUS on neurite extension in differentiated SH-SY5Y neuroblastoma cells and to compare three commonly used cytotoxicity tests.

MATERIALS AND METHODS

Cell culture conditions and differentiation of SH-SY5Y cells

SH-SY5Y human neuroblastoma cells purchased from American Type Culture Collection (ATCC® CRL-2266™, ATCC, VA, USA), which was cultured with Dulbecco's minimum essential medium/nutrient mixture F-12 (DMEM/F-12) (Cegrogen Biotech GmbH, Germany) supplemented by 10% fetal bovine serum (FBS) (Cegrogen Biotech GmbH, Germany) and 1% penicillin-streptomycin antibiotic mixture at 37°C with 5% CO_2 in a humidified incubator. The culture medium was renewed every 3 days and subcultured the cells by detaching them with trypsin ethylenediaminetetraacetic acid (0.05%) in Dulbecco's phosphate-buffered saline (Cegrogen Biotech GmbH, Germany). SH-SY5Y cells then was incubated for 48 h for attachment. Finally, the culture medium was replaced with differentiation medium (DMEM supplemented with 3% FBS and 10 µM all-trans-RA) for 7 days until treatment in the dark at 37°C with 5% CO_2 in a humidified incubator.

Treatment of FLUS

First, FLUS was dissolved (PESTANAL®, analytical standard, Merck KGaA, Darmstadt, Germany) in dimethyl sulfoxide (Applichem, Darmstadt, Germany) to prepare 0.1 g/mL stock solution. Then the working concentrations were prepared by diluting the stock solution with cell culture medium. Next, the differentiated SH-SY5Y cells were incubated with 0-500 µM FLUS concentrations and performed crystal violet cell viability assay to calculate the IC_{50}, which was found at 182.42 µM. The cell viability (15%) at high concentrations (500 µM) was found very toxic. The working concentrations were based on the calculated IC_{50} value for further analyses. It is defined low and middle doses as those with slightly toxic concentrations lower than the IC_{50} and for high dose selection while high doses are those with concentrations higher than the IC_{50} value. Finally, 50-, 100-, and 200-µM FLUS concentrations were selected for further analyses.

Crystal violet cell viability assay

First, the differentiated SY-SY5Y cells were seeded at 1×10^4 cells/well into a 96-well culture plate and incubated them for 24 h for cell attachment. Then the cells were treated with 0, 50, 100, and 200 µM FLUS at 37°C and 5% CO_2 in a humidified incubator for 24 h after which we performed a crystal violet cell viability assay.[14] Briefly, the culture medium was discarded with FLUS and mixed the cells with 4% neutral buffered formalin for 1 h. After removing the fixative, the cells was stained with 0.1% crystal violet solution for 30 min on a shaker at room temperature. The cells then were washed with distilled water several times to remove excess crystal violet dye. The crystal violet dye was extracted in the cells using 10% acetic acid solution until the dye was dissolved and then measured the absorbance at 595 nm wavelength using a microplate spectrophotometer (BIO-TEK µQuant, BIO-TEK Instruments, Inc., USA). Finally, the cell viability was calculated based on the 100% viability of untreated cells.

Neutral red uptake assay

Similarly, the differentiated SH-SY5Y cells were seeded into a 96-well culture plate at a density of 1×10^4 cells/well and allowed them to attach onto the surface and grow for 24 h. Afterwards, the cells were treated with FLUS concentrations (0, 50, 100, 200 µM) and were incubated at 37°C and 5% CO_2 in a humidified

incubator for 24 h. A neutral red uptake assay was performed to determine the cell viability. Briefly, the differentiated SH-SY5Y cells were incubated with 40 µg/mL neutral red dye containing the culture media for 4 h at 37°C and 5% CO_2 in a humidified incubator. Then the culture medium was discarded, the cells were washed twice with phosphate buffer saline twice, and extracted the dye using a neutral red desorb solution (1% glacial acetic acid, 50% ethanol in distilled water) for 20-45 min on a shaker at room temperature. Afterwards, the absorbance was measured at 540 nm wavelength for 1 h using a microplate spectrophotometer (BIO-TEK µQuant, BIO-TEK Instruments, Inc., USA). Finally, the cell viability was calculated based on the 100% viability of untreated cells.

Lactate dehydrogenase (LDH) leakage assay

LDH is a stable cytosolic enzyme that is released from cells when cell membrane damage occurs. Consequently, LDH leakage assay is commonly used to determine cell membrane damage. We performed an LDH assay using a commercial kit (Biovision, K313-500, USA). Briefly, the differentiated SY-SY5Y cells were seeded at a density of 2×10^4 cells/well into a 96-well culture plate and incubated them at 37°C and 5% CO_2 in a humidified incubator for 24 h. Then the culture medium was discarded and the cells were treated with FLUS concentrations (0, 50, 100, and 200 µM) for 24 h. At the end of the incubation time, the cells were centrifuged at 600 g for 10 min using a plate rotor (5810R Centrifuge, Ependorf AG, Hamburg, Germany). Afterwards, I incubated 10 µL sample with 100 µL LDH reaction solution for 30 min in the dark at room temperature. This assay utilizes the enzymatic coupling reaction in which LDH oxidized lactate to generate nicotinamide adenine dinucleotide and where the water-soluble tetrazolium salt present in the reaction solution generates yellow to amber color. The generated color intensity directly correlates with the damaged cell amount. Finally, at the end of the incubation time, we measured the absorbance at 450 nm wavelength using a microplate spectrophotometer (BIO-TEK µQuant, BIO-TEK Instruments, Inc., USA). The percentage of the cytotoxicity was calculated based on the 100% viability of untreated cells.

Cell morphology analysis

The cell mofphology analysis was performed by capturing micrographs of undifferentiated or differentiated treated cells using an inverted microscope (Olympus CKX 41 inverted microscope, CellSence Imaging Software, Olympus, Japan). Each experiment was performed by measuring the neurite lengths of undifferentiated or differentiated neurons using an Image J Package with Neuron J.[15,16]

Statistical analysis

The statistical analyses were performed using the package program of SPSS for Windows and calculated the IC_{50} value through probit analysis. In order to determine the significant differences between FLUS treatment and non-treatment groups, ANOVA test was performed with 95% confidence interval followed by Tukey post-hoc test. The data were expressed as mean ± standard error. All experiments were performed in independent triplicates.

RESULTS

Morphological features of undifferentiated and differentiated SH-SY5Y cells

The SH-SY5Y cells were differentiated by treating them with 10 µM RA for 7 days. Figure 1 demonstrates morphological features of undifferentiated and differentiated cells. Undifferentiated cells can be distinguished by the presence of clustered round cells and short neurites (Figure 1A). On the other hand, morphologically differentiated SH-SY5Y cells are characterized by extensive neurites as well as pyramid-shaped cells (Figure 1B). To better distinguish the differences, the neurite lengths of undifferentiated and differentiated SH-SY5Y cells were measured, as shown in Figure 1C. While undifferentiated cells showed shorter neurites, neurites were longer in cells that underwent 7-day RA-induced differentiation. Differentiated SH-SY5Y cells were treated with different FLUS concentrations. Figure 2 demonstrates the morphological effects of FLUS on RA-induced differentiated SH-SY5Y cells. Accordingly, results showed that FLUS treatment caused remarkable morphological changes in differentiated SH-SY5Y cells, including apoptotic cell death, which is characterized by round and small nuclei and a decrease in neurite length (Figure 2). Apoptotic cells increased in FLUS treatment groups, and neurite length decreased in response to the highest FLUS concentration, which was statistically significant compared with those in the non-treatment group.

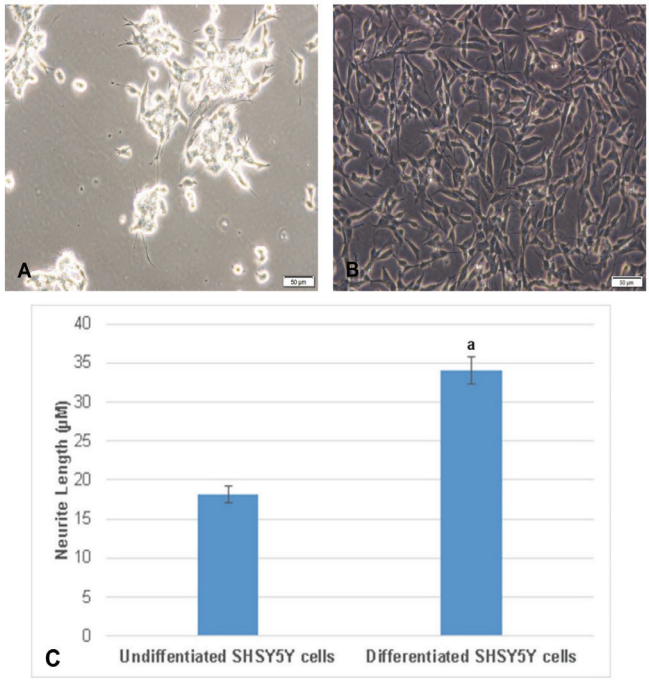

Figure 1. A) Undifferentiated SH-SY5Y cells with clustered, round-shaped cell body and short neurites; B) RA-induced differentiated SH-SY5Y cells with pyramidal-shaped cell body and extended neurites; C) neurite lengths of undifferentiated and differentiated SH-SY5Y cells

RA: Retinoic acid

Cell viability assay results

The cytotoxic effects of FLUS was evaluated by performing different cytotoxicity assays (i.e., crystal violet, LDH, and neutral red cell viability assays). Crystal violet assay revealed an IC_{50} value of 182.42 µM, which was the basis of our working concentrations. As demonstrated in Figure 3, the decrease in cell viability was statistically significant in 100- and 200-µM FLUS treatment groups as compared with that in the control and 50-µM FLUS treatment groups. Meanwhile, as shown in Figure 4, LDH leakage assay results revealed that occurrences of cell death increased in response to increasing FLUS concentrations. At higher concentrations, FLUS increased the percentage of cell death viability, which was statistically significant in the 100- and 200-µM FLUS treatment groups when compared with that in the non-treatment and 50-µM FLUS treatment groups. On the other hand, according to neutral red cell viability assay results (Figure 5), remarkable decreases in cell viability were statistically significant in all treatment groups. Significant decreases were found between non-treatment and FLUS treatment groups. Additionally, the cell viability in the 200-µM FLUS treatment group was significantly different from that in the 50- and 100-µM FLUS treatment groups.

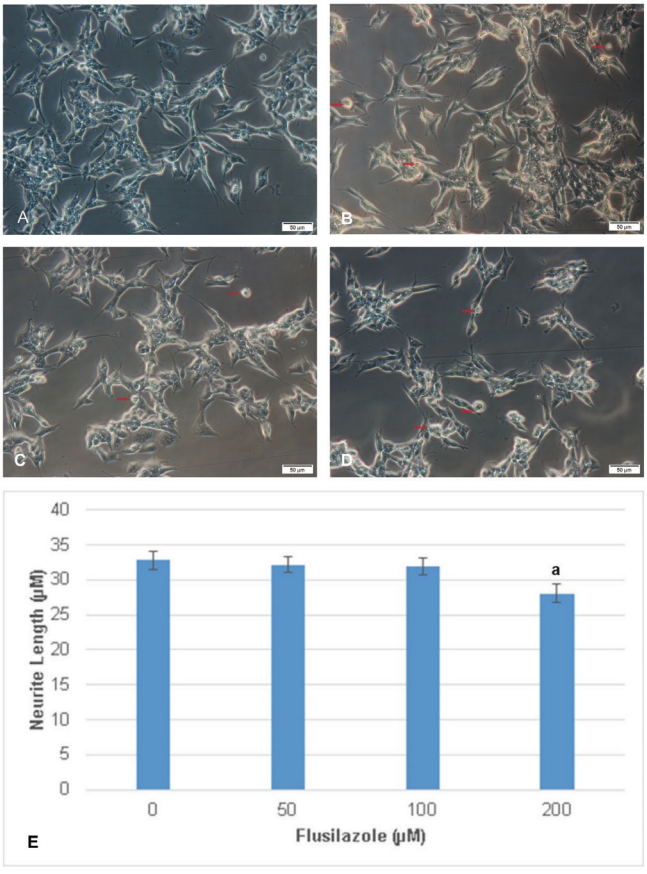

Figure 2. Morphological micrographs of differentiated SH-SY5Y cells in the FLUS treatment groups: A) Control group; B) 50-µM FLUS treatment group; C) 100-µM FLUS treatment group; D) 200-µM FLUS treatment group; (→) apoptotic cell

FLUS: Flusilazole

DISCUSSION

Triazole fungicides have been used globally in various areas including agriculture and medicine. However, excessive use of fungicides could leave harmful residues in the environment and cause risks in human health via consumption of contaminated food and water.[17] For example, studies have shown that triazole

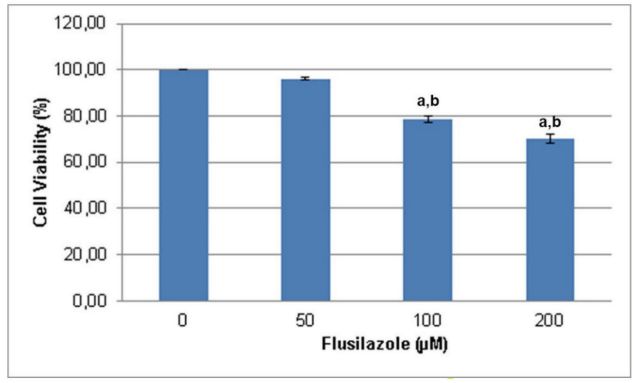

Figure 3. Crystal violet cell viability assay results (%). aSignificantly different from control group. bSignificantly different from 50-µM FLUS group

FLUS: Flusilazole

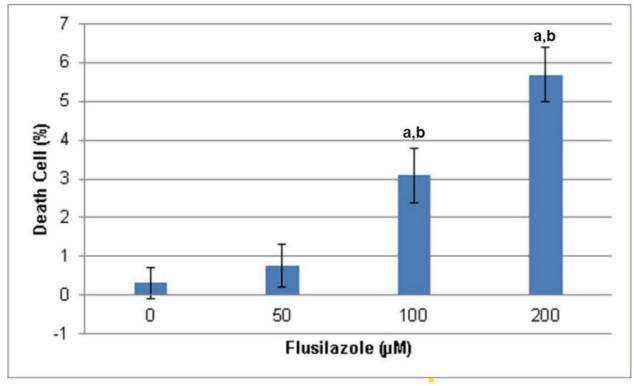

Figure 4. LDH leakage assay results, cell death (%). [a]Significantly different from control group. [b]Significantly different from 50-µM FLUS group

LDH: Lactate dehydrogenase, FLUS: Flusilazole

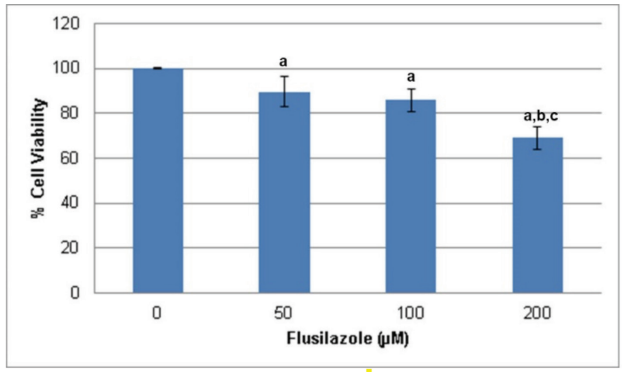

Figure 5. Neutral red cell viability assay results. [a]Significantly different from control group. [b]Significantly different from 50-µM FLUS group. [c]Significantly different from 100-µM FLUS group

FLUS: Flusilazole

fungicides, which are used to inhibit fungal CYP51 and increase fungal cell wall permeability to kill fungi,[6,7] cause harmful effects on the nervous system via neuropathological defects in the murine brain as well as neuropathological lesions in the peripheral nervous system.[18] Other studies also reported several adverse effects of azole fungicides such as birth defects, craniofacial malformations, and inhibition of steroidogenesis in mammals.[5,19,20] Despite the wide range of risks in human health caused by triazole fungicides, studies about the effects of FLUS on human health are very limited.[6,7] Because of the limited information on the effects of FLUS on differentiated neurons, this study aimed to elucidate the toxicity mechanism of FLUS on neurite outgrowth and to compare cytotoxicity tests using FLUS treatment.

In the field of neuroscience, *in vitro* models functionally resembling neurons are lacking, especially for neurodegenerative diseases including Alzheimer's disease. Although cell lines such as SH-SY5Y cells are often used, these cells lack mature neuronal functions and morphology, have ceased cell division, and express specific markers.[21] However, SH-SY5Y cells could be differentiated into mature neuron, and differentiated neuron cells could serve as homogenous cell types, as demonstrated in previous studies where SH-SY5Y cells were differentiated into mature neuron-like cells by RA induction on a 7-day treatment in dark conditions, and differentiated cells morphologically changed as characterized by extensive neurites outgrowth.[22,23] Hence, the present study aimed to investigate the cytotoxic mechanisms of FLUS on differentiated SH-SY5Y cells. The action mechanism of RA was characterized by the activation of transcription via binding to non-steroid nuclear hormone receptors. Additionally, RA was shown to induce the Wnt signaling pathway and play a role in the regulation of the neurotrophin receptor gene transcription.[13] In this study, it was observed that morphologically differentiated SH-SY5Y cells had typical neurons with extensive neurites and pyramid-shaped cell bodies. On the other hand, undifferentiated cells tend to form clusters and had round-shaped cell bodies.[11] According to these results, I can say that the morphological differentiation of SH-SY5Y cells was successful.

In vitro cytotoxicity assays can be useful in determining toxicity levels in humans in toxicological studies. Cytotoxicity assays differ in the types of assays as well as results depending on the test principle.[24] It is important to carry out multiple markers to exert reversible or irreversible effects of toxic substances.[25] In this study, three cytotoxicity assays were performed based on different test principles for differentiated SH-SY5Y cells to evaluate the mechanism of toxicity. The crystal violet assay was selected to evaluate cell viability because of its reliable and quick method and because crystal violet specifically binds to DNA to reveal the cell viability. Neutral red uptake assay as performed to evaluate the percentage of cell viability in terms of lysosomal activity and the LDH leakage assay to evaluate necrotic cell death.

To evaluate the viability of differentiated SH-SY5Y cells, we performed crystal violet cell viability assay, which is a basic method for determining cell viability by staining with crystal violet dye that binds to DNA and proteins. This method depends on staining attached viable cells because dead cells lose their absorption and the amount of crystal violet dye is reduced.[26] Results from this assay showed that FLUS treatment caused the decrease in differentiated SH-SY5Y cells in a dose-dependent manner. A previous study with 9.5-day-old rat embryos *in vitro* reported that triazole treatment altered hindbrain development and caused cranial nerve anomalies. The same study also found that FLUS and other triazole derivatives were teratogenic.[20] The present study has shown that FLUS can induce cell death at higher concentrations, consistent with previous studies.

Results showed that the release of LDH, an intracellular enzyme found in the inner compartment of the cell, was significantly increased at higher concentrations in the FLUS treatment groups. Consequently, LDH leakage assay is described as a cytotoxicity marker that reveals cell membrane damage as irreversible cell death.[27] As necrotic cells have permeable cell membrane, leakage of LDH into the culture media as a result of membrane damage is considered a hallmark of necrotic cell death.[28] Hence, in the present study the LDH leakage assay was used to determine the necrotic cell death percentage. A previous study treated zebra fish liver cell line with triazole fungicides and evaluated the effects using LDH leakage assay. That study revealed remarkable increases in LDH leakage at higher concentrations of FLUS.[29] Similarly, the results of the present study were consistent with the previously reported study as is another previous study that also used triazole fungicide to induce necrotic cell death in L929 cells.[30] The present study revealed that FLUS could adversely affect human neuronal cells as membrane damage occurred in differentiated SH-SY5Y cells after FLUS treatment, which eventually induced necrotic cell death.

The neutral red uptake assay was performed to determine cytotoxicity. The principle of this assay is based on the uptake of neutral red dye (a water-soluble dye) into the lysosomes, which processes energy required for cells.[31] The neutral red uptake depends on pH gradients during the ATP production process. As the net charge of the dye is zero, neutral red dye could enter the cell. However, the interior of the lysosomes has a lower pH than the cytoplasm via proton gradient. Because of the pH gradient, the neutral red dye keeps the cytoplasm positively charged so that the dye could retain inside the lysosomes. Conversely, neutral red dye could not be retained in the lysosomes in case of cell death or pH gradient changes. Studies reported that this assay is highly sensitive to cell viability quantification.[32] When plasma or lysosomal membranes are damaged by chemicals, the ability of the endocytosis, which requires energy for the process, to uptake the neutral red dye decreases. According to neutral red uptake assay results in this study, high concentrations of FLUS in SH-SY5Y cells adversely affected cell viability. These results indicate that FLUS may cause lysosomal damage especially at higher concentrations. All cytotoxicity test results demonstrated a downward trend in cell viability. Despite some variations, it seemed that the most

sensitive test for FLUS in differentiated SH-SH5Y cells was the crystal violet assay.

Environmental neurotoxins including pesticides and fungicides have been reported to play a crucial role in the development of neurodegenerative disorders.[33-35] In differentiated neurons, changes in morphology or neurite growth could be a sign of neurodegenerative diseases. To date, several cell lines including SH-SY5Y have been used to study the effects of chemicals on neurite growth.[36] Consequently, SH-SY5Y cells differentiated via RA induction could serve as a good *in vitro* model for revealing neurotoxicity mechanisms[37] as differentiated SH-SY5Y cells were reported to have the longest neurite measurement after treatment with 10 µM RA for 3 days.[38] In the present study, differentiated SH-SY5Y cells had longer neurites than undifferentiated cells. Neurite growth induced by RA treatment were >1.9 fold compared with that in undifferentiated cells. Previous *in vitro* studies involving organophosphates reported a reduction in neurite outgrowth in N2a mouse neuroblastoma and C6 glioma cells,[39] We observed that FLUS treatment caused the inhibition in neurite outgrowth of differentiated SH-SY5Y cells.

CONCLUSION

As mentioned earlier, FLUS is widely used as a fungicide in agriculture for preventing fungal diseases. However, intensive usage of these compounds has potential health risks for both humans and the environment. The present study has demonstrated that FLUS caused neurotoxicity at higher concentrations resulting in neuronal cell death and adversely affecting neurite growth in differentiated neurons, indicating that FLUS could cause neuronal degeneration in mammals. The results in this study may serve as preliminary data for further studies to elucidate the mechanism of action.

Conflict of interest: No conflict of interest was declared by the author. The author are solely responsible for the content and writing of this paper.

REFERENCES

1. Martin MT, Brennan RJ, Hu W, Ayanoglu E, Lau C, Ren H, Wood CR, Corton JC, Kavlock RJ, Dix DJ. Toxicogenomic study of triazole fungicides and perfluoroalkyl acids in rat livers predicts toxicity and categorizes chemicals based on mechanisms of toxicity. Toxicol Sci. 2007;97:595-613.
2. de Jong E, Barenys M, Hermsen SAB, Verhoef A, Ossendorp BC, Bessems JGM, Piersma A. Comparison of the mouse embryonic stem cell test, the rat whole embryo culture and the zebrafish embryotoxicity test as alternative methods for developmental toxicity testing of six 1,2,4-triazoles. Toxicol Appl Pharmacol. 2011;253:103-111.
3. Farag AT, Ibrahim HH. Developmental toxic effects of antifungal flusilazole administered by gavage to mice. Birth Defects Res B Dev Reprod Toxicol. 2007;80:12-17.
4. Menegola E, Broccia ML, Di Renzo F, Giavini E. Antifungal triazoles induce malformations *in vitro*. Reprod Toxicol. 2001;15:421-427.
5. Zarn JA, Brüschweiler BJ, Schlatter JR. Azole fungicides affect mammalian steroidogenesis by inhibiting sterol 14 alpha-demethylase and aromatase. Environ Health Perspect. 2003;111:255-261.
6. Heusinkveld HJ, Molendijk J, van den Berg M, Westerink RH. Azole fungicides disturb intracellular Ca2+ in an additive manner in dopaminergic PC12 cells. Toxicol Sci. 2013;134:374-381.
7. Dimopoulou M, Verhoef A, van Ravenzwaay B, Rietjens IM, Piersma AH. Flusilazole induces spatio-temporal expression patterns of retinoic acid-differentiation-and sterol biosynthesis-related genes in the rat Whole Embryo Culture. Reprod Toxicol. 2016;64:77-85.
8. Mineshima H, Fukuta T, Kato E, Uchida K, Aoki T, Matsuno Y, Mori C. Malformation spectrum induced by ketoconazole after single administration to pregnant rats during the critical period – comparison with vitamin A-induced malformation spectrum. J Appl Toxicol. 2012;32:98-107.
9. Food and Agriculture Organization of the United Nations, World Health Organization, FAO Panel of Experts on Pesticide Residues in Food and the Environment & WHO Core Assessment Group on Pesticide Residues. (2009). Pesticide residues in food: 2007, Toxicological Evaluations Last Accessed Date: 02.01.2021. Available from: https://apps.who.int/iris/handle/10665/44064
10. Krishna A, Biryukov M, Trefois C, Antony PM, Hussong R, Lin J, Heinäniemi M, Glusman G, Köglsberger S, Boyd O. Systems genomics evaluation of the SH-SY5Y neuroblastoma cell line as a model for Parkinson's disease. BMC Genomics. 2014;15:1154.
11. Kovalevich J, Langford D. Considerations for the use of SH-SY5Y neuroblastoma cells in neurobiology. Neuronal cell culture. London: Springer; 2013:9-21.
12. Janesick A, Wu SC, Blumberg B. Retinoic acid signaling and neuronal differentiation. Cell Mol Life Sci. 2015;72:1559-1576.
13. Xie HR, Hu LS, Li GY. SH-SY5Y human neuroblastoma cell line: *in vitro* cell model of dopaminergic neurons in Parkinson's disease. Chin Med J. 2010;123:1086-1092.
14. Akinrinde A, Koekemoer T, Van De Venter M, Bradley G. *In vitro* investigation of potential anti-diabetic activity of the corm extract of Hypoxis argentea Harv. Ex Baker. Acta Pharm. 2018;68:389-407.
15. Pemberton K, Mersman B, Xu F. Using ImageJ to assess neurite outgrowth in mammalian cell cultures: research data quantification exercises in undergraduate neuroscience lab. J Undergrad Neurosci Educ. 2018;16:A186.
16. Schneider CA, Rasband WS, Eliceiri KW. NIH Image to ImageJ: 25 years of image analysis. Nat Methods 2012;9:671-675.
17. Faro LRF. Neurotoxic effects of triazole fungicides on nigrostriatal dopaminergic neurotransmission. Fungicide. 2010:405-420.
18. EPA. Reregistration eligibility decision for triadimefon and tolerance reassessment for triadimenol. 2006. Available from. https://archive.epa.gov/pesticides/reregistration/web/pdf/triadimefon_red.pdf
19. Crofton K. A structure-activity relationship for the neurotoxicity of triazole fungicides. Toxicol Lett. 1996;84:155-159.
20. Menegola E, Broccia ML, Di Renzo F, Massa V, Giavini E. Study on the common teratogenic pathway elicited by the fungicides triazole-derivatives. Toxicol In Vitro. 2005;19:737-748.
21. Agholme L, Lindström T, Kågedal K, Marcusson J, Hallbeck M. An *in vitro* model for neuroscience: differentiation of SH-SY5Y cells into cells with

morphological and biochemical characteristics of mature neurons. J Alzheimers Dis. 2010;20:1069-1082.

22. Cheung YT, Lau WK, Yu MS, Lai CS, Yeung SC, So KF, Chang RC. Effects of all-trans-retinoic acid on human SH-SY5Y neuroblastoma as *in vitro* model in neurotoxicity research. Neurotoxicology. 2009;30:127-135.
23. Sarkanen JR, Nykky J, Siikanen J, Selinummi J, Ylikomi T, Jalonen TO. Cholesterol supports the retinoic acid-induced synaptic vesicle formation in differentiating human SH-SY5Y neuroblastoma cells. J Neurochem. 2007;102:1941-1952.
24. Weyermann J, Lochmann D, Zimmer A. A practical note on the use of cytotoxicity assays. Int J Pharm. 2005;288:369-376.
25. Rausch O. High content cellular screening. Curr Opin Chem Biol. 2006;10:316-320.
26. Feoktistova M, Geserick P, Leverkus M. Crystal violet assay for determining viability of cultured cells. Cold Spring Harbor Protocols. 2016;2016:pdb. prot087379.
27. Fotakis G, Timbrell JA. *In vitro* cytotoxicity assays: comparison of LDH, neutral red, MTT and protein assay in hepatoma cell lines following exposure to cadmium chloride. Toxicol Lett. 2006;160:171-177.
28. Chan FK, Moriwaki K, De Rosa MJ. Detection of necrosis by release of lactate dehydrogenase activity. Methods Mol Biol. 2013;979:65-70.
29. Bopp SK, Lettieri T. Comparison of four different colorimetric and fluorometric cytotoxicity assays in a zebrafish liver cell line. BMC Pharmacol. 2008;8:8.
30. Süloğlu AK, Karacaoğlu E, Koçkaya EA, Selmanoğlu G, Loğoglu E. Cytotoxic effects of a novel thialo benzene derivative 2, 4-dithiophenoxy-1-iodo-4-bromobenzene ($C_{18}H_{12}S_2IBr$) in L929 cells. Int J Toxicol. 2014;33:319-324.
31. Putnam K, Bombick D, Doolittle D. Evaluation of eight *in vitro* assays for assessing the cytotoxicity of cigarette smoke condensate. Toxicol In Vitro. 2002;16:599-607.
32. Repetto G, del Peso A, Zurita JL. Neutral red uptake assay for the estimation of cell viability/cytotoxicity. Nat Protoc. 2008;3:1125-1131.
33. Sanchez M, Gastaldi L, Remedi M, Cáceres A, Landa C. Rotenone-induced toxicity is mediated by Rho-GTPases in hippocampal neurons. Toxicol Sci. 2008;104:352-361.
34. Kara M, Oztas E, Ramazanoğulları R, Kouretas D, Nepka C, Tsatsakis AM, Veskoukis AS. Benomyl, a benzimidazole fungicide, induces oxidative stress and apoptosis in neural cells. Toxicol Rep. 2020;7:501-509.
35. Kanat ÖN, Selmanoğlu G. Neurotoxic effect of fipronil in neuroblastoma SH-SY5Y cell line. Neurotox Res. 2020;37:30-40.
36. Itano Y, Nomura Y. 1-Methyl-4-phenyl-pyridinium ion (MPP+) causes DNA fragmentation and increases the Bcl-2 expression in human neuroblastoma, SH-SY5Y cells, through different mechanisms. Brain Res. 1995;704:240-245.
37. Pak EJ, Son GD, Yoo BS. Cadmium inhibits neurite outgrowth in differentiating human SH-SY5Y neuroblastoma cells. Int J Toxicol. 2014;33:412-418.
38. Dwane S, Durack E, Kiely PA. Optimising parameters for the differentiation of SH-SY5Y cells to study cell adhesion and cell migration. BMC Res Notes. 2013;6:1-11.
39. Almami IS, Aldubayan MA, Felemban SG, Alyamani N, Howden R, Robinson AJ, Pearson TDZ, Boocock D, Algarni AS, Garner AC, Griffin M, Bonner PLR, Hargreaves AJ. Neurite outgrowth inhibitory levels of organophosphates induce tissue transglutaminase activity in differentiating N2a cells: evidence for covalent adduct formation. Arch Toxicol. 2020;94:3861-3875.

Turk J Pharm Sci 2021;18(5):604-608
DOI: 10.4274/tjps.galenos.2021.04903

ORIGINAL ARTICLE

In Vitro Cytotoxicity and Oxidative Stress Evaluation of Valerian (*Valeriana officinalis*) Methanolic Extract in Hepg2 and Caco2 Cells

Valeriana officinalis'in Metanol ile Hazırlanmış Ekstresinin HepG2 ve Caco2 Hücrelerinde *İn Vitro* Sitotoksisite ve Oksidatif Stres Değerlendirmesi

Mehtap KARA[1]*, Ecem Dilara ALPARSLAN[2], Ezgi ÖZTAŞ[1], Özlem Nazan ERDOĞAN[3]

[1]İstanbul University Faculty of Pharmacy, Department of Pharmaceutical Toxicology, İstanbul, Turkey
[2]İstanbul Physical Therapy Rehabilitation Training and Research Hospital, Department of Pharmacy, İstanbul, Turkey
[3]İstanbul University Faculty of Pharmacy, Department of Pharmacy Management, İstanbul, Turkey

ABSTRACT

Objectives: Traditional treatment methods are becoming popular and commonly used in many societies and have become the first treatment option for most people. While some of these methods are helpful, they can interact with medications the patient is taking for another disease and cause a variety of life-threatening risks. Valerian (catweed) plant is used in traditional medicine as a sleep aid due to its sedative effects. Valerian may also exert anticancer effect *in vitro*.

Materials and Methods: In this study, the cytotoxicty and oxidative stress effects of valerian root extract were evaluated in human liver hepatocellular carcinoma (Hepg2) and human colorectal adenocarcinoma (Caco2) cell lines. The cytotoxicity was evaluated via the 3-(4,5-dimethythiazol-2-yl)-2,5-diphenyl tetrazolium bromide test. Total reactive oxygen species analysis was performed via a 2',7'-dichlorodihydrofluorescein diacetate assay in flow cytometry.

Results: Inhibition concentration 50 values were calculated as 936.6 and 1097.5 µg/mL in the Hepg2 and Caco2 cell lines, respectively. It was observed that valerian root extract did not induce oxidative stress in HepG2 and Caco2 cell lines.

Conclusion: These results indicate that the use of valerian root extract as an alternative method in cancer treatment may not be effective and may cause a risk for public health. On the other hand, it may be safe at recommended tolerated concentrations since it does not cause oxidative stress.

Key words: *Valeriana officinalis*, HepG2, Caco2, oxidative stress, MTT

ÖZ

Amaç: Geleneksel tedavi yöntemleri, birçok toplumda yaygın olarak kullanılmakta, popüler hale gelmekte ve birçok kişi için ilk tedavi seçeneği olarak karşımıza çıkmaktadır. Bu yöntemlerden bazıları yararlı olmakla birlikte, kişinin başka bir hastalık için kullandığı ilaçlarla etkileşime girebilir ve çeşitli yaşamı tehdit edici risklere neden olabilir. Kediotu (catweed) bitkisi yatıştırıcı etkisi nedeniyle geleneksel tıp uygulamalarında uyku düzenleyici amaçlı kullanılmaktadır. Ayrıca *in vitro* olarak kanser önleyici etkiye sahip olabileceği bildirilmiştir.

Gereç ve Yöntemler: Bu çalışmada, kediotu kökü ekstresinin sitotoksisite ve oksidatif stres etkileri Hepg2 ve Caco2 hücre hatlarında değerlendirilmiştir. Sitotoksisite değerlendirmesi 3-(4,5-dimethylthiazol-2-yl)-2,5-diphenyltetrazolium bromide testi ile gerçekleştirildi. Total-reaktif oksijen bileşikleri analizi, hücre akış sitometrisinde 2',7'-dichlorodihydrofluorescein diacetate testi ile gerçekleştirildi

Bulgular: İnhibisyon konsantrasyonu 50 değerleri Hepg2'de 936,6 µg/mL ve Caco2 hücre hatlarında 1097,5 µg/mL olarak hesaplandı. Kediotu kökü ekstresinin HepG2 ve Caco2 hücre hatlarında da oksidatif strese neden olmadığı gözlenmiştir.

Sonuç: Bu sonuçlar, kanser tedavisinde alternatif bir yöntem olarak kediotu kökü ekstresi kullanımının etkili olamayacağını ve halk sağlığı açısından risk oluşturabileceğini, diğer yandan oksidatif strese neden olmadığı için tavsiye edilen tolere edilen konsantrasyonlarda güvenli olabileceğini göstermektedir.

Anahtar kelimeler: *Valeriana officinalis*, HepG2, Caco2, oksidatif stres, MTT

***Correspondence:** matost@gmail.com, **Phone:** +90 507 349 24 78, **ORCID-ID:** orcid.org/0000-0001-7764-5593

Received: 10.11.2020, **Accepted:** 19.02.2021

INTRODUCTION

The use of herbal products for the treatment of several diseases has been widespread from the past to the present. In developed countries, herbal remedies are considered over-the counter drugs with strict regulations. However, in developing countries, the use of herbal therapy methods and products lacks control. Most of herbal drugs in the market have not been fully evaluated from the toxicological aspect; thus, these products may cause several adverse effects during therapy of the different body systems.[1]

Valeriana belongs to Valerianaceae family, which includes approximately 300 species. *Valeriana officinalis* has been generally used as an alternative traditional medicine for insomnia and depression therapy. This medical plant has sedative, anticonvulsant, hypnotic, and anxiolytic effects. In addition, this plant has treatment potential for gastrointestinal and urinary system problems. The *V. officinalis* compounds obtained by extraction methods (EMs) include flavonoids, monoterpenes, sesquiterpenes, valepotriates, iridoids, alkaloids, acid-like gamma-aminobutyric acid (GABA), glutamine, and lignans, which affect the central nervous system and have antioxidant and vasorelaxant effects. Given these effects, *V. officinalis* is a popular herbal remedy choice to cure insomnia, headache, gastrointestinal system, cardiovascular system, and urinary tract problems.[2-5]

Valeriana herbal remedy can be effective in cancer patients. Valerian herb ingredients with anticancer effects have been given great concern by the scientific area. However, herbal therapy implementers have been attempting to cure cancer patients with insufficient valerian products.[6]

In this work, we have observed the cytotoxic and oxidative stress-inducing effects, which play important roles in killing cancer cells, of methanolic extract of *V. officinalis* on HepG2 and CaCo2 cell lines.

MATERIALS AND METHODS

Valeriana officinalis extraction

V. officinalis roots were purchased commercially from a traditional herbal drug store in İstanbul and pulverized in a porcelain mortar. A total of 75 mL methanol was added to 15 g powdered *V. officinalis* roots and incubated at room temperature in a shaker for 24 h. After the incubation period, the extraction solution was filtered with a Whatman no.1 filter, and methanol was evaporated with fractional distillation.[7]

Cell culture and 3-(4,5-dimethylthiazol-2-yl)-2,5-diphenyltetrazolium bromide (MTT) test human liver hepatocellular carcinoma (HepG2- HB-8065™) and human colorectal adenocarcinoma (Caco2- HTB-37™) cell lines were purchased from the American Type Culture Collection (Virginia, USA), and the cells were maintained as per manufacturer's instructions. Exactly 1000 mg/mL extract was prepared by dissolving *V. officinalis* roots in 100% dimethyl sulfoxide (DMSO) and stored at +4°C until the experiments. Before the cell treatments, the extract was diluted with DMSO at a final concentration of 1%. Given the selected concentrations for cytotoxicity assay, the root extract was dissolved in a cell culture medium to prepare the desired concentrations. The treatments were performed at a concentration range for 24 h to evaluate the dose-dependent effects. All study experiments were performed in triplicates in three different days.

The HepG2 and Caco2 cells were seeded into 96-well plates ($1x10^4$ cells/100 µL cell culture medium/well). After overnight incubation, the cells were treated with *V. officinalis* extract at the concentrations of 200, 400, 600, 800, and 1000 µM and control for 24 h. In the control group, the final DMSO concentration was 1%. Then, MTT was added into the wells, and the wells were incubated for another 3 h at 37°C in the dark. Optical densities were measured at 570 nm using a microplate reader (Biotek, Epoch, Vermont, USA).[8]

Total reactive oxygen species (Total-ROS) assay with 2',7'-dichlorodihydrofluorescein diacetate (H_2DC-FDA).

Different pathological conditions were associated with the ROS increase in cells. Thus, changes in the ROS level are detected in basic studies. Given the short half-life of ROS, effective detection methods are important during observations. H_2DC-FDA is a non-fluorescent dye, and in the presence of ROS, it returns a green fluorescent with oxidation.[9] In the present study, the ROS production was evaluated with H_2DC-FDA dye with by a flow cytometer. The $5x10^5$ HepG2 and Caco2 cells in 2 mL medium per well were seeded into six-well plates and incubated overnight. The cells were treated with 100, 200, 100, and 600 µg/mL concentrations. These concentrations exerted a cell viability higher than 70% in the MTT assay for 24 h. The 1% DMSO solution was used as the negative control for the experiment. After 24 h, the cells were washed with phosphate-buffered saline (PBS) twice and incubated with 20 µM H_2DC-FDA at 37°C for 30 min. The cells were detached with trypsin-ethylenediaminetetraacetic acid after the incubation period and washed with PBS. Then, the cells were re-suspended with 1% BSA in 150 µL PBS. The fluorescence intensity of 10^4 cells was measured with an ACEA NovoCyte flow cytometer (San Diego, California, USA), and the results were expressed as the percentage of median fluorescence intensity (MFI %) as previously described.[10]

Statistical analysis

All the experiments were performed as three replicates; the results were presented as the mean ± standard deviation. The statistical comparison results were analyzed using the one-way analysis of variance followed by Tukey's test for post hoc analysis, and the statistical significance was set at $p<0.05$ (SPSS, version 21.0, USA)

RESULTS

Cell viability

According to MTT results, the percentage of cell inhibition in Caco2 and HepG2 cell lines with *V. officinalis* methanolic extract exposure increased and was concentration dependent for 24 h (Figure 1, Table 1). The inhibition concentration 50 (IC_{50}) values

were calculated by graph slope formulations. The IC_{50} values were 939.68 µg/mL for HepG2 cells and 1097.58 µg/mL for Caco2 cells.

Total-ROS induction

The IC_{30} values of *V. officinalis* methanolic extract in HepG2 and Caco2 cell lines were calculated for the Total-ROS evaluation. The calculated IC_{30} values were 600.12 µg/mL for HepG2 cells and 672.95 µg/mL for CaCo2 cells. The 100, 200, 400, and 600 µg/mL concentrations were selected for the Total-ROS analysis to determine the ROS production with a flow cytometer via H_2DC-FDA. No statistically significant difference was observed between the concentration groups for MFI for both cell lines. The *V. officinalis* methanolic extract did not cause an increase in the ROS production after a 24 h exposure (Figure 2).

DISCUSSION

Valerian belongs to Valerianaceae family, which includes approximately 300 species existing only in Western countries, and contains several different phytochemicals that may have nervous system protection, diuretic, antispasmodic, anthelmintic, antioxidant, antimicrobial, anti-inflammatory, antirheumatic sedative, anticonvulsant, and diaphoretic effects.[6] As a medicinal herbal plant, valerian is important in traditional therapy for sleeping and anxiety disorders due to its effects on the GABA A receptor system.[11] *V. officinalis* products are widely used for different type of diseases. In recent years, the usage of valerian products in cancer cure increased due to herbal implementers.[2]

Several people die worldwide due to different cancer types, and new therapeutic development studies pique the interest of scientists. Oxidative stress induction plays an important role in cancer cell death induction via chemotherapeutics. Oxidative stress has evident effects on cancer cell induction and cancer cell death mechanisms. Oxidative stress may induce cancer cell proliferation via DNA damage or can be a therapeutic strategy to cure cancer via inducing cancer cell death through

Table 1. MTT results of *Valeriana officinalis* extract exposure

Concentration (µg/mL)	Cell viability inhibition (%)	
	HepG2	Caco2
200	4.99	6.81
400	18.36	17.30
600	33.36	29.28
800	40.15	33.71
1000	52.95	45.72

MTT: 3-(4,5-dimethylthiazol-2-yl)-2,5-diphenyltetrazolium bromide, HepG2: Human liver hepatocellular carcinoma, Caco2: Human colorectal adenocarcinoma

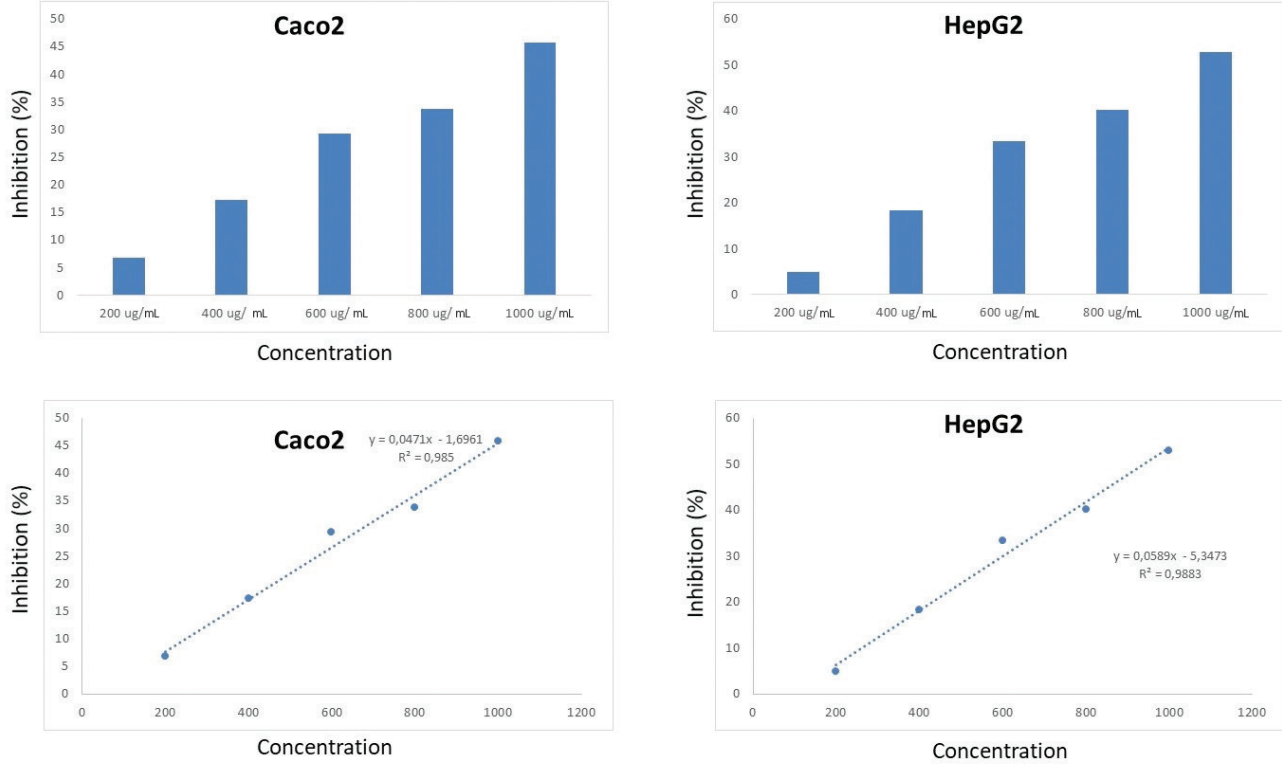

Figure 1. Cell viability inhibition (%) values of *Valeriana officinalis* methanolic extract on HepG2 and Caco2 cell lines increased with concentration dependence. Graph slope formulations are shown on the graphs

HepG2: Human liver hepatocellular carcinoma, Caco2: Human colorectal adenocarcinoma

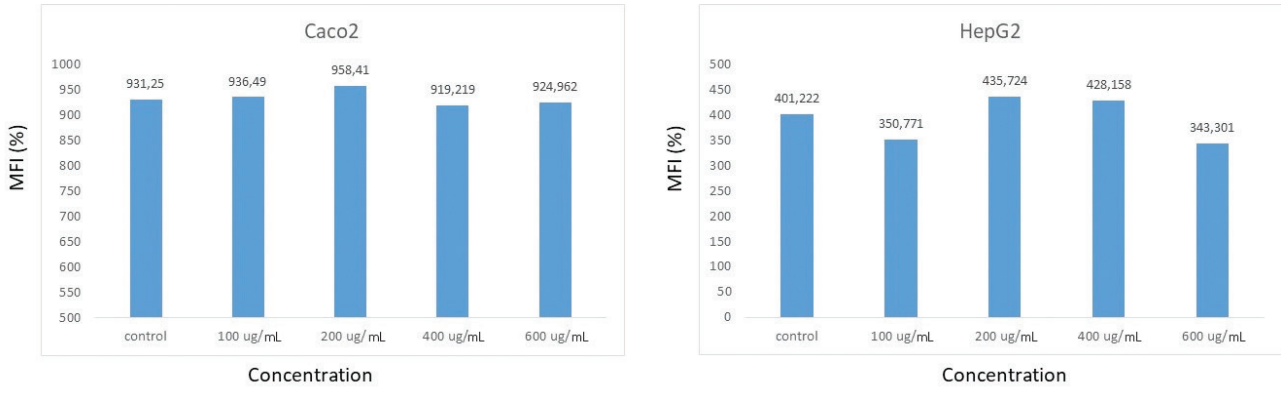

Figure 2. DC-FDA analysis results for HepG2 and Caco2 cell lines after 24 h exposure to *Valeriana officinalis* methanolic extract. ROS production was not induced (p>0.05)

DC-FDA: 2',7'-dichlorodihydrofluorescein diacetate, HepG2: Human liver hepatocellular carcinoma, Caco2: Human colorectal adenocarcinoma, ROS: Reactive oxygen species

apoptosis.[12,13] In different clinical trials, varied results were reported on valerian species *in vitro* and *in vivo*. In human neuroblastoma (SH-SY5Y) cell line, de Oliveria et al.[2] reported that aqueous *V. officinalis* extract exerted a protective role against apoptosis with rotenone exposure. Wang et al.[13] showed the antioxidant effects of *V. jatamansi* on HepG2, human cervix carcinoma, breast cancer (MDA-MB-231), and human umbilical vein endothelial cells. Kakehashi et al.[11] reported that *V. sitchensis* added in drinking water of male F344 rats significantly suppressed the 8-hydroxy-29-deoxyguanosine generation after hepatocarcinogenesis initiation by diethylnitrosamine at 50, 500, and 5000 ppm concentrations. The antioxidant catalase levels and apoptosis increased, and cell proliferation significantly decreased. The apoptosis induction was associated with the suppression of c-myc, Mafb, and cyclin D1 expression and increased expression levels of p21Waf1/Cip1, p53, and Bax. These results indicated that *V. sitchensis* administration can be associated with carcinogenesis inhibition.[11] Zhu et al.[14] showed the anticancer effects of *V. jatamansi* F3 fraction *in vitro* and *in vivo*. In MCF-10A cells, the F3 fraction administration increased the intracellular ROS production and induced apoptosis, which play key roles in cancer inhibition. Sudati et al.[15] reported that *V. officinalis* ethanolic extract has an antioxidant effect against different toxic agents in rat brain homogenates. In addition, different studies showed the antioxidant effect of *V. officinalis*.[16-18] Tian et al.[19] reported that a *V. jatamansi* ingredient, valtrate, induced apoptosis in MDA-MB-231 and MCF-7 cells and inhibited cell migration. In another study, Han et al.[20] reported that valeric acid, one of the important ingredients of valerian root extract, inhibits liver cancer development via histone deacetylase inhibition.

Quan et al.[21] isolated different iridoids from *V. jatamansi* roots, and two of these iridoids showed inhibitory effects on human glioma stem cells. Sen-Utsukarci et al.[22] reported that *V. alliariifolia* ethanolic extracts obtained with different EMs (EM1 and EM2) have a high antioxidant capacity. Additionally, two different ethanolic extracts had different IC_{50} values (EM1 >200 µg/mL and EM2 <10 µg/mL). Bos et al.[23] showed the cytotoxic effects of different ingredients isolated from *V. officinalis* on human small-cell lung cancer cell and human colorectal cancer cell line (COLO 320) with MTT test. Valerenic acid and its derivatives, such as acetoxyvalerenic acid, hydroxyvalerenic acid, and methyl valerenate, which are obtained from *V. officinalis*, exhibited extremely low toxicity in both cell lines at the 100-200 µM concentration range.[23]. In our study, the calculated IC_{50} values of *V. officinalis* methanolic extracts were 939.68 µg/mL for HepG2 cells and 1097.58 µg/mL for Caco2 cells. Differences in cytotoxicity results among studies of *Valeriana* species may depend on the different subtypes of the plant, plant section differences, EM differences, and study cell type.

In our study, the exposure of HepG2 and CaCo2 to the methanolic extract of *V. officinalis* in all exposure groups did not induce significant ROS production levels. Our results indicate that the methanolic extracts of *V. officinalis* may not induce cell death in cancer cell lines via oxidative stress induction. These results can be associated with commercial products obtained from different herbalists, which are less effective or ineffective in cancer cells.

CONCLUSION

In conclusion, the effects of *V. officinalis* extracts on cancer cells should be analyzed in detail with further studies that include different extraction protocols and with cultivated medical plants to define the anticancer effects of *V. officinalis*.

ACKNOWLEDGMENTS

The present study was supported by İstanbul University Scientific Research Projects Department (project no: 33246).

Conflicts of interest: No conflict of interest was declared by the authors. The authors alone are responsible for the content and writing of the paper.

REFERENCES

1. Ekor M. The growing use of herbal medicines: issues relating to adverse reactions and challenges in monitoring safety. Front Pharmacol. 2014;4:177.
2. de Oliveria DM, Barreto G, De Andrade DV, Saraceno E, Aon-Bertolino L, Capani F, Dos Santos El Bachá R, Giraldez LD. Cytoprotective effect of *Valeriana officinalis* extract on an *in vitro* experimental model of Parkinson disease. Neurochem Res. 2009;34:215-220.
3. Hamaidia M, Barez P, Carpentier A, Lebecque S, Miazek K, Paul A, Sriramareddy SN, Staumont B, Danthine S, Deleu M, Frédérich M, Pauw ED, Delaplace P, Delvigne F, Goffin D, Ongena M, Duysinx B, Louis R, Cosse J, Willems L. From *Valeriana officinalis* to cancer therapy: the success of a bio-sourced compound. Biotechnol Agron Soc Environ. 2016;20(Suppl 1):314-320.
4. Şen B, Mat A. Chemical and medicinal evaluations of the *Valeriana* species in Turkey. Istanbul Journal of Pharmacy. 2015;45:267-276.
5. EMA reports, Assessment report on *Valeriana officinalis* London, Doc. Ref. EMEA/HMPC/167391/2006. Last Accessed Date: 29.11.2007. Available from:https://www.ema.europa.eu/en/documents/herbal-report/superseded-assessment-report-valeriana-officinalis-l-radix_en.pdf
6. Nandhini S, Narayanan KB, Ilango K. *Valeriana officinalis*: a review of its traditional uses, phytochemistry and pharmacology. Asian J Pharm Clin Res. 2018;11;36-41.
7. Pandey A, Tripathi S. Concept of standardization, extraction and pre phytochemical screening strategies for herbal drug. J Pharmacogn Phytochem. 2014;2:115-119.
8. Oztas E, Abudayyak M, Celiksoz M, Özhan G. Inflammation and oxidative stress are key mediators in AKB48-induced neurotoxicity *in vitro*. Toxicol In Vitro. 2019;55:101-107.
9. Wu D, Yotnda P. Production and detection of reactive oxygen species (ROS) in cancers. J Vis Exp. 2011:3357.
10. Kara M, Oztaş E, Ozhan G. Acetamipride induced cyto-and genotoxicity in pancreatic cell line. Turk J Pharm Sci. 2020;17:474-479.
11. Kakehashi A, Kato A, Ishii N, Wei M, Morimura K, Fukushima S, Wanibuchi H. Valerian inhibits rat hepatocarcinogenesis by activating GABA(A) receptor-mediated signaling. PLoS One. 2014;9:e113610.
12. Matés JM, Segura JA, Alonso FJ, Márquez J. Oxidative stress in apoptosis and cancer: an update. Arch Toxicol. 2012;86:1649-1665.
13. Wang F, Zhang Y, Wu S, He Y, Dai Z, Ma S, Liu B. Studies of the structure-antioxidant activity relationships and antioxidant activity mechanism of iridoid valepotriates and their degradation products. PLoS One. 2017;12:e0189198.
14. Zhu Z, Shen W, Tian S, Yang B, Zhao H. F3, a novel active fraction of Valeriana jatamansi Jones induces cell death via DNA damage in human breast cancer cells. Phytomedicine. 2019;57:245-254.
15. Sudati JH, Fachinetto R, Pereira RP, Boligon AA, Athayde ML, Soares FA, de Vargas Barbosa NB, Rocha JB. *In vitro* antioxidant activity of *Valeriana officinalis* against different neurotoxic agents. Neurochem Res. 2009;34:1372-1379.
16. Yoo DY, Jung HY, Nam SM, Kim JW, Choi JH, Kwak YG, Yoo M, Lee S, Yoon YS, Hwang IK. *Valeriana officinalis* extracts ameliorate neuronal damage by suppressing lipid peroxidation in the gerbil hippocampus following transient cerebral ischemia. J Med Food. 2015;18:642-647.
17. Sudati JH, Vieira FA, Pavin SS, Dias GR, Seeger RL, Golombieski R, Athayde ML, Soares FA, Rocha JB, Barbosa NV. *Valeriana officinalis* attenuates the rotenone-induced toxicity in Drosophila melanogaster. Neurotoxicology. 2013;37:118-126.
18. Santos G, Giraldez-Alvarez LD, Ávila-Rodriguez M, Capani F, Galembeck E, Neto AG, Barreto GE, Andrade B. SUR1 receptor interaction with hesperidin and linarin predicts possible mechanisms of action of *Valeriana officinalis* in Parkinson. Front Aging Neurosci. 2016;8:97.
19. Tian S, Wang Z, Wu Z, Wei Y, Yang B, Lou S. Valtrate from Valeriana jatamansi Jones induces apoptosis and inhibits migration of human breast cancer cells *in vitro*. Nat Prod Res. 2020;34:2660-2663.
20. Han R, Nusbaum O, Chen X, Zhu Y. Valeric acid suppresses liver cancer development by acting as a novel HDAC inhibitor. Mol Ther Oncolytics. 2020;19:8-18.
21. Quan LQ, Hegazy AM, Zhang ZJ, Zhao XD, Li HM, Li RT. Iridoids and bis-iridoids from *Valeriana jatamansi* and their cytotoxicity against human glioma stem cells. Phytochemistry. 2020;175:112372.
22. Sen-Utsukarci B, Taskin T, Goger F, Tabanca N, Estep AS, Kessler SM, Akbal-Dagistan O, Bardakci H, Kurkcuoglu M, Becnel J, Kiemer A, Mat A. Chemical composition and antioxidant, cytotoxic, and insecticidal potential of *Valeriana alliariifolia* in Turkey. Arh Hig Rada Toksikol. 2019;70:207-218.
23. Bos R, Hendriks H, Scheffer JJ, Woerdenbag HJ. Cytotoxic potential of valerian constituents and valerian tinctures. Phytomedicine. 1998;5:219-225.

Turk J Pharm Sci 2021;18(5):609-615
DOI: 10.4274/tjps.galenos.2021.34676

ORIGINAL ARTICLE

Wound Healing Effectivity of the Ethanolic Extracts of *Ageratum conyzoides* L. Leaf (White and Purple Flower Type) and *Centella asiatica* and Astaxanthin Combination Gel Preparation in Animal Model

Ageratum conyzoides L. Yaprağı (Beyaz ve Mor Çiçekli Tür) ve *Centella asiatica* Etanol ile Hazırlanmış Ekstreleri Astaksantin Kombinasyonunu İçeren Hazırlanmış Jelin Hayvan Modelinde Yara İyileştirici Etkisi

Yedy Purwandi SUKMAWAN[1]*, Ilham ALIFIAR[1], Lusi NURDIANTI[2], Widar Rahayu NINGSIH[1]

[1]Bakti Tunas Husada Health Science College, Department of Pharmacology and Clinical Pharmacy, Tasikmalaya, Indonesia
[2]Bakti Tunas Husada Health Science College, Department of Pharmaceuthics, Tasikmalaya, Indonesia

ABSTRACT

Objectives: The study's objective was to determine the wound healing activity of the combination of ethanolic extracts of *Ageratum conyzoides* L. leaf (white and purple), *Centella asiatica,* and astaxanthin gel preparation.

Materials and Methods: For in-gel preparation, three different formulas of gelling agents, namely carbopol 934 (1%), hydroxypropyl methylcellulose (HPMC) (9%), and natirum-carboxymethylcellulose (Na-CMC) (4%), were employed. Then, the organoleptic, pH, spreadability, and viscosity of the formulas were evaluated. To determine wound healing activity, six treatments, including negative control (placebo), positive control (bioplacenton), BP5 (*A. conyzoides* L. leaf ethanolic extract of white flower type 5%, *C. asiatica* L. Urb leaf ethanolic extract 2.5%, astaxanthin 0.05%), BU5 (*A. conyzoides* L. leaf ethanolic extract of purple flower type 5%, *C. asiatica* L. Urb leaf ethanolic extract 2.5%, astaxanthin 0.05%), BU10 (*A. conyzoides* L. leaf ethanolic extract of purple flower type 10%, *C. asiatica* L. Urb leaf ethanolic extract 5%, and astaxanthin 0.1%), and BP10 (*A. conyzoides* L. leaf ethanolic extract of white flower type 10%, *C. asiatica* L. Urb leaf ethanolic extract 5%, and astaxanthin 0.1%) were evaluated. All treatments were applied to an incision wound (1.5 cm). Measurement of the wound length was conducted daily for 14 days.

Results: The results showed that the carbopol 934 (1%) gelling agent formula was better than HPMC and Na-CMC. Meanwhile, the percentages of wound healing activity for negative, positive, BP5, BU5, BU10, and BP10 groups were 72.51%, 69.36%, 70.14%, 81.70%, 86.54%, and 80.21%, respectively. The BU5 and BU10 showed significant activity ($p<0.05$) compared with positive and negative controls.

Conclusion: BU10 provided the best wound healing activity and can be developed as a commercial product.

Key words: *Ageratum conyzoides* L., astaxanthin, *Centella asiatica,* gel preparation, wound healing

ÖZ

Amaç: Çalışmanın amacı, *Ageratum conyzoides* L. yaprağı (beyaz ve mor), *Centella asiatica* ve astaksantin jel preparatının etanol ekstrelerinin kombinasyonunun yara iyileştirici aktivitesini belirlemekti.

Gereç ve Yöntemler: Jel hazırlamada, 3 farklı jelleştirme ajanı formülümüz vardı: Karbopol 934 (%1), hidroksipropil metilselüloz (HPMC) (%9) ve sodyum-karboksimetil selüloz (Na-CMC) (%4). Daha sonra bu formülleri organoleptik özellikleri, pH'leri, yayılabilirlikleri ve viskoziteleri dahil olmak üzere farklı parametreler ile değerlendirdik. Yara iyileştirme aktivitesini belirlemek için oluşturulan altı grup: Negatif kontrol (plasebo), pozitif kontrol (bioplasenton), BP5 (beyaz çiçekli *A. conyzoides* L. yaprağının etanol ekstresi %5, *C. asiatica* L. Urb yaprağı etanol ekstresi %2,5 ve astaksantin %0,05), BU5 (mor çiçekli *A. conyzoides* L. yaprağının etanol ekstresi %5, *C. asiatica* L. Urb yaprağı etanol ekstresi %2,5 ve astaksantin %0,05), BU10

*Correspondence: yedipur@gmail.com, Phone: +6287827070970, ORCID-ID: orcid.org/0000-0002-9017-8990
Received: 13.07.2020, Accepted: 21.02.2021

(mor çiçekli *A. conyzoides* L. yaprağının etanol ekstresi %10, *C. asiatica* L. Urb yaprağı etanol ekstresi %5 ve astaksantin %0,1), BP10 (beyaz çiçekli *A. conyzoides* L. yaprağının etanol ekstresi %10, *C. asiatica* L. Urb yaprağı etanol ekstresi %5 ve astaksantin %0,1) şeklindeydi. Tüm gruplar 1,5 cm uzunluğunda kesi ile tedavi edildi. Yara uzunluğunun ölçümü 14 gün boyunca günlük olarak gerçekleştirildi.

Bulgular: Karbopol 934 (%1) jelleştirici madde formülü, değerlendirme testine göre HPMC ve Na-CMC'den daha iyiydi. Negatif, pozitif, BP5, BU 5, BU10 ve BP10 grupları için yara iyileştirme aktivitesi yüzdesi sırasıyla; %72,51, %69,36, %70,14, %81,70, %86,54 ve %80,21 olarak bulundu. BU5 ve BU10, pozitif ve negatif gruplara kıyasla anlamlı aktivite gösterdi ($p<0,05$).

Sonuç: BU10, en iyi yara iyileştirme aktivitesi gösteren formül olarak ticari olarak geliştirilme potansiyeli olan formülasyon olarak belirlendi.

Anahtar kelimeler: *Ageratum conyzoides* L, astaksantin, *Centella asiatica*, jel hazırlama, yara iyileşmesi

INTRODUCTION

A wound is defined as a physical, chemical, or thermal injury or insult that results in an opening or breaking in the integrity of the skin or disruption of anatomical and functional integrity of living tissues.[1] Global wound prevalence has reached ~8.2 million people, and medical care costs range from $28.1 to $96.8 billion.[2] Many wound healing products are available in the market. To date, there is no standard topical treatment for wound healing. Bioplacenton is a topical preparation that is available in the market. This product is commonly used for wound healing treatment by Indonesians.[3] The ingredients of bioplacenton include neomycin sulfate 0.5% and placenta extract 10%.[4] Placenta extract accelerates the healing of the wound size, followed by reduction of transforming growth factor and elevation of vascular endothelial growth factor and $CD31^+$.[5]

Ageratum conyzoides, *Centella asiatica*, and astaxanthin have been shown to have wound healing activity.[6,7] Ethanolic extract of *A. conyzoides* exhibits a 40% increase in tissue tensile strength and a 33% decrease in re-epithelialization time, high collagen, and cellular infiltration.[8] Different extractions of *C. asiatica* (hexane, ethyl acetate, methanol, and water extract) show tensile strength and develop epithelization and keratinization of the wounds.[9] Asiaticoside and madecassoside from *C. asiatica* play an essential role in this wound healing activity.[10] Astaxanthin is a powerful antioxidant, which is isolated from a lobster.[11] Besides that, astaxanthin provides wound healing activity by reducing iNOS and increasing Col1A1 and bFGF.[12] Col1A1 provides instructions for making collagen, which supports many tissues, including the skin. Meanwhile, bFGF regulates many biological functions, including tissue repair.[13,14] However, the wound healing activity of these combinations is still unknown. Therefore, this study aimed to evaluate the wound healing activity of *A. conyzoides, C. asiatica,* and astaxanthin combination gel preparation.

MATERIALS AND METHODS

Ethical clearance

All the procedures were performed according to the Guide for the Care and Use of Laboratory Animals and approved by Bakti Tunas Husada Health Sciences College Ethical Committee (no: 03/kepk-bth/04/20).

Plant materials and extract preparation

A. conyzoides and *C. asiatica* leaves were collected from the Galunggung Mountain area, Tasikmalaya, West Java. The plants were authenticated by the School of Life Science and Technology, Institut Teknologi Bandung. Astaxanthin was obtained from Sigma Aldrich. The leaves were shade-dried and coarsely powdered by a grinder and stored in an airtight container at room temperature. The dried leaves of *A. conyzoides* L. (1000 g, purple flower type and 1000 g white flower type) and *C. asiatica* (2000 g) were used for maceration by ethanol 96% for 24 h, and this process was repeated thrice. The extract was filtered and concentrated using a rotary evaporator at 60°C. The percentage yield was calculated, and the extract was preserved in a refrigerator at 4°C until further use.

Standardization of simplicia

Simplicia was standardized using organoleptic, microscopic, and secondary metabolite analysis. The secondary metabolites, including alkaloid, flavonoid, polyphenol, quinone, tannin, monoterpenes-sesquiterpenes, triterpenoid, and steroid, were determined according to Fransworth's methods.[15]

Preformulation of gel preparation

The objective of the gel preformulation was to determine the best gel formula from three bases, including carbopol 934 1%, hydroxypropyl methylcellulose (HPMC) 9%, and natirum-carboxymethylcellulose (Na-CMC) 4%. The preformulation was checked for organoleptic, pH, homogeneity, viscosity, and spreadability.

Wound healing activity test

The treatments were

(i) Negative control (placebo),

(ii) Positive control (Bioplacenton),

(iii) BP5 (*A. conyzoides* L. of white flower 5%, *C. asiatica* L. Urb 2.5%, astaxanthin 0.05%),

(iv) BU5 (*A. conyzoides* L. of purple flower 5%, *C. asiatica* L. Urb 2.5%, astaxanthin 0.05%),

(v) BU10 (*A. conyzoides* L. of purple flower 10%, *C. asiatica* L. Urb 5%, and astaxanthin 0.1%), and

(vi) BP10 (*A. conyzoides* L. of white flower 10%, *C. asiatica* L. Urb 5%, and astaxanthin 0.1%).

All treatments were applied to an incision wound of 1.5 cm. The wound healing capacity was determined by daily measurement of the wound length using calipers for 14 days.

Statistical analysis

The obtained data were analyzed using analysis of variance, followed by posthoc test of least significant difference. The data were considered significant if the p value was ⟨0.05. All statistical analyses were performed using SPSS 16.00.

RESULTS AND DISCUSSION

Standardization of simplicia

The standard was evaluated based on organoleptic, microscopic, and non-specific parameters as well as phytochemical screening. The results of the organoleptic and microscopic parameters (Table 1), and non-specific parameters such as water content, ash content, dry shrinkage, and yields (Table 2) fulfilled the Indonesia Materia Medica Standard and Indonesia Herbal Pharmacopeia criteria.[16,17] Therefore, these simplicia were qualified for further wound healing test activity. Phytochemical screening study was positive for flavonoid, alkaloid, saponin, polyphenol, tannin, quinone, steroid-triterpenoid, and monoterpene-sesquiterpene, but negative for tannin (Table 3).

Evaluation of the gel preparation

In the organoleptic evaluation, carbopol 934 gel preparation gave the best texture and color compared with Na-CMC and HPMC (Table 4, Figure 1). Thus, carbopol 934 bases in three concentrations (0.5%, 1%, and 1.5%) were used for further gel preparation formula evaluation (Table 5). The parameters, including stability, organoleptic, pH, viscosity, and spreadability for three cycles at two temperatures, 2°C and 40°C (Table 6).

Table 1. Organoleptic and microscopic data

Simplicia	Organoleptic	Microscopic
Centella asiatica L. Urb	Form: Powder Color: Green Odor: Aromatic typical Taste: Bitter	Stomata, hair cover, oxalic acid, sklerenkim, epidermis, wooden vessel
Ageratum conyzoides L. leaf (white flower type)	Form: Powder Color: Pale green Odor: Aromatic typical Taste: Bitter	Stomata, hair cover, secretion cells and essential oil, stomata
Ageratum conyzoides L. leaf (purple flower type)	Form: Powder Color: Green Odor: Aromatic typical Taste: Bitter	Stomata, hair cover, secretion cells, epidermis, wooden vessels

Table 2. Non-specific parameters

No.	Parameters	Results (%)	Standard (%)
1	Water content a. *Ageratum conyzoides* L. leaf (white flower type) b. *Ageratum conyzoides* L. leaf (purple flower type) c. *Centella asiatica* L. Urb	 5.33 5.33 6.67	 ⟨10
2	Ash content a. *Ageratum conyzoides* L. leaf (white flower type) b. *Ageratum conyzoides* L. leaf (purple flower type) c. *Centella asiatica* L. Urb	 11.84 10.57 10.60	 ⟨13 ⟨13 ⟨18.05
3	Dry shrinkage a. *Ageratum conyzoides* L. leaf (white flower type) b. *Ageratum conyzoides* L. leaf (purple flower type) c. *Centella asiatica* L. Urb	 8.7 9.91 9.68	 ⟨10 ⟨10 ⟨11
4	Yields a. *Ageratum conyzoides* L. leaf (white flower type) b. *Ageratum conyzoides* L. leaf (purple flower type) c. *Centella asiatica* L. Urb	 20.16 13.87 11.74	 ⟩7.2

Table 3. Phytochemical screening

Secondary metabolite	*Ageratum conyzoides* L. leaf		*Centella asiatica* L. Urb	
	Simplicia	Extract	Simplicia	Extract
Flavonoid	+	+	+	+
Alkaloid	+	+	+	+
Saponin	+	+	+	+
Polyphenol	+	+	+	+
Tannin	-	-	-	-
Quinone	+	+	+	+
Steroid/triterpenoid	+	+	+	+
Monoterpene/sesquiterpene	+	+	+	+

+: Positive results, -: Negative results

HPMC
Texture: Bubbly and liquid
Colour: Yellowish

Na CMC
Texture: Liquid
Colour: Clear

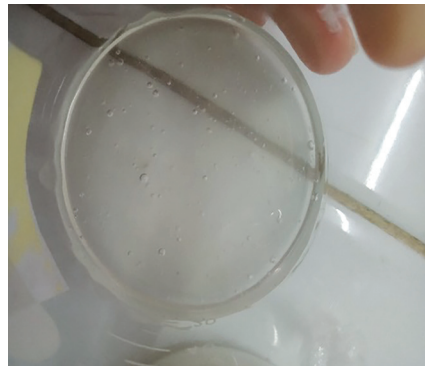

Carbopol 934
Texture: Viscous
Colour: Clear

Figure 1. Organoleptic evaluation of three basis gel preformulation
HPMC: hydroxypropyl methylcellulose, Na-CMC: Natirum-carboxymethylcellulose

Table 4. Preformulation of gel preparation

Substances	F1 (%)	F2 (%)	F3 (%)
Carbopol 934	-	-	1
Hydroxypropyl methylcellulose	9	-	-
Na-carboxymethylcellulose	-	4	-
Propylenglycol	15	2.5	2
Triethinolamine	-	-	qs
Propyl paraben	0.15	0.2	-
Methyl paraben	0.18	0.18	-
Tween 80	-	2	-
Aquades	Ad 20 g	Ad 20 g	Ad 20 g

Table 5. Formulation of gel preparation

Substances	F3a (%)	F3b (%)	F3c (%)
Carbopol 934	0.5	1	1.5
Propylenglycol	2	2	2
Triethanolamine	qs	qs	qs
DMDM hyndantoin	0.5	0.5	0.5
Aquades	Ad 15 g	Ad 15 g	Ad 15 g

Table 6. Evaluation of gel preparation

Parameter	Hasil			Standard
	F3a (%)	F3b (%)	F3c (%)	
Organoleptic	Yellowish	Clear	Clear	Clear
Homogenity	Homogen	Homogen	Homogen	Homogen
Consistency	Viscous	Viscous	Viscous	Viscous
pH	7	6.25	6	4-6.5
Spreadability	7.2 cm	5.8 cm	4.8 cm	4-6 cm

The results of the evaluation showed that carbopol 1% gave the best formulas and fulfilled the criteria.[18-20] Hence, carbopol 1% (F3b) was combined with *A. conyzoides* L. leaf ethanolic extract (white and purple flower type), *C. asiatica* leaf ethanolic extract, and astaxanthin.

The determination of wound healing activity

Wound healing is comprised of three phases: Inflammation, proliferation, and remodeling. The first phase involves polymorphonuclear and macrophage inflammation, which last 3-5 days. The second phase is marked with a new tissue formation, fibroblast, endotel, and collagen formation. The third phase is the maturation phase that provides tensile strength, epithelium, and new tissue growth.[21-23]

The BU10 treatment showed the best wound healing activity compared with other groups ($p<0.05$) (negative and positive controls, BP5, and BP10), but not superior ($p>0.05$) than BU5 (Figure 2, 3). The wound healing percentage of BU10 was 86.54%, with complete remission time on the 8th day (Figure 2). Meanwhile, the positive control (bioplacenton) showed no difference from the negative control ($p>0.05$). Currently, we could not confirm this phenomenon.

The wound healing activity of BU10 may be due to the secondary metabolite composition in *A. conyzoides* L. leaf (purple flower type), *C. asiatica*, and the antioxidant activity of astaxanthin.[13-14,24-29] The flavonoids in *A. conyzoides* L. leaf, such as kaempferol and quercetin, showed anti-inflammation, antioxidant, and immunomodulatory activity.[24,25] Alkaloid and saponin composition of *A. conyzoides* L. leaf also has a role in wound healing activity through fibroblast initiation, anti-inflammation, cell repairing, and strength of the skin cells.[26,27]

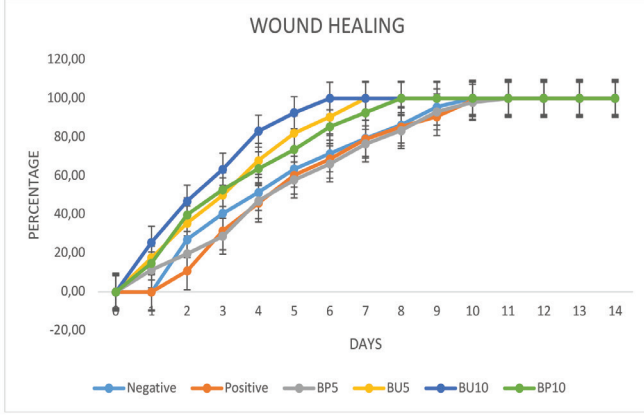

Figure 2. Wound healing activity test

Besides, *C. asiatica* secondary metabolites such as asiaticoside and madecassoside play an important role in wound healing activity although madecassoside is more effective than asiaticoside.[10,28] Asiaticoside stimulates collagen, epidermis formation, antioxidant activity, and anti-inflammation activity, resulting in the inhibition of scar formation.[28,29]

CONCLUSION

The combination of *A. conyzoides* L. leaf ethanolic extract (purple flower type) 10%, *C. asiatica* L. Urb leaf ethanolic extract 5%, and astaxanthin 0.1% showed the best wound healing activity and can be developed as a commercial product. Future studies are required to determine the relationships between antioxidants and wound healing activities.

Time (days)	Negative	Groups positive	BU10
1		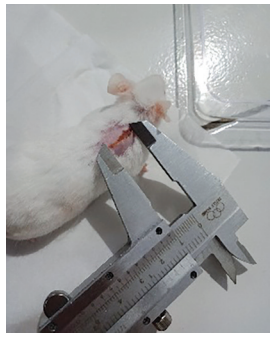	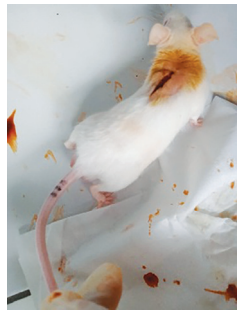
6		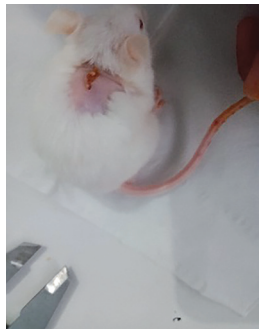	
10	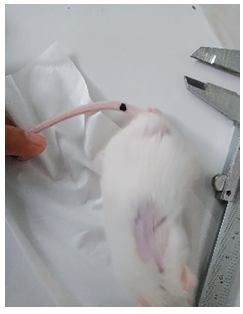	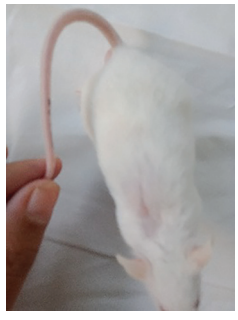	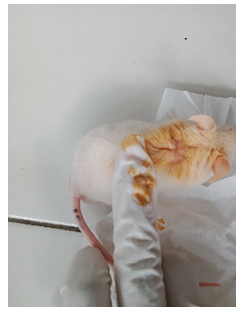
14	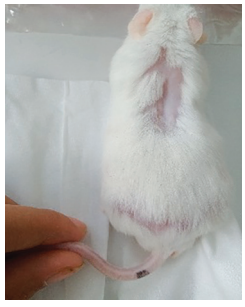		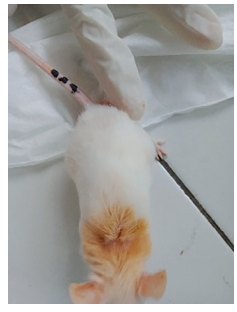

Figure 3. Wound healing comparison between negative control vs. positive control vs. BU10

ACKNOWLEDGMENTS

The authors thank Yusuf Firmansyah for helping in animal care.

Conflict of interest: No conflict of interest was declared by the authors. The authors are solely responsible for the content and writing of this paper.

REFERENCES

1. Boakye YD, Agyare C, Ayande GP, Titiloye N, Asiamah EA, Danquah KO. Assessment of wound-healing properties of medicinal plants: the case of phyllanthus muellerianus. Front Pharmacol. 2018;9:945.
2. Sen CK. The Launch of advances in wound care: strengthening the interdisciplinary continuum of wound care. Adv Wound Care (New Rochelle). 2012;1:1-2.

3. Wandasari C. Efektivitas gel putih telur pada penyembuhan luka bakar tikus putih (Rattus novergicus) melalui pengamatan jumlah fibroblas dan sel makrofag. Accessed date: 21.01.2021. Available from: http://repository.wima.ac.id/8052/2/BAB1%202443012253.pdf
4. MIMS. Bioplacenton. Accessed date: 21.01.2021. Available from: https://www.mims.com/indonesia/drug/info /bioplacenton?lang=id
5. Hong JW, Lee WJ, Hahn SB, Kim BJ, Lew DH. The effect of human placenta extract in a wound healing model. Ann Plast Surg. 2010;65:96-100.
6. Shedoeva A, Leafley D,Upton Z, Fan C. Wound healing and the use of medicinal plants. Evidence Based Complementary and Altern Med. 2019;2684108:1-30.
7. Sukmawan YP, Aryani R. Uji aktivitas penyembuhan luka formula gel ekstrak etanol daun babadotan (*Ageratum conyzoides* L) terhadap tikus jantan wistar. Jurnal STIKes BTH. 2016;16:88-93.
8. Arulprakash K, Murugan R, Ponrasu T, Iyappan K, Gayathri VS, Suguna L. Efficacy of *Ageratum conyzoides* on tissue repair and collagen formation in rats. Clin Exp Dermatol. 2012;37:418-424.
9. Somboonwong J, Kankaisre M, Tantisira B, Tantisira MH. Wound healing activities of different extracts of *Centella asiatica* in incision and burn wound models: an experimental animal study. BMC Complement Altern Med. 2012;12:103.
10. Wu F, Bian D,Xia Y,Gong Z, Tan Q, Chen J, Dai Y. Identification of major active ingredients responsible for burn wound healing of centella asiatica herbs. Evid Based Complement Alternat Med. 2012;848093:1-13.
11. Davinelli S, Nielsen ME, Scapagnini G. Astaxanthin in skin health, repair, and disease: a comprehensive review. Nutrients. 2018;10:522.
12. Meephansan J, Rungjang A, Yingmema W, Deenonpoe R, Ponnikorn S. Effect of astaxanthin on cutaneous wound healing. Clin Cosmet Investig Dermatol. 2017;10:259-265.
13. US. National Library of Medicine. Genetics Home Reference: COL1A1 Gene. Accessed date: July 7, 2020. Available from: https://ghr.nlm.nih.gov/gene/COL1A1#:~:text=Normal%20Function,the%20eye%20(the%20sclera).
14. Yun YR, Won JE, Jeon E. Fibroblast growth factors: biology, function, and application for tissue regeneration. J Tissue Eng. 2010;2010:218142.
15. Fransworth NR. Biological and phytochemical screening of plants. J Pharm Sci. 1996;55:225-276.
16. Departemen Kesehatan RI. Materia Medika Indonesia Jilid VI. Jakarta: Departemen Kesehatan RI; 1995.
17. Departemen Kesehatan RI. Farmakope Herbal Indonesia, Edisi 1. Jakarta : Departemen Kesehatan RI. 2009. Available from: https://farmalkes.kemkes.go.id/2020/08/farmakope-herbal-indonesia-edisi-ii-tahun-2017-3/
18. Garg AD, Garg AS, Sigla AK. Spreading of semisolid formulation: an update. Pharm Technol. 2002;26:84-102.
19. Voigt, R. Buku Pengantar Teknologi Farmasi, diterjemahkan oleh Soedani, N. Edisi V. Yogyakarta: Universitas Gadjah Mada Press; 1994.
20. Voigt, R. Buku Pengantar Teknologi Farmasi. Yogyakarta: Universitas Gadjah Mada Press; 1995.
21. Carville K. Wound care: Manual (5th ed). Osborne Park: Silver Chain Foundation; 2007.
22. Landen NX, Li D, Stahle M. Transition from Inflammation to proliferation: a critical step during wound healing. Cell Mol Life Sci. 2016;73:3861-3885.
23. Velnar T, Bailey T, Smrkolj V. The wound healing process: an overview of the cellular and molecular mechanism. J Int Med Res. 2009;37:1528-1542.
24. Suhendy H, Sukmawan YP. Aktivitas immunomodulator ekstrak etanol daun babadotan [*Ageratum conyzoides* (L .)]. J Pharmacopol. 2019;2:9-14.
25. Sukmawan YP, dan Aryanti R. Uji aktivitas penyembuhan luka formula gel ekstrak etanol daun babadotan (*Ageratum conyzoides* L) terhadap tikus. Jurnal Kesehatan Bakti Tunas Husada. 2016;16:88-93.
26. Safani EE, Kunharjito WAC, Lestari A, Purnama ER. Potensi ekstrak daun bandotan (*Ageratum conyzoides* L.) sebagai spray untuk pemulihan luka mencit diabetik yang terinfeksi *Staphylococcus aureus*. J Tropic Biol. 2019;3:69.
27. Sartika DD. Efek lumatan daun dewa (gynura segetum) dalam memperpendek waktu penyembuhan luka bersih pada tikus putih. Jurnal Keperawatan Soedirman. 2010;5:127-135.
28. Kurnianto S, Kusnanto K, Padoli P. Penyembuhan luka bakar pada tikus putih dengan menggunakan ekstrak daun pegagan (*Centella asiatica*) 25% dan ekstrak daun petai cina (leucaena leucocephala) 30%. Jurnal Ilmiah Kesehatan. 2017;10:250-255.
29. Mizuta M, Hirano S, Hiwatashi N, Tateya I, Kanemaru S, Nakamura T, Ito J. Effect of astaxanthin on vocal fold wound healing. Laryngoscope. 2014;124:E1-E7.

Turk J Pharm Sci 2021;18(5):616-627
DOI: 10.4274/tjps.galenos.2021.33958

ORIGINAL ARTICLE

Phytochemical Characterization of Phenolic Compounds by LC-MS/MS and Biological Activities of *Ajuga reptans* L., *Ajuga salicifolia* (L.) Schreber and *Ajuga genevensis* L. from Turkey

Türkiye'den *Ajuga reptans* L., *Ajuga salicifolia* (L.) Schreber ve *Ajuga genevensis* L.'nin LC-MS/MS ile Fenolik Bileşiklerinin Fitokimyasal Karakterizasyonu ve Biyolojik Aktiviteleri

Gamze GÖGER[1]*, Yavuz Bülent KÖSE[2], Fatih DEMİRCİ[3,4], Fatih GÖGER[3]

[1]Trakya University Faculty of Pharmacy, Department of Pharmacognosy, Edirne, Turkey
[2]Anadolu University Faculty of Pharmacy, Department of Pharmaceutical Botany, Eskişehir, Turkey
[3]Anadolu University Faculty of Pharmacy, Department of Pharmacognosy, Eskişehir, Turkey
[4]Eastern Mediterranean University Faculty of Pharmacy, Mersin, Turkey

ABSTRACT

Objectives: In this study, it was aimed to characterize the phenolic contents of *Ajuga reptans* L., *Ajuga salicifolia* (L.) Schreber and *Ajuga genevensis* L. and to investigate their *in vitro* antioxidant and antimicrobial activities.

Materials and Methods: Air dried aerial parts of *A. reptans* L., *A. salicifolia* (L.) Schreber, and *A. genevensis* L. collected from Turkey were extracted with methanol (70%), and the phenolic composition of the crude extracts was analyzed by liquid chromatography with tandem mass spectrometry (LC-MS/MS) method. To determine the total phenolic content the Folin-Ciocalteu method was used. The radical scavenging activities of the extracts were evaluated by the photometric 1,1-diphenyl-2-picrylhydrazyl radical, and trolox equivalent antioxidant capacity assays (TEAC). Furthermore, *Ajuga* sp. extracts were tested against *Escherichia coli* NRRL B3008, *Staphylococcus areus* ATCC 6538, *Salmonella thyphimurium* ATCC 13311, *Bacillus cereus* NRRL B-3711, *Candida albicans* ATCC 90028, *Candida tropicalis* ATCC 1369, and *Candida parapsilosis* ATCC 22019 using the *in vitro* broth dilution assay.

Results: The LC-MS/MS analyses identified 19 compounds. The amount of total phenolics ranged from 30.0 to 42.2 mg gallic acid equivalent/g in all extracts. According to the results of TEAC assay, the tested extracts were found to have relatively high activity at 1.2-1.5 mM concentrations. *Ajuga* sp. extracts inhibited all tested microorganisms; however, *C. albicans, C. tropicalis,* and *C. parapsilosis* exhibited relatively more susceptibility (minimum inhibitory concentration: 156.25 µg/mL) compared to the bacteria tested.

Conclusion: The antioxidant activities of all extracts were determined for the first time by the TEAK method, and the *in vitro* antimicrobial activity of *A. salicifolia* was investigated for the first time against selected strains.

Key words: *Ajuga reptans, Ajuga salicifolia, Ajuga genevensis*, LC-MS/MS, antioxidant activity, antimicrobial activity

ÖZ

Amaç: Bu çalışmada Türkiye'de yetişen *Ajuga reptans* L., *Ajuga salicifolia* (L.) Schreber ve *Ajuga genevensis* L.'nin fenolik içeriklerinin karakterizasyonu, *in vitro* antioksidan ve antimikrobiyal aktivitelerinin araştırılması amaçlanmıştır.

Gereç ve Yöntemler: *A. reptans* L., *A. salicifolia* (L.) Schreber ve *A. genevensis* L'nin toprak üstü kısımları metanol (%70) ile ekstre edilmiş ve liyofilize edilerek ardından sıvı kromatografi tandem kütle/kütle spektrometre (LC-MS/MS) ile karakterizasyonları yapılmıştır. Toplam fenolik madde miktarları Folin-Ciocaltaeu yöntemi ile belirlenmiştir Ekstrelerin radikal süpürücü etkileri 1,1-difenil-2-pikrilhidrazil ve troloks eşdeğeri antioksidan

*Correspondence: gamzegoger@trakya.edu.tr, Phone: +90 284 235 40 10/3251, ORCID-ID: orcid.org/0000-0003-2978-5385
Received: 17.01.2021, Accepted: 23.02.2021

kapasite (TEAK) yöntemleri kullanılarak değerlendirilmiştir. Ayrıca, *Ajuga* sp. ekstrelerinin antimikrobiyal aktiviteleri, *Escherichia coli* NRRL B3008, *Staphylococcus areus* ATCC 6538, *Salmonella thyphimurium* ATCC 13311, *Bacillus cereus* NRRL B-3711, *Candida albicans* ATCC 90028, *Candida tropicalis* ATCC 1369 ve *Candida parapsilosis* ATCC 22019'a karşı *in vitro* mikrodilüsyon yöntemiyle çalışılmıştır.

Bulgular: LC-MS/MS analizleriyle 19 fenolik bileşik tanımlanmıştır. Tüm ekstrelerde toplam fenol miktarı 30,0-42,2 mg gallik asit eşdeğeri/g arasında bulunmuştur. TEAK antioksidan aktivite sonucunda ekstreler (1,2-1,5 mM) konsantrasyonlarda nispeten yüksek aktivite göstermiştir. *Ajuga* sp. ekstreleri, test edilen tüm mikroorganizmalara karşı antimikrobiyal aktivite göstermiştir. Ancak ekstreler, test edilen bakterilere kıyasla *C. albicans, C. tropicalis* ve *C. parapsilosis* suşlarına karşı nispeten daha fazla etkili (minimal inhibisyon konsantrasyonu: 156,25 µg/mL) bulunmuştur.

Sonuç: TEAK yöntemi ile tüm ekstrelerin ilk defa antioksidan aktiviteleri belirlenmiştir ve *A. salicifolia*'nın *in vitro* antimikrobiyal aktivitesi seçilen suşlara karşı ilk kez incelenmiştir.

Anahtar kelimeler: *Ajuga reptans, Ajuga salicifolia, Ajuga genevensis*, LC-MS/MS, antioksidan aktivite, antimikrobiyal aktivite

INTRODUCTION

The Lamiaceae family includes more than 245 genera and 7886 species distributed worldwide.[1] *Ajuga* L. is a genus of annual and perennial herbaceous flowering plants in the Lamiaceae family, with most species native to Asia, Africa, and Europe. *Ajuga* is represented by 14 species and 27 taxa in Turkey.[2]

Ajuga has a long history of use for wound healing preparation, and although little used today, it is well known in Anatolia as "Mayasil otu". Some *Ajuga* species are widely consumed as diuretic, diaphoretic, astringent, antipyretic, and tonic in Turkish traditional medicine.[3]

Ajuga sp. plants are reported for their *in vitro* antimalarial,[4] antimicrobial,[5,6] antioxidant,[5] anti-inflammatory,[7] lipoxygenase, acetylcholinesterase, and butyrylcholinesterase inhibition,[8] antipyretic,[9] and antiproliferative[10] activities.

Phytochemical constituents diterpenoids, such as phenylethanoid glycosides, sterols, phytoecdysteroids, flavonoids, and iridoids were reported as the main active compounds in *Ajuga* L. species.[11]

Ajuga salicifolia sterol glycosides were isolated and tested for antimicrobial and cytotoxic activity.[12] Iridoid, ionone, and phenylethanoid glycosides from the same group were also reported for this species.[13]

Phytochemical profile of Romanian *Ajuga genevensis* L. and *A. reptans reptans* were recently reported.[6] A summary of phytochemical investigations on *A. salicifolia*, *A. reptans,* and *A. genevensis* species are listed in Table 1.[6-36] *In vitro* antioxidant and antimicrobial activity of different extracts of Romanian *A. genevensis* L. and *A. reptans* were recently reported.[6] Previous antimicrobial activity results of *A. reptans*, *A. genevensis* and *A. salicifolia* are listed in Table 2.[37-40]

Table 1. Literature data on phytochemical profile for *Ajuga* species

Species	Compounds	References
Ajuga reptans	Iridoid glycoside (ajureptaside)	19
Ajuga reptans	Iridoid glucosides (ajureptaside A-D)	24
Ajuga salicifolia	Iridoid, ionone and phenylethanoid glycosides (8-O-acetylharpagide corchoionoside C, leonosides A)	13
Ajuga genevensis	Neo-clerodane diterpenoids (ajugavensins A-C)	18
Ajuga salicifolia	Clerodane diterpene (ajugachin a derivative)	20
Ajuga reptans	Neo-clerodane diterpenes (ajugatansins)	21
Ajuga salicifolia	Sterol glycosides (ajugasalicioside A-E)	12
Ajuga reptans	Phytoecdysteroids (28-Epi-sengosterone)	36
Ajuga salicifolia	Stigmastane sterols (ajugasalicigenin)	22
Ajuga reptans	Anthocyanins (cyanidin)	25
Ajuga reptans	Anthocyanins (delphinidin)	26
Ajuga reptans	Anthocyanins (cyanidin and delphinidin glucosides)	27
Ajuga genevensis *Ajuga reptans*	Hydroxycinnamic acids (caffeic acid, chlorogenic acid), flavonoids (apigenin and luteolin-7-O-glucoside)	17
Ajuga genevensis	Hydroxycinnamic acids (caffeic acid, *p*-coumaric acid, ferulic acid), flavonoids (hyperoside, isoquercitrin, rutin, quercitrin, luteolin, apigenin)	6
Ajuga reptans	Hydroxycinnamic acids (*p*-coumaric acid, ferulic acid), flavonoids (isoquercitrin, rutin, quercitrin, luteolin, apigenin)	6

Table 2. Literature survey of antimicrobial activity for *Ajuga salicifolia, Ajuga genevensis, and Ajuga reptans*

Componuds/species	Microorganisms	MIC (mg/mL) inhibition zone (mm)	References
Ajugasalicioside A, B, C, D, E compounds from *A. salicifolia*	*B. cereus* ATCC 10702, *S. epidermidis* ATCC 12228 *S. aureus* ATCC 25923 *M. luteus* ATCC 99431 *P. aeruginosa* ATCC 27853 *C. albicans* ATCC 2579	No activity was found	12
MeOH extract of *A. reptans* MeOH extract of *A. reptans*	*F. oxysporum, F. verticillioides* *P. brevicompactum, P. expansum* *A. flavus, A. fumigatus* *F. oxysporum, F. verticillioides* *P. brevicompactum*	Range of 2.65 mm-31.65mm	37
Water extract from aerial parts of *A. genevensis*	*S. aureus* 209, *S. aureus* (Makarov) *S. aureus* Type, *S. epidermidis* Wood 46, *E. coli* 675, *S. gallinarum*, *P. vulgaris* *B. subtilis* L2, *B. anthracoides* 96	Range of 7 mm-15 mm	38
MeOH extract from *A. reptans*	*B. subtilis* ATCC 6633 *E. coli* ATCC 25922	8.5 mm-10.00 mm	39
Water, MeOH and EtOH extracts from aerial parts of *A. reptans*	*E. coli* ATCC 25922, *P. aeruginosa* ATCC 27853, *S. typhimurium* ATCC 14028, *S. marcescens* ATCC 8100 *P. vulgaris* ATCC 13315, *E. cloacae* ATCC 23355, *K. pneumoniae* ATTC 13883, *S. pyogenes* ATTC 19615 *S. aureus* ATTC 25923, *S. epidermidis* ATCC 12228	7.0 mm-11.7 mm	40
MeOH and EtOH extracts from flowers of *A. genevensis*	*S. aureus* ATCC 49444, *P. aeruginosa* ATCC 27853, *L.monocytogenes* ATCC 19114, *E. coli* ATCC 25922 *S. typhimurium* ATCC 14028	MIC value of 1.56-6.25	29
MeOH and EtOH extracts from flowers of *A. reptans*	*S. aureus* ATCC 49444, *P. aeruginosa* ATCC 27853, *L. monocytogenes* ATCC 19114, *E. coli* ATCC 25922 *S. typhimurium* ATCC 14028	MIC value of 1.56-6.25	28
EtOH, PE and Chl. extracts from aerial parts of *A. genevensis*	*A. flavus* ATCC 9643, *A. niger* ATCC 6275, *C. albicans* ATCC 10231, *C. parapsilosis* ATCC 22019, *P. funiculosum* ATCC 56755, *A. flavus* ATCC 9643	MIC value of 0.05-0.1	6
EtOH, PE and Chl. extracts from aerial parts of *A. reptans*	*A. niger* ATCC 6275 *C. albicans* ATCC 10231 *C. parapsilosis* ATCC 22019 *P. funiculosum* ATCC 56755	MIC value of 0.05-0.025	6

A. genevensis was used in traditional Austrian medicine and consumed as medicinal tea in treating respiratory tract disorders,[14] and *in vitro* anticancer activity studies were reported from Europe, Asia, and America.[15]

A. reptans grows natively in Europe and have bluish-purple flowers colored with anthocyanin pigments.[11] It was used in Mediterranean traditional medicine for cardiovascular complications and skin disorders[16] and in traditional Austrian medicine as a medicinal tea for the treatment of respiratory tract disorders.[14] A previous study showed that *A. reptans* L. is used due to the anti-inflammatory effects of its polyphenols, its wound healing properties, and antidiarrhea, antiulcerogenic, and hepatoprotective effects due to the presence of iridoids.[17]

In the present study, 70% methanol extract of aerial parts of *A. reptans* L., *A. salicifolia* (L.) Schreber, and *A. genevensis* L. from Turkey were evaluated for their phytochemical profiles, total phenol, and total flavonoid contents, as well as their *in vitro* antioxidant and antimicrobial activities. LC-MS/MS techniques

were used for phytochemical analyses. *In vitro* 1,1-diphenyl-2-picrylhydrazyl (DPPH) radical, and trolox equivalent antioxidant capacity (TEAC) assays were performed. Additionally, antimicrobial properties of *Ajuga* extracts were assessed against microbial strains of *Escherichia coli* NRRL B3008, *Staphylococcus areus* ATCC 6538, *Salmonella thyphimurium* ATCC 13311, *Bacillus cereus* NRRL B-3711, *Candida albicans* ATCC 90028, *Candida tropicalis* ATCC 1369, and *Candida parapsilosis* ATCC 22019.

To the best of our knowledge, this is the first study to perform the TEAC antioxidant activity for all extracts and the *in vitro* antimicrobial activity of *A. salicifolia*.

MATERIALS AND METHODS

Chemicals

Antimicrobial standards, Mueller Hinton Broth, and RPMI-1640 medium were purchased from Sigma-Aldrich Chemical Co (Sigma-Aldrich Corp., St. Louis, MO). All chemicals and solvents used were of analytical grade.

Plant materials

A. reptans L.: [A1(E) Kırklareli: İğneada, Fidanlık kavşağı, 350 m, N 41 52' 25.3'' E 27 56' 11'', 21 ıv 2009], *A. salicifolia* (L.) Schreber: (B3, Eskişehir: Çağlan köyü, 1000 m, K 390 39' 971'' D 300 31' 185'', 31 vi 2010), and *A. genevensis* L. [A1(E) Kırklareli: Dereköy yolu, 449 m, K 410 50' 6.13 D 270 18' 3.18'', 22 ıv 2009] were collected and identified by Dr. Y.B Köse, and herbarium materials were deposited in the Herbarium of Anadolu University, Faculty of Pharmacy under herbarium code YBK1560, YBK1575, and YBK 1561, respectively.

Preparation of extracts

The aerial parts of the plants were dried in the shade at room temperature and ground to powder in a mechanical grinder. Each species (1 g) was extracted with methanol (70%, 100 mL) for 24 h, three times a day. After filtration, the solvents were evaporated under vacuo.

Phytochemical analysis by liquid chromatography with tandem mass spectrometry (LC-MS/MS)

The phytochemical analyses were performed using LC-MS/MS techniques.[5]

Determination of phenolic compounds

The total phenols contained in the extracts were calculated using the Folin-Ciocalteu method equivalent to gallic acid (GA).[30] A sample solution (100 µL) and Folin-Ciocalteu reagent (500 µL) were added to a 10 mL scale vessel containing 6 mL of distilled water. After 1 min, 1.5 mL of 20% aqueous Na_2CO_3 was added and completed with water to reach 10 mL. The reagent-free of extracts was used as the control. After incubation at 25ºC for 2 h, the absorbance was read at 760 nm and compared with the GA calibration curve. The total amount of phenolic was calculated as equivalent to GA. Three parallel experiments were performed, and the results were reported as mean values.

Biological activity

DPPH radical scavenging assay

The DPPH radical scavenging activity was performed according to Kumarasamy et al.[31] For this purpose, 100 µL of methanol and samples were transferred to the first column of 96-well microtiter plates. A 10-well dilution was made in an equal amount of MeOH via a multi-channel pipette and stirred in the vortex for 5 min. The DPPH stock solution was prepared by dissolving 2 mg of DPPH• in 25 mL of MeOH, and solution was added to each well and left in a dark place for 30 min. Butylated hydroxy toluene (BHT) and GA at the same concentration were used as positive controls, and ultraviolet (UV) absorbance was measured at room temperature using a Biotek microplate spectrophotometer at 517 nm.

The following equations using 50% inhibition concentration (IC_{50}) (equation 1) and percentage (%) inhibition values (equation 2) were calculated as follows:

$$IC_{50} = [(A_0-A_1)/A_0] \times 100 \quad \text{equation (1)}$$

$$\text{Percentage Inhibition} = \left[\frac{(\text{Abs}_{\text{control}} - \text{Abs}_{\text{sample}})}{\text{Abs}_{\text{control}}}\right] x100 \quad \text{equation (2)}$$

TEAC assay

Experiments were performed as declared by Papandreou et al.[32] sweeping $ABTS^{\bullet+}$ (2,2'-azino-bis-3-ethylbenzothiazoline-6-sulfonic acid) radical and vitamin E. It is based on the comparison of water-soluble analog with trolox. The mixture of 7 mM $ABTS^{\bullet+}$ and 2.5 mM sodium persulfate was kept in the dark for 12-16 h, resulting in the formation of blue-colored radicals. A sample (10 µL) and $ABTS^{\bullet+}$ solution (990 µL) were mixed, and absorbance was measured at 734 nm per minute intervals for 30 min. To find out the TEAC activity results, the $ABTS^{\bullet+}$ radical was plotted using Trolox's 2.5-2-1.5-1-0.5-0.1 (mM) concentrations, according to the % inhibition values. For quantification, a Trolox calibration curve was used where all experiments were repeated in triplicates.

Antimicrobial activity

Antimicrobial activity testing was performed according to the guidelines of broth microdilution methods.[33-35] Standard strains, *E. coli* NRRL B3008, *S. areus* ATCC 6538, *S. thyphimurium* ATCC 13311, *B. cereus* NRRL B-3711, *C. tropicalis* ATCC 1369, *C. parapsilosis* ATCC 22019, and *C. albicans* ATCC 90028, as well as antimicrobial standards, such as ampicillin, tetracycline, ketoconazole, and oxiconazole, were used in this study. Methanol extracts were prepared at 1250-2.44 µg/mL concentrations and dissolved in dimethylsulfoxide and initial test solutions. Serial dilutions were prepared at 64-0.125 µg/mL for ampicillin, tetracycline, and ketoconazole. All experiments were evaluated in triplicates, and mean values were reported.

Statistical analysis

Data obtained from antioxidant and total phenolic content experiments were expressed as mean standard error. IC_{50} values were estimated using a non-linear regression algorithm.

RESULTS AND DISCUSSION

LC-MS/MS analysis of the extracts

Screening of the extracts by LC-MS/MS enabled the identification of phenolic acids, such as coumaroyl glucoside, flavonoids, and phenylethanoid glycosides. Figures 1-3 show the 280 nm UV chromatograms of *A. reptans*, *A. genevensis* and *A. salicifolia*, respectively. The compounds detected from *Ajuga* sp. methanol extracts are listed in Table 3.

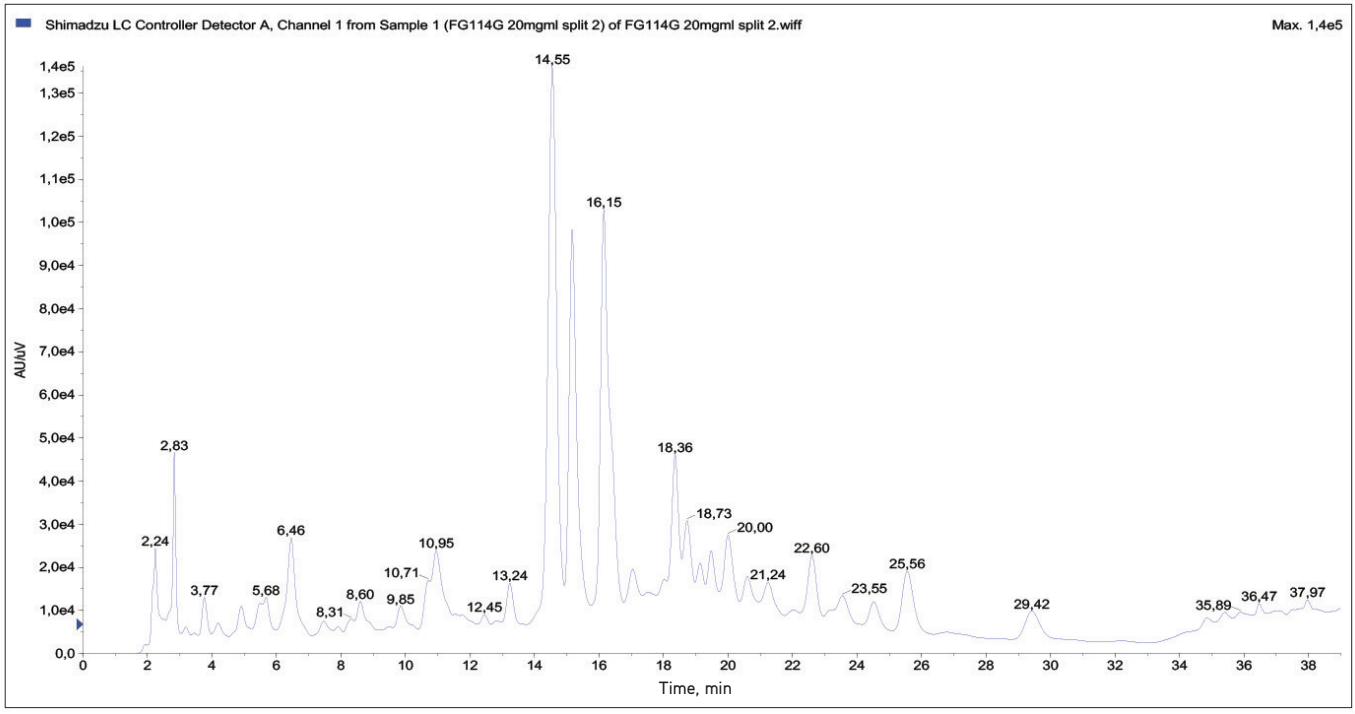

Figure 1. HPLC-UV chromatogram (280 nm) of *A. reptans*

HPLC: High performance liquid chromatography, UV: Ultraviolet

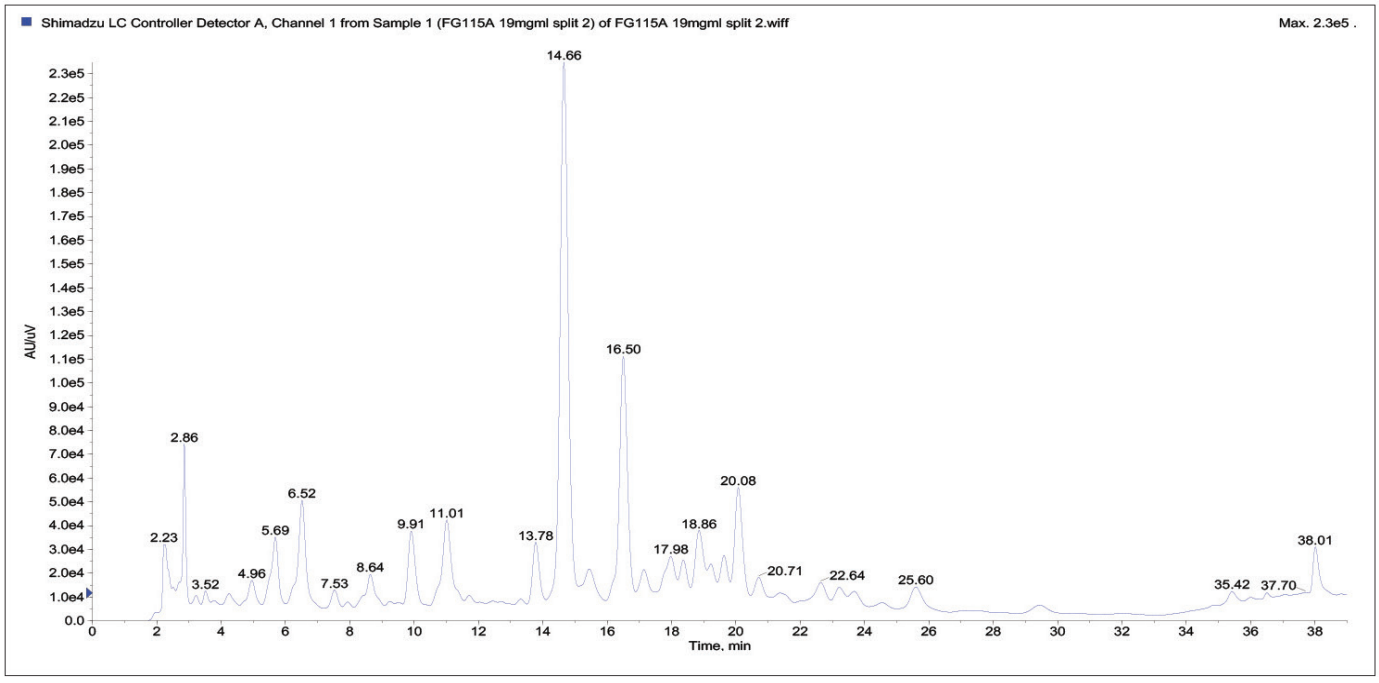

Figure 2. HPLC-UV chromatogram (280 nm) of *A. genevensis*

HPLC: High performance liquid chromatography, UV: Ultraviolet

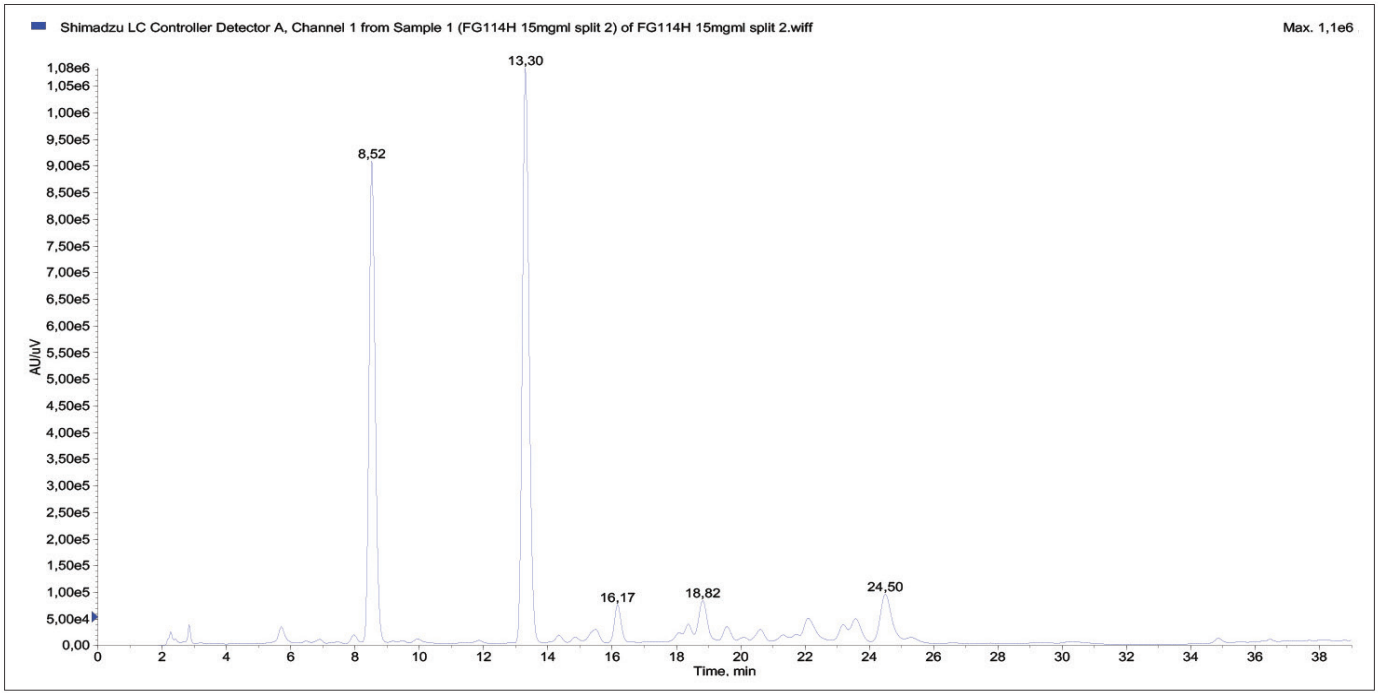

Figure 3. HPLC-UV chromatogram (280 nm) of *A. salicifolia*
HPLC: High performance liquid chromatography, UV: Ultraviolet

Table 3. Phytochemical composition of *A. reptans*, *A. salicifolia* and *A. genevensis* extracts

No	Compound	Rt	$[M-H]^-$	Fragments	Plant	Reference
1	Caffeoyl glucose	6.4	341	179, 161, 133	R	[41]
2	Coumaroyl glucoside	8.5	325	163, 119	S (major), G	[41,42]
3	Caffec acid	11.2	179	135	G	-
4	Coumaroyl glucoside isomer	13.3	325	163, 119	S (major), G	[41,42]
5	Luteolin derivative	14.6	487	285, 133, 117	R (major), G (major)	[43]
6	Apigenin-C-hexoside-C-pentoside	14.7	563	443, 383, 353	G	[44]
7	Echinocoside	15.4	785	623, 461, 161	R (major)	[44]
8	Forsythoside B	15.6	755	593, 461, 161	S	[45]
9	Forsythoside A	16.3	623	461, 315, 161	R (major), G (major)	[45]
10	Cistanoside A	18.5	799	623, 461, 175, 193	S, R	[45]
11	Leonosides A	18.9	769	593, 461, 315, 193, 175	S	-
12	Quercetin glucuronide	19.0	477	301, 227, 133	G	[47]
13	Verbascoside	19.2	623	461,315, 161	R	-
14	Leucoseptoside A	19.6	637	461, 175	R, S	[45]
15	Luteolin glucuronide	20,1	461	285	R, G (major)	[43]
16	Luteolin glucoside	21.6	447	285	S	[46]
17	Luteolin	35.4	285	175,133	G	[6,29]
18	Apigenin	37.9	269	149,117	G	[29]

R: *A. reptans*, S: *A. salicifolia*, G: *A. genevensis*

As a result, the only substance commonly identified in all *Ajuga* species was forsythoside A and luteolin glucuronide.

The coumaroyl glucose and its glucoside isomer (Figure 4, 5) were determined for *A. salicifolia* extract. The echinacoside (Figure 6) was detected in *A. reptans* extract. The LC-MS/MS sprectrum of luteoline derivative (Figure 7), forsytoside A (Figure 8), and luteoline glucuronide (Figure 9) were observed in both *A. reptans* and *A. genevensis* extracts.

The phenolic acids as caffeic acid and flavonoids; apigenin-C-hexoside-C-pentoside, quercetin glucuronide, luteolin, and apigenin were identified only for *A. genevensis.* Furthermore, the phenylethanoid glycosides forsythoside B and leonosides A were identified only for *A. salicifolia*. The phytochemical research on *Ajuga* species focus on the isolation of flavonoids, caffeic and chlorogenic acid type derivates, phenylethanoid glycosides, phytoecdysteroids, iridoids, and diterpenes.[12,13,17-24] Some anthocyanins, delphinidin, and cyanidin 3-*O*-sophoroside-5-*O*-glucosides, were acylated with *p*-coumaric acid, while ferulic acid and malonic acid were isolated from the flowers of cell cultures of *A. reptans.*[25-27]

Total phenolic amounts of the extracts

The amount of total phenolics ranged from 30.0 to 42.2 mg GA equivalent (GAE)/g of the extracts. The phenolic amounts equivalent to GA in all three methanol extracts are shown in Table 4. The highest total phenolic level was found in the methanol extract of *A. reptans.* In previous studies, the total phenolic content of methanol extracts of *A. reptans* and *A. genevensis* has been evaluated to be 20.86±0.53 mg RE/g dw[28] and 22.63±0.61 mg GAE/g.[29]

DPPH radical scavenging activity

DPPH radical scavenging activity results are presented in Table 4. The positive control, BHT with IC_{50} value of 0.06 mg/mL, was found as the most potent antioxidant. The highest radical scavenging activity were obtained for *A. salicifolia* (IC_{50}: 0.28±0.01 mg/mL) and *A. reptans* (IC_{50}: 0.30±0.01 mg/mL) extracts. A correlation was also found between radical scavenging capacity and total phenol content. Previous studies showed the antioxidant activity of the methanol extract of *A. genevensis* flowers as IC_{50}: 72.08±6.02 µg/mL[29] and *A. reptans* as IC_{50}: 83.16±5.21.[28]

However, there have been no reports on the antioxidant activity of *A. salicifolia.* This study is the first to determine the antioxidant activity of *A. salicifolia*.

TEAC assay

The results obtained for the evaluation of the antioxidant activity using TEAC assay are presented in Table 4. $ABTS^{\bullet+}$ radical sweeping impact results are in parallel with the results of the DPPH radical scavenging effect. Extracts from all three plants show $ABTS^{\bullet+}$ radical scavenging activity at 1% concentrations, but these effects are not as high as the BHT used as the standard.

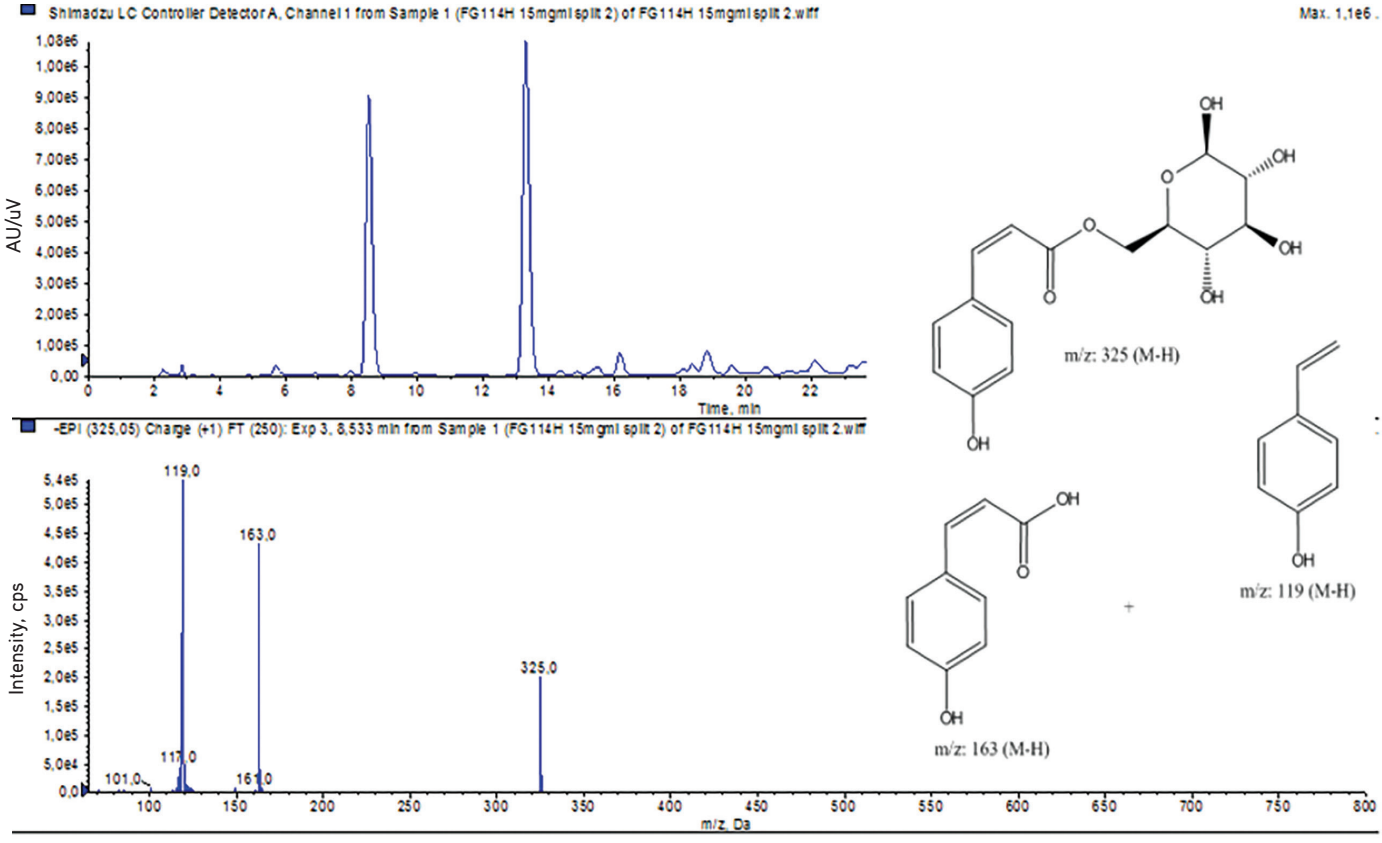

Figure 4. LC-MS/MS sprectrum of in coumaroyl glucose (2) in *A. salicifolia* extract

LC-MS/MS: Liquid chromatography with tandem mass spectrometry

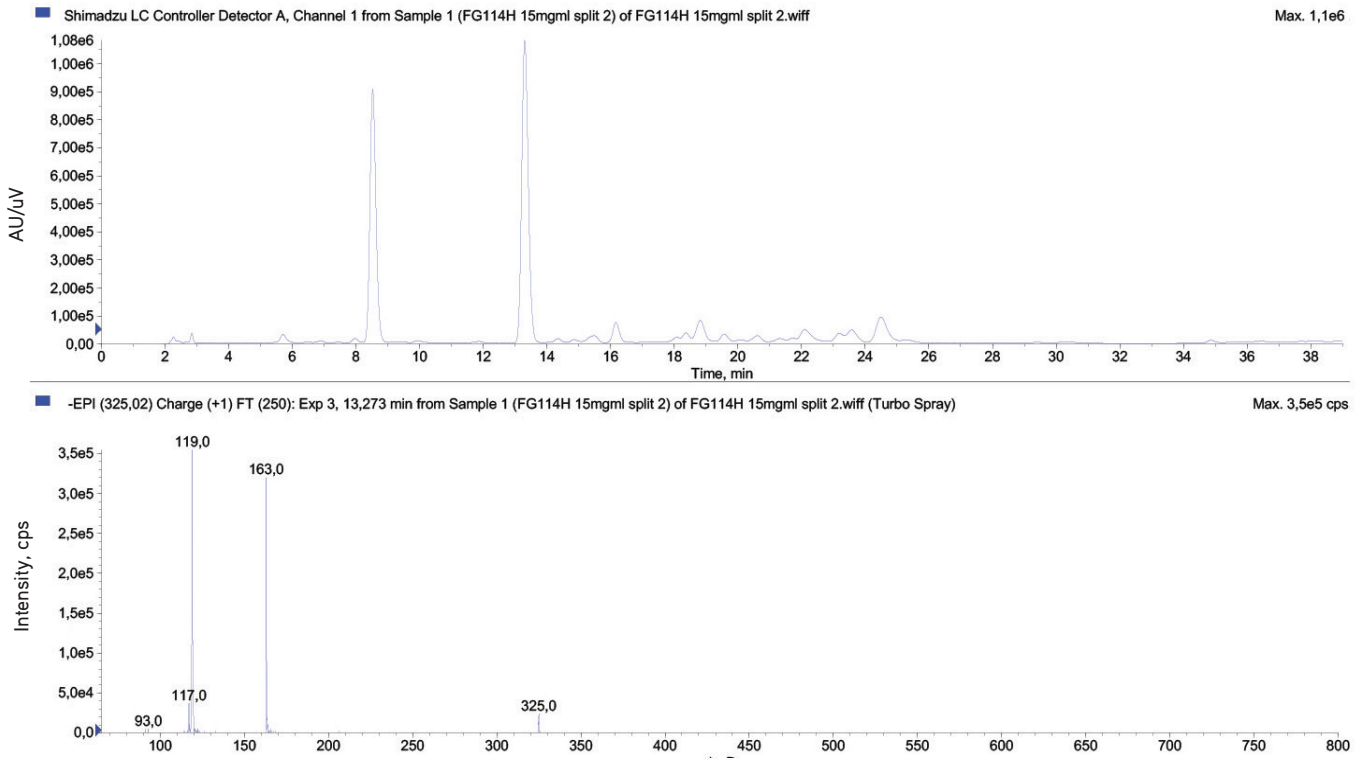

Figure 5. LC-MS/MS sprectrum of in coumaroyl glucoside isomer (4) in *A. salicifolia* extract
LC-MS/MS: Liquid chromatography with tandem mass spectrometry

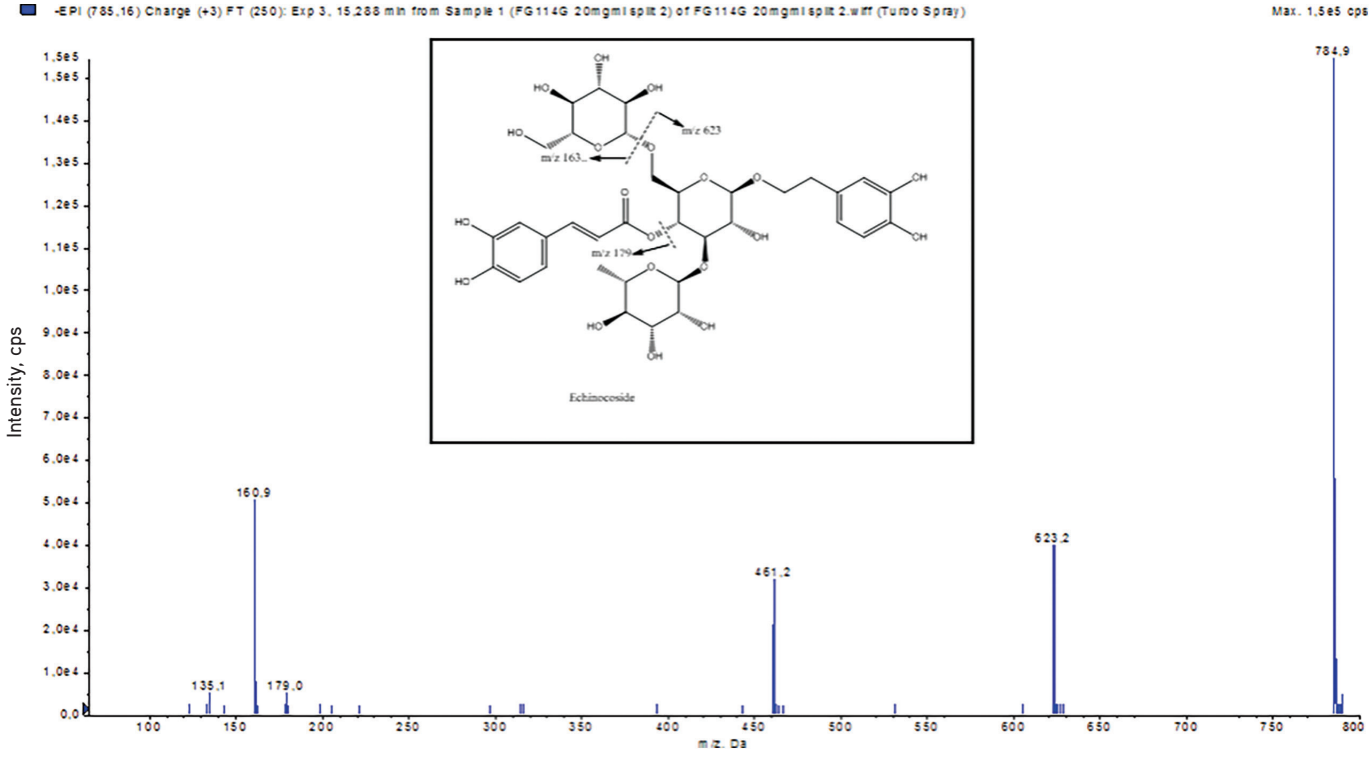

Figure 6. LC-MS/MS sprectrum of echinacoside (7) in *A. reptans* extract
LC-MS/MS: Liquid chromatography with tandem mass spectrometry

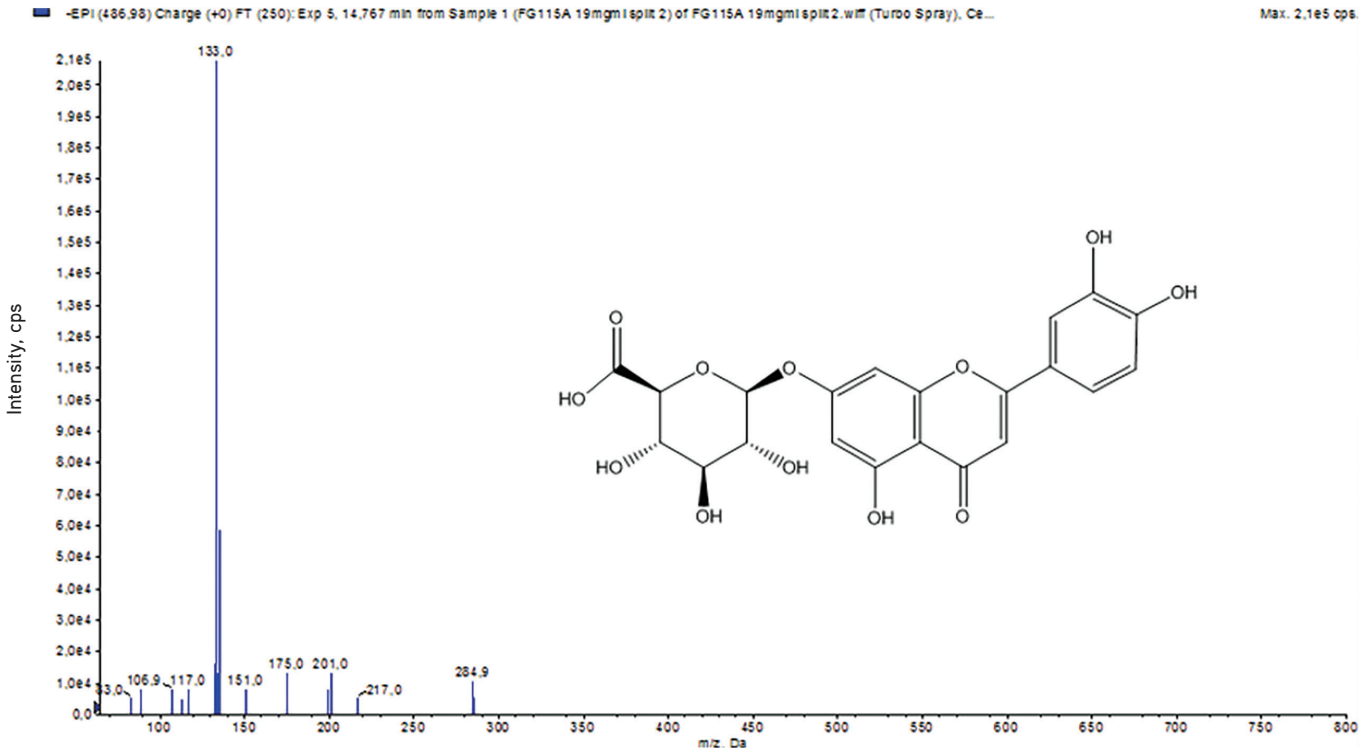

Figure 7. LC-MS/MS sprectrum of luteoline derivative (5) in *A. reptans* and *A. genevensis* extracts
LC-MS/MS: Liquid chromatography with tandem mass spectrometry

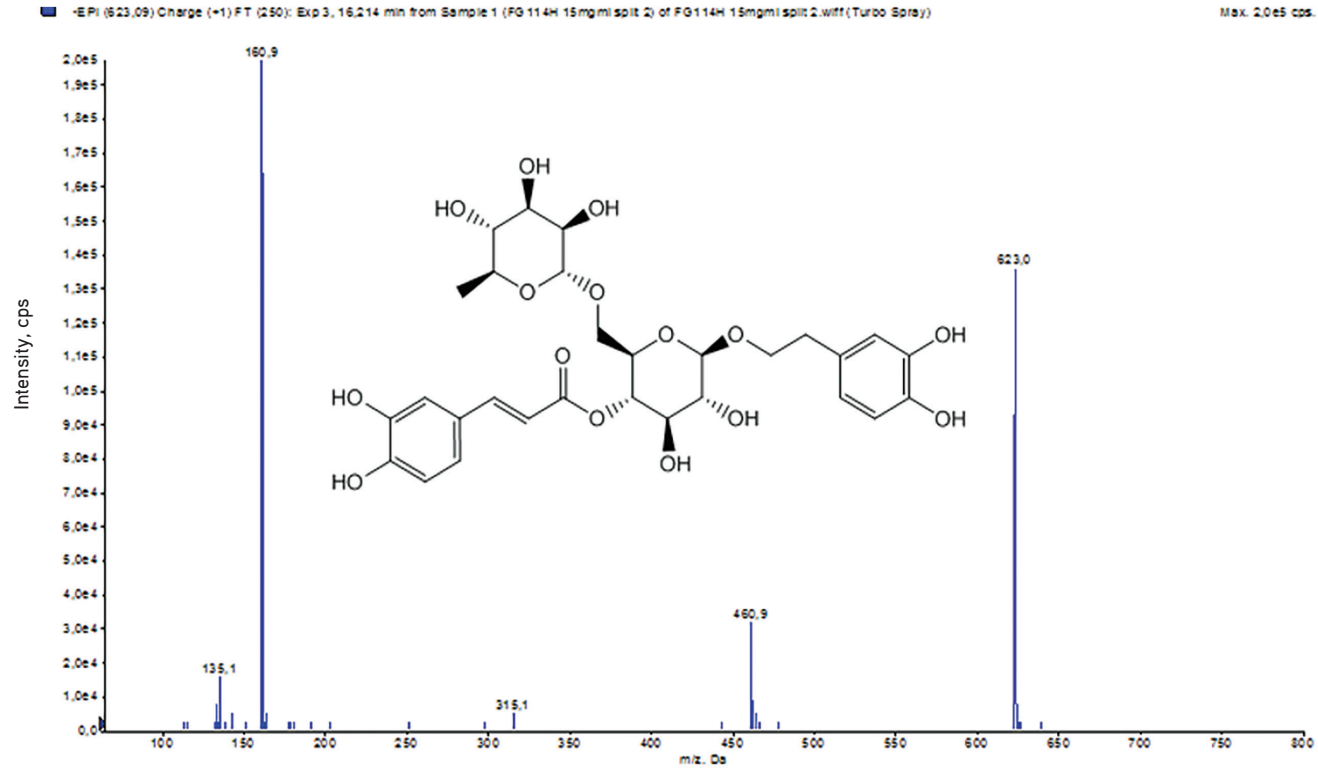

Figure 8. LC-MS/MS sprectrum of forsytoside A (9) in *A. reptans* and *A. genevensis* extracts
LC-MS/MS: Liquid chromatography with tandem mass spectrometry

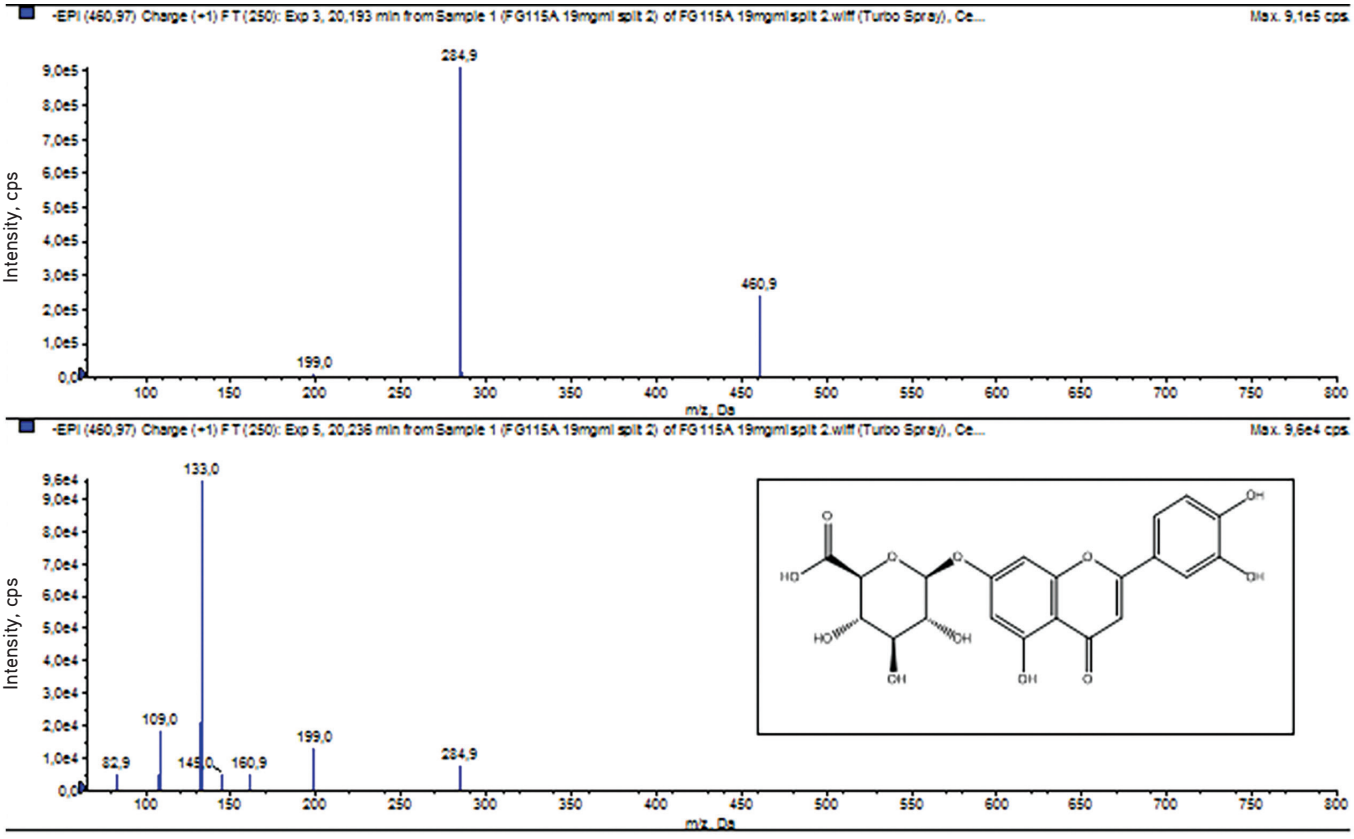

Figure 9. LC-MS/MS sprectrum of luteoline glucuronide (15) in *A. reptans* and *A. genevensis* extracts
LC-MS/MS: Liquid chromatography with tandem mass spectrometry

Table 4. Total phenolic contents and antioxidant activities of the extracts

Extract	Total phenolic content (mg GAE/g extract)*	DPPH activity (IC_{50}, mg/mL)	TEAC (mM)
A. reptans	42.0±0.01	0.30±0.01	1.4±0.02
A. salicifolia	38.0±0.00	0.28±0.01	1.5±0.02
A. genevensis	30.0±0.01	0.44±0.02	1.2±0.04
BHT	-	0.06±0.00	1.9±0.03

*Total phenolic content was expressed as GAE, each value in the table is represented as the mean ± SD (n=3). TEAC: Trolox equivalent antioxidant activity, GAE: Gallic acid equivalent, BHT: Butylated hydroxy toluene, DPPH: 1,1-diphenyl-2-picrylhydrazyl, SD: Standard deviation, IC: Inhibition concentration

There have been no reports on the antioxidant activity performed by a TEAC assay. Antioxidant activity was performed for the first time in this study for *A. reptans* L., *A. salicifolia* (L.) Schreber, and *A. genevensis* L. species found in Turkey.

Antimicrobial activity

The seven different strains tested in this study are presented in Table 5. *Ajuga* L. extracts showed antimicrobial effect against all microorganisms tested and were more effective against yeasts than bacteria [minimum inhibitory concentration (MIC): 156.25 µg/mL]. The MIC was 312.5 µg/mL for *E. coli* NRRL B-3008, *S. areus* ATCC 6538, *S. thyphimurium* ATCC 13311, and *B. cereus* NRRL B-3711 for methanol *Ajuga* extracts. As a result, the antimicrobial activity was observed in *Ajuga* extracts, especially against *Candida* strains.

Data from previous studies on the antimicrobial activity of *A. reptans*, *A. genevensis,* and *A. salicifolia* are listed in Table 2. To the best of our knowledge, this is the first report on the antimicrobial evaluation for methanol extract of *A. salicifolia,* which was more effective against yeast than bacteria.

CONCLUSION

We disclose the phytochemical profiles of *A. reptans*, *A. salicifolia,* and *A. genevensis* collected from Turkey.

Table 5. Minimum inhibitory concentrations (µg/mL)

Microorganisms	Extracts			Standard antimicrobials			
	A. genevensis	*A. reptans*	*A. salicifolia*	KT	OXC	AMP	TCY
Escherichia coli NRRL B-3008	312.5	312.5	312.5	-	-	4	16
Staphylococcus aureus ATCC 6538	312.5	312.5	312.5	-	-	2	8
Salmonella typhimurium ATCC 13311	312.5	312.5	312.5	-	-	2	8
Bacillus cereus NRRL B-3711	312.5	312.5	312.5	-	-	0.5	4
Candida albicans ATCC 90028	156.25	156.25	156.25	4	1	-	-
Candida tropicalis ATCC 1369	156.25	156.25	156.25	2	0.5	-	-
Candida parapsilosis ATCC 22019	156.25	156.25	156.25	2	2	-	-

KT: Ketoconazole, OXC: Oxiconazole, AMP: Ampicillin, TCY: Tetracycline, (-): Not tested

The extracts were found to contain valuable metabolites; phenolics acids, coumaroyl glucoside, flavonoids, and phenylethanoid glycosides. The phytochemicals could be employed as potential chemotaxonomic markers because different phytochemicals were observed between the three *Ajuga* species.

The scope of this study included the biological potential of methanol extracts of *A. reptans*, *A. salicifolia,* and *A. genevensis* evaluated for the first time against some pathogenic strains.

Ajuga species may be considered a valuable natural source against *Candida* infections and candidal resistance. However, further *in vitro* and *in vivo* experiments using different alternative *Candida* and fungal species are required to validate these screening results.

ACKNOWLEDGMENTS

This work was supported by the Anadolu University Research Funding (project number: BAP: 080307).

*This work is dedicated to late Hulusi Malyer Prof. MD. for his outstanding contributions to pharmaceutical botany.

Conflict of interest: No conflict of interest was declared by the authors. The authors are solely responsible for the content and writing of this paper.

REFERENCES

1. The Plant List, 2013 Version 1.1. Last Accessed Date: 07.11.2020. Available from: http://www.theplantlist.org/
2. Köse Ajuga YB. In: Güner A, Aslan S, Ekim T, Vural M, Babaç MT, (eds). Türkiye Bitkileri Listesi (Damarlı Bitkiler). İstanbul: Flora Araştırmaları Derneği ve Nezahat Gökyiğit Botanik Bahçesi Yayını; 2012.
3. Baytop T. Türkiye'de Bitkiler ile Tedavi: Geçmişte ve Bugün. Nobel Tıp Kitabevleri: Ankara; 1999.
4. Njoroge GN, Bussmann RW. Diversity and utilization of antimalarial ethnophytotherapeutic remedies among the Kikuyus (Central Kenya). J Ethnobiol Ethnomed. 2006;2:8.
5. Göger F, Köse YB, Göger G, Demirci F. Phytochemical characterization of phenolics by LC-MS/MS and biological evaluation of *Ajuga* orientalis from Turkey. Bangladesh J Pharmacol. 2015;10:639-644.
6. Toiu A, Mocan A, Vlase L, Parvu AE, Vodnar DC, Gheldiu AM, Oniga I. Comparative phytochemical profile, antioxidant, antimicrobial and *in vivo* anti-inflammatory activity of different extracts of traditionally used Romanian *Ajuga genevensis* L. and *A. reptans* L. (Lamiaceae). Molecules. 2019;24:1597.
7. Matu EN, Van Staden J. Antibacterial and anti-inflammatory activities of some plants used for medicinal purposes in Kenya. J Ethnopharmacol. 2003;87:35-41.
8. Riaz N, Nawaz SA, Mukhtar N, Malik A, Afza N, Ali S, Choudhary MI. Isolation and enzyme-inhibition studies of the chemical constituents from *Ajuga bracteosa*. Chem Biodivers. 2007;4:72-83.
9. Debell A, Makonnen E, Zerihun L, Abebe D, Teka F. *In-vivo* antipyretic studies of the aqueous and ethanol extracts of the leaves of *Ajuga remota* and *Lippia adoensis*. Ethiop Med J. 2005;43:111-118.
10. Mamadalieva NZ, El-Readi MZ, Ovidi E, Ashour ML, Hamoud R, Sagdullaev SS, Wink M. Antiproliferative, antimicrobial and antioxidant activities of the chemical constituents of *Ajuga turkestanica*. Phytopharmacology. 2013;4:1-18.
11. Luan F, Han K, Li M, Zhang T, Liu D, Yu L, Lv H. Ethnomedicinal uses, phytochemistry, pharmacology, and toxicology of species from the genus *Ajuga* L.: a systematic review. Am J Chin Med. 2019;47:959-1003.
12. Akbay P, Gertsch J, Çalıs I, Heilmann J, Zerbe O, Sticher O. Novel antileukemic sterol glycosides from *Ajuga salicifolia*. Helv Chim Acta. 2002;85:1930-1942.
13. Akbay P, Çalış I, Heilmann J, Sticher O. Ionone, iridoid and phenylethanoid glycosides from *Ajuga salicifolia*. Z. Naturforsch C. 2003;58:177-180.
14. Vogl S, Picker P, Mihaly-Bison J, Fakhrudin N, Atanasov AG, Heiss EH, Kopp B. Ethnopharmacological *in vitro* studies on Austria's folk medicine-an unexplored lore *in vitro* anti-inflammatory activities of 71 Austrian traditional herbal drugs. J Ethnopharmacol. 2013;149:750-771.
15. Israili ZH, Lyoussi B. Ethnopharmacology of the plants of genus Ajuga. Pak J Pharm Sci. 2009;22:4.
16. Gonzalez-Tejero MR, Casares-Porcel M, Sánchez-Rojas CP, Ramiro-Gutiérrez JM, Molero-Mesa J, Pieroni A, ElJohrig S. Medicinal plants in the Mediterranean area: synthesis of the results of the project Rubia. J Ethnopharmacol. 2008;116:341-357.

17. Ghita G, Cioanca O, Gille E, Necula R, Zamfirache MM, Stanescu U. Contributions to the phytochemical study of some samples of *Ajuga reptans* L. and *Ajuga genevensis* L. Med Sci. 2011;4:7.

18. Malakov PY, Papanov GY, María C, Rodríguez B. Neo-clerodane diterpenoids from *Ajuga genevensis*. Phytochemistry. 1991;30:4083-4085.

19. Shoji N, Umeyama A, Sunahara N, Arihara S. Ajureptoside, a novel C9 iridoid glucoside from *Ajuga reptans*. J Nat Prod. 1992;55:1004-1006.

20. Bozov PI, Papanov GY, Malakov PY, María C, Rodriguez B. A clerodane diterpene from *Ajuga salicifolia*. Phytochemistry. 1993;34:1173-1175.

21. Carbonell P, Coll J. Ajugatansins, neo-clerodane diterpenes from *Ajuga reptans*. Phytochem Anal. 2001;12:73-78.

22. Akbay P, Çalıs I, Heilmann J, Sticher O. New stigmastane sterols from *Ajuga salicifolia*. J Nat Prod. 2003;66:461-465.

23. Ramazanov NS. Phytoecdysteroids and other biologically active compounds from plants of the genus *Ajuga*. Chem Nat Compd. 2005;41:4.

24. Ono M, Furusawa C, Ozono T, Oda K, Yasuda S, Okawa M, Nohara T. Four new iridoid glucosides from *Ajuga reptans*. Chem Pharm Bull. 2011;59:1065-1068.

25. Callebaut A, Hendrickx G, Voets AM, Motte JC. Anthocyanins in cell cultures of *Ajuga reptans*. Phytochemistry. 1990;29:2153-2158.

26. Terahara N, Callebaut A, Ohba R, Nagata T, Ohnishi-Kameyama M, Suzuki M. Triacylated anthocyanins from *Ajuga reptans* flowers and cell cultures. Phytochemistry. 1996;42:199-203.

27. Terahara N, Callebaut A, Ohba R, Nagata T, Ohnishi-Kameyama M, Suzuki M. Acylated anthocyanidin 3-sophoroside-5-glucosides from *Ajuga reptans* flowers and the corresponding cell cultures. Phytochemistry. 2001;58:493-500.

28. Toiu A, Vlase L, Gheldiu AM, Vodnar D, Oniga I. Evaluation of the antioxidant and antibacterial potential of bioactive compounds from *Ajuga reptans* extracts. Farmacia. 2017;65:351-355.

29. Toiu A, Vlase L, Arsene AL, Vodnar DC, Oniga I. LC/UV/MS profile of polyphenols, antioxidant and antimicrobial effects of *Ajuga genevensis* L. extracts. Farmacia. 2016;64:53-57.

30. Singleton VL, Orthofer R, Lamuela-Raventos RM. Analysis of total phenols and other oxidation substrates and antioxidants by means of folin-ciocalteu reagent. Methods Enzymol. 1999;299:152-178.

31. Kumarasamy Y, Byres M, Cox PJ, Jaspars M, Nahar L, Sarker SD. Screening seeds of some Scottish plants for free radical scavenging activity. Phytother Res. 2007;2:615-621.

32. Papandreou MA, Kanakis CD, Polissiou MG, Efthimiopoulos S, Cordopatis P, Margarity M, Lamari FN. Inhibitory activity on amyloid-β aggregation and antioxidant properties of Crocus sativus stigmas extract and its crocin constituents. J Agric Food Chem. 2006;54:8762-8768.

33. Clinical and Laboratory Standards Institute (CLSI). Reference method for broth dilution antifungal susceptibility testing of yeast. Approved standard CLSI 27-A3. (3rd ed). Pennsylvania, USA: Clinical and Laboratory Standards Institute; 2008.

34. Clinical and Laboratory Standarts Institute (CLSI). Methods for dilution antimicrobial susceptibility tests for bacteria that grow aerobically CLSI M7-A7. Pennsylvania, USA: Clinical and Laboratory Standards Institute; 2006.

35. Göger G, Demirci B, Ilgın S, Demirci F. Antimicrobial and toxicity profiles evaluation of the chamomile (*Matricaria recutita* L.) essential oil combination with standard antimicrobial agents. Ind Crops Prod. 2018;120:279-285.

36. Calcagno MP, Camps F, Coll J, Mele, E, Sanchez-Baeza, F. New phytoecdysteroids from roots of Ajuga reptans varieties. Tetrahedron. 1996;52:10137-10146.

37. Zabka M, Pavela R, Gabrielova-Slezakova L. Promising antifungal effect of some Euro-Asiatic plants against dangerous pathogenic and toxinogenic fungi. J Sci Food Agric. 2011;91:492-497.

38. Butenko LE, Kuleshova SA, Postnikova NV, Lovyagina SA. The *Ajuga genevensis* L. chemical composition and the biological activity study. Eur J Nat Hist. 2011;5:31-33.

39. Abdullah E, Raus RA, Jamal P. Extraction and evaluation of antibacterial activity from selected flowering plants. Am J *Med*. 2012;3:27-32.

40. Yildirim AB, Karakas FP, Turker AU. *In vitro* antibacterial and antitumor activities of some medicinal plant extracts, growing in Turkey. Asian Pac J Trop Med. 2013;6:616-624.

41. Gavrilova V, Kajdzanoska M, Gjamovski V, Stefova M. Separation, Characterization and quantification of phenolic compounds in blueberries and red and black currants by HPLC- DAD- ESI-MS^n. J Agric Food Chem. 2011;59:4009-4018.

42. Shimomura H, Sashida Y, Ogawa K. Iridoid glucosides and phenylpropanoid glycosides in *Ajuga* species of Japan. Phytochemistry. 1987;26:1981-1983.

43. Cvetkovikj I, Stefkov G, Acevska J, Stanoeva JP, Karapandzova M, Stefova M, Kulevanova S. Polyphenolic characterization and chromatographic methods for fast assessment of culinary *Salvia* species from South East Europe. J Chromatogr A. 2013;1282:38-45.

44. Ferreres F, Silva BM, Andrade PB, Seabra RM, Ferreira MA. Approach to the study of C-glycosyl flavones by ion trap HPLC-PAD-ESI/MS/MS: application to seeds of quince (*Cydonia oblonga*). Phytochem Anal. 2003;14:352-359.

45. Mitreski I, Stanoeva JP, Stefova M, Stefkov G, Kulevanova S. Polyphenols in representative teucrium species in the flora of R. Macedonia: LC/DAD/ESI-MS n profile and content. Nat Prod Commun. 2014;9:175-180.

46. Petreska J, Stefova M, Ferreres F, Moreno DA, Tomás-Barberán FA, Stefkov G, Gil-Izquierdo A. Potential bioactive phenolics of Macedonian Sideritis species used for medicinal "Mountain Tea". Food Chem. 2011;125:13-20.

47. Tao Y, Chen Z, Zhang Y, Wang Y, Cheng Y. Immobilized magnetic beads based multi-target affinity selection coupled with high performance liquid chromatography-mass spectrometry for screening anti-diabetic compounds from a Chinese medicine "Tang-Zhi-Qing". J Pharm Biomed. 2013;7:190-201.

Turk J Pharm Sci 2021;18(5):628-636
DOI: 10.4274/tjps.galenos.2021.93457

ORIGINAL ARTICLE

Investigation of the Rheological Properties of Ointment Bases as a Justification of the Ointment Composition for Herpes Treatment

Herpes Tedavisi İçin Merhem Bileşiminin Doğrulanması Amacıyla Merhem Bazlarının Reolojik Özelliklerinin Araştırılması

Tanya IVKO[1]*, Vita HRYTSENKO[2], Lydmila KIENKO[2], Larisa BOBRYTSKA[2], Halyna KUKHTENKO[2], Tamara GERMANYUK[1]

[1]National Pirogov Memorial Medical University, Department of Pharmacy, Vinnytsya, Ukraine
[2]National University of Pharmacy, Department of Industrial Technology of Drugs, Kharkiv, Ukraine

ABSTRACT

Objectives: Combinatorial drugs are among the leading pharmacotherapeutic agents, including those used for the treatment of herpetic infections, which require complex treatment. We have developed a soft dosage form of ointment, which includes acyclovir and miramistin, which have antimicrobial, anti-inflammatory, and local immunoadjuvant activity. The study aimed to investigate the rheological properties of ointment bases in order to substantiate the composition of a soft dosage form with antiviral effect using the active ingredients miramistin and acyclovir.

Materials and Methods: The object of the study was to determine the heterogeneous and homogeneous composition models of the bases made using a wide range of excipients. Structural and mechanical studies were performed using the "Rheolab QC" rotary viscometer by Anton Paar (Austria) with coaxial cylinders CC27/S-SN29766. The rheological parameters were investigated at a temperature of 25°C±0.5°C. The samples were thermostated using a thermostat MLM U15c. The batch of sample weighing about 15.0±0.5 g was placed in the container of an external stationary cylinder. The required temperature of the experiment was set and the thermostating time was 20 min. The device is equipped with RheoPlus 32 V3.62 software.

Results: The rheological behavior of the model compositions was analyzed in terms of indicators, such as yield strength, hysteresis square, coefficients of dynamic flow, and mechanical stability. It was found that all samples have a non-Newtonian pseudoplastic type of flow. The model of spreading optimums was used to evaluate consumer properties. According to the rheological parameters, it is advisable to use the sample based on paraffin and vaseline oil for further research.

Conclusion: The findings from this study will be relevant in the development of the soft dosage form for the treatment of herpes viral diseases.

Key words: Ointment bases, soft dosage forms, rheology, structural and mechanical properties

ÖZ

Amaç: Kombinatoryal (birleşimsel) ilaçlar, karmaşık tedavi gerektiren herpetik enfeksiyonların tedavisinde kullanılanlar da dahil olmak üzere önde gelen farmakoterapötik ajanlar arasındadır. Antimikrobiyal, anti-inflamatuvar ve lokal immünoadjuvan aktiviteye sahip asiklovir ve miramistin içeren merhemin yumuşak bir dozaj formunu geliştirdik. Çalışma, miramistin ve asiklovir aktif bileşenleri kullanılarak antiviral etkiye sahip yumuşak bir dozaj formunun bileşimini doğrulamak için merhem bazlarının reolojik özelliklerini araştırmayı amaçladı.

Gereç ve Yöntemler: Çalışmanın amacı, çok çeşitli yardımcı maddeler kullanılarak yapılan merhem bazlarının heterojen ve homojen bileşim modellerini belirlemektir. Yapısal ve mekanik çalışmalar, koaksiyel silindirler CC27/S-SN29766 ile Anton Paar (Avusturya) tarafından üretilen "Rheolab QC" döner viskozimetre kullanılarak gerçekleştirilmiştir. Reolojik parametreler 25°C±0,5°C sıcaklıkta belirlenmiştir. Numunelerde, bir termostat MLM U15c kullanılarak sıcaklık kontrolü sağlandı. Yaklaşık 15,0±0,5 g ağırlığındaki numune yığını, harici bir sabit silindirin kabına yerleştirildi. Deney için gerekli sıcaklık ayarlandı ve termostatlama süresi 20 dakikaydı. Cihaz RheoPlus 32 V3.62 yazılımı ile donatılmıştır.

Bulgular: Model kompozisyonlarının reolojik davranışı, akma dayanımı, histerezis karesi, dinamik akış katsayıları ve mekanik kararlılık gibi göstergeler açısından analiz edildi. Tüm örneklerin Newtonyen olmayan bir psödoplastik akış tipine sahip olduğu bulundu. Tüketici özelliklerini değerlendirmek

*Correspondence: ivkot1981@gmail.com, Phone: +380982640560, ORCID-ID: orcid.org/0000-0003-2873-1473
Received: 03.07.2020, Accepted: 24.02.2021

için yayılma optimumları modeli kullanıldı. Reolojik parametrelere göre, daha fazla araştırma için parafin ve vazelin bazlı numunenin kullanılması tavsiye edilir.

Sonuç: Bu çalışmanın bulguları, herpes viral hastalıklarının tedavisi için yumuşak dozaj formunun geliştirilmesinde yararlı olacaktır.

Anahtar kelimeler: Merhem bazları, yumuşak dozaj formları, reoloji, yapısal ve mekanik özellikler

INTRODUCTION

Soft dosage forms are dispersed systems with a viscous-plastic dispersed medium characterized by a non-Newtonian type of flow.[1] Their viscosity at a given temperature and shear stress varies non-linearly, depending on the shear rate.[2,3]

When developing the composition of soft dosage drugs, much attention is paid to the study of their rheological properties and the structural and mechanical parameters determine the stability of viscose-dispersed systems.[4] A comprehensive study of rheological characteristics is of both theoretical and practical interest, since they can be an effective and objective criterion for quality control at the stage of creation, production, storage, and use of drugs.[5,6] The rheological properties affect the release of medicinal substances, therapeutic efficacy of drugs, consumer requirements (the process of extrusion from tubes, convenience, and ease of lubrication on the skin), and production characteristics (the process of dispersion and packaging).[7-9]

Soft dosage forms are complex systems that contain a base and active ingredients.[10] Properly selected base provides the necessary speed and completeness of the medicinal substances released, comfort in usage, and stability during storage of drugs.[11,12] Therefore, the study of the structural and mechanical properties of ointment bases is an important step in the development of soft dosage forms.[13-15]

Today, combinatorial drugs are among the leading pharmacotherapeutic agents, including those used for the treatment of herpetic infections, which require complex treatment. Choice of drug combination allows the expansion of drug action and the complex influence on diseases, enhances the activity of every ingredient, improves tolerability, and reduces side effects.[16-19]

Herpetic infections occur in the form of mono-, mixed and coinfections and can be asymptomatic (latent), in an acute, chronic persistent form with a recurrent course, as well as in the form of an atypical chronic active infection.[20] Currently, the combined drugs are leading among pharmacotherapeutic agents, including the treatment of herpetic infections, which require complex treatment. Drug combination choice allows to expand the range of action of the drug and the complex influence on the disease, activity of the every ingredient, as well to improve tolerability.[21-26] We have developed a soft dosage form in the form of an ointment, which includes acyclovir [TEVA Pharmaceutical and Chemical (Hang-zhou) Co., Ltd, China] and miramistin (Infamed LLC, Russia), which has antimicrobial, anti-inflammatory and local immunoadjuvant action.

MATERIALS AND METHODS

The objects of the study were ointment bases (Table 1). The ointment bases, which have been developed using excipients that are widely used in soft dosage technology, were obtained were obtained at National University of Pharmacy, Department of Industrial Technology of Drugs. The excipients used includes propylene glycol (BASF SE, Germany),[27] proxanol-268 (NPF "Perftoran" OJSC, Russia), polyethylene oxide-400 (Dow Chemical, Germany),[28] vaseline oil (Borma wachs, Italy),[27] paraffin (LLC "Novokhim," Ukraine), cetostearyl alcohol (Guangzhou Yiming Chemical Material Co., Ltd., China),[29] twin-80 (MN & Gustav Heess Ukraine, Ukraine), carbopol 934 (Kylin Chemicals Co., Ltd., China), triethanolamine (LLC "Novokhim", Ukraine),[27] corn oil (Nordolio, Italy), eucerit (LLC NPP "Electrogazokhim" Ukraine), aristoflex AVC (Clariant, Switzerland), vaseline (Balea, Germany),[27] emulsifier "Solid-2" (LLC NPP "Electrogazokhim", Ukraine), isopropylmyristate[30] (MN & Gustav Heess Ukraine, Ukraine),[23] and hydroxyethylcellulose (LLC "Linkchem", Ukraine). The rheological (structural-mechanical) properties of the bases were determined using a "Rheolab QC" rotary viscometer (Anton Paar, Austria) with coaxial cylinders CC27/S-SN29766. The rheological parameters were investigated at a temperature of 25°C±0.5°C. The samples were thermostated using a thermostat MLM U15c.

The batch of sample weighing about 15.0±0.5 g was placed in the container of an external stationary cylinder; the required temperature of the experiment was set and the time of thermostating was 20 min. The device is equipped with RheoPlus 32 V3.62 software. Measurements of the rheological flow curve were performed in 3 stages:

1. Linear increase at the rate of shear velocity from 0.1 s^{-1} to 350 s^{-1} with 105 measurement points and duration of the measurement point is 1 s;

2. Constant shift at a speed of 350 s^{-1} for 1 s of duration;

3. Linear decrease at the rate of shear velocity from 350 s^{-1} to 0.1 s^{-1} with 105 measurement points and duration of the measurement point is 1 s.

The range of the shear rate gradient 0.1-350 s^{-1} corresponds to the range speed of 0.075-270 revolutions per minute.

The device allows the measurement of tangential bias voltage (t) in the range of 0.5-3.0 10^4 Pa, gradient of the shear rate (γ) from 0.1 to 4000 s^{-1}, and viscosity (h) from 1 to 10^6 Pa sec. Using RheoPlus 32 V3.62 software, the hysteresis square (A, Pa/sec) was calculated. The points (yield) strength (τ_0, Pa) and viscosity at the infinite shear rate (η_∞, Pa·s) was calculated using the Casson model:[5,6]

Table 1. Composition of the ointment bases

Ingredients	Numbers of bases/contents of components, g							
	№ 1	№ 2	№ 3	№ 4	№ 5	№ 6	№ 7	№ 8
Propylene glycol	24.0	-	10.0	-	-	10.0	-	-
Proxanol-268	54.0	-	-	-	-	-	-	-
Polyethylene oxide-400	22.0	-	10.0	-	12.0	10.0	-	-
Vaseline oil	-	85.0	-	-	25.0	-	5.2	-
Paraffin	-	15.0	-	-	-	-	-	-
Cetostearyl alcohol	-	-	-	-	25.0	-	-	-
Twin-80	-	-	-	-	2.0	-	-	-
Carbopol 934	-	-	1.5	-	-	-	-	-
Triethanolamine	-	-	1.5	-	-	-	-	-
Corn oil	-	-	10.0	20.0	-	-	-	-
Emulsifier № 1	-	-	6.0	-	-	-	-	-
Aristoflex AVC	-	-	-	2.0	-	-	-	-
Vaseline	-	-	-	-	-	55.0	93.6	-
Emulsifier T-2	-	-	-	-	-	10.0	-	-
Isopropylmyristate	-	-	-	-	-	-	1.2	-
Hydroxyethylcellulose	-	-	-	-	-	-	-	2.0
Purified water to	-	-	100.0	100.0	100.0	100.0	-	100.0

$$\tau^{\frac{1}{2}} = \tau_0 + (\eta \cdot \dot{\gamma})^{\frac{1}{2}}$$

where τ_0 - yield strength, Pa;

η - dynamic viscosity, Pa·s;

γ - shear rate, s^{-1}

The Casson model describes an imperfect plastic type of flow, in which there is a disproportionate relationship between shear rate and stress and most closely corresponds to the nature of the flow of the investigated ointment bases.

A coefficient of dynamic flow was determined at the speed rates of 3.4 and 10.2 s^{-1}, which correspond to the velocity of the palm, while soft dosage form distribution over the surface and viscosity of the system was determined at the velocity rates of 27.0 and 155 s^{-1}, which display the velocity of the processing procedure while manufacturing. Based on the results obtained, the values of coefficients of the dynamic flow of the system were calculated by the formulas:[5,6]

$$K_{d1} = \frac{\eta_{3.4} - \eta_{10.2}}{\eta_{3.4}} \cdot 100\%$$

$$K_{d2} = \frac{\eta_{27} - \eta_{155}}{\eta_{27}} \cdot 100\%$$

where K_{d1}, K_{d2} - the dynamic flow coefficients;

η - apparent viscosity at specified shear rates

For a more complete study of samples, the parameters of their mechanical stability (MS) were calculated. It is known that the optimal value of MS is 1.[15] The MS value is defined as the ratio of the strength of the structure to failure (τ_1) to the strength value after fracture (τ_2) at a shear rate of 3.4 s^{-1}, according to the formula:[5,6]

$$MS = \frac{\tau_1}{\tau_2}$$

Statistical data was not used in this research.

RESULTS AND DISCUSSION

To study the structural and mechanical properties of the experimental samples, complete rheograms of the dependence of the shear stress (t) from the shear rate gradient (γ) were constructed (Figure 1). A comprehensive assessment of the behavior of the ointment bases during the step-by-step destruction and subsequent restoration (Figure 1) also shows the dependence of viscosity from the shear rate. Sample values of the shear stress and viscosity of the model bases are given in Table 2.

The profile of rheological behavior depends on the composition of the ointment base and varies in a wide range of structural and mechanical parameters (Figure 1). All samples have a pseudoplastic type of flow and the viscosity of the samples decreases disproportionately with increasing shear rate. The samples were exposed to the flow in different ways, which is expressed in the value of the yield strength calculated by the Casson equation: 105.8 Pa, 1.3 Pa, 49.3 Pa, 12.6 Pa, 104.5 Pa, 77.2 Pa, 65.9 Pa, and 0.3 Pa for the samples № 1, № 2, № 3, № 4, № 5, № 6, № 7, and № 8, respectively (Figure 2-8).

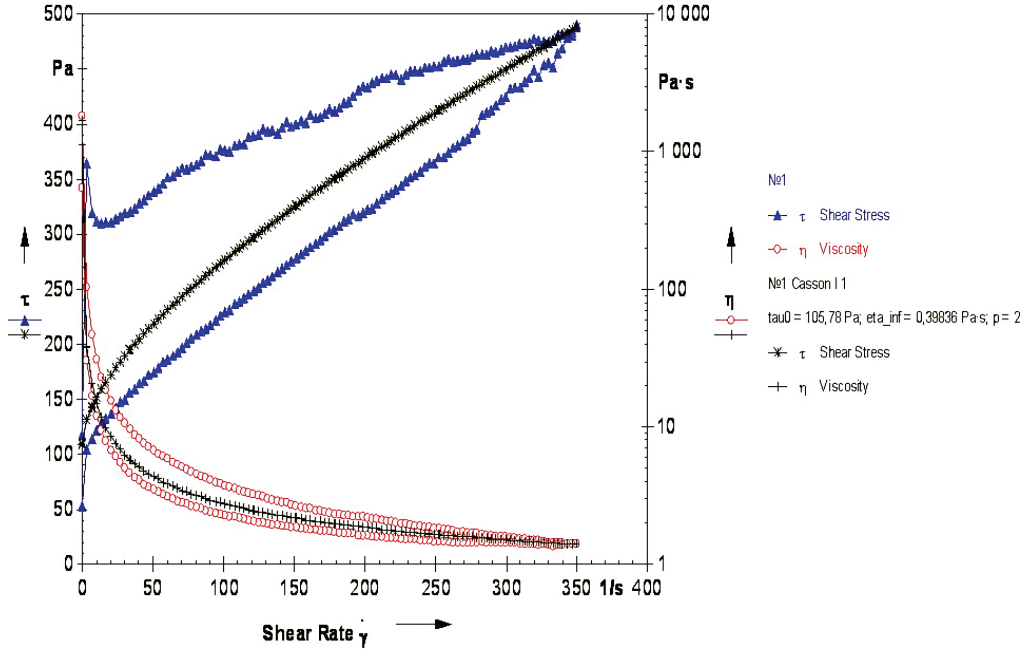

Figure 1. Profile of rheological behavior of sample № 1

Table 2. Parameters of shear stress and structural viscosity of the ointment bases at appropriate shear rate

Gradient of shear rate, (γ, s^{-1})	Shear stress with increasing (τ_1, Pa) / decreasing (τ_2, Pa) shear rate gradient (γ, s^{-1})															
	№ 1		№ 2		№ 3		№ 4		№ 5		№ 6		№ 7		№ 8	
	τ_1	τ_2	τ_1	τ_2	τ_1	τ_2	τ_1	τ_2	τ_1	τ_2	τ_1	τ_2	τ_1	τ_2	τ_1	τ_2
0.1	118	52.9	43.7	0.745	8.31	21.4	2.16	29.8	128	66.1	106	37.9	381	16.6	0.178	2.04
3.4	365	104	189	6.68	162	121	130	82.9	164	106	371	74.4	399	79	18.3	17
6.8	320	114	219	9.53	206	167	144	93	178	130	320	81.2	416	87	28.3	26.6
10.2	312	122	230	11.7	225	196	149	99.9	194	149	314	86.3	467	91.7	35.1	33.6
13.6	310	127	234	13.7	244	217	151	105	209	165	317	90.3	511	95.9	40.8	39.6
16.9	310	132	233	15.5	259	233	157	110	228	178	319	94.3	550	99.7	45.7	44.5
27.0	316	147	222	20.9	296	260	175	121	275	207	319	104	621	111	57.8	57.2
155.0	403	282	171	83.5	381	386	246	185	607	415	381	202	433	204	122	124
350.0	490	488	199	196	419	418	282	283	742	737	386	380	380	384	167	167
	Structural viscosity with increasing (η_1, Pa·s) / decreasing (τ_2, Pa) shear rate gradient (γ, s^{-1})															
	η_1	η_2	η_1	η_2	η_1	η_2	η_1	η_2	η_1	η_2	η_1	η_2	η_1	η_2	η_1	η_2
0.1	1820	546	437	7.54	4340	5870	3100	2900	859	661	1530	386	4 620	166	1.81	19.7
3.4	103	30.1	54.3	1.93	49.1	35.9	38.6	24.7	46.9	30.7	105	21.5	112	22.9	5.28	4.91
6.8	46.4	16.7	31.9	1.4	30.4	24.9	21.4	13.8	26	19	46.4	11.9	60.3	12.8	4.14	3.9
10.2	30.5	11.9	22.5	1.15	22.2	19.5	14.7	9.9	19	14.6	30.7	8.48	45.5	9	3.44	3.3
13.6	22.8	9.41	17.2	1.01	18.1	16.1	11.2	7.84	15.4	12.2	23.3	6.66	37.5	7.08	3.01	2.92
16.9	18.3	7.8	13.7	0.916	15.4	13.8	9.31	6.51	13.5	10.5	18.8	5.57	32.4	5.89	2.7	2.63
27.0	11.7	5.45	8.21	0.774	11	9.66	6.51	4.49	10.2	7.67	11.8	3.86	22.9	4.1	2.14	2.12
155.0	2.61	1.82	1.1	0.539	2.46	2.5	1.59	1.2	3.92	2.68	2.5	1.3	2.8	1.32	0.787	0.799
350.0	1.4	1.39	0.569	0.561	1.2	1.19	0.805	0.807	2.12	2.11	1.1	1.08	1.09	1.1	0.476	0.476

The yield strength is an indicator that shows the force at which the dispersed system begins to flow. In accordance with the value, it is possible to draw a conclusion about how easily the system will be squeezed out, whether the self-flow of the system will be observed, and about the adhesive properties of the drug. Thus, since the sample № 8 has low rheological parameters, the system has a pronounced ability to self-flow due to insufficient concentration of gelling agent.[4-6] The plan of the experiment envisages a stepwise increase in the rate of destruction of the dispersed system, the flow reflected in the ascending curve, and a subsequent decrease in the rate with the same step. The flow of the system is described by a descending curve.

The ascending curve is located above the descending one and this arrangement of curves is called positive thixotropy, since

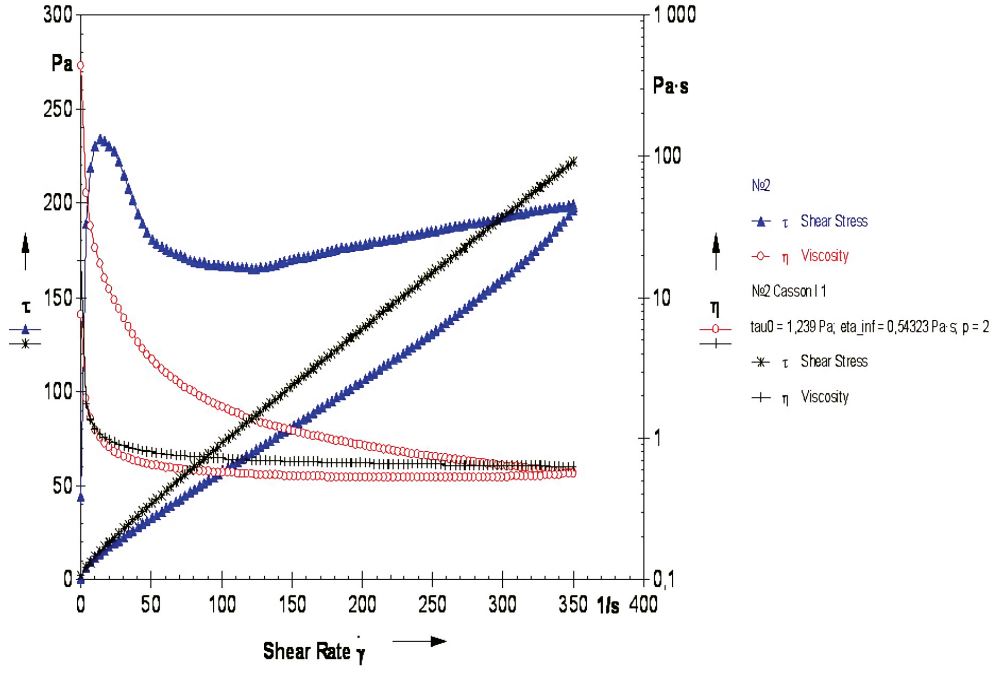

Figure 2. Profile of rheological behavior of sample № 2

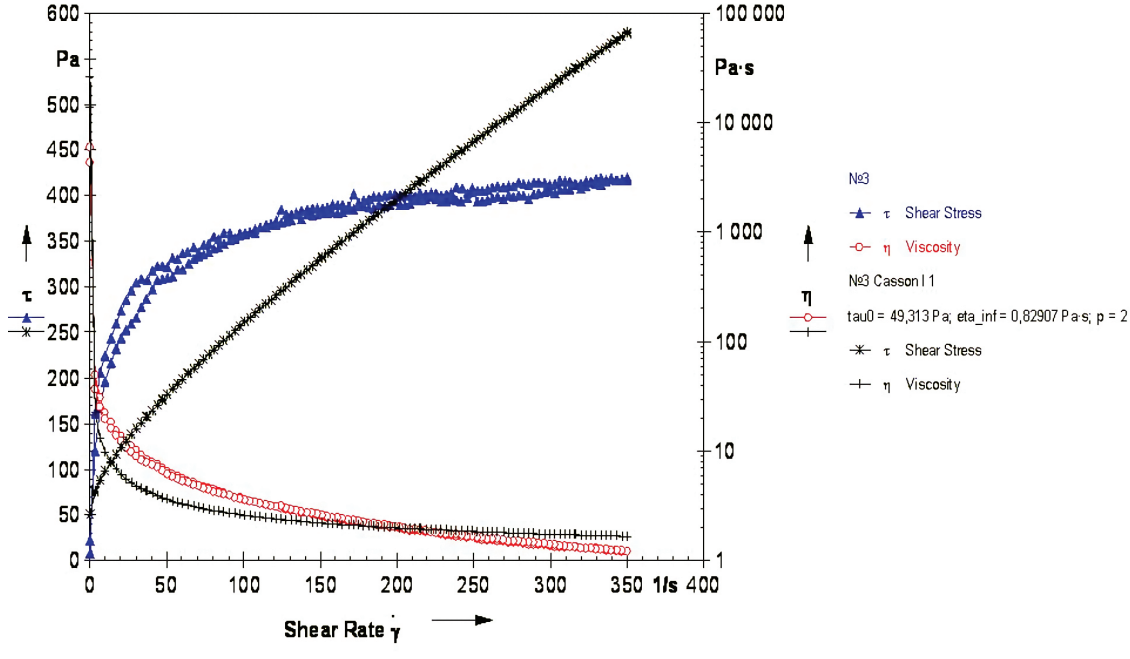

Figure 3. Profile of rheological behavior of sample № 3

there are such dispersed systems that have antitixotropic or reopective properties. In such systems, the ascending and descending curves are opposite. The investigated ointment bases were restored to varying degrees and the surface area between the ascending and descending curves indicates the thixotropy of the system or ability to recover.[11,15] On one hand, the smaller the area of the hysteresis loop, the faster the system recovers and, on the other hand, the larger the area, the easier the system is distributed on the surface and on a larger surface area. The first aspect is important in the production process and speaks of the reproducibility of the structured system after the technological process of processing, while

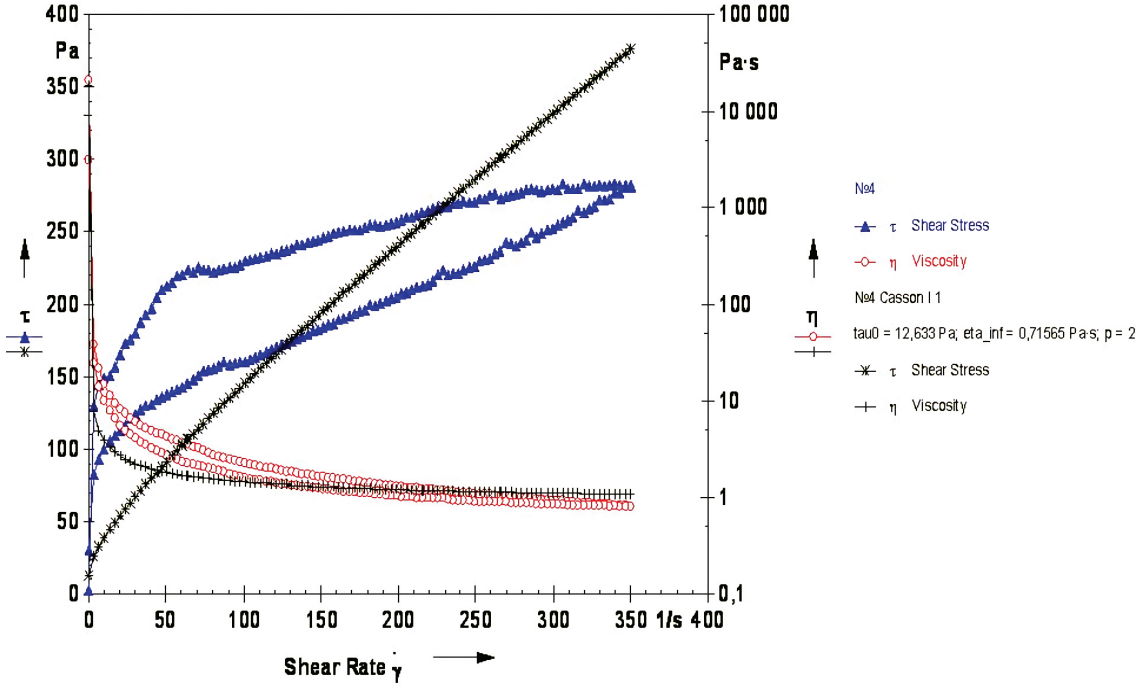

Figure 4. Profile of rheological behavior of sample № 4

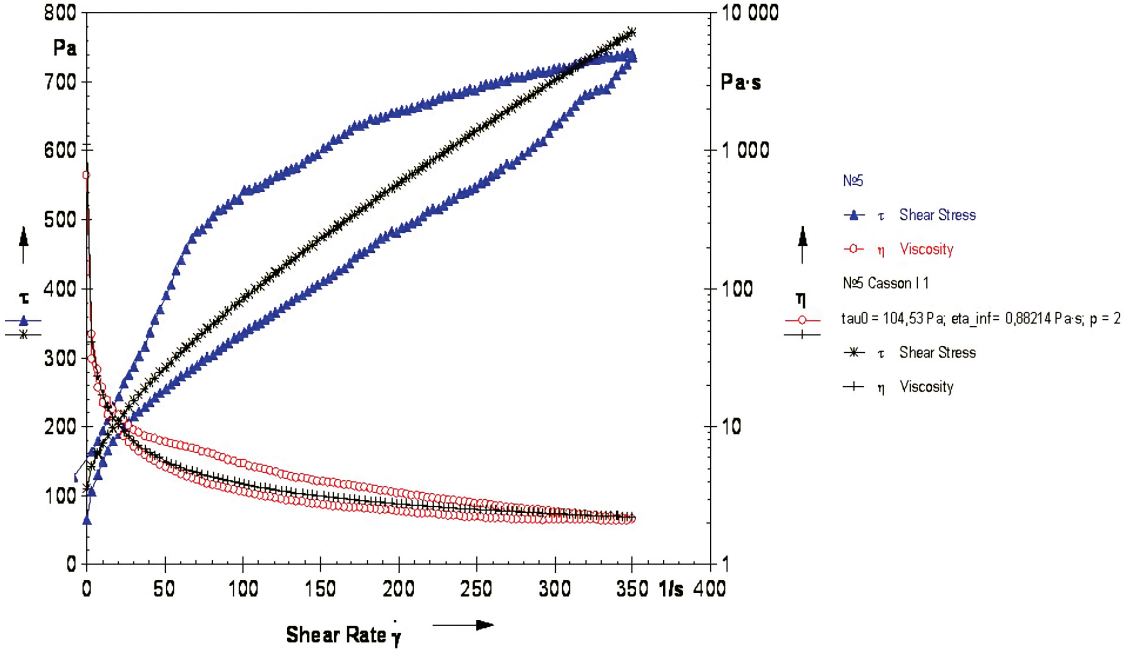

Figure 5. Profile of rheological behavior of sample № 5

the other is important as a consumer indicator of quality. The hysteresis square for base № 1, № 2, № 3, № 4, № 5, № 6, № 7, and № 8 was 38780.5 Pa/s, 30887.8 Pa/s, 40.2 Pa/s, 17242.8 Pa/s, 49174, 4 Pa/s, 49521.1 Pa/s, 82587.0 Pa/s, and 319.5 Pa/s. respectively.

During the period of destruction of structured systems by means of increasing speed of rotation of the internal cylinder, there is a rarefaction of systems, which never comes to an end because some share of communications is restored back, even at high speeds. The viscosity at the infinite shear rate calculated by the Casson model was 0.39 Pa/s, 0.54 Pa/s, 0.83 Pa/s, 0.72 Pa/s, 0.88 Pa/s, 0, 34 Pa/s, 0.44 Pa/s, and 0.65 Pa/s for sample № 1, № 2, № 3, № 4, № 5, № 6, № 7, and № 8, respectively (Table 3). According to this indicator, the most resistant to the applied

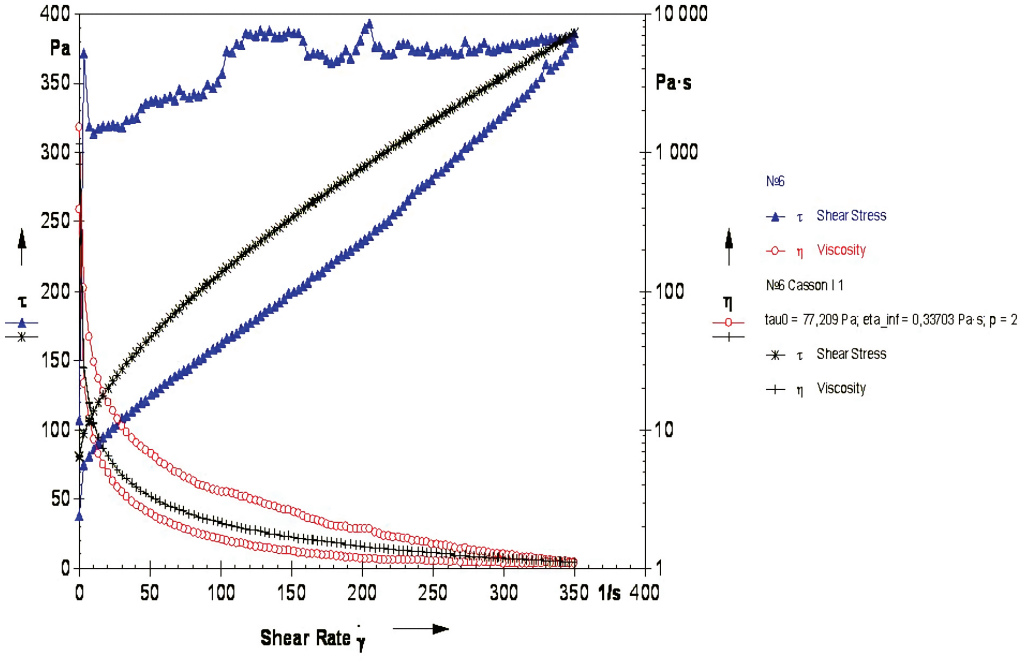

Figure 6. Profile of rheological behavior of sample № 6

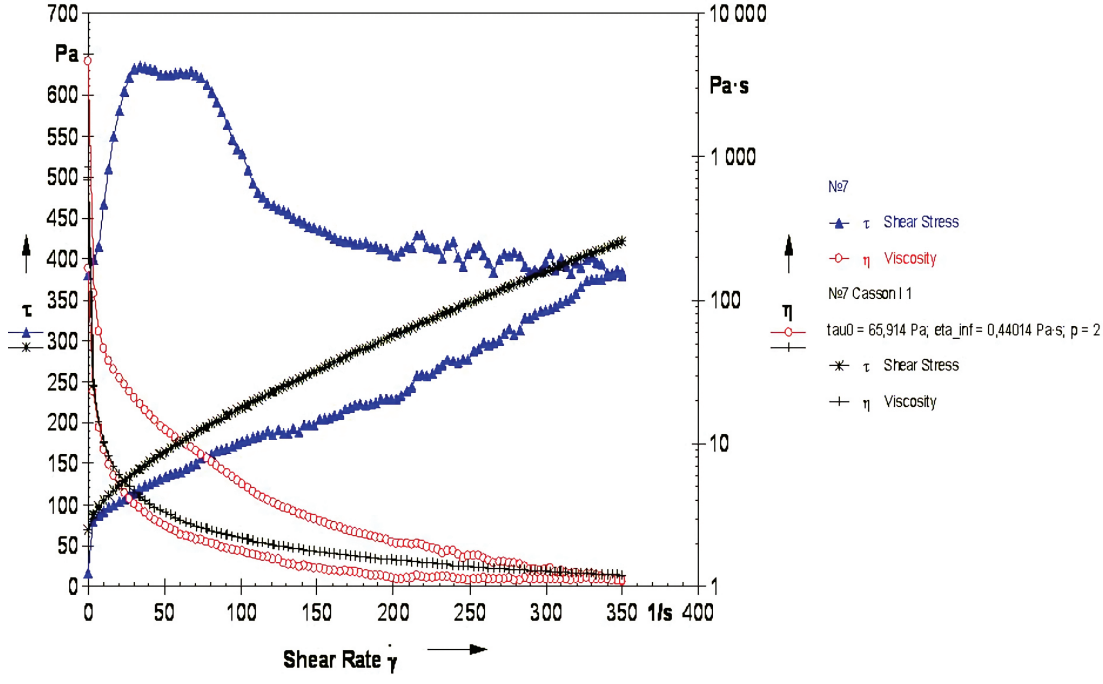

Figure 7. Profile of rheological behavior of sample № 7

shear force is sample № 8, which had a hydroxyethylcellulose base. Emulsion samples are liquefied to the greatest extent.

The behavior of dispersed systems during destruction is also evaluated by the coefficients of dynamic flow and MS. The coefficient of dynamic flow Kd_1 at shear rates of 3.4 and 10.3 s^{-1} varies in the range from 34.8% to 95.9%. The coefficient of dynamic flow Kd_2 is in the range of even higher values, since systems at higher shear rates are destroyed to a greater extent. The coefficient of MS, calculated as γ 3,4 s-1, serves as a measure of the assessment of the restoration of the structure after the full cycle of destruction-restoration. The closer the calculated value is to 1, the faster the system recovers, thus indicating a high instantaneous thixotropic properties. From Table 2, we see that the lowest value of the MS index was recorded by sample № 8, which was made using hydroxyethylcellulose. For gel systems, this behavior is typical because as the speed of rotation of the cylinder increases, there is elongation of the molecules of macromolecular matter and, after the cessation of the driving force, the structured orientation of the molecule is restored. In emulsion dispersed systems, which include samples № 3, № 4, № 5, and № 6, the change in viscoplastic properties is due to the sol-gel transition and such systems are restored over time. Homogeneous hydrophobic dispersed systems (samples № 2 and № 7) recover more slowly and the reason for this may be a violation of thermodynamic equilibrium in the system as a result of forced mixing of one layer relative to another or because the viscosity of hydrophobic systems is sensitive to temperature changes.

Samples № 6 and № 7 (Figure 1) have an unstable flow at high shear rates, which can be interpreted as an unstable structure that can stratify over time.

Sample № 2 (based on paraffin and vaseline oil) has a stable homogeneous flow over the entire range of the shear rates, the system is easily propelled, and is characterized by good consumer properties according to the optimum lubrication. According to the set of the rheological parameters, we consider it expedient to use the sample of the ointment base № 2 for further research on the development of the composition of the ointment with antiviral activity.

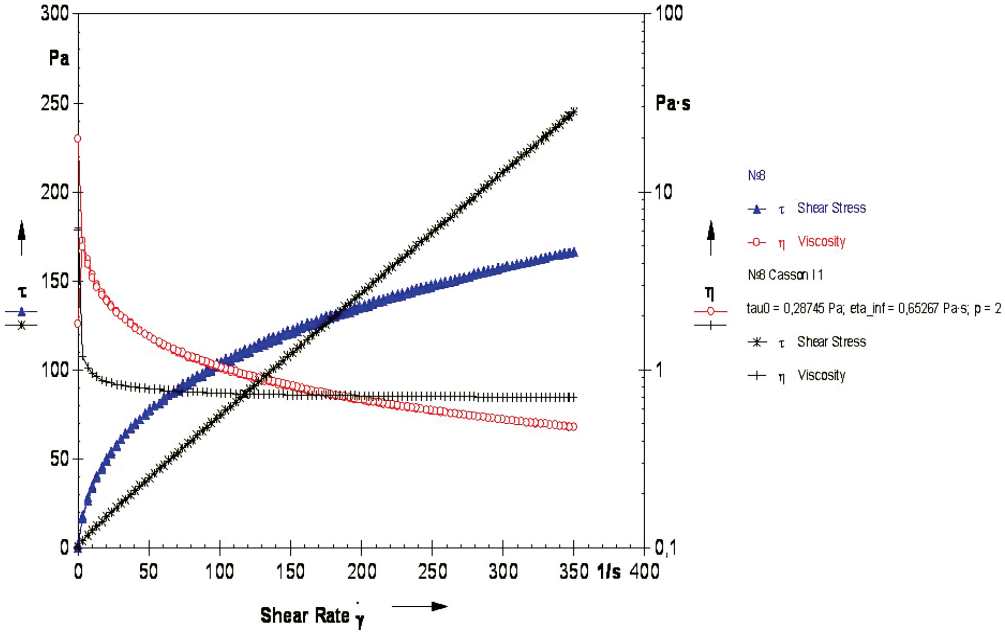

Figure 8. Profile of rheological behavior of sample № 8

Table 3. Structural and mechanical parameters of the ointment bases are calculated

Indicator	№ 1	№ 2	№ 3	№ 4	№ 5	№ 6	№ 7	№ 8
Hysteresis square, Pa/s	38780.5	30887.8	40.2	17242.8	49174.4	49521.1	82587.0	319.5
Yield strength at Casson τ_0, Pa	105.8	1.3	49.3	12.6	104.5	77.2	65.9	0.3
Structural viscosity at the infinite shear rate at Casson $\eta\infty$, Pa·s	0.39	0.54	0.83	0.72	0.88	0.34	0.44	0.65
The coefficient of dynamic flow Kd1, %	70.4	58.6	27.1	61.9	59.5	70.8	95.9	34.8
The coefficient of dynamic flow Kd2, %	77.7	86.6	77.6	75.6	61.6	78.8	97.7	63.2
Mechanical stability at γ 3,4 s-1	3.51	27.84	1.34	1.56	1.55	4.99	5.05	1.08

CONCLUSION

The structural and mechanical activity of the ointment bases was studied with help of the rotary viscometer "Rheolab QC" by Anton Paar (Austria) with coaxial cylinders CC27/S-SN29766. It was found that all samples have a non-Newtonian pseudoplastic type of flow. It is established that the ointment base № 2, which includes vaseline oil and paraffin, exhibits a homogeneous rheological flow.

Further research will focus on the development of composition of ointments with the antiviral effect.

Conflict of interest: No conflict of interest was declared by the authors. The authors are solely responsible for the content and writing of this paper.

REFERENCES

1. Shegokar R, Shaal LAL, Mishra PR. SiRNA Delivery. Challenges and role of carrier systems. Die Pharmazie. 2011;66:313-318.
2. Mezger TG. The Rheology Handbook. Hanover: Vincentz Network; 2014:432.
3. Goodwin JW, Hughes RW. Rheology for Chemists: An Introduction. Cambridge: Cambridge University Press; 2000:299.
4. Rukhmakova OA, Yarnykh TG, Kovalenko SN. The development of industrial technology of the ointment codenamed "Alergolik". Res J Pharm Tech. 2017;10:1994-1997.
5. Kukhtenko H, Gladukh I, Kukhtenko O, Soldatov D. Influence of excipients on the structural and mechanical properties of semisolid dosage forms. Asian J Pharm. 2017;11:575-578.
6. Gladukh I, Grubnik I, Kukhtenko H. Structural-mechanical studies of phytogel "Zhivitan". J Pharm Sci Res. 2017;9:1672-1676.
7. Ivko T, Aslanian M, Bobrytska L, Popova N, Nazarova O, Bereznyakova N, Germanyuk T. Development of the composition and manufacturing technology of the new combined drug Lavaflam. Turk J Pharm Sci. 2018;3:263-270.
8. Nwoko VE. Semi solid dosage forms manufacturing: tools, critical process parameters, strategies, optimization and validation. Sch Acad J Pharm. 2014;3:153-161.
9. Fares R, Bobrytska L, Germanyuk T. Diaplant: manufacturing technology and rationalization of costs of acute intestinal infection pharmacotherapy. Int J Green Pharm. 2017;11:584-589.
10. Caggioni M, Spicer PT, Blair DL, Lingerg SE. Rheology and microrheology of a microstructured fluid the gellan. J Rheology. 2007;51:851-865.
11. Kolpakova OA, Kucherenko NV, Kukhtenko HP. Research of rheological properties of ointment with water-saluble protein-polysaccharide complex of oyster mushroom. J Pharm Sci Res. 2019;11:1880-1883.
12. Neel JM, Neel DP, Jay P, Divyesh HS, Pragna KS. Development and evaluation of antiarthritic herbal ointment. Res J Pharm Biol Chem Sci. 2013;4:221-228.
13. Hrytsenko VI, Kienko LS, Bobrytska LO. The study of the antimicrobial activity of a soft dosage form with the antiviral effect. Clin Pharm. 2019;2:25-28.
14. Rebecca CB, David IB. Treatment of herpes simplex virus infections. Antiviral Res. 2004;61:73-81.
15. Grubnik I, Gladukh I. Study of the rheological properties of natural gums. Br J Educ Stud. 2015;2:689-669.
16. Aslanyan MA, Bobrytska LO, Nazarova ES, Mirnaya TA, Zborovskaya TV. Development and validation of method for the quantitative determination of lavender oil in lavaflam preparation by gas chromatography. Pharm Chem J. 2016;50:47-51.
17. Aslanyan M, Bobrytska L, Hrytsenko V, Shpychak O, Popova N, Germanyuk T, Kryvoviaz O, Ivko T. Technological aspects of development of a new drug in tablets called "Lavaflam" and its pharmacoeconomic evaluation. Res J Pharm Biol Chem Sci. 2017;4:808-814.
18. Aslanian M, Bobrytska L, Bereznyakova N, Shpychak H, Hrytsenko V, Germanyuk T, Ivko T. Biochemical research of hepatoprotective activity of tablets Lavaflam in rats with subchronic hepatitis. Curr Issues Pharm Medical Sci. 2020;32:10-13.
19. Bobrytska LO, Kovalev VV, Spyrydonov SV, Ivko TI, Germanyuk TA, Gordzievska NA. Diaplant-NEO: Complex therapy of acute intestinal infections. Trends Pharm Res Dev. 2020;2:145-153.
20. Nesterova IV, Khalturina EO. Mono- and mixed-herpesvirus infections: association with clinical syndromes of im-munodeficiency. RUDN J Med. 2018;22:226-234.
21. Bobrytska LO, Fares R, Goncharov MI, Nazarova OS, Popova NV, Litvinenko VI. Drug of antimicrobial, anti-inflammatory and antispasmodic action: patent 103886 Ukraine. № u2015 04344; declared 05.05.2015; published 12.01.2016, Bulletin no: 1.
22. Gritsenko VI, Kienko LS, Bobritskaya LO, Shpychak OS, Germanyuk TA, Nazarova OS. Pharmaceutical composition of soft dosage form with antiviral action: patent 134507 of Ukraine on utility model: international patent classification A61P 31/04. № in 201811079; declared 11/09/18; publ. 27.05.19, Bull. no: 10.
23. Kienko L, Hrytsenko V, Iakovlieva L, Bobrytska L. Marketing analysis of the assortment of drugs for the treatment of herpes viral diseases at the pharmaceutical market of Ukraine. Eureka: Health Sciences. 2020;3:70-76.
24. Hrytsenko VI, Kienko LS, Bobrytska LA, Rybalko SL, Starosila DB. Study of anti-herpetic activity of a soft dosage form with acyclovir and miramistin. J Glob Pharma Technol. 2020;12:397-404.
25. Aslanian MA, Bobrytska IA, Bereznyakova NL, Shpychak OS, Germanyuk T, Ivko TI. Histological research of hepatoprotective activity of tablets Lavaflam in rats with subchronic hepatitis. Zaporozhye Medical Journal. 2018;182-187.
26. Hrytsenko V, Gubar S, Ruban O, Kutsenko S, Bobrytska L, Germanyuk T. Development of the method of identification and quantitation of active ingredients in suppositories "phytoprost". Asian J Pharm. 2018;49-53.
27. Rowe RC, Sheskey PJ, Owen SC. Handbook of Pharmaceutical Excipiets. London: Pharmaceutical Press; 2006.
28. Dhawan S, Varma M, Sinha VR. High molecular weight poly(ethylene oxide)-based drug delivery systems. Part 1: hydrogeles and hydrophilic matrix systems. Pharm Technol. 2005;29:72-80.
29. WHO. State Pharmacopoeia of Ukraine. V. 2. Ch. 2. Kharkiv 2014. Available from: https://www.who.int/medicines/areas/quality_safety/quality_assurance/resources/Ukranian_Pharmacopoeia.pdf?ua=1
30. Schaefer MJ, Singh J. Effect of isopropyl myristic acid ester on the physical characteristics and in vitro release of etoposide from PLGA microspheres. AAPS PharmSciTech. 2000;1:E32.

Turk J Pharm Sci 2021;18(5):637-644
DOI: 10.4274/tjps.galenos.2021.36599

ORIGINAL ARTICLE

Cytotoxic Effects of Verbascoside on MCF-7 and MDA-MB-231

Verbaskositin MCF-7 ve MDA-MB-231 Üzerindeki Sitotoksik Etkileri

Hülya ŞENOL[1]*, Pınar TULAY[2,3], Mahmut Çerkez ERGÖREN[2,3], Azmi HANOĞLU[4], İhsan ÇALIŞ[4], Gamze MOCAN[5]

[1]Near East University Faculty of Medicine, Department of Medical Biology, Nicosia, North Cyprus
[2]Near East University Faculty of Medicine, Department of Medical Genetics, Nicosia, North Cyprus
[3]Near East University, Desam Research Institute, Nicosia, Cyprus
[4]Near East University Faculty of Pharmacy, Department of Pharmacognosy, Nicosia, North Cyprus
[5]Near East University Faculty of Medicine, Department of Medical Pathology, Nicosia, North Cyprus

ABSTRACT

Objectives: Verbascoside, also known as acteoside/kusaginin, has attracted a great attention due to its pharmacological features. In this study, we aimed to determine the cytotoxic effects of pure verbascoside isolated from *Phlomis nissolii L*. plant in both MCF-7 and MDA-MB-231 cell lines *in vitro.*

Materials and Methods: MCF-7 and MDA-MB 231 cells were treated with verbascoside (100, 48, 25, 10, 1, 0.5, and 0.1 µM) for 24, 48, and 72 hours. Cytotoxic effect of verbascoside in MCF-7 and MDA-MB-231 cells was assessed using TEBU-BIO cell counting kit 8.

Results and Conclusion: IC_{50} values for 24, 48, and 72 h verbascoside exposure of MCF-7 cells were determined as 0.127, 0.2174, and 0.2828 µM, respectively. R^2 values were calculated as 0.9630, 0.8789 and 0.8752, respectively. Two-Way ANOVA multiple comparison test results showed that 100 µM verbascoside has the highest cytotoxic effect on MCF-7 breast cancer (BC) cells after 72 h of exposure. IC_{50} values for 24, 48 and 72 h verbascoside exposure of MDA-MB 231 cells were determined as 0.1597, 0.2584 and 0.2563 µM, respectively and R^2 values were calculated as 0.8438, 0.5107 and 0.9203, respectively. Two-Way ANOVA multiple comparisons test results showed that 100 µM verbascoside has the highest cytotoxic effect on MDA-MB 231 BC cells after 24, 48 and 72 h of exposure.

Key words: Cytotoxicity, MCF-7, MDA-MB-231, *Phlomis nissolii* L., verbascoside

ÖZ

Amaç: Akteosit/kusaginin olarak bilinen verbaskosit, farmakolojik özelliklerinden dolayı büyük ilgi görmüştür. Bu çalışmada, *Phlomis nissolii* L. bitkisinden izole edilen saf verbaskositin MCF-7 ve MDA-MB-231 hücre hatlarında *in vitro* koşullarda sitotoksik etkilerini belirlemeyi amaçladık.

Gereç ve Yöntemler: MCF-7 ve MDA-MB 231 hücreleri, 24, 48 ve 72 saat süreyle 100, 48, 25, 10, 1, 0,5 ve 0,1 µM verbaskosit ile muamele edildi. Verbaskositin MCF-7 ve MDA-MB-231 hücrelerinde sitotoksisite etkisi TEBU-BIO hücre sayım kiti 8 kullanılarak değerlendirildi.

Bulgular ve Sonuç: MCF-7 hücrelerinin 24, 48 ve 72 saatlik verbaskosit maruziyetine ilişkin IC_{50} değerleri sırasıyla 0,127, 0,2174 ve 0,2828 µM olarak belirlendi. R^2 değerleri sırasıyla 0,9630, 0,8789 ve 0,8752 olarak hesaplanmıştır. İki yönlü ANOVA çoklu karşılaştırma testi sonuçları, 100 µM verbaskositin 72 saatlik maruziyetinin MCF-7 meme kanseri (BC) hücrelerinde en yüksek sitotoksik etkiye sahip olduğunu gösterdi. MDA-MB 231 hücrelerinin 24, 48 ve 72 saatlik verbaskosite maruziyeti için IC_{50} değerleri sırasıyla 0,1597, 0,2584 ve 0,2563 µM olarak belirlendi. R^2 değerleri sırasıyla 0,8438, 0,5107 ve 0,9203 olarak hesaplandı. İki yönlü ANOVA çoklu karşılaştırma test sonuçları, 100 µM verbaskositin 24, 48 ve 72 saatlik maruziyettinin MDA-MB 231 BC hücrelerinde en yüksek sitotoksik etkiye sahip olduğunu gösterdi.

Anahtar kelimeler: MCF-7, MDA-MB-231, *Phlomis nissolii* L., verbaskosit

***Correspondence:** hulya.senol@emu.edu.tr, **Phone:** +90 392 630 39 23, **ORCID-ID:** orcid.org/0000-0003-1701-8103
Received: 27.10.2020, **Accepted:** 24.02.2021

INTRODUCTION

Breast cancer (BC) is the most frequent cancer type found among women, affecting 2.1 million women each year.[1] In 2018, the female deaths due to BC was 627, which compromises 15% of all cancer deaths among women. Furthermore, BC rates in women are higher in more developed regions than in developing countries, and threateningly, these rates are still increasing in every region globally.[1] According to statistical data obtained by the Ministry of Health in North Cyprus, a total of 1.854 men and 1.809 women were diagnosed with cancer between 2012 and 2016. BC has the highest incidence (62.2%) among women in North Cyprus, and this value is lower than the incidence in Europe but unfortunately, however, higher than the BC incidence globally.[2] The current treatment strategies for BC include radiotherapy + adjuvant chemotherapy, radiation therapy, hormone therapy, and surgery have side effects.[3] These may include rib fracture, second non-breast infield malignancies, tissue necrosis, brachial plexopathy in radiation therapy, reduced number of white and red blood cells, elevated risk of infection, anemia, diarrhea, fatigue, hair loss, sore throat, ulcers, nausea, constipation, loss of appetite, and change in skin color during chemotherapy.[3] Due to these side effects, there has been a growing interest in alternative treatment modalities with reduced side effects.[4] There are many studies that have identified anti-cancer properties of herbal medicines that are used in developing countries for medical treatment for many years.[5]

Verbascoside ($C_{29}H_{36}O_{15}$), known as acteoside/kusaginin, is a phenylethanoid glycoside. Verbascoside has been isolated from many different plant species such as: *Verbascum sinuatum L.*,[6] *Syringa vulgaris*,[7] *Orobancherapum-genistae*,[8] *Clerodendron trichotomum* Thunb,[9] *Phlomis nissolii L.* (*Lamiaceae*),[10] *Buddleja brasiliensis, Striga asiatica, Olea europea, Paulownia tomentosa var. tomentosa, Lippia javanica, Lantana camara, and Lippia citriodora*.[11] In addition, verbascoside is abundant in olive mill wastewater.[12,13] There are total of 34 genus *Phlomis species* L. found in Turkey and Aegean islands.[14] The project performed on the 33 *Phlomis* species recorded in the Flora of Turkey resulted in the isolation and characterization of 33 phenylethanoid glycosides, of which verbascoside and forsythoside B were the common compounds for all of the *Phlomis* species.[15] Recently, two compounds were isolated from the two endemic *Phlomis* species, *P. brevibracteata,* and *P. cypria* growing in Cyprus.[16] Verbascoside attracted great attention due to its pharmacological features,[17] such as anti-inflammatory effect,[18-24] antioxidative effect,[25-32] neuroprotective effect,[33-43] antimicrobial effect[44-46] ultraviolet radiation protective effect[47-51] antimetastatic effect,[52] and cytotoxic effects on many types of cancer such as myeloma and leukemia[53-56] human gastric carcinoma,[57] colorectal cancer,[58] human oral squamous cell carcinoma,[59] glioblastoma,[60] and inhibitory effect on tumor cell proliferation.[61] In this study, we aimed to determine the cytotoxic effects of pure verbascoside isolated from the *Phlomis nissolii* L. plant in both MCF-7 and MDA-MB-231 cell lines *in vitro.*

MATERIALS AND METHODS

Cell culture conditions

The compound verbascoside used in this study was provided from the studies performed on *Phlomis* species L. Çalış et al.[15] Human BC cells MCF-7 and MDA-MB-231 (ATCC) were cultured in DMEM/F-12 media supplemented with 10% fetal bovine serum, human insulin of 4 mg/mL, penicillin streptomycin (1%) at 37°C, in a 5% CO_2 containing humidified chamber. The medium was refreshed every other day.

Cell viability/cytotoxicity

MCF-7 and MDA-MB 231 BC cells were plated in 96-well plates in triplicate with a density of 5000 cells/well. The cells were treated with verbascoside after 24 h of culturing at a different concentrations (100, 48, 25, 10, 1, 0.5, and 0.1 μM) for 24, 48, and 72 h. CCK-8 (Tebu, France) analysis was performed according to the manufacturer's protocol. The absorbencies were measured using Versa max tunable microplate reader at 450nm wavelength.

Statistical analysis

GraphPad® Prism software version 8 was used to calculate IC_{50} values by applying a non-linear regression curve fit analysis. Further, statistical analysis was performed using Two-Way ANOVA multiple comparisons test to determine the significance of a mean difference between the control and varying concentrations of verbascoside.

RESULTS

Cytotoxic effects of verbascoside in MCF-7 cells

To assess the cytotoxicity of verbascoside, MCF-7 BC cells were treated with several concentrations of verbascoside (100, 48, 25, 10, 1, 0.5, and 0.1 μM) for 24, 48, and 72 h. IC_{50} values of verbascoside in MCF-7 cells are shown in Table 1.

Significance ofamean difference between control and other concentrations of verbascoside for MCF-7 cell line after 24, 48, and 72 h was determined using Two-Way ANOVA multiple comparisons test, and the results are shown in Figure 1-3, respectively.

Two-Way ANOVA multiple comparisons test results for MCF-7 cell line after 24 h exposure to different concentrations of verbascoside showed tha the, mean difference wasnot significant at the 95% confidence level (CI) between the control and the test group at 48, 25, and 10 μM verbascoside concentrations. However, significance (at $p<0.05$) was observed at 100, 1, 0.5, and 0.1 μM verbascoside concentrations, and the control group after 24 h exposure. When concentration of verbascoside was decreased from 100-10 μM, absorbency

Table 1. IC_{50} and R^2 values for MCF-7 cell line

Exposure time to verbascoside	IC_{50} (μM)	R^2
24 h	0.127	0.9630
48 h	0.2174	0.8789
72 h	0.2828	0.8752

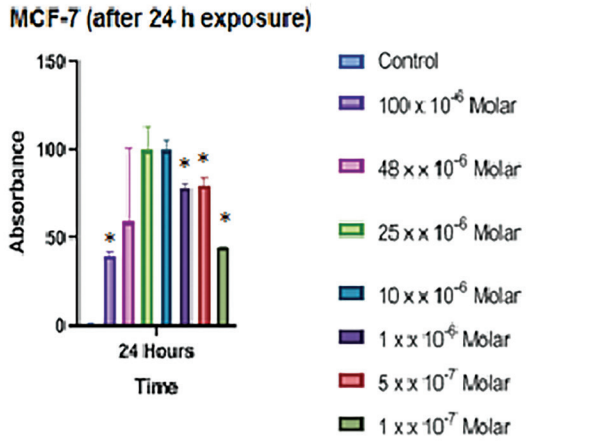

Figure 1. Two-Way ANOVA multiple comparisons test results for MCF-7 cell line after 24 h exposure to a different concentration of verbascoside (*significance at p<0.05)

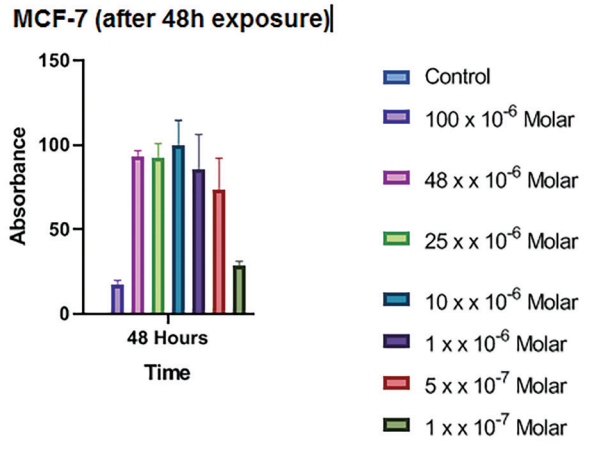

Figure 2. Two-Way ANOVA multiple comparisons test results for MCF-7 cell line after 48 h exposure to a different concentration of verbascoside (*significance at p<0.05)

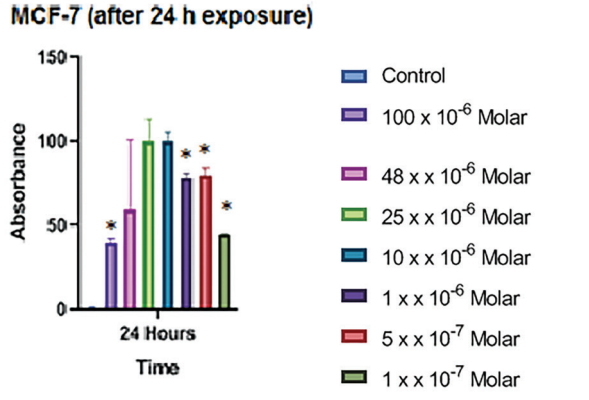

Figure 3. Two-Way ANOVA multiple comparisons test results for MCF-7 cell line after 72 h exposure to different concentrations of verbascoside (*significance at p<0.05)

increased so that the number of alive cells increased. When the concentration of verbascoside was further decreased from 10-0.1 µM, absorbency decreased so that number of alive cells decreased but number of dead cells increased. All absorbency values were higher than the control group, indicating that 100, 48, 25, 10, 1, 0.5, and 0.1 µM concentrations of verbascoside were not effectively toxic to the MCF-7 BC cells after 24h exposure (Figure 1).

The mean difference was not significant at 95% CI between the control absorbency value and absorbency values obtained at 100, 48, 25, 10, 1, 0.5, and 0.1 µM verbascoside concentrations after 48 h exposure of MCF-7 cell line. When the concentration of verbascoside was decreased from 100-10 µM, absorbency increased so that the number of alive cells increased. When the concentration of verbascoside was further decreased from 10-0.1 µM, absorbency decreased so that number of alive cells decreased, but the number of dead cells increased. All absorbency values were higher than the control so that 100, 48, 25, 10, 1, 0.5, and 0.1 µM concentrations of verbascoside were not effective on MCF-7 BC cells after 48 h exposure (Figure 2).

The mean difference calculated by Two-Way ANOVA multiple comparisons test was not significant at the 95% CI between the control absorbency value and absorbency values obtained at 100, 48, 25, 10, 1, 0.5, and 0.1 µM verbascoside concentrations after 72 h exposure of the MCF-7 cell line. When the concentration of verbascoside decreased from 100-25 µM, absorbency increased so that number of alive cells increased. When the concentration of verbascoside was further decreased from 25-0.1 µM, absorbency decreased so that number of alive cells decreased but number of dead cells increased. The absorbency value at 100 µM verbascoside was the lowest among the other absorbency values, so that lowest number of alive cells but highest number of dead cells was at this concentration. Verbascoside of 100 µM had the highest cytotoxic effect on MCF-7 BC cells after 72 h exposure (Figure 3).

Cytotoxic effects of verbascoside in MDA-MB 231 cells

MDA-MB 231 BC cells were treated with a several concentrations of verbascoside (100, 48, 25, 10, 1, 0.5, and 0.1 µM) for 24, 48, and 72 h to assess the cytotoxicity of verbascoside by using TEBU-BIO cell counting kit 8. IC_{50} values of verbascoside in MDA-MB 231 cells are shown in Table 2.

Two-Way ANOVA multiple comparisons test results for MDA-MB 231BC cell line after 24, 48, and 72 h are shown in Figure 4-6.

Analysis of the results showed that the mean difference between the control absorbency value and absorbency values

Table 2. IC_{50} and R^2 values for MDA-MB 231 breast cancer cell line

Exposure time to verbascoside	IC_{50} (µM)	R^2
24 h	0.1597	0.8438
48 h	0.2584	0.5107
72 h	0.2563	0.9203

obtained at 100, 48, 25, 10, 1, 0.5, and 0.1 µM verbascoside concentrations was not significant at 95% CI. Absorbency increased when concentration of verbascoside decreased from 100-0.5 µM. This result showed that the number of alive cells increased. A further decrease of concentration of verbascoside from 0.5-0.1 µM caused a decrease of absorbency indicating the decreased number of number of alive cells, but the number of dead cells increased. Absorbency value at 100 µM verbascoside was the lowest among the other absorbency values. This result indicated that lowest number of alive cells, but the highest number of dead cells were at this concentration. Verbascoside of 100 µM had the highest cytotoxic effect on MDA-MB 231 BC cells after 24 h exposure (Figure 4).

The mean difference was not significant at 95% CI between control the absorbency value and absorbency values obtained at 100, 48, 25, 10, 0.5, 1, and 0.1 µM verbascoside concentrations. When concentration of verbascoside was decreased from 100-25 µM, absorbency increased so that the number of alive cells increased. When the concentration of verbascoside further decreased from 25-0.1 µM, absorbency decreased. This result indicated that the number of alive cells decreased, but the number of dead cells increased. The absorbency value at 100 µM verbascoside was the lowest among the other absorbency values. This result showed that the lowest number of alive cells, but the highest number of dead cells, was at this concentration. Verbascoside 100 µM had the highest cytotoxic effect on MDA-MB 231 BC cells after 48 h exposure (Figure 5).

Although the calculated mean difference between the control absorbency value and absorbency values obtained at 48, 25, 10, and 1 µM verbascoside concentrations was not significant at the 95% CI. The mean difference was significant at 95% CI (*significance at $p<0.05$) between the control absorbency value and absorbency values obtained at 100, 0.5, and 0.1 µM verbascoside concentrations. Absorbency increased when the concentration of verbascoside was decreased from 100-0.5 µM indicating that the number of alive cells increased. When the concentration of verbascoside was further decreased from 0.5-0.1 µM, absorbency decreased so that the number of alive cells decreased but the number of dead cells increased. The absorbency value at 100 µM verbascoside was the lowest among the other absorbency values so that the lowest number of alive cells, but the highest number of dead cells, was at this concentration. Verbascoside of 100 µM had the highest cytotoxic effect on MDA-MB 231 BC cells after 72 h exposure (Figure 6).

CONCLUSION AND DISCUSSION

The prevalence of BC has been rising rapidly in the past decades; however, diagnosis and treatment in the early stages is very important.[62] Despite advances in treatment in the early stage of BC, many women experience recurrence and metastasis. Although treatment strategies are limited, the main focus is on medical therapy. The importance of classical treatment methods in cancer therapy is indisputable.[63] Increasing cancer cases and developing resistance to drugs has urged the need for new diagnostic and treatment approaches. Since the success of traditional treatments is limited, most cancer

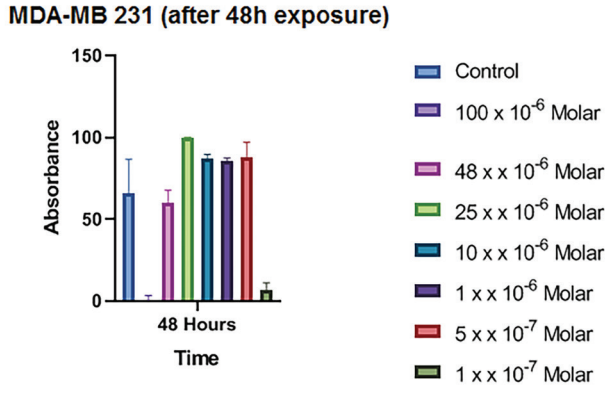

Figure 5. Two-Way ANOVA multiple comparisons test results for MDA-MB231 cell line for 48 h exposure of verbascoside (*significance at $p<0.05$)

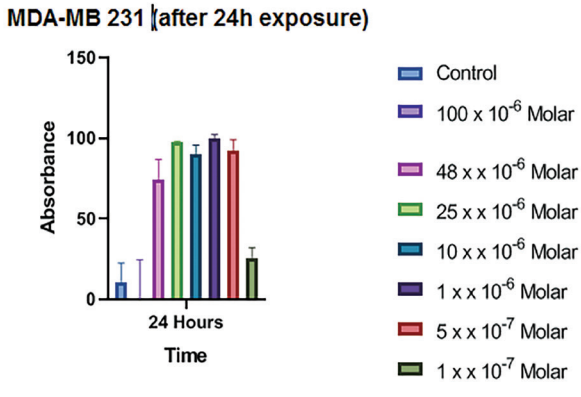

Figure 4. Two-Way ANOVA multiple comparisons test results for MDA-MB231 cell line for 24 h exposure of verbascoside (*significance at $p<0.05$)

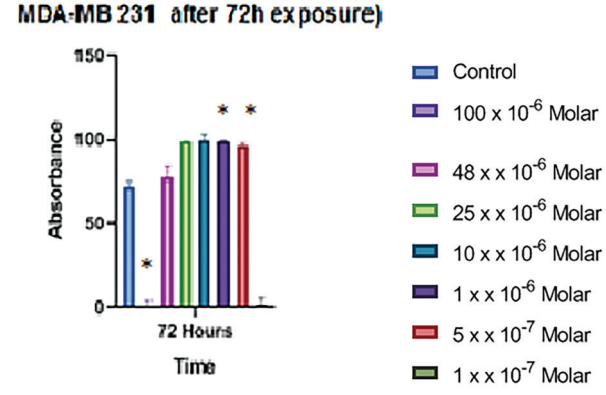

Figure 6. Two-Way ANOVA multiple comparisons test results for MDA-MB231 cell line for 72 h exposure of verbascoside (*significance at $p<0.05$)

patients try complementary medical therapies. There has been a growing interest in alternative treatment modalities. Finding alternative therapies with less or no side effects are essential. In recent years, alternative treatment modalities, such as natural products and anti-cancer drugs, have gained importance in BC therapy. Thus, the main aim of this study was to evaluate the cytotoxic effect of verbascoside isolated from *Phlomis nissolii* L. plant (Lamiaceae) in MCF-7 and MDA-MB 231 BC cell lines *in vitro*.

IC_{50} values for MCF-7 BC cell line after 24, 48, and 72 h exposure to a different concentration of verbascoside were found as 0.127, 0.2174, and 0.2828 µM, respectively. R^2 values for 24, 48, and 72 h exposure to verbascoside were calculated as 0.9630, 0.8789, and 0.8752, respectively. Concentrations of 48, 25, 10, 1, 0.5, and 0.1 µM verbascoside were not toxic on MCF-7 BC cells after 24, 48, and 72 h exposure. Verbascoside of 100 µM had the highest cytotoxic effect on MCF-7 BC cells only after 72 h exposure. In a study, verbascoside was isolated from *Scrophularia subaphylla* L., and researchers examined the effect of 1-1000 µg/mL verbascoside on MCF-7 cells and found IC_{50} value as 0.39 (±0.015) µg/mL after 48 h of exposure.[64] In another study, 5β,6β-dihydroxyantirrhide was isolated from *Pseuderanthemum carruthersii (Seem.) Guill. var. atropurpureum (Bull.) Fosb.* (Acanthaceae) leaves with13 different compounds, including verbascoside and the cytotoxic activities of these chemicals, and acetylcholinesterase inhibition against MCF-7 and HeLa cells at a concentration of 100 µg/mL were analyzed. Isoverbascoside and verbascoside showed fairly weak AChE inhibitory activity but showed cytotoxic activity against MCF-7 cells strongly.[65] This result supports the results of our study. In another study, acteoside was isolated from the crude methanolic extract of *Leucas indica* flowers, and a range of concentrations of acteoside (250.00, 125.00, 62.50, 31.25, 15.63, 7.81, 3.91, 1.95, 0.98 µg/mL) was tested on the MCF-7 cell line after 48 h of incubation. Researchers evaluated the *in vitro* cytotoxicity of acteoside on MCF-7 cell by using the (3-(4,5-dimethylthiazol-2-yl)-2,5-diphenyltetrazolium bromide) (MTT) assay. This study tested a higher range of acteoside concentration on MCF-7 cell line than our present study, that used a range of concentrations of 100, 48, 25, 10, 1, 0.5, and 0.1 µM verbascoside (acteoside) and obtained higher values of IC_{50} and R^2 as 7.7 and 0.9968 than the current study.[66] Researchers also concluded that acteoside isolated from *Leucas indica* flowers extract showed a significant cytotoxic activity on MCF-7 cell line, and results indicated that the antiproliferative effect strengthens with an increase in the concentration of the extract (p.2). Results of another study with verbascoside isolated from the aerial parts of *Plantago lagopus* L. showed that verbascoside had strong cytotoxic activities against MCF-7 cell line, and histological analysis proved the apoptotic cell death of MCF-7 cells after the treatment of 50-100 µg/mL verbascoside.[67] In one report, the effect of different concentrations of verbascoside isolated from *V. ovalifolium Donn ex Sims* (Scrophulariaceae) on cell viability of MCF-7 cells was measured using the MTT colorimetric assay after 48 h of incubation. The IC_{50} value for verbascoside was calculated as 58.3 µg/mL, and it was observed that verbascoside decreased viability by 69.6% in MCF-7 cells at 100 µg/mL but did not affect the viability of non-tumor MCF-10A cells (up to 100 µg/mL).[68] Acteoside may be effective to prevent MCF-7 BC cells because of its antiestrogenic effect. Acteoside isolated from aerial parts of *Verbascum macrurum* exhibited an ER-mediated significant antiestrogenic activity at a low concentration range 10^{-7}-10^{-9}M in both the ERα and and ERß assay systems, indicating that acteoside may act as antagonist by itself. Acteoside at low concentration (10^{-7} M) demonstrated a potent inhibitory effect against estradiol (10^{-9} M) mainly via Erα, so that acteoside functions as antagonist for ERα-mediated transcription.[69] In contrast, in another study, 12 chemical constituents from the *Callicarpa nudiflora* were isolated and their cytotoxicity was evaluated by the MTT assay. The cytotoxicity assay demonstrated that the flavonoids luteoloside, lutedin-4'-O-β-D-glucoside, 6-hydroxyluteolin-7-O-β-glucoside, lutedin-7-O-neohesperidoside, rhoifolin, luteolin-7, and 4'-di-O-glucoside showed monolithic proliferation inhibitory activities against Hela, A549, and MCF-7 cell lines in various concentrations. Compounds 6-hydroxyluteolin-7-O-β-glucoside and rhoifolin and iridoid glycoside nudifloside exhibited higher cytotoxicactivities.[70]

IC_{50} values for MDA-MB 231 cell line after 24, 48, and 72 h of exposure to different concentrations of verbascoside were found as 0.1597, 0.2584, and 0.2563 µM, respectively. R^2 values for 24, 48, and 72 h of exposure to verbascoside were calculated as 0.8438, 0.5107, and 0.9203, respectively. Concentrations of 48, 25, 10, 1, 0.5, and 0.1 µM verbascoside are not toxic on MDA-MB 231 BC cells after 24, 48, and 72 h exposure. Verbascoside 100 µM has the highest cytotoxic effect on MDA-MB 231 BC cells after 24, 48, and 72 h exposure. There are few studies about the cytotoxic effects of verbascoside on MDA-MB 231 BC cell line in the literature. In a study, antiproliferative effect of *Strobilanthes crispus* containing verbascoside on MDA-MB 231 cells was evaluated using MTT assay, and the IC_{50} value of methanolic extract was found as 27.2 µg mL^{-1}.[71] Another study examined the effect of dry olive mill residue water containing verbascoside and found that dry olive mill residue water inhibited MDA-MB 231 cell growth by EC value of 57.15±1.04 c.[72] Both of these studies support the idea that plant extracts containing verbascoside have cytotoxic effects on MDA-MB 231 BC cell line; however researchers in these studies examined the cytotoxic effects of the plant extracts containing verbascoside and any other chemicals on MDA-MB 231 cell line, unlike pure verbascoside in our study.

This study proved that verbascoside isolated from *Phlomis species L.* has cytotoxic effects on MCF-7 and MDA-MB 231 BC cells. Further studies would be performed to assess the underlying mechanisms for apoptotic induction of verbascoside extracted from *Phlomis species* L. In addition, detailed investigations maybe performed to evaluate the synergic effects of verbascoside isolated from *Phlomis species* L. with other plant extracts used in the BC treatment.

ACKNOWLEDGEMENTS

The authors would like to thank Prof. A. Elif Erson Bensan from the Faculty of Arts and Sciences, Department of Biology, Middle East Technical University for supplying MDA-MB 231 cell lines.

Funding: This study was supported in terms of equipment and laboratories by DESAM Institute, Faculty of Medicine and Faculty of Pharmacy of Near East University, Nicosia, Yakın Doğu Bulvarı, 99138, North Cyprus, Mersin 10, Turkey.

Conflict of interest: No conflict of interest was declared by the authors. The authors are solely responsible for the content and writing of this paper.

REFERENCES

1. World Health Organization. Breast Cancer (2019). Available from: https://www.who.int/cancer/prevention/diagnosis-screening/breast-cancer/en/
2. TRNC Ministry of Health, Kuzey Kıbrıs Türk Cumhuriyeti'nde Kanser Kayıtçılık Projesi (2019). Available from: https://saglik.gov.ct.tr/Portals/107/KK-Kidem%202012 2016%20BesYllkKanserIstatistikleri%20%282%29.pdf
3. Agrawal S. Late effects of cancer treatment in breast cancer survivors. South Asian J Cancer. 2014:3:112-115.
4. Mitra S, Dash R. Natural products for the management and prevention of breast cancer. Evid Based Complement Alternat Med. 2018;2018:8324696.
5. Greenwell M, Rahman PK. Medicinal plants: their use in anticancer treatment. Int J Pharm Sci Res. 2015;6:4103-4112.
6. Scarpati ML, Monache D. Isolation from Verbascum sinuatum of two new glucosides, verbascoside and isoverbascoside. Ann Chlm. 1963:53:356-367.
7. Birkofer L, Kaiser C, Thomas U. Acteosid und neoacteosid: Zukerester aus Syringa vulgaris. Z Naturforsch B. 1968:23:1051-1058.
8. Andary C, Wylde R, Laffite C, Privat G, Winternitz F. Structures of verbascoside and orobanchoside, caffeic acid sugar esters from Orobanche rapum-genistae. Phytochemistry. *1982:21*:1123-1127.
9. Sakurai A, Kato T. A new glycoside, kusaginin isolated from Clerodendron trichotomum. Bull Chem Soc Jpn. 1983;56:1573-1574.
10. Kırmızıbekmez H, Piacente S, Pizza C, Dönmez AA, Çaliş İ. Iridoid and phenylethanoid glycosides from Phlomis nissolii and P. capitata. Z. Naturforsch. 2004:59:609-613.
11. Alipieva K, Korkina L, Orhan IE, Georgiev MI. Verbascoside--a review of its occurrence, (bio)synthesis and pharmacological significance. Biotechnol Adv. 2014;32:1065-1076.
12. De Marco E, Savarese M, Paduano A, Sacchi R. Characterization and fractionation of phenolic compounds extracted from olive oil mill waste waters. Food Chem. 2006;104:858-867.
13. Dell'Aquila ME, Bogliolo L, Russo R, Martino NA, Filioli Uranio M, Ariu F, Amati F, Sardanelli AM, Linsalata V, Ferruzzi MG, Cardinali A, Minervini F. Prooxidant effects of verbascoside, a bioactive compound from olive oil mill wastewater, on in vitro developmental potential of ovine prepubertal oocytes and bioenergetic/oxidative stress parameters of fresh and vitrified oocytes. Biomed Res Int. 2014;2014:878062.
14. Huber-Morath A. Phlomis. In Davis PH, eds. Flora of Turkey and the East Aegean Islands. (7th ed). Edinburgh: Edinburg University Press; 1982:102-126.
15. Çalış İ, Saracoğlu İ, Ersöz T, Kırmızıbekmez H, Yalçın FN, Harput Ş. Chemotaxonomy of Turkish Phlomis L. (Lamiaceae) Genus. The Scientific and Technological Research Council of Turkey, 2004: Project Number: SBAG-2304.
16. Hanoğlu A. Phytochemical Studies on the endemic phlomis species growing in Northern Cyprus. Doctorial Thesis. Kyrenia: Near East University, Graduate School of Health Sciences; 2019.
17. Schönbichler SA, Bittner LK, Pallua JD, Popp M, Abel G, Bonn GK, Huck CW. Simultaneous quantification of verbenalin and verbascoside in Verbena officinalis by ATR-IR and NIR spectroscopy. J Pharm Biomed Anal. 2013;84:97-102.
18. Lee JH, Lee JY, Kang HS, Jeong CH, Moon H, Whang WK, Kim CJ, Sim SS. The effect of acteoside on histamine release and arachidonic acid release in RBL-2H3 mast cells. Arch Pharm Res. 2006;29:508-513.
19. Li Y, Gan L, Li GQ, Deng L, Zhang X, Deng Y. Pharmacokinetics of plantamajoside and acteoside from Plantago asiatica in rats by liquid chromatography-mass spectrometry. J Pharm Biomed Anal. 2014;89:251-256.
20. Mazzon E, Esposito E, Di Paola R, Riccardi L, Caminiti R, Dal Toso R, Pressi G, Cuzzocrea S. Effects of verbascoside biotechnologically produced by Syringa vulgaris plant cell cultures in a rodent model of colitis. Naunyn Schmiedebergs Arch Pharmacol. 2009;380:79-94.
21. Rao YK, Fang SH, Hsieh SC, Yeh TH, Tzeng YM. The constituents of Anisomeles indica and their anti-inflammatory activities. J Ethnopharmacol. 2009;121:292-296.
22. Lenoir L, Rossary A, Joubert-Zakeyh J, Vergnaud-Gauduchon J, Farges MC, Fraisse D, Texier O, Lamaison JL, Vasson MP, Felgines C. Lemon verbena infusion consumption attenuates oxidative stress in dextran sulfate sodium-induced colitis in the rat. Dig Dis Sci. 2011;56:3534-3545.
23. Kostyuk VA, Potapovich AI, Suhan TO, de Luca C, Korkina LG. Antioxidant and signal modulation properties of plant polyphenols in controlling vascular inflammation. Eur J Pharmacol. 2011;658:248-256.
24. Pesce M, Franceschelli S, Ferrone A, De Lutiis MA, Patruno A, Grilli A, Felaco M, Speranza L. Verbascoside down-regulates some pro-inflammatory signal transduction pathways by increasing the activity of tyrosine phosphatase SHP-1 in the U937 cell line. J Cell Mol Med. 2015;19:1548-1556.
25. Vertuani S, Beghelli E, Scalambra E, Malisardi G, Copetti S, Dal Toso R, Baldisserotto A, Manfredini S. Activity and stability studies of verbascoside, a novel antioxidant, in dermo-cosmetic and pharmaceutical topical formulations. Molecules. 2011;16:7068-7080.
26. Caturla N, Funes L, Pérez-Fons L, Micol V. A randomized, double-blinded, placebo-controlled study of the effect of a combination of lemon verbena extract and fish oil omega-3 fatty acid on joint management. J Altern Complement Med. 2011;17:1051-1063.
27. Mestre-Alfaro A, Ferrer MD, Sureda A, Tauler P, Martínez E, Bibiloni MM, Micol V, Tur JA, Pons A. Phytoestrogens enhance antioxidant enzymes after swimming exercise and modulate sex hormone plasma levels in female swimmers. Eur J Appl Physiol. 2011;111:2281-2294.
28. Carrera-Quintanar L, Funes L, Viudes E, Tur J, Micol V, Roche E, Pons A. Antioxidant effect of lemon verbena extracts in lymphocytes of university students performing aerobic training program. Scand J Med Sci Sports. 2012;22:454-461.
29. Cardinali A, Pati S, Minervini F, D'Antuono I, Linsalata V, Lattanzio V. Verbascoside, isoverbascoside, and their derivatives recovered from olive mill wastewater as possible food antioxidants. J Agric Food Chem. 2012;60:1822-1829.

30. Sgarbossa A, Dal Bosco M, Pressi G, Cuzzocrea S, Dal Toso R, Menegazzi M. Phenylpropanoid glycosides from plant cell cultures induce heme oxygenase 1 gene expression in a human keratinocyte cell line by affecting the balance of NRF2 and BACH1 transcription factors. Chem Biol Interact. 2012;199:87-95.

31. Alipieva K, Korkina L, Orhan IE, Georgiev MI. Verbascoside--a review of its occurrence, (bio)synthesis and pharmacological significance. Biotechnol Adv. 2014;32:1065-1076.

32. Di Giancamillo A, Rossi R, Vitari F, Carollo V, Deponti D, Corino C, Domeneghini C. Changes in nitrosative stress biomarkers in swine intestine following dietary intervention with verbascoside. Histol Histopathol. 2013;28:715-723.

33. Sheng GQ, Zhang JR, Pu XP, Ma J, Li CL. Protective effect of verbascoside on 1-methyl-4-phenylpyridinium ion-induced neurotoxicity in PC12 cells. Eur J Pharmacol. 2002;451:119-124.

34. Pu X, Song Z, Li Y, Tu P, Li H. Acteoside from Cistanche salsa inhibits apoptosis by 1-methyl-4-phenylpyridinium ion in cerebellar granule neurons. Planta Med. 2003;69:65-66.

35. Backhouse N, Delporte C, Apablaza C, Farías M, Goïty L, Arrau S, Negrete R, Castro C, Miranda H. Antinociceptive activity of Buddleja globosa (matico) in several models of pain. J Ethnopharmacol. 2008;119:160-165.

36. Deng M, Ju X, Fan D, Tu P, Zhang J, Shen Y. Verbascoside rescues the SHSY5Y neuronal cells from MPP+ induced apoptosis. Chin Pharmacol Bull. 2008;24:1297-1302.

37. Wang H, Xu Y, Yan J, Zhao X, Sun X, Zhang Y, Guo J, Zhu C. Acteoside protects human neuroblastoma SH-SY5Y cells against beta-amyloid-induced cell injury. Brain Res. 2009;1283:139-147.

38. Esposito E, Mazzon E, Paterniti I, DalToso R, Pressi G, Caminiti R, Cuzzocrea. PPAR-α contributes to the anti-inflammatory activity of verbascoside in a model of inflammatory bowel disease in mice. PPAR Res. 2010;2010:917312.

39. Kahraman C, Tatli II, Orhan IE, Akdemir ZS. Cholinesterase inhibitory and antioxidant properties of Verbascum mucronatum Lam. and its secondary metabolites. Z Naturforsch C J Biosci. 2010;65:667-674.

40. Filho AG, Morel AF, Adolpho L, Ilha V, Giralt E, Tarragó T, Dalcol II. Inhibitory effect of verbascoside isolated from Buddleja brasiliensis Jacq. ex Spreng on prolyl oligopeptidase activity. Phytother Res. 2012;26:1472-1475.

41. Lin J, Gao L, Huo SX, Peng XM, Wu PP, Cai LM, Yan M. [Effect of acteoside on learning and memory impairment induced by scopolamine in mice]. Zhongguo Zhong Yao Za Zhi. 2012;37:2956-2959.

42. Wang HQ, Xu YX, Zhu CQ. Upregulation of heme oxygenase-1 by acteoside through ERK and PI3 K/Akt pathway confer neuroprotection against beta-amyloid-induced neurotoxicity. Neurotox Res. 2012;21:368-378.

43. Kurisu M, Miyamae Y, Murakami K, Han J, Isoda H, Irie K, Shigemori H. Inhibition of amyloid β aggregation by acteoside, a phenylethanoid glycoside. Biosci Biotechnol Biochem. 2013;77:1329-1332.

44. Azimi H, Fallah-Tafti M, Khakshur AA, Abdollahi M. A review of phytotherapy of acne vulgaris: perspective of new pharmacological treatments. Fitoterapia. 2012;83:1306-1317.

45. Funari CS, Gullo FP, Napolitano A, Carneiro RL, Mendes-Giannini MJ, Fusco-Almeida AM, Piacente S, Pizza C, Silva DH. Chemical and antifungal investigations of six Lippia species (Verbenaceae) from Brazil. Food Chem. 2012;135:2086-2094.

46. Maquiaveli CDC, Rochetti AL, Fukumasu H, Vieira PC, da Silva ER. Antileishmanial activity of verbascoside: Selective arginase inhibition of intracellular amastigotes of Leishmania (Leishmania) amazonensis with resistance induced by LPS plus IFN-γ. Biochem Pharmacol. 2017;127:28-33.

47. Korkina L, Pastore S. The role of redox regulation in the normal physiology and inflammatory diseases of skin. Front Biosci (Elite Ed). 2009;1:123-141.

48. Pastore S, Lulli D, Fidanza P, Potapovich AI, Kostyuk VA, De Luca C, Mikhal'chik E, Korkina LG. Plant polyphenols regulate chemokine expression and tissue repair in human keratinocytes through interaction with cytoplasmic and nuclear components of epidermal growth factor receptor system. Antioxid Redox Signal. 2012;16:314-328.

49. Kostyuk VA, Potapovich AI, Lulli D, Stancato A, De Luca C, Pastore S, Korkina L. Modulation of human keratinocyte responses to solar UV by plant polyphenols as a basis for chemoprevention of non-melanoma skin cancers. Curr Med Chem. 2013;20:869-879.

50. Muñoz E, Avila JG, Alarcón J, Kubo I, Werner E, Céspedes CL. Tyrosinase inhibitors from Calceolaria integrifolia s.l.: calceolaria talcana aerial parts. J Agric Food Chem. 2013;61:4336-4343.

51. Potapovich AI, Kostyuk VA, Kostyuk TV, de Luca C, Korkina LG. Effects of pre- and post-treatment with plant polyphenols on human keratinocyte responses to solar UV. Inflamm Res. 2013;62:773-780.

52. Korkina LG. Phenylpropanoids as naturally occurring antioxidants: from plant defense to human health. Cell Mol Biol (Noisy-le-grand). 2007;53:15-25.

53. Wartenberg M, Budde P, De Mareés M, Grünheck F, Tsang SY, Huang Y, Chen ZY, Hescheler J, Sauer H. Inhibition of tumor-induced angiogenesis and matrix-metalloproteinase expression in confrontation cultures of embryoid bodies and tumor spheroids by plant ingredients used in traditional chinese medicine. Lab Invest. 2003;83:87-98.

54. Zhang F, Jia Z, Deng Z, Wei Y, Zheng R, Yu L. In vitro modulation of telomerase activity, telomere length and cell cycle in MKN45 cells by verbascoside. Planta Med. 2002;68:115-118.

55. Lee KW, Kim HJ, Lee YS, Park HJ, Choi JW, Ha J, Lee KT. Acteoside inhibits human promyelocytic HL-60 leukemia cell proliferation via inducing cell cycle arrest at G0/G1 phase and differentiation into monocyte. Carcinogenesis. 2007;28:1928-1936.

56. Chen M, Bin Huang YZ, Yang X, Wu Y, Liu B, Yuan Y, Zhang G. Evaluation of the antitumor activity by ni nanoparticles with verbascoside. J Nanomater. 2013;2013:62349.

57. Zhang F, Jia Z, Deng Z, Wei Y, Zheng R, Yu L. *In vitro* modulation of telomerase activity, telomere length and cell cycle in MKN45 cells by verbascoside. Planta Med. 2002;68:115-118.

58. Zhou L, Feng Y, Jin Y, Liu X, Sui H, Chai N, Chen X, Liu N, Ji Q, Wang Y, Li Q. Verbascoside promotes apoptosis by regulating HIPK2-p53 signaling in human colorectal cancer. BMC Cancer. 2014;14:747.

59. Zhang Y, Yuan Y, Wu H, Xie Z, Wu Y, Song X, Wang J, Shu W, Xu J, Liu B, Wan L, Yan Y, Ding X, Shi X, Pan Y, Li X, Yang J, Zhao X, Wang L. Effect of verbascoside on apoptosis and metastasis in human oral squamous cell carcinoma. Int J Cancer. 2018;143:980-991.

60. Jia WQ, Wang ZT, Zou MM, Lin JH, Li YH, Zhang L, Xu RX. Verbascoside inhibits glioblastoma cell proliferation, migration and ınvasion while promoting apoptosis through upregulation of protein tyrosine phosphatase shp-1 and ınhibition of stat3 phosphorylation. Cell Physiol Biochem. 2018;47:1871-1882.

61. Wartenberg M, Budde P, De Mareés M, Grünheck F, Tsang SY, Huang Y, Chen ZY, Hescheler J, Sauer H. Inhibition of tumor-induced angiogenesis and matrix-metalloproteinase expression in confrontation cultures of embryoid bodies and tumor spheroids by plant ingredients used in traditional chinese medicine. Lab Invest. 2003;83:87-98.

62. Parkin DM, Bray F, Ferlay J, Pisani P. Global cancer statistics, 2002. CA Cancer J Clin. 2005;55:74-108.

63. Aggarwal BB, Shishodia S. Molecular targets of dietary agents for prevention and therapy of cancer. Biochem Pharmacol. 2006;71:1397-1421.

64. Delazar A, Asnaashari S, Nikkhah E, Asgharian P. Phytochemical analysis and antiproliferative activity of the aerial parts of Scrophularia subaphylla. Res Pharm Sci. 2019;14:263-272.

65. Nga VT. Constituents of the leaves of Pseuderanthemum carruthersii (Seem.) Guill. var. atropurpureum (Bull.) Fosb. Amsterdam, Netherlands: Elsevier; 2017.

66. Vinayagam A, Sudha PN. In Vitro cytotoxicity activity of acteoside from leucas Indica flowers. Indian J Appl Resç 2014:4:1-3.

67. Harput US, Genc Y, Saracoglu I. Cytotoxic and antioxidative activities of Plantago lagopus L. and characterization of its bioactive compounds. Food Chem Toxicol. 2012;50:1554-1559.

68. Vasincu A, Neophytou CM, Luca SV, Skalicka-Woźniak K, Miron A, Constantinou AI. 6-O-(3″, 4″-di-O-trans-cinnamoyl)-α-l-rhamnopyranosylcatalpol and verbascoside: Cytotoxicity, cell cycle kinetics, apoptosis, and ROS production evaluation in tumor cells. J Biochem Mol Toxicol. 2020;34:e22443.

69. Papoutsi Z, Kassi E, Mitakou S, Aligiannis N, Tsiapara A, Chrousos GP, Moutsatsou P. Acteoside and martynoside exhibit estrogenic/antiestrogenic properties. J Steroid Biochem Mol Biol. 2006;98:63-71.

70. Ma YC, Zhang M, Xu WT, Feng SX, Lei M, Yi B. [Chemical constituents from Callicarpa nudiflora and their cytotoxic activities]. Zhongguo Zhong Yao Za Zhi. 2014;39:3094-3101.

71. Rahmat A, Edrini S, Akim A, Ismail P, Hin TYY, Abu Bakar MF. Anticarcinogenic properties of strobilanthes crispus extracts and its compounds in vitro. Int J Cancer Res. 2006:2:47-49.

72. Ramos P, Santos SAO, Guerra AR, Guerreiro O, Felício L, Jerónimo E, Silvestre AJD, Neto CP, Duarte M. Valorization of olive mill residues: Antioxidant and breast cancer antiproliferative activities of hydroxytyrosol-rich extracts derived from olive oil by-products, Ind Crops and Prod. 2013;46:359-368.

Turk J Pharm Sci 2021;18(5):645-651
DOI: 10.4274/tjps.galenos.2021.71354

ORIGINAL ARTICLE

Electrochemical Detection of Linagliptin and its Interaction with DNA

Linagliptinin Elektrokimyasal Tespiti ve DNA ile Etkileşimi

Seda Nur TOPKAYA[1]*, Hüseyin Oğuzhan KAYA[1], Arif E. CETIN[2]

[1]İzmir Katip Çelebi University Faculty of Pharmacy, Department of Analytical Chemistry, İzmir, Turkey
[2]İzmir Biomedicine and Genome Center, İzmir, Turkey

ABSTRACT

Objectives: Linagliptin (Lin) is a drug used in treatment of type 2 diabetes mellitus. In this study, the electrochemical detection of Lin and its interaction with DNA was analyzed for the first time using voltammetric methods by measuring the oxidation currents of the adenine bases of DNA before and after the interaction. In addition, the electrochemical properties of the Lin were studied.

Materials and Methods: The interaction between Lin and DNA was evaluated using differential pulse voltammetry. A three-electrode system comprising of a pencil graphite electrode as the working electrode, reference electrode (Ag/AgCl), and platinum wire as the auxiliary electrode was used in the electrochemical studies. Experimental conditions, such as the concentration, pH of the supporting electrolyte, and immobilization time were optimized to obtain maximum analytical signals.

Results: The adenine bases of DNA were evaluated as an analytical signal obtained at approximately +1.2 V vs. Ag/AgCl. After the Lin-DNA interaction, the oxidation currents of adenine decreased as proof of interaction. No reports have been published on Lin interacting with DNA. Based on our results, a diffusion-controlled irreversible redox process involving independent oxidation was revealed for Lin. Under optimum conditions, the detection limit was 6.7 µg/mL for DNA and 21.5 µg/mL for Lin. Based on the observations, Lin has a toxic effect on DNA.

Conclusion: We successfully demonstrated that Lin interacts with DNA, and its influence on DNA could play a vital role in the medical effect of the drug.

Key words: DNA, linagliptin, DNA-drug interaction, electrochemistry, voltammetry

ÖZ

Amaç: Linagliptin (Lin), tip 2 diabetes mellitusun tedavisi için kullanılan bir ilaçtır. İlaçlar, ligandlar ve kimyasallar gibi küçük moleküller, kovalent ve kovalent olmayan etkileşimler yoluyla DNA ile etkileşime girebilmektedir. İlaçlar farmakolojik aktivitelerini farklı mekanizmalarla gösterdiklerinden, DNA ile etkileşimlerinin altında yatan mekanizmasını anlamak son derece önemlidir. Bu çalışmada Lin'in elektrokimyasal tespiti ve ilk defa DNA ile etkileşimi çalışması yapılmıştır. Bu etkileşim süreci birbirleriyle etkileşim öncesi ve sonrasında DNA adenin bazlarının yükseltgenme akımları ölçülerek voltametrik yöntemlerle analiz edilmiştir. Ayrıca çalışmamızda Lin'in elektrokimyasal özellikleri incelenmiştir.

Gereç ve Yöntemler: Lin ve DNA arasındaki etkileşim, diferansiyel puls voltametrisi kullanılarak değerlendirilmiştir. Bu elektrokimyasal temelli çalışmada; çalışma elektrodu olarak grafit uçlu kurşun kalem, bir referans elektrot (Ag/AgCl) ve yardımcı elektrot olarak bir platin telden oluşan üçlü elektrot sistemi kullanılmıştır. Maksimum analitik sinyalleri elde etmek için konsantrasyon, destekleyici elektrolitin pH'si ve immobilizasyon süresi gibi deneysel koşullar araştırılmıştır.

Bulgular: Çalışmamızda DNA-Lin etkileşimi; DNA ve Lin'in birbirleriyle etkileşimi öncesi ve sonrası adenine bazlarının Ag/AgCl referans elektroda karşı + 1.2 V'de verdiği yükseltgenme akımları karşılaştırılarak değerlendirilmiştir. DNA etkileşiminden sonra, adenin yükseltgenme akımları azalmıştır. Lin'in elektrokimyasal özelliklerinin araştırılması sonucu, bu molekül için difüzyon kontrollü, yükseltgenmeye bağlı ve geri dönüşümsüz bir redoks sürecinin meydana geldiği açığa çıkarılmıştır. Optimum koşullar altında, tespit sınırı DNA için sırasıyla 6,7 µg/mL ve Lin için 21,5 µg/mL olarak bulunmuştur. Elde edilen sonuçlar değerlendirildiğinde, Lin'in DNA üzerinde toksik bir etkiye sahip olduğu sonucuna varılmıştır.

Sonuç: Bu çalışmada elde edilen sonuçlar değerlendirildiğinde; elektrokimyasal metotlar kullanarak Lin'in DNA ile etkileşime girdiği hızlı ve başarılı bir şekilde gösterilmiştir.

Anahtar kelimeler: DNA, linagliptin, DNA-ilaç etkileşimi, elektrokimya, voltametri

***Correspondence:** sedanur6@gmail.com, **Phone:** +90 507 444 16 07, **ORCID-ID:** orcid.org/0000-0002-7816-3155

Received: 07.01.2021, **Accepted:** 28.02.2021

INTRODUCTION

The interaction of small molecules, such as drugs, with DNA is important in pharmaceutical sciences.[1,2] Such interactions can occur in a covalent or non-covalent manner. In covalent interactions, the bonding of a drug to DNA is irreversible, causing cell death.[3] In non-covalent interactions, the bonding is reversible. A non-covalent interaction occurs mainly in three ways: Intercalation, groove binding, and electrostatic interaction.[4] Among them, intercalation is the most powerful interaction mechanism. In minor groove binding, a close interplay with the groove wall occurs, and hydrogen bonds form between drugs and DNA. In a major groove, hydrogen binds to DNA, forming a DNA triplex. In electrostatic interactions, the interaction occurs between the molecule and negatively charged phosphates (PBS) yerine negatively charged phosphates.[5] The interaction between drugs and DNA can be monitored using voltammetry,[6] electrochemical impedance spectroscopy,[7] ultraviolet-visible spectroscopy,[8] fluorescence spectroscopy,[9] high-performance liquid chromatography (HPLC),[10] fourier transform infrared and Raman spectroscopy,[11] surface plasmon resonance,[12] and molecular modeling methods.[13] Among them, electrochemical methods, such as voltammetry and impedimetry, are generally preferred owing to their low cost, rapidness, and high sensitivity. In addition, compared with optical, chromatographic, or other transducers, electrochemical transduction is more dynamic and tunable.

Linagliptin (Lin) is a drug used for curing type 2 diabetes mellitus.[14] Lin can be electrochemically detected through cyclic voltammetry (CV) and square wave voltammetry using Fe_2O_3-modified carbon paste electrodes,[15] and Co_3O_4 nanoparticles, and multiwalled carbon nanotubes-modified carbon paste electrodes.[16] Spectrofluorometric[17] and HPLC methods[18] have also been reported for Lin quantification in human plasma and rat plasma, respectively. In addition, the HPLC-DAD method for Lin quantification in the presence of its degradation products in tablets has been studied.[19]

Herein, for the first time, we detected the interaction of Lin with DNA electrochemically using differential pulse voltammetry (DPV). In our study, the electrochemical properties of Lin were analyzed in the first step. Subsequently, we examined the oxidation signals of the adenine bases of DNA before and after the interaction with Lin. As DNA can acts as a molecular wire or a conductive bridge, the intrinsic electro-activity of DNA bases, such as adenine and guanine, could be used as an indicator for drug-DNA interaction in a label-free assay. In our study, we explored how the presence of Lin influenced the oxidation of adenine. Upon interaction with Lin, adenine oxidation currents decreased dramatically. In addition, experimental parameters, such as the concentration, pH of the supporting electrolyte, and immobilization time, were optimized to obtain the maximum current signals.

MATERIALS AND METHODS

Equipment

AUTOLAB apparatus connected to NOVA software (Metrohm, The Netherlands) was used for performing the voltammetric measurements. In all the experiments, pencil graphite electrodes (PGEs), Ag/AgCl, and platinum wire were used as the working, reference, and auxiliary electrodes, respectively.

DNA and Lin

Fish sperm double-stranded DNA (dsDNA) was purchased from Sigma-Aldrich (Germany). Stock solutions of DNA were prepared with tris-EDTA buffer (TE, pH: 8.0) and stored at -20 °C. Lin was purchased from Sigma-Aldrich, and 1 mg/mL of Lin stock solution was prepared with ultrapure water. During the experiments, 0.5-M acetate [(ACB), pH: 4.8], 0.05-M (PBS, pH: 7.4), and 0.1-M sodium borate (pH: 8.1) buffers containing 0.02-M NaCl were used.

Method

Figure 1 shows the scheme for the experimental steps.

Activation

+1.4 V was applied to PGEs for 30 s in ACB for activation.

DNA and its immobilization (when only DNA is immobilized)

The stock solutions of DNA were diluted with ACB. The activated electrodes were immersed in 200 µg/mL of DNA solution for 1 h, and the electrodes were rinsed with ACB.

Lin and its immobilization (when only Lin is immobilized)

The stock solutions of Lin were diluted with ACB. The activated electrodes were immersed in 600 µg/mL of the drug solution

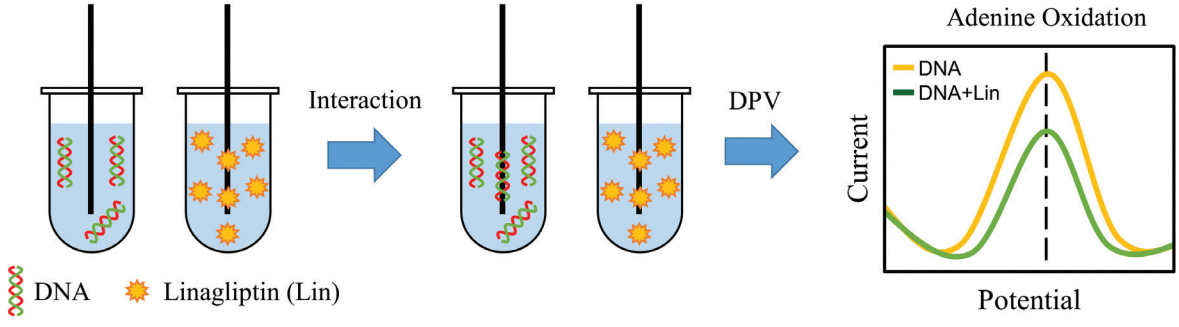

Figure 1. Experimental steps for the electrochemical detection of the interaction between DNA and Lin
DPV: Differential pulse voltammetry

for 1 h in the dark. Subsequently, the Lin-immobilized electrodes were rinsed with ACB.

Interaction

400 µg/mL of DNA and 1200 µg/mL of Lin were mixed in the ratio of 1:1 in ACB. Thus, 200 µg/mL of DNA and 600 µg/mL of Lin solutions were obtained. Subsequently, 100 µL of the solution was transferred into the vials. The electrodes were immersed in these vials for 1 h in the dark. Finally, the modified electrodes were rinsed with ACB.

Measurement

DPV measurements were carried out from +0.4 to +1.4 V at a scan rate of 50 mV/s in ACB.

Statistical analysis

No standard statistical procedure was performed in the current study.

RESULTS and DISCUSSION

The electrochemical oxidation of DNA has been performed using carbon electrodes, among which PGEs have been applied to the largest extent.[20] DNA bases are oxidized electrochemically at graphite electrodes, resulting in well-separated oxidation peaks on differential pulse voltammograms. The purine bases, such as guanine and adenine are negatively charged; on the other hand, the pyrimidine bases, such as cytosine and thymine, are positively charged.[21] Consequently, the oxidation potential of guanine and adenine that is much lower when compared to the oxidation potential of cytosine and thymine.[22] In general, the more negative peak (+1.0 V vs. Ag/AgCl) corresponds to the electro-oxidation of guanine, whereas the more positive peak (+1.2 V vs. Ag/AgCl) belongs to electro-oxidation of adenine. A dramatic decrease/increase at the oxidation/reduction peak currents of the drug (if the drug can be oxidized or reduced) or DNA, or potential shifts to the more positive or negative values can be used for the proof of interaction. Optimization studies for DNA, such as the concentration, immobilization time, and buffer prepared, were performed, and the corresponding results are shown in Figure 2.

To obtain maximum surface coverage, 25-200 µg/mL of DNA were adsorbed on the PGEs. As shown in Figure 2A, the peak currents of adenine increased with DNA concentrations (only linear values are shown in Figure 2A). A gradual increase was obtained until 200 µg/mL of DNA at PGE, and after this concentration, there was almost no change in the response. Thus, a DNA concentration of 200 µg/mL was selected as the optimum DNA concentration.

The limit of detection (LOD) and the limit of quantification (LOQ) were calculated in the concentration range between 25 and 200 µg/mL of DNA. According to the calibration plot (Figure 2A), LOD and LOQ for DNA were calculated to be 6.7 and 22.3 µg/mL, respectively, using the equation LOD: 3 s/m, and LOQ: 10 s/m (s is the standard deviation for the blank solution, and m is the slope of the related calibration curve).[23]

Figure 2B shows the histograms of adenine oxidation currents as a function of immobilization time of DNA on the electrodes from 40 to 120 min. Adenine oxidation currents slightly increased with time and remained nearly unchanged after 60 min. As shown, long immobilization duration had no remarkable effect on the response. Thus, 60 min was selected.

The effect of the buffer solution where DNA prepared was investigated. Figure 2C shows the results. Clearly, the highest guanine (+1.0 V) and adenine (+1.2 V) oxidation currents were obtained with ACB and further experiments were performed in ACB for the preparation of DNA solution.

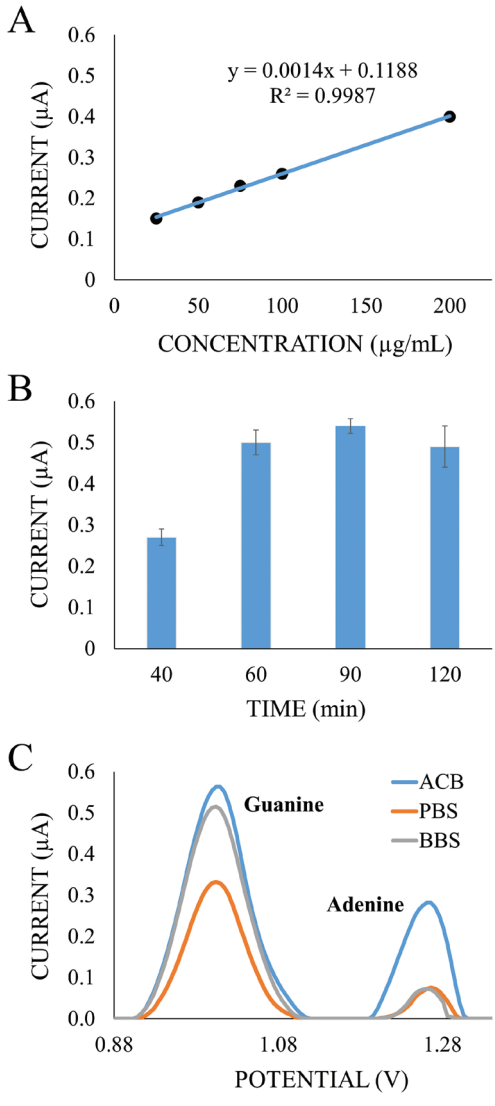

Figure 2. DNA optimization studies: (A) Calibration plot presenting adenine oxidation currents for DNA concentrations ranging from 25 to 200 µg/mL. (B) Histograms for average adenine oxidation currents for different immobilization times of DNA on the activated PGEs surface, e.g., 40 to 120 min. (C) Differential pulse voltammograms of guanine and adenine oxidation currents obtained from different buffers where DNA prepared

PGEs: Pencil graphite electrodes

In Figure 3A, a differential pulse voltammogram is shown for the oxidation of Lin by scanning from +0.7 to +1.1 V vs. Ag/AgCl in ACB. As shown in Figure 3A, Lin has an irreversible anodic peak at nearly +0.9 V. Lin's chemical structure is also shown in Figure 3B. As shown previously, one proton could involve to the oxidation process resulting from the oxidation of amine group of piperidine ring.[16]

To optimize oxidation signals of Lin, various concentrations from 100 to 600 µg/mL of Lin were prepared, and their oxidation currents were measured with DPV (only calibration plot-linear values were showed in Figure 4A). As shown in Figure 4A, Lin oxidation currents obtained from nearly +0.9 V signals were increased with the increased Lin concentration. The highest and reproducible Lin oxidation currents were measured in the presence of 600 µg/mL of Lin, and thus, this concentration was selected as the optimum concentration.

LOD and LOQ were calculated in the concentration range between 100 and 600 µg/mL of Lin. According to the calibration plot (Figure 4A), LOD and LOQ for Lin were calculated to be 21.5 and 71.67 µg/mL, respectively.

The immobilization time, another parameter affecting the oxidation currents of Lin, was examined in the range of 5-120 min (Figure 4B). Lin oxidation current increased with time and remained nearly unchanged after 60 min. Therefore, Lin immobilization time was chosen as 60 min.

The effect of pH of the supporting electrolytes on the oxidation peak currents was investigated in the pH range from 3.7 to 9.8 (Figure 4C). The Lin oxidation currents disappeared at pH 9.8. Therefore, we used three pH values (3.7, 4.8, and 7.4) to analyze the effect of pH. As shown in Figure 4C, the peak potential shifted toward more negative values as pH increased, demonstrating the involvement of protons during the oxidation process.[24] The highest peak current was observed in pH: 4.8, and thus, this supporting electrolyte was chosen.

Over the pH range 3.7-7.4, the anodic peak potential (Ep_a) of Lin varied linearly as a function of pH (Figure 4D). According to Ep_a-pH behavior results, the equation is as follows:

$Ep_a = -0.0189\ pH + 1.02\ R^2 = 0.9997$ (equation 1)

The slope of equation 1 (19 mV/pH) is far from the ideal slope value of 59 mV/pH, which suggests that the number of transferred protons and electrons are not equal. According to the literature, this result can be explained due to deprotonation or adsorption oxidation products that block electrode surface.[25]

The effect of scan rate (ν) on Lin oxidation currents was also analyzed with CV. The peak currents (Ip_a) of Lin increased with increasing scan rate (10 to 100 mV/s). According to the results, the equation is as follows:

$\log Ip_a = 0.6098 \log (\nu) + 0.746\ (R^2 = 0.9756)$ (equation 2)

According to equation 2, the slope of the above equation (0.6) is close to the theoretical value of 0.5, which showed the occurrence of a diffusion-controlled electrode process.[26]

The relationship of Ep_a between scan rates was analyzed with CV. According to the results, the equation is as follows:

$Ep_a = 0.0478 \log (\nu) + 1.0426\ (R^2 = 0.9618)$ (equation 3)

The peak potential shifted slightly positively with increasing scan rate (10 to 100 mV/s). This indicates that an irreversible electrochemical process has occurred.[27]

The relationship of the peak currents of Lin (Ip_a) between roots of scan rate ($\nu^{1/2}$) was also analyzed. According to the results, the equation is as follows:

$Ip_a\ (\mu A) = 3.5219\ (\nu)^{1/2} + 0.0598\ (R^2 = 0.9808)$ (equation 4)

The linear increase in Ip_a with the $\nu^{1/2}$ indicates a diffusion-controlled redox process.[25]

The mechanism of interaction between drug molecules and DNA could be explored in three different ways. The first one is the evaluation of the changes in the electrochemical responses of DNA before and after the interaction with drugs. In addition, the interaction could be assessed by obtaining a dramatic decrease/increase at the drug's oxidation/reduction peak currents, which selectively binds to DNA. In general, the appearance or disappearance of redox signals in typical voltammograms of the drug of interest after incubating with DNA in an electrochemical cell is preferred. Finally, potential

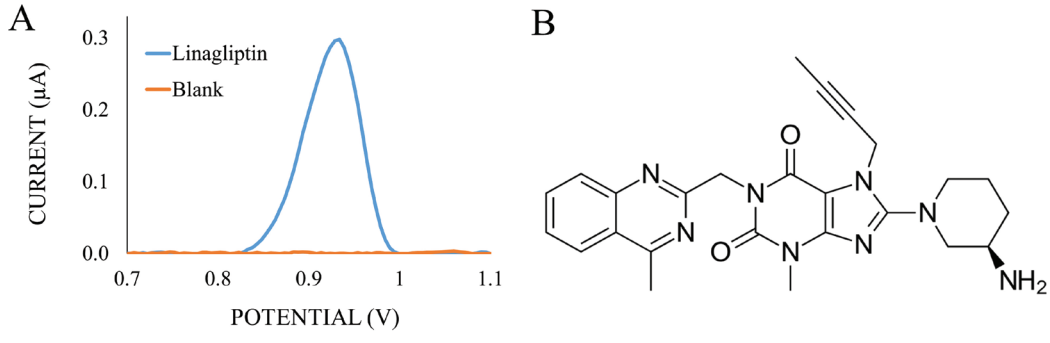

Figure 3. (A) Differential pulse voltammograms for oxidation currents of Lin obtained at nearly +0.9 V in ACB. (B) Chemical structure of Lin molecule
ACB: 0.5-M acetate

shifts to the more positive or negative side by the intercalation of nucleic acid-binding molecules into DNA could help understand the underlying mechanism of the interaction.

Our study aimed to investigate the interaction between DNA and Lin and to understand the interaction mechanism. Hence, interaction studies were performed. To optimize DNA-Lin interaction, different interaction times from 30 to 90 min were performed. Figure 5A shows the results. In the study, 400 µg/mL of DNA and 1200 µg/mL of Lin were mixed in a ratio of 1:1 in ACB. Thus, 200 µg/mL of DNA and 600 µg/mL of Lin solutions were obtained. Subsequently, 100 µL of the solution was transferred into the vials, and these vials were kept at interaction times ranging from 30 to 90 min. The adenine oxidation signal was measured as 0.51 (for 30 min), 0.72 (for 60 min), and 0.61 µA (for 90 min) before DNA-Lin interaction. After the interaction between DNA and Lin, the adenine oxidation signals were 0.25 (for 30 min), 0.32 (for 60 min), and 0.33 µA (for 90 min). The highest difference between before and after the signal was observed with 60 min. Therefore, the optimum interaction time was selected as 60 min.

After finding the optimum conditions, the interaction between DNA and Lin was performed to investigate the behavior of Lin on DNA to understand how Lin could interact with DNA (Figure 5B). The Lin-DNA interaction was investigated in comparison to the alterations in the adenine oxidation currents in the absence and presence of Lin. In our study, guanine currents were not analyzed because their signals were close to Lin oxidation signals and could interfere.

After the interaction with Lin, adenine oxidation signals were decreased. The adenine peak potential did not shift after the interaction. We assumed that the interaction of DNA with Lin leading to conformational changes in the DNA structure followed by the interaction of Lin to the adenine bases, which attenuates the electrochemical signal of adenine. This phenomenon could be explained by the shielding of the oxidizing groups of adenine or fewer base molecules being available for oxidation.[28]

According to the results based on adenine signals obtained from Figure 5B, the toxicity effect (S %) of Lin on DNA was calculated using equation 5:[29]

$$S\ \% = (S_a/S_b) \times 100 \qquad \text{(equation 5)}$$

S %: Percentage of the adenine peak current change,

S_a: Height of the adenine peak current after the interaction with Lin,

S_b: Height of the adenine peak current before the interaction with Lin.

Generally, if the S % value is more than 85, it is assumed to be non-toxic. If this value is between 50 and 85, it could be moderately toxic, and if less than 50, it is considered toxic. With this equation, the S % value was calculated to be 44%, demonstrating the toxicity of Lin to DNA.

Based on our voltammetric measurements and toxicity calculation, Lin could have toxic effects on DNA.

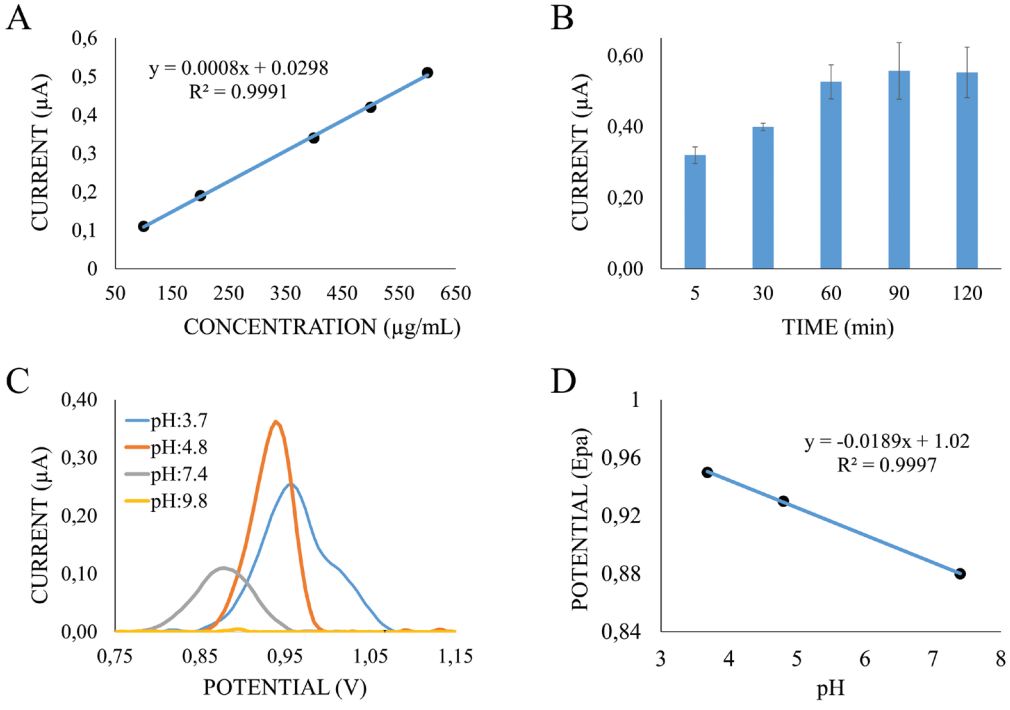

Figure 4. Lin optimization studies. (A) Calibration plot presenting Lin oxidation currents from 100 to 600 µg/mL of Lin. (B) Histograms for average Lin oxidation currents for different immobilization time of Lin on the activated PGEs surface, e.g., 5 to 120 min. (C) Differential pulse voltammograms of Lin oxidation currents from different supporting electrolytes with pH ranging from 3.7 to 9.8. (D) Plots of Ep_a vs. pH

Lin: Linagliptin, PGEs: Pencil graphite electrodes, Ep_a: Anodic peak potential

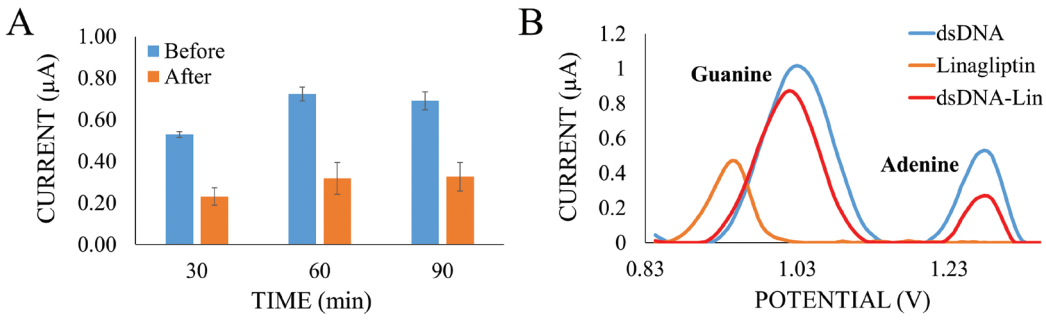

Figure 5. Interaction of DNA and Lin. (A) Histograms for average adenine oxidation signals for different interaction times between Lin and DNA e.g., 30 to 90 min. (B) Differential pulse voltammograms of guanine and adenine oxidation currents after interaction with Lin

Lin: Linagliptin, dsDNA: Double-stranded DNA

CONCLUSION

This is the first study demonstrating the electrochemical detection of the interaction between DNA and Lin using electrochemical techniques. The electrochemical properties of Lin were investigated, and the effects of DNA-Lin interaction have been explored in comparison with the alterations in the adenine oxidation peak. The interaction that occurred in the solution phase was characterized by the change in the adenine oxidation peak current before and after the incubation. According to our study, the diffusion-controlled irreversible redox process involving independent oxidation was revealed for Lin. After the interaction with Lin, the adenine oxidation signals of DNA decreased as proof of interaction. The adenine peak potential did not shift after the interaction with Lin. Our results also showed that Lin is toxic to dsDNA.

Conflict of interest: No conflict of interest was declared by the authors. The authors are solely responsible for the content and writing of this paper.

REFERENCES

1. Guarra F, Marzo T, Ferraroni M, Papi F, Bazzicalupi C, Gratteri P, Pescitell, G, Messori L, Biver T, Gabbiani C. Interaction of a gold(ı) dicarbene anticancer drug with human telomeric DNA G-quadruplex: solution and computationally aided X-ray diffraction analysis. Dalton Trans. 2018;47:16132-16138.
2. Morawska K, Poplawski T, Ciesielski W, Smarzewska S. Electrochemical and spectroscopic studies of the interaction of antiviral drug Tenofovir with single and double stranded DNA. Bioelectrochemistry. 2018;123:227-232.
3. Sirajuddin M, Ali S, Badshah A. Drug-DNA interactions and their study by UV-Visible, fluorescence spectroscopies and cyclic voltametry. J Photochem Photobiol B. 2013;124:1-19.
4. Topkaya SN, Cetin AE. Determination of Electrochemical interaction between 2-(1H-benzimidazol-2-yl) phenol and DNA sequences. Electroanalysis. 2019;31:1554-1561.
5. Shahabadi N, Fili SM, Kheirdoosh F. Study on the interaction of the drug mesalamine with calf thymus DNA using molecular docking and spectroscopic techniques. J Photochem Photobiol B. 2013;128:20-26.
6. Lima D, Hacke ACM, Inaba J, Pessôa CA, Kerman K. Electrochemical detection of specific interactions between apolipoprotein E isoforms and DNA sequences related to Alzheimer's disease. Bioelectrochemistry. 2020;133:107447.
7. Ensafi AA, Kazemnadi N, Amini M, Rezaei B. Impedimetric DNA-biosensor for the study of dopamine induces DNA damage and investigation of inhibitory and repair effects of some antioxidants. Bioelectrochemistry. 2015;104:71-78.
8. Bi S, Yan L, Wang Y, Pang B, Wang T. Spectroscopic study on the interaction of eugenol with salmon sperm DNA in vitro. J Lumin. 2012;132:2355-2360.
9. Kirsch P, Jakob V, Elgaher WAM, Walt C, Oberhausen K, Schulz TF, Empring M. Discovery of Novel Latency-Associated Nuclear Antigen Inhibitors as Antiviral Agents Against Kaposi's Sarcoma-Associated Herpesvirus. ACS Chem Biol. 2020;15:388-395.
10. Khan RA, Arjmand F, Tabassum S, Monari M, Marchetti F, Pettinari C. Organometallic ruthenium(II) scorpionate as topo IIα inhibitor; in vitro binding studies with DNA, HPLC analysis and its anticancer activity. J Organomet Chem. 2014;771:47-58.
11. Asghar F, Fatima S, Rana S, Badshah A, Butler IS, Tahir MN. Synthesis, spectroscopic investigation, and DFT study of N,N'-disubstituted ferrocene-based thiourea complexes as potent anticancer agents. Dalton Trans. 2018;47:1868-1878.
12. Loo FC, Ng SP, Wu CML, Kong SK. An aptasensor using DNA aptamer and white light common-path SPR spectral interferometry to detect cytochrome-c for anti-cancer drug screening. Sens Actuators B Chem. 2014;198:416-423.
13. Adeniji SE, Adamu Shallangwa G, Ebuka Arthur D, Abdullahi M, Mahmoud AY, Haruna A. Quantum modelling and molecular docking evaluation of some selected quinoline derivatives as anti-tubercular agents. Heliyon. 2020;6:e03639.
14. McGill JB. Linagliptin for type 2 diabetes mellitus: a review of the pivotal clinical trials. Ther Adv Endocrinol Metab. 2012;3:113-124.
15. El-Shal MA, Azab SM, Hendawy HAM. A facile nano-iron oxide sensor for the electrochemical detection of the anti-diabetic drug linagliptin in the presence of glucose and metformin. Bulletin of the National Research Centre. 2019;43:95.
16. Rizk M, Attia AK, Mohamed HY, Elshahed MS. Validated voltammetric method for the simultaneous determination of anti-diabetic drugs,

linagliptin and empagliflozin in bulk, pharmaceutical dosage forms and biological fluids. Electroanalysis. 2020;32:1737-1753.

17. Aref HA, Hammad SF, Elgawish MS, Darwish KM. Novel spectrofluorimetric quantification of linagliptin in biological fluids exploiting its interaction with 4-chloro-7-nitrobenzofurazan. J Lumin. 2020;35:626-635.
18. Hanafy A, Mahgoub H. A Validated HPLC method for the determination of linagliptin in rat plasma. Application to a pharmacokinetic study. J Chromatogr Sci. 2016;54:1573-1577.
19. Mourad SS, El-Kimary EI, Hamdy DA, Barary MA. Stability-indicating HPLC-DAD method for the determination of linagliptin in tablet dosage form: application to degradation kinetics. J Chromatogr Sci. 2016;54:1560-1566.
20. Ahmadi M, Ahour F. An electrochemical biosensor based on a graphene oxide modified pencil graphite electrode for direct detection and discrimination of double-stranded DNA sequences. Analytical Methods. 2020.
21. Zhang Y, Zhang WB, Liu C, Zhang P, Balaeff A, Beratan DN. DNA charge transport: Moving beyond 1D. Surface Science. 2016;652:33-38.
22. Kogikoski S, Paschoalino WJ, Cantelli L, Silva W, Kubota LT. Electrochemical sensing based on DNA nanotechnology. Trends Anal Chem. 2019;118:597-605.
23. J. N. miller JCm. Statistics and Chemometrics for Analytical Chemistry: 5th pearson education, Essex, London 2005. 121 p.
24. Aftab S, Kurbanoglu S, Ozcelikay G, Bakirhan NK, Shah A, Ozkan SA. Carbon quantum dots co-catalyzed with multiwalled carbon nanotubes and silver nanoparticles modified nanosensor for the electrochemical assay of anti-HIV drug Rilpivirine. Sensors and Actuators B: Chemical. 2019;285:571-583.
25. Fekry AM, Shehata M, Azab SM, Walcarius A. Voltammetric detection of caffeine in pharmacological and beverages samples based on simple nano- Co (II, III) oxide modified carbon paste electrode in aqueous and micellar media. Sensors and Actuators B: Chemical. 2020;302:127172.
26. Mahmoud BG, Khairy M, Rashwan FA, Banks CE. Simultaneous voltammetric determination of acetaminophen and isoniazid (hepatotoxicity-related drugs) utilizing bismuth oxide nanorod modified screen-printed electrochemical sensing platforms. Analytical Chemistry. 2017;89:2170-2178.
27. Mohamed MA, El-Gendy DM, Ahmed N, Banks CE, Allam NK. 3D spongy graphene-modified screen-printed sensors for the voltammetric determination of the narcotic drug codeine. Biosensors and Bioelectronics. 2018;101:90-95.
28. Rauf S, Nawaz H, Akhtar K, Ghauri MA, Khalid AM. Studies on sildenafil citrate (Viagra) interaction with DNA using electrochemical DNA biosensor. Biosensors and Bioelectronics. 2007;22:2471-2477.
29. Bagni G, Osella D, Sturchio E, Mascini M. Deoxyribonucleic acid (DNA) biosensors for environmental risk assessment and drug studies. Analytica Chimica Acta. 2006;573-574:81-89.

Turk J Pharm Sci 2021;18(5):652-664
DOI: 10.4274/tjps.galenos.2020.59319

REVIEW

Nanoemulsions as Ophthalmic Drug Delivery Systems

Oftalmik İlaç Taşıyıcı Sistemler Olarak Nanoemülsiyonlar

Rasha Khalid DHAHIR, Amina Mudhafar AL-NIMA*, Fadia Yassir AL-BAZZAZ

Department of Pharmaceutics, College of Pharmacy, University of Mosul, Mosul, Iraq

ABSTRACT

Nanoemulsions are liquid-in-liquid dispersion with a droplet size of about 100 nm. They have a transparent appearance, high rate of bioavailability, and increased shelf life. Nanoemulsions mainly consist of oil, water, surfactant, and cosurfactant and can be prepared by high- and low-energy methods. Diluted nanoemulsions are utilized for the delivery of ophthalmic drugs due to their capability to penetrate the deep layers of the ocular structure, provide a sustained release effect, and reduce the frequency of administration and side effects. These nanoemulsions are subjected to certain tests, such as safety, stability, pH profile, rheological studies, and so on. Cationic nanoemulsions are prepared for topical ophthalmic delivery of active ingredients from cationic agents to increase the drug residence time on the ocular surface, reducing their clearance from the ocular surface and improving drug bioavailability. This review article summarizes the main characteristics of nanoemulsions, ophthalmic nanoemulsions, and cationic nanoemulsions and their components, methods of preparation, and the evaluation parameters for ophthalmic nanoemulsions.

Key words: Nanoemulsion, cationic nanoemulsions, ophthalmic drug delivery

ÖZ

Nanoemülsiyonlar, yaklaşık 100 nm'lik bir damlacık boyutuna sahip sıvı içinde sıvı dispersiyonudur. Şeffaf bir görünüme, yüksek biyoyararlanıma ve artırılmış raf ömrüne sahiptirler. Nanoemülsiyonlar esas olarak yağ, su, yüzey aktif madde ve yardımcı yüzey aktif maddeden oluşur ve yüksek ve düşük enerjili yöntemlerle hazırlanabilir. Seyreltilmiş nanoemülsiyonlar, oküler yapının derin katmanlarına nüfuz etme, sürekli salım etkisi sağlama ve uygulama sıklığını ve yan etkileri azaltma kabiliyetleri nedeniyle oftalmik ilaçların verilmesi için kullanılır. Bu nanoemülsiyonlar, güvenlik, stabilite, pH profili, reolojik çalışmalar vb. gibi belirli testlere tabi tutulur. Katyonik nanoemülsiyonlar, ilacın oküler yüzey üzerinde kalış süresini artırmak, oküler yüzeyden klirensini azaltmak ve ilaç biyoyararlanımını geliştirmek için katyonik ajanlardan aktif bileşenlerin topikal olarak oftalmik taşınımı için hazırlanır. Bu derleme, nanoemülsiyonların, oftalmik nanoemülsiyonların ve katyonik nanoemülsiyonların temel özelliklerini ve bileşenlerini, hazırlama yöntemlerini ve oftalmik nanoemülsiyonlar için değerlendirme parametrelerini özetlemektedir.

Anahtar kelimeler: Nanoemülsiyon, katyonik nanoemülsiyonlar, oftalmik ilaç verilmesi

INTRODUCTION

Ophthalmic drug delivery system is one of the most important routes of drug administration, but it is regarded as a challenging attempt encountered by pharmaceutical scientists.[1] Most ophthalmic diseases are treated by topical eye drop instillation; however, several problems, such as poor bioavailability, are associated with these formulations.[2]

The drug is removed from the precorneal area within several minutes after instillation due to lacrimal secretion and nasolacrimal drainage.[3,4]

Various problems, including the issue on stability, high cost, and tedious preparation methods, are associated with the scalingup of nanoemulsions.[5]

*Correspondence: amnah.mudhafar@uomosul.edu.iq, Phone: 009647736976794, ORCID-ID: orcid.org//0000-0003-4090-0698
Received: 16.03.2020, Accepted: 22.06.2020

For the above reasons, pharmaceutical scientists attempt to formulate ophthalmic preparations that can overcome such problems. Although the incorporation of drugs in different pharmaceutical vehicles, such as ointments, suspensions, and emulsions, can improve the bioavailability and provide sustained drug release, they cannot be regarded as the formulation of choice given their ocular adverse effects, including irritation, redness of the eye, interference with vision, and low product stability. In addition, chronic administration may increase systemic availability and cause severe systemic complications. Formulations containing preservatives also induce adverse reactions upon systemic absorption.[3,6,7]

Nanotechnology is one of the most important promising approaches for ophthalmic drug delivery. This technology is currently being applied for drug delivery to the anterior and posterior segments of the eye. Nanotechnology-based systems with an appropriate particle size can be formulated to ensure low irritation to the patient's eye, adequate bioavailability, and compatibility with the ocular tissue. Such systems are an excellent approach for the delivery of lipophilic drugs, which involves the application of cationic nanoemulsion, benefitting from the negatively charged corneal and conjunctival cells that can prolong the drug residence time on the ocular surface and improve drug absorption and bioavailability.[8,9]

Barriers for intraocular drug transport

Each layer of the ocular tissue has distinct features and poses a diverse barrier following drug administration via a certain route (Figure 1).[10]

Tears

Tears can influence the administration of ophthalmic drugs through binding with the administered drug, resulting in enhanced clearance and drug dilution. Tear turnover is one of the dynamic barriers that significantly decrease drug availability, leading to inhibition of therapeutic effect.[1,11]

Cornea

The cornea, which is a non-vascular structure, consists of three main layers: the outer epithelial layer which is a lipophilic layer, the middle stromal layer which is hydrophilic in nature, and the inner endothelial layer that separates the aqueous humour and the stroma.[5] The corneal epithelium forms the most important barrier to drug absorption by topical administration; the corneal cells of glycosyl amino glycans lining the ocular surface are negatively charged at physiological pH.[5,6] When applying a positively charged formulation to the eye, an electrostatic

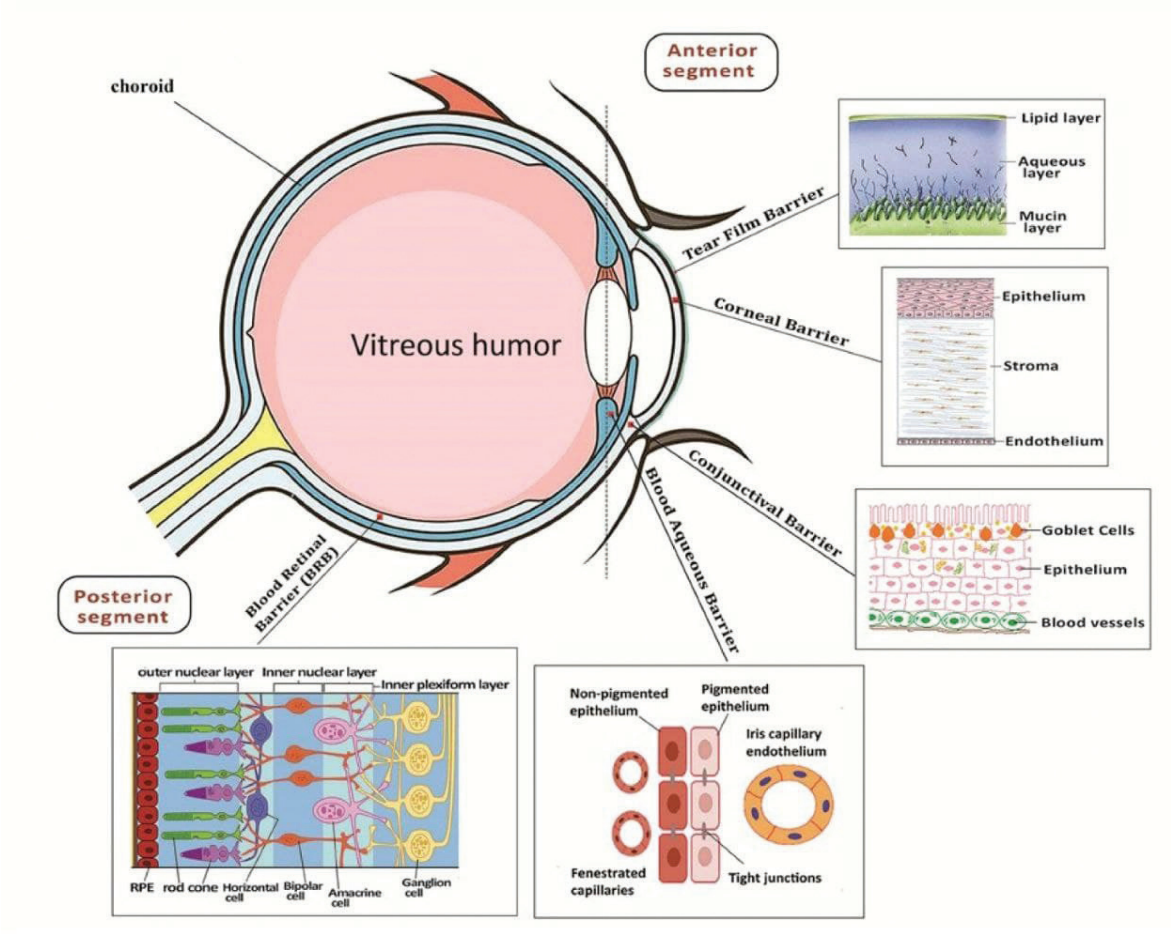

Figure 1. Ocular barriers for drug transport[10]

Permission has been obtained from the author for the use of the figure

attraction will possibly occur, which will prolong the residence time of the formulation on the ocular surface.[5,12]

Conjunctiva

The conjunctiva of the eye is a thin layer that lines the inside of eyelids and maintains the tear film. The stroma between the outer conjunctival epithelium and inner sclera has an abundance of blood and lymphatic vessels throughout the subconjunctiva, and it acts as a dynamic barrier to hydrophobic drug absorption. Given the rich capillaries and lymphatic vessels in the stroma, the drug administered to the conjunctival sac can be rapidly cleared.[8,12] The conjunctival epithelium is more penetrable to larger molecules and has 20 times larger surface area than the cornea because of its wider intercellular spaces. The conjunctival pathway favors the absorption of large hydrophilic molecules (with molecular weight nearly less than 20 kDa), such as proteins and peptides, different from the corneal route which favors lipophilic small molecules (the majority of drugs). Meanwhile, the retardation of the passive pathway can occur by the tight junctions present in the conjunctival epithelium. Therefore, if drug absorption through the conjunctiva is compared with that through the cornea, the former is considered as non-productive, leading to the low bioavailability of ophthalmic drugs.[11,12]

Sclera

The sclera is the outer layer of the eyeball and is known as the white of the eye. This part can maintain the eye shape through its fibrous structure. The hydrophobic nature of drugs affects the permeability of sclera; when the lipophilicity of a drug increases, the permeability across the sclera will decrease, and vice versa.[8] Moreover, the permeation of therapeutic molecules, including drugs, depends on the hydration degree of sclera and its intraocular pressure. Intraocular pressures in the normal range of 15-20 mmHg have negligible effects on permeability, whereas the trans-scleral permeability of solute molecules is affected by their high intraocular pressure up to (>20-60 mmHg).[11]

Choroid/Bruche's membrane

This part of the eye is regarded as the most vascularized part of the body. The choroidal thickness decreases with age. By contrast, the thickness of Bruch's membrane increases with age, and the changes in the thickness of choroid and Bruch's membrane may affect drug penetration into the retina.[8] With aging, the choroid becomes thinner, and the Bruch's membrane becomes thicker, leading to alteration in the barrier property which in turn alters drug permeation of drug molecules over the years.[11]

Retina

The retina is located at the back of the eye, on which an image is formed from the light that enters the eye from the cornea, passing across the anterior part until it reaches the retina in the posterior part of the eye, where it can then be interpreted in the brain. The retina may be subjected to diseases that affect the posterior segment of the eye, such as age-related macular degeneration and diabetic retinopathy. All of the drugs in the vitreous can be eliminated by anterior and posterior route; the drugs can be eliminated across the retina after passing through the internal limiting membrane that separates the retina and the vitreous.[8,9]

CD44 is over expressed on the retina surface and is important in targeting a number of drugs and gene-based therapeutics.

Table 1. Anatomical barriers for intraocular drug transport[13]

Anatomical barriers	Characteristics
Cornea	Epithelium is a major barrier to passage of hydro-philic drugs; tight intercellular junctions restrict paracellular diffusion. Stroma is a barrier to passage of highly lipophilic drugs.
Tear	Drugs bind with mucin, dilution of topical drugs. Induced lacrimation and tear film turnover increase drug clearance.
Conjunctiva	More permeable than cornea to hydrophilic drugs and macromolecules; has greater surface area. Epithelium-tight intercellular junctions.
Sclera	Hydrated stroma better absorption of hydrophilic drugs. More permeability to macromolecules. Molecular radius is an important parameter to determine permeation.
Choroid	Receives less blood flow, resulting in less drug permeation from the systemic circulation. Choroid Bruch's membrane limits permeation of lipophilic drugs.
Vitreous humour	Hyaluronan- is more permeable to anionic drugs (due to negatively charge). Large, lipophilic/hydrophilic drugs retained more in vitreous humor.
Retina	Permeable to small, lipophilic, or hydrophilic molecules. Inner limiting membrane limits entry of drugs from vitreous into retina.
Blood ocular barriers	Blood aqueous barrier- tight junctions limit entry of solutes into aqueous humour and entry of hydrophilic drugs from plasma into aqueous humour. Outer blood retinal barrier- major barrier to hydrophilic drugs. Inner blood retinal barrier- major barrier which limits entry of systemic drugs into retina.

Retina demonstrates the presence of 15-20 nm-wide intercellular spaces without tight junctions. As a result, small hydrophilic/lipophilic drugs can permeate the retina. However, large cationic molecules exhibit resistance to permeation in the retina. Inner and outer plexiform layers are major barriers to the diffusion of large molecules in human retina. This condition is supported by observations showing the persistence of hard exudates in hypertensive or diabetic retinopathy for months in the retina because molecules greater than 76 kDa diffuse through the retina very slowly, whereas macromolecules with a molecular weight greater than 150 kDa are arrested by the inner limiting membrane.[10-12]

Table 1 presents all the above barriers and their characteristics.[13]
Main challenges and key considerations in ocular drug delivery

Challenges

The eye is a unique organ anatomically and physiologically, and it contains highly varied structures with independent physiological functions. This complexity of the eye provides special challenges to ocular drug delivery strategies.[13] One of the challenges is the absorption; as with traditional eye drops, ocular bioavailability after topical administration is low at 3%-4% due to the eye's impermeable nature and small surface area. Other challenges include poor drug solubility. Lipophilic drugs cannot be incorporated in conventional aqueous eye drops. For this reason, they must be formulated as suspensions. Regarding patient compliance, frequent instillations are usually needed with eye drops to reach the desired therapeutic range of the drug. High tolerability or comfort demands limit the formulation options. As for excipient choice, limited numbers of expedients are listed in ophthalmology. Finally, the delivery of conventional eye drops to the posterior segment of the eye is impossible.[8,9]

Considerations

Ocular drugs typically achieve <10% ocular bioavailability. If a drug is applied to the outer surface of the eye, it may pass ocular blood barriers where it will encounter metabolizing enzymes and cellular transporters before it reaches the site of action. Thus, the anatomy and physiology of the eye, including the mucus layer, eyelids, metabolism, and blink drainage, must be considered. Other considerations include tear composition, such as enzymes, lipid outer layer, and stability of the tear film; disease state and occurrence of keratitis or inflammation on absorption, drug clearance, and ocular comfort and tolerability of the formulation, including viscosity, drop size, pH, and osmolality. In addition to the above considerations, patient anticipation, squeeze capability, and type of packaging must be accounted for.[8,9,14]

Efflux transporters and ophthalmic drug bioavailability

The primary barriers result in poor absorption of the drug and poor bioavailability, especially for anterior segment ophthalmic drug delivery. Several of these barriers have been identified in epithelial cells of various ocular tissues in humans and rabbits; these barriers include p-glycoprotein (also called multidrug resistance protein 1), multidrug resistance-associated proteins (MRP1, MRP2, MRP3, MRP4, MRP5, MRP6, MRP7, MRP8, and MRP9), lung resistance proteins, and breast cancer resistance proteins. Current studies focus on the role of these barriers in ophthalmic drug delivery.[15,16] Efflux transporters for anticancer drugs, antibiotics (ofloxacin and erythromycin), and steroids are recognized and limit drug bioavailability.[14] However, different studies suggest various concepts, such as the conjugation of drugs to the dendrimer to enable the bypassing of efflux transporters, resulting in an increased drug solubility and therefore increased drug bioavailability. In a study, propranolol (a calcium channel blocker), a well-known substrate of the p-glycoprotein efflux transporter, was conjugated to lauroyl-G3 dendrimers. This conjugation showed enhanced drug solubility.[17] However, the oral application of dendrimers for drug delivery is in its infancy but may emerge as a promising strategy in the future.[18]

Definition of nanoemulsion

Nanoemulsions can be defined as a clear and stable dispersion of oil and water. They are mainly composed of the internal, dispersed, and external phases or the dispersion medium. The surfactant and cosurfactant molecules play an effective role in the formation of nanoemulsions due to their capability to reduce the interfacial tension and create a small particle size due to their function in the formation of stable preparations as a result of the repulsive electrostatic interaction and steric hindrance. In general, surfactants are molecules that have a bipolar structure composed of hydrophilic and hydrophobic parts.[8,19]

Nanoemulsions are colloidal carriers of drug molecules with a droplet size in the range of 500-1000 nm (preferably from 100 nm to 500 nm). As a drug delivery system, they increase the therapeutic efficacy and minimize the adverse effects and toxic reactions of the administered drug.[20,21]

Nanoemulsions can be distinguished from microemulsions in terms of their droplet size and physical stability characteristics. Microemulsions are isotropic and transparent systems that contain spherical droplets of the water or oil phase (diameter range: 10-100 nm) and dispersed in an external oil or water phase, respectively. Microemulsions are thermodynamically more stable than nanoemulsions given the necessity of introducing thermal and/or mechanical energy in the preparation of nanoemulsions (i.e., mixing and heating) and phase separation after a certain period after the preparation of nanoemulsions. This condition is one of the most distinctive differences between microemulsions and nanoemulsions in terms of stability.[20,22]

The preparation of nanoemulsion can be classified into two main classes, namely, high-energy methods such as highpressure homogenization and ultrasonication, and low-energy methods such as phase inversion.[23]

The translucent appearance of nanoemulsions is due to a droplet size of less than 100 nm. With such a small droplet size, the nanoemulsion is thermodynamically unstable during dispersion. The required high-concentration of surfactants results in the sticky texture of the formulation. A yellowish appearance and rancid odor occur after storage due to the presence of phospholipids, which are generally used to stabilize nanoemulsions. Thus, a formulation was developed and

presented to overcome these problems (US6335022b1); this formulation utilizes oxyethylenated and non-oxyethylenated sorbitan fatty esters as surfactants.[16] The contrivers believed that the use of surfactants selected from oxyethylated or nonoxyethylated sorbitan fatty esters with a molecular weight of more than 400 g per mole, which are solid at a temperature of less than 45°C, can result in a stable formulation. In addition, a similar formulation-stabilizing effect can result from amphiphilic lipids from a group of alkaline salts of cholesterol; these formulations can be used as effective delivery vehicles for antiglaucoma, anti-inflammatory, antiviral, and antiallergic effects.[23,24]

The bioavailability of ophthalmic preparations can be improved by enhancing the drug residence time on the cornea through increasing the viscosity of formulations. This effect can be achieved by increasing the fraction of the dispersed oil phase and by incorporating water-soluble polymers, which can form a gel with the continuous aqueous phase. Certain studies demonstrated that caution should be recommended in considering the ideal concentration of water-soluble polymers to obtain the required viscosity with a transparency of the preparation.[25]

Prostaglandins affect a wide range of physiological activities, such as blood pressure, pain awareness, and clotting mechanisms. Several of these analogs are utilized in ophthalmic antiglaucoma preparations, such as travoprost, latanoprost, and bimatoprost. However, such analogs are chemically unstable in aqueous preparations and have a poor water solubility.

Thus, various strategies have been suggested to avoid these challenges. These strategies include pH adjustment and complexation with cyclodextrin to improve solubility and stability. Solubility can also be improved by the addition of benzalkonium chlorides. The problem associated with these preparations is the ocular intolerability associated with the positively charged resultant preparation. Carli et al.[26] discovered that neutral zeta potential and non-toxic preparations can be obtained from a nanoemulsion formulation that consists of prostaglandin containing oil phase as an internal phase and is dispersed in the aqueous external phase, utilizing two or more non-ionic surfactants.[27] Cyclosporin A is used widely for the treatment of dry eye disease. However, precipitation of the drug occurs as a result of its poor solubility in the aqueous medium. In patent disclosures US4649047 and US6582718, the improved formulation of this drug has been reported.[28]

Positively charged ophthalmic preparation strategy is applied by utilizing the negative charge of corneal barriers. United States patent no. 6007826 describes an oil/water preparation consisting of surfactants/lipid; this preparation has a positively charged polar group, resulting in a cationic preparation that can bind strongly to the corneal surface.[29]

Wang et al.[30] and colleagues from Hainan University, China developed coconut oil-in-water emulsions that were formulated using three polysaccharides. The main effects of the ratio of compounded polysaccharides on their apparent viscosity and interfacial activity were studied. Various data, in addition to the physical stability of the formulated emulsions with different compound polysaccharides, were studied. The results showed that emulsions formulated with compound polysaccharides manifested small average particle sizes, and the stability analysis showed that the emulsion formulated by compounding polysaccharides had preferable physical stability.[30]

Components of nanoemulsions

The prime components of nanoemulsions are oil, aqueous phase, and emulsifying agents. Different types of oils, such as medium-chain triglycerides, mineral oils, and vegetal oils including castor oil, can be used in ophthalmic nanoemulsions.[31] Emulsifying agents are important in maintaining product stability because without these agents, the oil and water phases will separate into two layers. These compounds may be surfactants, such as polysorbates, cremophors, poloxamers, tyloxapol, and vitamin E-TPGS. Emulsifying agents should have certain properties, including compatibility with the product and non-toxicity.[5,21]

Desirable properties of emulsifying agents[21,32,33]

1. They should have the capability to reduce the surface tension to less than 10 dyne/cm.

2. They should form a stable and coherent film around the dispersed phase globules to prevent coalescence.

3. They should provide adequate viscosity and zeta potential for optimum stability.

4. They should be effective in low concentration.

Types of films around dispersed globules in nanoemulsions[34,35]

Monomolecular film

The surfactants that stabilize nanoemulsions form a monolayer of ions or adsorbed molecules at the interface, and this monolayer reduces the interfacial tension; to date, a combination of emulsifying agents can be used; such a combination is composed of a hydrophilic emulsifying agent at the aqueous layer and lipophilic one at the lipoid layer to produce a complex film at the interface.[36]

Multimolecular film

A multimolecular film around the droplets is formed by hydrated lyophilic colloids; these agents do not lower the surface tension significantly but can increase emulsion stability through their tendency to enhance the viscosity of the external phase.[34]

Solid particulate film

This type of film is produced by emulsifying agents, which are small solid particles and form a film around the dispersed droplets, hence inhibiting their coalescence.[34,35]

Preparation of nanoemulsions

Two main methods are used for nanoemulsion preparation: High-energy and low-energy methods. Low-energy methods involve changing the composition or temperature, which results in system reversal and the formation of small droplets. The most common low-energy methods are emulsion inversion point (EIP) and phase inversion temperature (PIT) methods.[32,37]

High-energy methods consist of two main steps, which result in the formation of the nanoemulsion. The first step involves the mixing of oil, water, and surfactant for a sufficient period in a simple stirrer system, resulting in the formation of oil/water macroemulsion. The second step includes the conversion of the macroemulsion into a nanoemulsion through a homogenizer, which forces the macroemulsion through a narrow gap; this homogenization is repeated several times until a constant droplet size is achieved (Figure 2a).[22,31,38] Zhang et al.[39] prepared tacrolimus-loaded cationic nanoemulsions by using a highpressure homogenization method. Meanwhile, Dukovski et al.[40] used a microfluidizer and homogenizer to prepare an ibuprofenloaded cationic nanoemulsion.

Different from high-energy methods, low-energy methods start with a water/oil emulsion, which is converted into an oil/water emulsion due to the changes in temperature and composition. The EIP method involves the conversion of a water/oil macroemulsion, which is formed initially at room temperature, into an oil/water nanoemulsion through gradual dilution until it passes over the inversion point, at which transformation occurs. This method requires no energy to form the emulsion owing to the low interfacial tension between the oil and water interface, which results in the formation of small droplets. In the PIT method, the initial water/oil macroemulsion is formed at a temperature higher than the PIT, and conversion occurs after cooling to produce the required oil/water emulsion without the need for energy (Figure 2b).[31,41,42] Figure 2 was used with the personal permission from Gupta et al.[31]

Instability of nanoemulsions[9,21]

1. Flocculation can be defined as an aggregation of small globules to form large floccules.
2. Creaming refers to the settling down or rising up of floccules, which form a concentrated layer. Upon agitation, the emulsion can be reconstituted.
3. Cracking is the permanent instability of a nanoemulsion, in which the internal phase separates as a layer. In this case, upon agitation, the emulsion cannot be reconstituted, and additional amounts of surfactants may be beneficial.

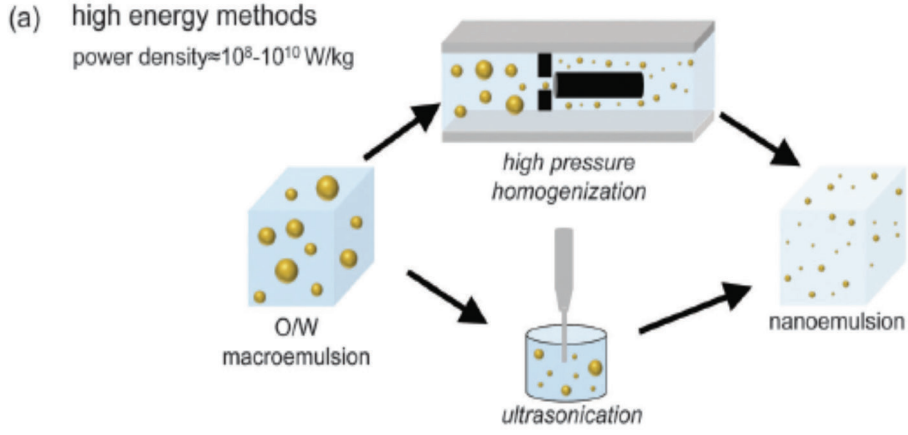

Figure 2a. Overview of high-energy methods, such as high-pressure homogenization and ultrasonication, for the preparation of oil/water nanoemulsion[31]

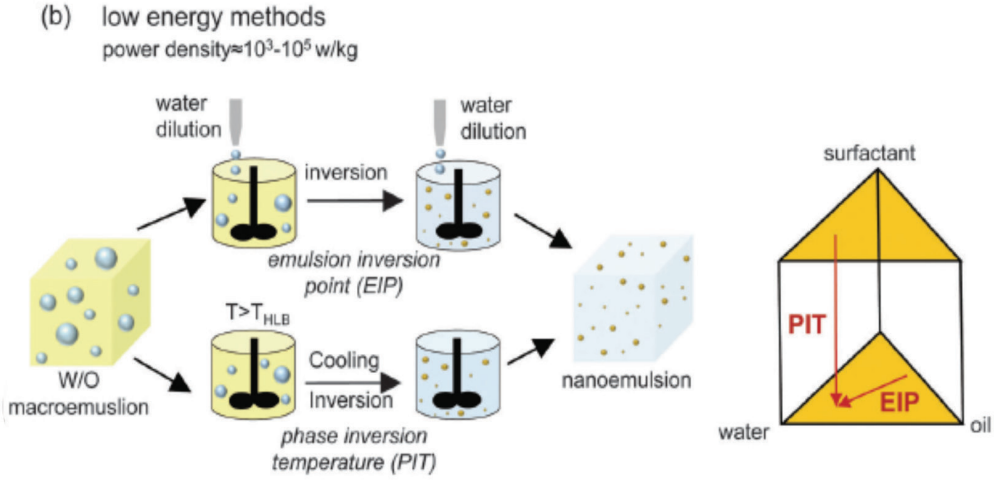

Figure 2b. Overview of low-energy methods for the preparation of oil/water nanoemulsion
Other nanoemulsion preparation methods, such as as bubble bursting, evaporative ripening, and microfluidization, are also employed[31]

4. Miscellaneous instability denotes the instability of a nanoemulsion due to extreme temperature and light. In this scenario, the emulsion should be stored in a tight-colored container.

5. Phase inversion occurs as a result of changes in the volume ratio of phases or addition of electrolytes, which lead to the changes in the emulsion type from water/oil to oil/water, and vice versa.

Important factors during the preparation of nanoemulsions[7-9,34]

One of the most important factor during nanoemulsion preparation is the careful choice of surfactants to achieve an extremely low interfacial tension. The concentration of surfactants must be sufficiently high to stabilize the microdroplets to yield the nanoemulsion. In addition to the above factors, adequate flexibility and fluidity of surfactants should be considered to support the formation of nanoemulsions.

Advantages of nanoemulsions[34,35]

Nanoemulsions enhance drug bioavailability, are non-irritant, non-toxic, and physically stable, and improve drug absorption due to their high surface area and small droplets size. Nanoemulsions can also be formulated in different formulations, dissolve lipophilic drugs, require less amount of energy, and promote taste masking.

Disadvantages of nanoemulsions[34,36]

Nanoemulsions require the addition of large amounts of surfactants and cosurfactants to maintain their stability; they have a limited capacity to solubilize high-melting-point substances. In addition, the toxicity of surfactants should be considered, and different environmental parameters can affect nanoemulsion stability. Table 2 summarizes the advantages and disadvantages of nanoemulsions and several of their physical properties.

Cationic oil-in-water nanoemulsion

Cationic nanoemulsions are preparations that utilize cationic surfactants, which concentrate around the surface of oil droplets to make them positively charged. Owing to the negative nature of the ocular surface, cationic nanoemulsions can improve the residence period of the product in the eye through the electrostatic interaction with the opposite charges of the eye surface mucus layer. Therefore, cationic nanoemulsions probably improve therapeutic efficacy due to an increase in the retention time at the ocular surface.[25,43] Cationic surfactants should have an adequate lipophilicity to be taken in by oil droplets, with a very small amount present in the aqueous phase. These preparations show an important role in prolonging the residence time of drugs on the ocular tissue, which is greater than that observed in anionic oil/water nanoemulsions. In addition to their important biological effects, cationic surfactants can stabilize nanoemulsions and prolong their shelf life through preventing the coalescence of oil droplets (Figure 3) due to their repulsive force.[44,45] Table 3 summarizes several important physicochemical features of a cationic oil/water nanoemulsion.

The reason behind the discovery of these cationic nanoemulsions is that different attempts that had been made to extend drug residence time at the ocular surface; the use of excipients with bioadhesive and viscosity enhancement properties, such as cellulose derivatives and propylene glycol, are associated with problems, including ocular disturbance; excipients are only applicable to hydrophilic drugs; in addition, many lipophilic drugs formulated as topical ocular oily or micellar solutions, ointments, and creams are not only uncomfortable to the patient but also show restricted efficacy.[46]

Protective properties of cationic oil-in-water nanoemulsion vehicle

Regarding lipophilic drugs, the application of cationic nanoemulsions to increase ocular bioavailability through prolonging the drug residence time and spreading properties is accompanied by surprising valuable effects on the ocular surface.[47]

By mixing the oil phase in cationic oil/water nanoemulsions with the lipid layer of the tear film, water evaporation from the

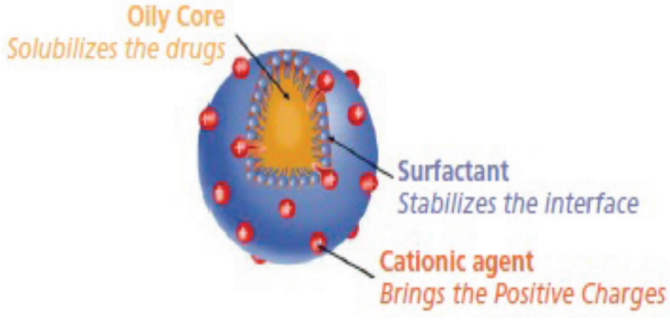

Figure 3. Schematic of one of the oil nanodroplets present in the cationic oil-in-water nanoemulsion[50]

Table 2. Advantages, disadvantages, and several properties of nanoemulsions

Advantages	Disadvantages	Other properties
Carrier of hydrophobic drugs	Requires large amount of surfactant and cosurfactant	Translucent/translucent system
Improves bioavailability of drugs	Low capability to solubilize high-melting-point drugs	High surface area/small droplet size
Good shelf stability	Low stability especially in acidic condition	Liquid morphology
Toxicologically safe	Toxicity of surfactants and cosufractants is possible	Has benefit to mask taste

Table 3. Summary of the physicochemical characteristics of a cationic oil-in-water nanoemulsion[50]

Parameter	Description
Aspect	White opaque to slightly translucent
pH	5.0-7.0
Osmolality (mOsmol/kg)	270
Droplet size (nm)	<200
Zeta potential (Mv)	Positive (+40)
Sterility	Sterile

aqueous phase is reduced, which can promote the restoration of the lacrimal film integrity and maintenance of product stability. Such benefits are important for patients suffering from short tear-film breakup time due to lipid deficiency in their tears (meibomian disease). Nanoemulsions are also important in the treatment of keratitis and in the reduction of dry eye disease symptoms by their capability to mechanically stabilize the tear film and increase the hypo-osmolarity of the aqueous film given that hyperosmolarity is a proinflammatory factor. In addition, these preparations have unexpected beneficial effects in the wound healing process by reducing the size of the scraped area.[48,49]

Choice of cationic agent

A high zeta potential of nanoemulsions is one of the most important factors to be considered before selecting a cationic agent. The entire cationic agent must be trapped in oil nanodroplets, with the positive charge positioned at the oilwater interface, to obtain a high zeta potential; a very small amount of these agents may exist in the aqueous phase, therefore requiring a high-lipophilicity cationic agent.[49]

The selection of cationic agent must be limited to those that have been previously registered, used in ophthalmic products, or submitted to the United States or European pharmacopoeia. Given the large numbers of cationic agents, such as stearylamine, oleylamine, polyethylenimine, polylysine, and benzalkonium chloride derivatives, not all of them can be selected due to their related toxicity.[49,50] Figure 4 (presented with personal permission from Jean-Sébastien Garrigue) shows a drawing of the phase spreading of diverse alkyl derivatives of benzalkonium chloride in (a) emulsion and (b) aqueous solution.[50]

Stearylamine is one of the most commonly used cationic agents. However, this primary amine is very reactive to various excipients. Thus, this compound is not described in pharmacopoeias. Oleylamine is a cationic lipid that has been used for manufacturing ophthalmic nanoemulsions; however, it has as stability problem owing to the existence of unsaturated sites in the aliphatic chain and the function of its primary amine.[49,51]

Additional cationic molecules that are used for DNA transfection, such as polyethylimine and poly-L-lysine, are

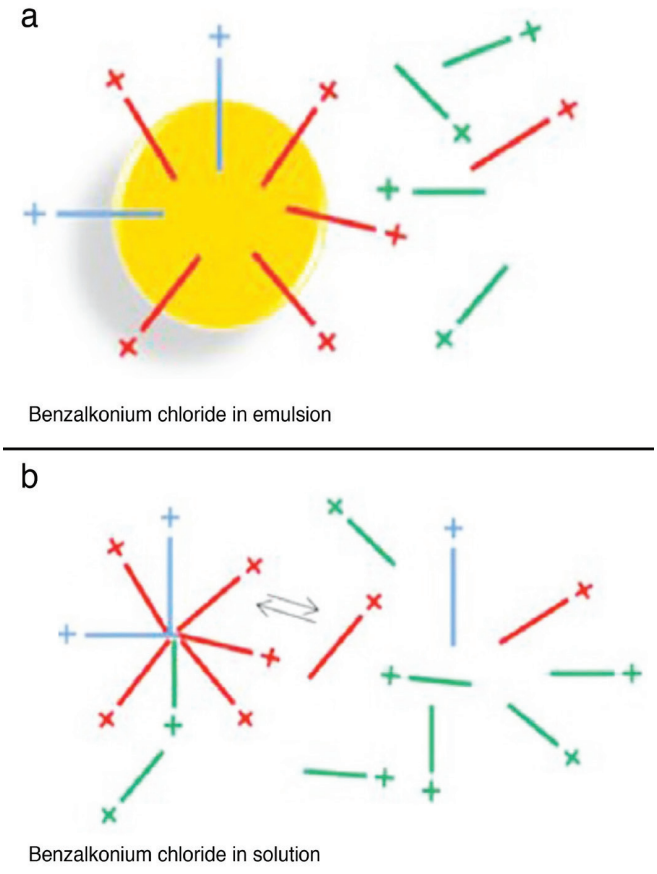

Figure 4. Illustration of the phase distribution for the different alkyl derivatives of benzalkonium chloride in (a) emulsion and (b) aqueous solution[50]

also used for cationic drug delivery systems; they are used in various nanoparticles as cationic agents, but several authors regard them as extremely toxic.[52]

Quaternary ammonium compounds, such as benzalkonium chloride, benzododecinium bromide, and cetrimide, are preservatives that have surfactant properties and provide nanoemulsions with a positive charge. Their preservative action is due to their capability to bind negatively charged bacteria and mycoplasma, which destroys their membrane. As a result,

their action is not only limited to microorganisms but also the epithelial cell lining of the ocular surface via an identical mechanism; in addition, the preservative action of these agents is neutralized by the emulsion because less amount of these agents is present freely in the aqueous medium, which limits their antimicrobial action and results in a toxic effect.[53]

EVALUATION OF OPHTHALMIC NANOEMULSION

Parameters for evaluation

Zeta potential

Zeta potential is the measurement of charge repulsion among oil nanodroplets. This variable is one of the most important parameters affecting the dispersed system stability. A high zeta potential results in a stable nanoemulsion. Its value depends on the differences between the electrical potential of the dispersion medium and the stationary layer of fluid close to the dispersed oil nanodroplets.[50,54]

The optimum zeta potential range is between +20 mV and +40 mV.5

Refractive index

The refractive index can be determined by using an Abbes refractometer. This index is used to determine any probable impairment of vision or distress after the administration of an eye drop.[50,55] The refractive index for the tear fluid is 1.340 to 1.360. Eye drops must have refractive index values not higher than 1.476.[56]

Percentage transmittance

The percentage transmittance can be measured by a spectrophotometer[50,54] at a specific wavelength with distilled water as a blank. The formulated nanoemulsion is considered transparent if the percentage transmittance is more than 99%.[57]

pH

The pH can be measured by using a pH meter, and the pH of nanoemulsions should be about 7.2±0.2 for maximum comfort. When the pH of the instilled solution is different from the tear pH, it results in discomfort and irritant effect, which depends on the contact period with the eye surface, solution composition, volume instilled, and buffering capacity. However, in most cases in which the preparation is not buffered or only slightly buffered, a nanoemulsion with a different pH can be tolerated because the tear pH can be adjusted to physiological levels; the accepted pH of preparations is between 3.5-8.5.[58,59]

Surface tension

The tear film becomes damaged when the surface tension of eye drops is greatly lower than that of the lachrymal fluid (40-50 mN/m).[60]

Rheological measurement

The influence of an ophthalmic preparation on the normal tear behavior should be as minimal as possible; a less viscous preparation allows limited blinking pain and good tolerance, whereas a more viscous one can improve the residence time of the drug and ocular bioavailability; the viscosity of eye drops should not be more than 20 mPa s.[60,61]

Osmolality

The lacrimal fluid osmolality is between 280-293 mOsm/kg. However, when the eye is opened, the osmolality is between 231-446 mOsm/kg due to evaporation. When the osmolality of a solution is less than 100 or greater than 640 mOsm/kg, the preparation will irritate the eye. However, the osmolality is reestablished 1-2 min after the instillation of a non-isotonic solution.[62]

Ocular irritation study

These studies should ensure that corneal integrity and structure are not affected.[62,63]

Thermodynamic stability studies

These studies involve subjecting the nanoemulsion formulation to six cycles between 4°C and 45°C. Then, the stable formulations are exposed to centrifugation test at about 3500 rpm; formulations that do not display phase separation will be obtained for the freeze-thaw stress test; during this test, the formulation is exposed to three freeze-thaw cycles under standard laboratory conditions.[56,64]

Analysis of droplet size

The droplet size is measured using a diffusion method, a particle size analyzer, light scattering, and LS 230. In addition, droplet sizes can be measured via correlation spectroscopy and transmission electron microscopy.[65]

Viscosity measurement

Viscosity can be determined by using a rotary viscometer at different temperatures.[54]

Dilution test

This test ensures that the stability of an ophthalmic nanoemulsion remains unchanged its after dilution; it involves the addition of the aqueous phase to the nanoemulsion without showing any problem.[54]

Drug content

A predetermined weight of nanoemulsion is extracted by dissolving it in an appropriate solvent, which is then investigated using a spectrophotometer or high-performance liquid chromatograph.[54]

Polydispersity

This test is performed to determine the droplet size uniformity using a spectrophotometer; the greater the polydispersity, the lesser the uniformity of droplet size.[54]

Cytotoxicity test

This test examines the effects of a preparation on a certain culture of mammalian cells.[66,67]

Examples of ophthalmic nanoemulsion studies and new products

Nanoemulsions are promising for ophthalmic disease treatment. Thus, diverse studies cover the use of nanoemulsions as ophthalmic drug delivery vehicles, as summarized in Table 4. When formulated as nanoemulsions, drugs, such as timolol, dexamethasone, indomethacin, levobunolol, pilocarpine, and chloramphenicol, exhibit preferred advantages over other traditional formulations (Table 4). Moreover, a number of nanoemulsion products are available either on the market, such as Restasis® (Allergan company) which is used as a nanoemulsion formulation for dry eye disease, or in clinical trials (brimonidine tartrate eye drops for dry eye disease under phase III). All these new examples are shown in Table 5.[68,69]

CONCLUSION

Owing to the innovation of nanoformulations, which is preferred over the systemic route, a significant improvement has been achieved in ocular disease therapy. Heating and/or mixing must be used in the preparation of nanoemulsions, whereas phase separation may occur after preparation. Thus, nanoemulsions are thermodynamically less stable than microemulsions.

The translucent appearance of nanoemulsions is due to a droplet size of less than 100 nm. As a result of this small droplet size, nanoemulsions exist as thermodynamically unstable dispersion. A high concentration of surfactants is required, resulting in the sticky texture of the formulation. A yellowish appearance and rancid odor occur after storage due to the presence of phospholipids, which are generally used to stabilize nanoemulsions. Nanoemulsions are easily manufactured system prepared by methods which may or may not rely on energy.

Unlike traditional ocular solutions and suspensions, which have considerable bioavailability and require frequent dosing, nanoemulsions have huge potential in enhancing bioavailability and reducing the frequency of drug administration. Surfactants

Table 4. Studies of several ophthalmic nanoemulsion formulations with types of surfactants and cosurfactants and oil used[68]

S. no.	Drug	Surfactants and co-surfactants	Oil	Comment
1	Timolol	Lecithin	Isopropyl myristate	Nanoemulsion bioavailability in aqueous humour was 3.5 times more than Timolol alone.
2	Dexamethasone	Cremophor EL, ropyleneglycol,	Isopropyl myristate	Enhanced ocular bioavailability (about three times compared with the conventional dosage form) and sustained effect of drug without ocular irritation.
3	Indomethacin	Phospholipids miranol-MHT	MCT	Significant increase in corneal permeability compared with the marketed formulation (Indocollyre®) and showed almost 4 times corneal permeability coefficient without toxicity in *ex vivo* studies.
4	Levobunolol	Lecithin, glycerol	Soybean oil	Improved *in vitro* permeability with a reservoir effect.
5	Pilocarpine	Macrogol 1500-glyceroltriricinoleate, 6PEG 200, propylene glycol,	Isopropyl myristate	Enhanced ocular bioavailability of up to 1.68 times with sustained effect and no ocular toxicity in comparison with aqueous solutions.
6	Chloramphenicol	Span20, Span80, Tween20, Tween80	Isopropyl palmitate and isopropyl myristate	Improved stability in nanoemulsion formulation in comparison to conventional system as chloramphenicol is relatively prone to degradation in conventional dosage form.

Table 5. Ophthalmic nanoemulsions products[69]

Nanoemulsions in the market for ophthalmic disease treatment				
Trade name	Drugs	Formulation	Disease	Company
Restasis®	0.05% cyclosporin A	Nanoemulsion	Dry eye disease	Allergan
Cyclokat®	0.1% cyclosporin A	Cationic nanoemulsion	Dry eye disease	Santen pharmaceuticals
Nanoemulsion under clinical trials for ophthalmic disease treatment				
Products	Administration method	Disease	Trial	Phase
Brimonidine tartrate	Eye drops	Dry eye disease	NCT03785340	III

and cosurfactants are important constituents of nanoemulsions and should be carefully selected. Their concentrations should be high enough to obtain ultra-low interfacial tension.

However, their toxicity presents a concern. In addition, cationic surfactants can be utilized to increase the product residence time on the eye. Accordingly, the use of nanoemulsion systems for topical ocular therapeutics can overcome the problem of multiple daily doses of traditional ocular therapy and improve patient compliance. To date, increasing interest surrounds nanoformulation studies, and the growing literature in this field is causing a great shift in the management of eye diseases, with the creation of successful products on the market and in clinical trials.

ACKNOWLEDGEMENTS

The authors are grateful to the College of Pharmacy, University of Mosul, Mosul, Iraq, for their support in this research.

Conflicts of interest: No conflict of interest was declared by the authors. The authors alone are responsible for the content and writing of this article

REFERENCES

1. Bucolo C, Drago F, Salomone S. Ocular drug delivery: a clue from nanotechnology. Front Pharmacol. 2012;3:1-3.
2. Al-bazzaz FY, Al-kotaji M. Ophthalmic *in-situ* sustained gel of ciprofloxacin, preparation and evaluation study. Int J Appl Pharm. 2018;10:153-161.
3. Ammar HO, Salama HA, Ghorab M, Mahmoud AA. Nanoemulsion as a potential ophthalmic delivery system for dorzolamide hydrochloride. AAPS PharmSciTech. 2009;10:808-819.
4. Kumari A, Sharma PK, Garg VK, Garg G. Ocular inserts: advancement in therapy of eye diseases. J Adv Pharm Technol Res. 2010;1:291-296.
5. Lallemand F, Daull P, Benita S, Buggage R, Garrigue JS. Successfully Improving Ocular Drug Delivery Using the Cationic Nanoemulsion, Novasorb. J Drug Deliv. 2012;2012:604204.
6. Shah J, Nair A, Jacob S, Patel R, Shah H, Shehata T, Morsy M. Nanoemulsion based vehicle for effective ocular delivery of moxifloxacin using experimental design and pharmacokinetic study in rabbits. Pharmaceutics. 2019;11:230.
7. SCCS. "Guidance on the safety assessment of nanomaterials in cosmetics"(2012). Avaialable from: https://ec.europa.eu/newsroom/sante/items/661871
8. Yen CC, Chen YC, Wu MT, Wang CC, Wu YT. Nanoemulsion as a strategy for improving the oral bioavailability and antiinflammatory activity of andrographolide. Int J Nanomedicine. 2018;13:669-680.
9. Patel A, Cholkar K, Agrahari V, Mitra AK. Ocular drug delivery systems: An overview. World J Pharmacol. 2013;2:47-64.
10. Huang D, Chen YS, Rupenthal ID. Overcoming ocular drug delivery barriers through the use of physical forces. Adv Drug Deliv Rev. 2018;126:96-112.
11. Gaudana R, Ananthula HK, Parenky A, Mitra AK. Ocular drug delivery. AAPS J. 2010;12:348-360.
12. Suri R, Beg S, Kohli K. Target strategies for drug delivery bypassing ocular barriers. J Drug Deliv Sci Technol. 2020;55:101389.
13. Singh V, Ahmad R, Heming T. The challenges of ophthalmic drug delivery: a review. Int J Drug Discov. 2011;3:56-62.
14. Agban Y, Thakur SS, Mugisho OO, Rupenthal ID. Depot formulations to sustain periocular drug delivery to the posterior eye segment. Drug Discov Today. 2019;24:1458-1469.
15. DeGorter MK, Xia CQ, Yang JJ, Kim RB. Drug transporters in drug efficacy and toxicity. Annu Rev Pharmacol Toxicol. 2012;52:249-273.
16. Ruponen M, Urtti A. Undefined role of mucus as a barrier in ocular drug delivery. Eur J Pharm Biopharm. 2015;96:442-446.
17. D'Emanuele A, Jevprasesphant R, Penny J, Attwood D. The use of a dendrimer-propranolol prodrug to bypass efflux transporters and enhance oral bioavailability. J Control Release. 2004; 95:447-453.
18. Parveen S, Misra R, Sahoo SK. Nanoparticles: a boon to drug delivery, therapeutics, diagnostics and imaging. Nanomedicine. 2012;8:147-166.
19. Zdziennicka A, Krawczyk J, Szymczyk K, Jańczuk B. Macroscopic and microscopic properties of some surfactants and biosurfactants. Int J Molecular Sci. 2018;19:1934.
20. Čalija B. Microsized and nanosized carriers for nonsteroidal anti-inflammatory drugs: formulation challenges and potential benefits. Belgrade: Academic Press; 2017.
21. Jaiswal M, Dudhe R, Sharma PK. Nanoemulsion: an advanced mode of drug delivery system. 3 Biotech. 2015;5:123.
22. Delmas T, Piraux H, Couffin AC, Texier I, Vinet F, Poulin P, Cates ME, Bibette J. How to prepare and stabilize very small nanoemulsions. Langmuir. 2011;27:1683-1692.
23. Park H, Han DW, Kim JW. Highly stable phase change material emulsions fabricated by interfacial assembly of amphiphilic block copolymers during phase inversion. Langmuir. 2015;31:2649-2654.
24. Ako-Adounvo AM, Nagarwal RC, Oliveira L, Boddu SHS, Wang XS, Dey S, Karla P. Recent Patents on ophthalmic nanoformulations and therapeutic implications. Recent Pat Drug Deliv Formul. 2014;8:193-201.
25. Subrizi A, del Amo EM, Korzhakov-Vlakh V, Tennikova T, Ruponen M, Urtti A. Design principles of ocular drug delivery systems: importance of drug payload, release rate, and material properties. Drug Discov Today. 2019;24:1446-1457.
26. Carli F, Baronian M, Schmid R, Chiellini E, inventors; AZAD Pharma AG, assignee. Ophthalmic oil-in-water emulsions containing prostaglandins. United States patent application. 2013; US 13/804,794.
27. Toris CB. Pharmacotherapies for glaucoma. Curr Mol Med. 2010;10:824-840.
28. Khan W, Aldouby YH, Avramoff A, Domb AJ. Cyclosporin nanosphere formulation for ophthalmic administration. Int J Pharm. 2012;437:275-276.
29. Benita S, Elbaz E, inventors; Yissum Research Development Co of Hebrew University, assignee. Oil-in-water emulsions of positively charged particles. United States patent US 6,007,826. 1999 Dec 28. Available from: https://patents.justia.com/assignee/yisum-research-development-company-of-the-hebrew-university-of-jerusalem
30. Wang B, Tian H, Xiang D. Stabilizing the oil-in-water emulsions using the mixtures of dendrobium officinale polysaccharides and gum arabic or propylene glycol alginate. Molecules. 2020;25:759.

31. Gupta A, Eral HB, Hatton TA, Doyle PS. Nanoemulsions: formation, properties and applications. Soft Matter. 2016;12:2826-2841.
32. Tadros TF. Emulsion formation, stability, and rheology. Emulsion formation and stability. 2013;1:1-75.
33. Qiu H, Chen X, Wei X, Liang J, Zhou D, Wang L. The emulsifying properties of hydrogenated rosin xylitol ester as a biomass surfactant for food: effect of ph and salts. Molecules. 2020;25:302.
34. Jaiswal M, Dudhe R, Sharma PK. Nanoemulsion: an advanced mode of drug delivery system. 3 Biotech. 2015;5:123.
35. Shakeel F, Baboota S, Ahuja A, Ali J, Aqil M, Shafiq S. Nanoemulsions as vehicles for transdermal delivery of aceclofenac. AAPS PharmSciTech. 2007;8:E104.
36. Nikam TH, Patil MP, Patil SS, Vadnere GP, Lodhi S. Nanoemulsion: a brief review on development and application in parenteral drug delivery. Adv Pharm J. 2018;3:43-54.
37. Sharma N, Mishra S, Sharma S, Deshpande RD, Sharma RK. Preparation and optimization of nanoemulsions for targeting drug delivery. Int J Drug Dev Res. 2013;5:37-48.
38. Chávez-Zamudio R, Ochoa-Flores AA, Soto-Rodríguez I, Garcia-Varela R, García HS. Preparation, characterization and bioavailability by oral administration of O/W curcumin nanoemulsions stabilized with lysophosphatidylcholine. Food Funct. 2017;8:3346-3354.
39. Zhang J, Liu Z, Tao C, Lin X, Zhang M, Zeng L, Chen X, Song H. Cationic nanoemulsions with prolonged retention time as promising carriers for ophthalmic delivery of tacrolimus. Eur J Pharm Sci. 2020;144:105229.
40. Dukovski BJ, Juretić M, Bračko D, Randjelović D, Savić S, Moral MC, Diebold Y, Filipović-Grčić J, Pepić I, Lovrić J. Functional ibuprofen-loaded cationic nanoemulsion: Development and optimization for dry eye disease treatment. Int J Pharm. 2020;576:118979.
41. Kumar M, Bishnoi RS, Shukla AK, Jain CP. Techniques for Formulation of Nanoemulsion Drug Delivery System: A Review. Prev Nutr Food Sci. 2019;24:225-234.
42. Kotta S, Khan AW, Ansari SH, Sharma RK, Ali J. Formulation of nanoemulsion: a comparison between phase inversion composition method and high-pressure homogenization method. Drug Deliv. 2015;22:455-466.
43. Henostroza MA, Melo KJ, Yukuyama MN, Löbenberg R, Bou-Chacra NA. Cationic rifampicin nanoemulsion for the treatment of ocular tuberculosis. Colloids Surf A Physicochem Eng. 2020;597:124755.
44. Chime SA, Kenechukwu FC, Attama AA. Nanoemulsions-advances in formulation, characterization and applications in drug delivery. Intechopen: London; 2014.
45. Frank SG. Emulsions: Theory and Practice. In: Becher P, Wilmington, DE, eds. Partnership with American Chemical Society. (3rd ed). Oxford: Oxford University Press; 2001.
46. Hussain A, Altamimi MA, Alshehri S, Imam SS, Shakeel F, Singh SK. Novel approach for transdermal delivery of rifampicin to induce synergistic antimycobacterial effects against cutaneous and systemic tuberculosis using a cationic nanoemulsion gel. Int J Nanomedicine. 2020;15:1073.
47. Kulkarni SK. Nanotechnology: principles and practices. Switzerland: Springer; 2014.
48. Daull P, Feraille L, Elena PP, Garrigue JS. Comparison of the anti-inflammatory effects of artificial tears in a rat model of corneal scraping. J Ocul Pharmacol Ther. 2016;32:109-118.
49. Dell SJ, Gaster RN, Barbarino SC, Cunningham DN. Prospective evaluation of intense pulsed light and meibomian gland expression efficacy on relieving signs and symptoms of dry eye disease due to meibomian gland dysfunction. Clin Ophthalmol. 2017;11:817-827.
50. Daull P, Lallemand F, Garrigue JS. Benefits of cetalkonium chloride cationic oil-in-water nanoemulsions for topical ophthalmic drug delivery. J Pharm Pharmacol. 2014;66:531-541.
51. Campbell PI. Toxicity of some charged lipids used in liposome preparations. Cytobios. 1983;37:21-26.
52. Manosroi A, Podjanasoonthon K, Manosroi J. Development of novel topical tranexamic acid liposome formulations. Int J Pharm. 2002;235:61-70.
53. Draz MS, Fang BA, Zhang P, Hu Z, Gu S, Weng KC, Gray JW, Chen FF. Nanoparticle-Mediated Systemic Delivery of siRNA for Treatment of Cancers and Viral Infections. Theranostics. 2014;4:872-892.
54. Wu TH, Craven A, Tran T, Tran K, So K, Levi DM, Li RW. Enhancing coarse-to-fine stereo vision by perceptual learning: An asymmetric transfer across spatial frequency spectrum. Invest Ophthalmol Vis Sci. 2014;55:751.
55. Liu DX, Zhao XT, Liang W, Li JW. The stability and breakage of oil-in-water from polymer flooding produced water. Pet Sci Technol. 2013;31:2082-2088.
56. Patel N, Nakrani H, Raval M, Sheth N. Development of loteprednol etabonate-loaded cationic nanoemulsified *in-situ* ophthalmic gel for sustained delivery and enhanced ocular bioavailability. Drug Deliv. 2016;23:3712-3723.
57. Gurpreet K, Singh SK. Review of nanoemulsion formulation and characterization techniques. Indian J Pharm Sci. 2018;80:781-789.
58. Mahran A, Ismail S, Allam AA. Development of Triamcinolone Acetonide-Loaded Microemulsion as a Prospective Ophthalmic Delivery System for Treatment of Uveitis: In Vitro and In Vivo Evaluation. Pharmaceutics. 2021;13:444.
59. Salimi A. Preparation and evaluation of celecoxib nanoemulsion for ocular drug delivery. Asian J Pharm. 2017;11:543-550.
60. Mahboobian MM, Foroutan SM, Aboofazeli R. Brinzolamide-loaded nanoemulsions: *in vitro* release evaluation. Iran J Pharm Sci. 2016;12:75-93.
61. Lallemand F, Schmitt M, Bourges JL, Gurny R, Benita S, Garrigue JS. Cyclosporine a delivery to the eye: a comprehensive review of academic and industrial efforts. Eur J Pharm Biopharm. 2017;117:14-28.
62. Sharif HR, Sharif MK, Zhong F. Preparation, characterization and rheological properties of vitamin E enriched nanoemulsion. Pak J Food Sci. 2017;27:7-14.
63. Sarı ES, Koç R, Yazıcı A, Şahin G, Çakmak H, Kocatürk T, SS Ermiş. Tear osmolarity, break-up time and schirmer's scores in parkinson's disease. Turk J Ophthalmol. 2015;45:142.
64. Gallarate M, Chirio D, Bussano R, Peira E, Battaglia L, Baratta F, Trotta M. Development of O/W nanoemulsions for ophthalmic administration of timolol. Int J Pharm. 2013;440:126-134.
65. Khan NU, Ali A, Khan H, Khan ZU, Ahmed Z. Stability Studies and Characterization of Glutathione-Loaded Nanoemulsion. Journal of cosmetic science. 2018;69:257-267.
66. Gupta A, Narsimhan V, Hatton TA, Doyle PS. Kinetics of the change in droplet size during nanoemulsion formation. Langmuir. 2016;32:11551-11559.

67. Al-Omari NA, Butrus NH. Preparation, characterization and cytotoxic evaluation of novel au(iii) complexes of thioglycolate and 2-mercaptoglycolate ligands. Iraqi J Pharm Sci. 2013;13:28-40.

68. Rao R, Upadhyay SC, Singh MK. Nanoemulsion in ophthalmics: a newer paradigm for sustained drug delivery and bioavailability enhancement in ophthalmic manifestations. Int J Pharm Sci Rev Res. 2018;50:18-24.

69. Meng T, Kulkarni V, Simmers R, Brar V, Xu Q. Therapeutic implications of nanomedicine for ocular drug delivery. Drug Discov Today. 2019;24:1524-1538.

NOTES

NOTES

PUBLICATION NAME	Turkish Journal of Pharmaceutical Sciences
TYPE OF PUBLICATION	Vernacular Publication
PERIOD AND LANGUAGE	Bimonthly-English
OWNER	Erdoğan ÇOLAK on behalf of the Turkish Pharmacists' Association
EDITOR-IN-CHIEF	Prof. Terken BAYDAR, Ph.D.
ADDRESS OF PUBLICATION	Turkish Pharmacists' Association, Mustafa Kemal Mah 2147.Sok No:3 06510 Çankaya/Ankara, TURKEY

TURKISH
JOURNAL OF PHARMACEUTICAL
SCIENCES

Volume: 18, No: 5, Year: 2021

CONTENTS